MIINA BJÖRNINEN

The Effects of Electroactive Polypyrrole on the Osteogenic Differentiation of Adipose Stem Cells and Bone Regeneration

■

ACADEMIC DISSERTATION
To be presented, with the permission of
the Board of the BioMediTech of the University of Tampere,
for public discussion in the Auditorium of Finn-Medi 5,
Biokatu 12, Tampere, on January 7th, 2015, at 12 o'clock.

UNIVERSITY OF TAMPERE

MIINA BJÖRNINEN

The Effects of Electroactive Polypyrrole on the Osteogenic Differentiation of Adipose Stem Cells and Bone Regeneration

Acta Universitatis Tamperensis 2008
Tampere University Press
Tampere 2015

UNIVERSITY
OF TAMPERE

ACADEMIC DISSERTATION
University of Tampere, BioMediTech
Finland
Zhongshan Hospital
China

Supervised by
Docent Suvi Haimi
University of Tampere
Finland
Docent Susanna Miettinen
University of Tampere
Finland

Reviewed by
Professor Reijo Lappalainen
University of Eastern Finland
Finland
Associate Professor Joselito Razal
Deakin University
Australia

The originality of this thesis has been checked using the Turnitin OriginalityCheck service in accordance with the quality management system of the University of Tampere.

Cover design by
Mikko Reinikka

Distributor:
kirjamyynti@juvenes.fi
http://granum.uta.fi

Acta Universitatis Tamperensis 2008
ISBN 978-951-44-9670-7 (print)
ISSN-L 1455-1616
ISSN 1455-1616

Acta Electronica Universitatis Tamperensis 1497
ISBN 978-951-44-9671-4 (pdf)
ISSN 1456-954X
http://tampub.uta.fi

Suomen Yliopistopaino Oy – Juvenes Print
Tampere 2015

To my husband Hannes

Abstract

While conventional bone treatment methods still struggle to address efficient bone regeneration in cases of critical-sized defects, bone tissue engineering could provide functional solutions by exploiting the body's own healing capacity. Due to the load-bearing nature of bone tissue, high mechanical performance is required of the biomaterials used as scaffold material in bone tissue engineering. Lactide-based polymers are commonly used for this purpose because they have an easily controllable degradation rate and possess mechanical properties with good biocompatibility. However, their lack of bioactivity and their hydrophobic surface properties do not encourage cell and tissue attachment to the scaffold's surface. For this reason, electroconductive and biocompatible polypyrrole (PPy) provides a potential coating method for scaffolds; it can be incorporated with different bioactive molecules and provides favourable surface properties for cell attachment. In addition, redox activity of PPy in combination with electrical stimulation (ES) provides an interesting stimulation method for osteogenic cells.

PPy has been reported to be a potential substrate for osteogenic cell lines, such as mesenchymal stem cells (MSCs). However, human adipose stem cells (hASCs), which are an MSC source of high potential due to their abundance and ease of accessibility, are yet to be explored in this area. Moreover, the effect of PPy on bone regeneration *in vivo* has not been studied.

This work evaluates the potential of PPy as a substrate in bone tissue engineering with hASCs *in vitro* and as an implant coating in bone regeneration *in vivo*. In the first part, electrochemically produced PPy, which is doped either with chondroitin sulphate (CS) or hyaluronic acid (HA), is studied as a coating for hASCs. In the second part, PPy is chemically produced in the presence of CS to form a coating on polylactide (PLA) fibre scaffolds that are then studied as a conductive platform for hASCs *in vitro*. ES is applied through PPy-coated systems in both *in vitro* studies. The cell response is evaluated by their morphology, viability, proliferation, and osteogenic differentiation. In the *in vivo* part of the work, chemically PPy-coated and CS-incorporated bioabsorbable poly(lactide-co-glycolide)-β-tricalcium phosphate (PLGA-β-TCP) composite bone fixation screws are implanted into rabbit bone tissue and examined in terms of biocompatibility and new bone formation.

The cells showed a good morphology and homogenous spreading on the CS-doped PPy films (PPy-CS), whereas the HA-doped PPy films (PPy-HA) triggered aggregation and a partial detachment of the cells. This was most probably due to the significantly rougher surface morphology of the PPy-HA films. Cells on PPy-CS also showed significantly higher mineralisation in comparison to PPy-HA when applying ES. A PPy-coated PLA scaffold enhances hASC proliferation significantly in

comparison to plain PLA scaffolds. The parameters used did not have an effect on cells in either of the *in vitro* studies in comparison to the unstimulated controls. PPy-coated bioabsorbable screws promoted new bone formation *in vivo* significantly better than the uncoated screws according to hard tissue histology, micro-computed tomography (micro-CT) and tetracycline labelling. In addition, no signs of acute, systematic or chronic toxicity were found in any of the rabbits.

In conclusion, electrochemically produced PPy-CS and chemically produced PPy incorporated with CS provided favourable conditions for hASCs in terms of morphology, proliferation and osteogenic differentiation, implying its great potential for bone tissue engineering applications. The chemically produced PPy coating also proved to be a potential conductive coating material for PLGA-β-TCP screws, promoting significantly greater new bone formation *in vivo*.

Tiivistelmä

Perinteiset luuvaurioiden hoitomenetelmät ovat usein riittämättömiä kriittisen koon luuvaurioiden hoidoissa. Luun kudosteknologia pystyisi tarjoamaan tähän toimivia ja tehokkaita ratkaisuja hyödyntäen kehon omaa parantumiskykyä.

Luun kudosteknologiassa käytettäviltä materiaaleilta vaaditaan mekaanista kestävyyttä johtuen luukudoksen tärkeästä roolista kehon tukirankana. Laktidipohjaiset polymeerit ovat yleisesti käytettyjä polymeereja luun kudosteknologiassa, sillä ne ovat mekaanisesti kestäviä, niiden hajoamista kehossa on helppo hallita ja ne on todettu erittäin kudosyhteensopiviksi polymeereiksi. Laktidipohjaiset polymeerit eivät kuitenkaan ole bioaktiivisia ja lisäksi niiden hydrofobisuus haittaa solujen ja kudoksen kiinnittymistä materiaalin pintaan.

Polypyrroli(PPy)-pinnoitus on potentiaalinen menetelmä edellä mainittujen ongelmien välttämiseksi, koska sillä on edulliset pintaominaisuudet solujen kiinnittymiselle ja lisäksi siihen voidaan sisällyttää erilaisia bioaktiivisia molekyylejä. PPy on myös redox-aktiivinen, minkä vuoksi sen käyttö sähkövirtaa välittävänä biomateriaalina avaa mielenkiintoisia mahdollisuuksia osteogeenisten solujen stimuloinnissa.

PPy:n on todettu olevan potentiaalinen substraatti osteogeenisille soluille, kuten mesenkymaalisille kantasoluille. Mesenkymaalisiin kantasoluihin lukeutuvat rasvan kantasolut ovat yksi potentiaalisimmista solutyypeistä niiden runsaslukuisuuden ja helpon saatavuuden ansiosta. Niitä ei ole kuitenkaan vielä tutkittu PPy:n ja sähköstimulaation yhdistelmässä.

Tässä työssä arvioitiin PPy:n mahdollisuudet ihmisen rasvan kantasolujen substraattina luun kudosteknologiassa *in vitro* ja sekä luun uudismuodostumista edistävänä implantin pinnoitemateriaalina *in vivo*. Tutkimuksen ensimmäisessä osassa sähkökemiallisesti valmistettu PPy seostettiin kondroitiinisulfaatilla tai hyaluronihapolla ja tutkittiin sen soveltuvuutta pinnoitemateriaaliksi ihmisen rasvan kantasoluille. Tutkimuksen toisessa osassa PPy valmistettiin kemiallisesti kondroitiinisulfaatin läsnäollessa ja tutkittiin sen ominaisuuksia sähköäjohtavana pinnoitteena polylaktidista (PLA) valmistetuissa kuiturakenteissa. Kummassakin *in vitro*-osatyössä sähköstimulaatiota syötettiin PPy substraattien läpi. Soluvastetta tutkittiin solujen morfologian, elinkyvyn, proliferaation ja luuerilaistumisen kannalta. Tutkimuksen *in vivo*-osassa luun korjaukseen tarkoitetut kemiallisesti, kondoitiinisulfaatin läsnäollessa pinnoitetut biohajoavat poly(laktidi-co-glykolidi)- β-trikalsiumfosfaatti (PLGA-β-TCP) komposiittiruuvit implantoitiin kanin luukudokseen ja niiden kudosyhteensopivuutta ja vaikutusta uudisluun muodostukseen tutkittiin.

Kondroitiinisulfaattiseostettujen PPy-pinnoitteiden (PPy-CS) päällä olevat solut osoittautuivat morfologialtaan hyviksi ja levittäytyivät tasaisesti pitkin pintaa. Sen

sijaan hyaluronihapposeostettujen PPy-pinnoitteiden (PPy-HA) päällä olevat solut olivat aggregoituneet ja osittain irrottautuneet pinnasta. Tämä johtui todennäköisimmin PPy-HA-pinnoitteen merkittävästi suuremmasta pintakarheudesta. Solun ulkoisen tilan mineralisaatio oli merkittävästi suurempaa sähköstimuloiduissa PPy-CS-pinnoitteen päällä olevissa soluissa verrattuna vastaavassa ryhmässä olevaan PPy-HA-pinnoitteeseen. Ihmisen rasvan kantasolujen proliferaatio oli merkittävästi suurempaa PPy-pinnoitetuissa PLA kuiturakenteissa verrattuna vastaaviin pinnoittamattomiin rakenteisiin. Sähköstimulaatiolla ei todettu olevan vaikutusta soluihin kummassakaan *in vitro*-tutkimuksessa verrattuna stimuloimattomiin kontrolleihin. Kovakudoshistologian, digitaalisen röntgenkuvauksen ja tetrasykliinileimauksen perusteella PPy-pinnoitetut biohajoavat ruuvit edistivät merkittävästi uudisluun muodostusta verrattuna vastaaviin pinnoittamattomiin ruuveihin. Lisäksi mitään merkkejä akuuttisesta, systemaattisesta tai kroonisesta toksisuudesta ei havaittu yhdessäkään kanista.

Tutkimuksen johtopäätös on, että sähkökemiallisesti valmistettu PPy-CS ja kemiallisesti kondoitiinisulfaatin läsnäollessa valmistettu PPy-pinnoite osoittautuivat sopiviksi substraateiksi ihmisen rasvan kantasoluille niiden morphologian, proliferaation ja luuerilaistumisen perusteella. Tämä osoittaa niiden suuren potentiaalin luun kudosteknologiassa. Kemiallisesti tuotettu PPy-pinnoite todettiin potentiaaliseksi luuimplanttien pinnoitemateriaaliksi myös PLGA-β-TCP-ruuveissa edistäen merkittävästi luun uudismuodostusta *in vivo*.

Abbreviations

AC	alternating current
AFM	atomic force microscope
ALP	alkaline phosphatase
ANOVA	one-way analysis of variance
APS	ammonium peroxydisulfate
ASC	adipose stem cell
ATP	adenosine triphosphate
BEC	biphasic electric current
BMP	bone morphogenic proteins
BMSC	bone marrow stromal cell
BSP	bone sialoprotein
Coll I	collagen type I
Coll III	collagen type III
Coll V	collagen type V
CP	conductive polymer
CPE	constant phase element
CS	chondroitin sulphate
CV	cyclic voltammetry
CXCL2	chemokine (C-X-C motif) ligand 2
DC	direct current
DMEM	Dulbecco's Modified Eagle Medium
DNA	deoxyribonucleic acid
ECM	extracellular matrix
EIS	electrochemical impedance spectroscopy
EMF	electromagnetic field
Erk	extracellular-signal-regulated kinases
ES	electrical stimulation
FACIT	fibril-associated collagens with interrupted triple helices
FBS	foetal bovine serum
FDA	US Food and Drug Administration
GAG	glycosaminoglycan
HA	hyaluronic acid
hASC	human adipose stem cells
HE	heparin
HEPES	4-(2-hydroxyethyl)-1-piperazineethanesulphonic acid
IGF-1	insulin-like growth factor 1
IL-8	interleukin 8

i.m.	intramuscular
MAPK	mitogen-activated protein kinase
MC	marrow cavity
microRNA	microribonucleic acid
MM	maintenance medium
mRNA	messenger ribonucleic acid
MS	mass spectrometry
MSC	mesenchymal stem cell
OC	osteocalcin
OM	osteogenic medium
OPN	osteopontin
PBS	phosphate-buffered saline
PEN	polyethylene-naphthalate
PLA	polylactide
PLC	phospholipase C
PPy	polypyrrole
PPy-CS	chondroitin sulphate-doped polypyrrole
PPy-HA	hyaluronic acid-doped polypyrrole
PS	polystyrene
Ra	surface roughness
ROS	reactive oxygen species
runx2	runt-related 2
s.c.	subcutaneous
SD	standard deviation
Smad	portmanteau of Sma in Drosophila and Mad in C. elegans
TCP	tricalcium phosphate
TGF-β	transforming growth factor-β
VEGF	vascular endothelial growth factor
Wnt	portmanteau of Wingless and integration1
$\|Z\|_{cell}$	magnitude of cell impedance
η	ideality coefficient of capacitance in the CPE model

Original publications

This dissertation is based on the following articles, which are referred to in the text by their Roman numerals (**I–III**):

I. **Björninen M**, Siljander A, Pelto J, Hyttinen J, Kellomäki M, Miettinen S, Seppänen R, Haimi S. "Comparison of chondroitin sulfate and hyaluronic acid doped conductive polypyrrole films for adipose stem cells". *Ann Biomed Eng.* 2014

II. Pelto J, **Björninen M**, Pälli A, Talvitie E, Hyttinen J, Mannerström B, Seppänen R, Kellomäki M, Miettinen S, Haimi S. "Novel polypyrrole-coated polylactide scaffolds enhance adipose stem cell proliferation and early osteogenic differentiation". *Tissue Eng Part A.* 2013 Apr; 19(7–8): 882–92.

III. Zhao M-D, **Björninen M**, Cao L, Wang H-R, Pelto J, Hyttinen J, Jiang Y-Q, Kellomäki M, Miettinen S, Haimi S, Dong J. "Polypyrrole coating on poly-(lactide/glycolide)-β-tricalcium phosphate screws enhances new bone formation in rabbits". Submitted to *Acta Biomaterialia.*

Table of contents

1 Introduction

Bone treatment methods have advanced over the decades, from amputation to reconstruction with bone grafts (Awad et al. 2014). An estimated 2.2 million bone graft procedures take place annually (Lewandrowski et al. 2000). Currently, the gold-standard treatment method uses autograft bone (bone tissue from the patient) from the iliac crest, as it provides a scaffold for bone ingrowth and contains living bone cells that stimulate osteoinduction (Cypher & Grossman 1996). However, there are several disadvantages, such as the limited availability of donor tissue, extended operation time, and the increased risk of complications, especially with elderly patients (Van der Stok et al. 2011, Brown, Kumbar & Laurencin 2013). Other methods currently used include allograft bone (human source of origin), xenograft bone (animal source of origin), synthetic and natural polymers, ceramics, and their composites (Lewandrowski et al. 2000, Brown, Kumbar & Laurencin 2013). Allograft and xenograft bone substitutes are sterilised, decellularised and demineralised, leaving only the collagens, non-collagenous proteins, and some growth factors from the original bone (Gazdag et al. 1995). They possess some major disadvantages, such as immunological issues and disease transmission (Asselmeier, Caspari & Bottenfield 1993, Stevenson & Horowitz 1992). Despite the wide variety of options for bone grafts, the bioactivity of the grafts remains an issue. For example, vascularisation is one of the key factors in bone regeneration that is difficult to achieve using conventional means (Rouwkema, Rivron & van Blitterswijk 2008).

Bone tissue engineering exploits the body's own regeneration capacity by combining cells, biomaterials and cell-inductive stimuli, such as growth factors (GF) or physical stimuli (Sarkar et al. 2013). The aim of bone tissue engineering is to restore bone function in critical-sized bone defects that are too large for the body to restore through its own regeneration capacity (Liu, Wu & de Groot 2010).

Approaches in bone tissue engineering can be classified into two main categories: 1) tissue-engineered constructs with cells and biomaterial scaffolds generated *in vitro* following *in vivo* transplantation, and 2) scaffolds implanted *in situ* without addition of cells in the constructs. Cells can be retrieved from various sources, including embryonic stem cells and somatic adult cells. However, the potential of adult somatic cells in tissue engineering is limited due to their low proliferation capability, loss of phenotype, dedifferentiation in the culture, and the limited number that can be harvested. (Sarkar et al. 2013)

Mesenchymal stem cells (MSCs) have shown great potential as a cell source in bone tissue engineering because they can be used as an abundant autologous cell source for patients. MSCs derived from adipose tissue – adipose stem cells (ASCs) – are receiving

increasing interest in the field due to their ease of isolation and high availability in adipose tissue when compared to bone marrow stromal cells (BMSCs) (Wen et al. 2013, Zuk et al. 2002).

Biomaterials provide a template for cells. This template gradually and controllably degrades to give way for the target tissue's regeneration process. The main role of the biomaterial is to act as a scaffold to provide mechanical support for cells and the surrounding target tissue, but it can also be used to direct growth, migration and differentiation of cells by supplying nutrients, drugs, and other bioactive factors, as well as physical cues (Sarkar et al. 2013).

One of the conductive polymers (CPs), polypyrrole (PPy), has shown great promise in tissue engineering, not only because it can mediate electrical currents, but also because it may enhance the bioactivity of extensively used lactide-based polymers in bone applications. Lactide-based polymers alone are relatively hydrophobic (Oh 2011) with a lack of bioactivity. PPy has been reported to possess good *in vivo* biocompatibility with soft tissues (Wang et al. 2004b, Wang et al. 2004a, Ramanaviciene et al. 2007, George et al. 2005, Wan et al. 2005, Jiang et al. 2002), but its effects on bone tissue are still unknown. However, excellent attachment, enhanced proliferation, and osteogenic differentiation of MSCs (Serra Moreno et al. 2012, Serra Moreno et al. 2009) and osteoblasts on PPy coatings (Hu et al. 2014) have been previously demonstrated. This indicates that PPy is a potential material in bone tissue regeneration *in vivo*. The combination of conducting polymers and electrical stimulation (ES) provides a range of new opportunities to mimic the electrophysiological phenomena of living tissues (Hu et al. 2014, Thompson et al. 2010, Richardson et al. 2009).

This doctoral dissertation introduces a novel approach in regulating stem cell behaviour by combining electrical cues with an electroactive PPy coating to provide an alternative method to the conventional chemical induction used in bone tissue engineering. Furthermore, this dissertation evaluates the significance of PPy coating in enhancing bone-implant interaction of the commonly used bioabsorbable bone fixation implant material. The first study compares two different PPy films, one doped with chondroitin sulphate (CS) and the other with hyaluronic acid (HA) as substrates for human ASCs (hASCs). The second *in vitro* study evaluates hASC response to chemically oxidised PPy that has been incorporated with CS and coated on PLA fibre scaffolds. ES is applied via the constructs in both *in vitro* studies. In the third study, the biocompatibility of PPy in bone tissue and the effect of PPy on bone regeneration is studied *in vivo* in a rabbit model by implanting PPy-coated bioabsorbable bone fixation screws into the rabbit's femur and tibia for 12 and 26 wks.

2 Literature review

2.1 Bone regeneration

The main role of bone tissue is to provide structural support and protection for the body and to serve as the body's mineral reservoir. It is a highly complex and dynamic tissue that is constantly changing under the regulation of hormones, cytokines, and the central and sympathetic nervous systems. (Martin, Wah Ng & Sims 2013, Elefteriou 2008)

Regulation in bone is controlled by three main cell types: osteoblasts, osteocytes, and osteoclasts. Osteoblasts are the bone matrix-forming cells that also regulate mineralisation. These cells are highly anchorage-dependent; their extensive cell-cell and cell-matrix contacts come via a variety of transmembranous proteins, such as integrins and connexins, and specific receptors (Lecanda et al. 1998, Sommerfeldt & Rubin 2001). As osteoblasts become trapped in their own calcified matrix, they change their phenotype and become osteocytes, which remain connected with other similar cells and quiescent bone-lining cells, forming an extensive network of intercellular communication (Martin, Wah Ng & Sims 2013, Sommerfeldt & Rubin 2001). Osteoclasts are multinucleated bone resorbing cells derived from haematopoietic stem cells. It is suggested that osteoclasts not only respond to stimuli from osteoblastic, stromal and immune cells, growing evidence shows that they can also act as immune cells and mutually regulate the function of these other cell types (Boyce, Yao & Xing 2009).

The extracellular matrix (ECM) of bone is composed of 70–90% mineral and 10–30% organic matrix (Boskey & Robey 2013). The composition of bone is presented in Table 1. The mineral matrix is composed mainly of hydroxyapatite ($Ca_{10}(PO4)_6(OH)_2$), which brings mechanical strength to the bone (Boskey & Robey 2013). Even though the organic matrix is mainly composed of collagen type I (Coll I), the osteoblasts secrete the same amount of collagenous and non-collagenous proteins on a molar basis (Clarke 2008). Collagen provides tensile strength to the bone structure and serves as an important "backbone" for mineral deposition by orientating the nucleation of mineralisation (Boskey & Robey 2013). More detailed explanations of the functions of some of the non-collagenous proteins are described later in Chapter 2.1.1.

Table 1. Bone composition. Modified from Boskey and Robey (2013), and Clarke (2008).

Matrix	Content	Specific composition
Mineral	70–90%	**$Ca_{10}(PO4)_6(OH)_2$** carbonate magnesium acid phosphate
Organic matrix	10–30%	**85–90% collagenous proteins:** Coll I, III and V, FACIT collagens **10–15% non-collagenous proteins:** proteoglycans, glycosylated proteins, γ-carboxylated proteins, growth factors
Water	5–10%	
Lipids	< 3%	

Coll I, III and V: collagen type I, III and V; FACIT: Fibril-associated collagens with interrupted triple helices.

The structure of a long bone encompasses cortical (compact) bone on the outer structure that surrounds the marrow space, and an interior scaffold of trabecular (spongy) bone interspersed in the bone marrow compartment (Figure 1). The ratios of cortical and trabecular bone vary depending on the bone's location in the body. Both cortical and trabecular bone consist of osteons. They are formed in concentric lamellae where the osteocytes are entrapped between lamellae. Osteons in cortical bone, called Haversian systems, are cylindrical in shape and formed of concentric lamellae. The outer surface of the cortical bone is called the periosteum and the inner surface is called the endosteum. The remodelling activity of the bone concentrates mostly on these surfaces; it is more active in the periosteum where the bone formation typically exceeds bone resorption, which is important for appositional growth and fracture repair. The reverse is typically true in the endosteum, where the marrow space expands with aging. Trabecular bone consists of rods and plates, and the osteons are semilunar in shape. (Clarke 2008)

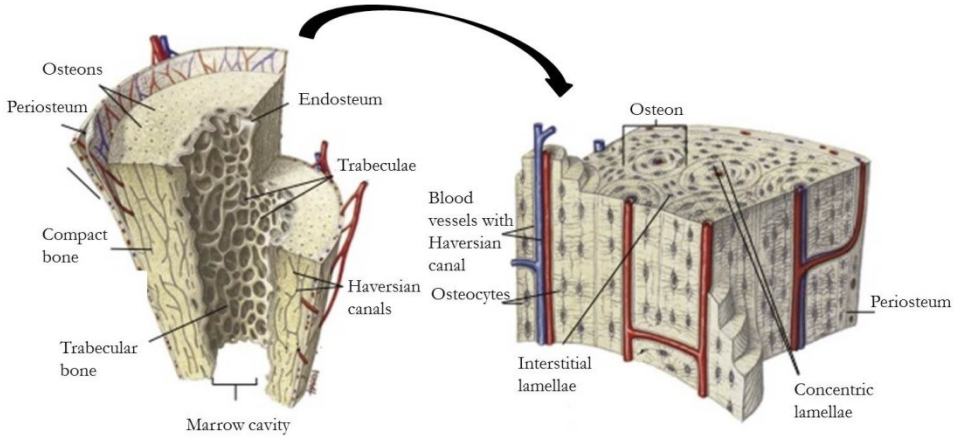

Figure 1**.** Structure of the long bone. Modified from Gunson, Gropp & Varela (2013).

2.1.1 Bone healing and regeneration

The periosteum, surrounding soft tissue, and MSCs are involved in bone healing, which can occur through intramembranous ossification and endochondral ossification (Li & Stocum 2014). Intramembranous ossification mainly occurs during embryonic development, especially in flat bones, and does not solely contribute to fracture healing (Li & Stocum 2014, Kanczler & Oreffo 2008, Cohen Jr. 2006). It involves invasion of capillaries into the mesenchymal zone and the migration and differentiation of MSCs into mature osteoblasts (Li & Stocum 2014, Kanczler & Oreffo 2008). In endochondral ossification, an inflammatory response triggers a series of subsequent events (Li & Stocum 2014). During fracture healing, cartilage is formed at the fracture site in response to the hypoxia caused by the lack of blood supply (Kanczler & Oreffo 2008). Cartilage-forming chondrocytes, derived from MSCs migrating from the periosteum and endosteum, enter a hypertrophic state after proliferation; their volume dramatically increases and they simultaneously secrete ECM (Mackie et al. 2008). Hypertrophic chondrocytes undergo apoptosis, allowing invasion of osteoclasts, precursor osteoblasts, and blood vessels into the callus (Li & Stocum 2014, Mackie et al. 2008). This triggers new bone formation as osteoclasts assist in the removal of cartilage, and the differentiating osteoblasts deposit bone at the remnants of the cartilage matrix (Mackie et al. 2008). After 3 to 4 wks of the fracture occurring, the newly formed woven bone is replaced by lamellar bone; it may take years to restore the original anatomic structure (Li & Stocum 2014).

Endochondral ossification also occurs in the growth plates of long bones during childhood development. This ossification causes longitudinal bone growth. (Cohen Jr. 2006, Mackie et al. 2008)

Proteoglycans play an essential role in endochondral ossification, and many of them remain in the mature bone matrix (Boskey & Robey 2013). Proteoglycans consist of a core protein and one or several covalently attached glycosaminoglycan (GAG) chains (Esko, Koji & Lindahl 2009). They bind large amounts of water and cations while excluding anions, and are responsible for matrix maintenance and organisation (Heinegård 2009). They may also play a role in regulation of cartilage calcification (Bertrand et al. 2010), and it is generally known that they block hydroxyapatite formation and growth (Boskey & Robey 2013). GAGs are linear repeating disaccharides that consist of an amino sugar and uronic acid or galactose. Hyaluronic acid (HA) is the only GAG that does not bind covalently with proteoglycans, and instead, interacts non-covalently with them (Esko, Koji & Lindahl 2009). Aggrecan, a large proteoglycan, binds to HA and one other GAG, chondroitin sulphate (CS). Aggrecan is commonly found in cartilage and, in lesser amounts, in bone, where its effect is largely unknown, but it is likely to have an effect on growth plate calcification (Boskey & Robey 2013).

In addition to collagen, glycoproteins and γ-carboxyglutamic acid-containing proteins are involved in bone regeneration. Alkaline phosphatase (ALP) is a specific marker of preosteoblasts and osteoblasts in areas of new bone, while less expression is found in a mature matrix (Martin, Wah Ng & Sims 2013). ALP has been reported to play a crucial role in mineralisation by regulating the levels of mineralisation inhibitor (Yadav et al. 2011, Whyte 2010). Another early marker in bone regeneration is ostepontin (OPN), which is an Arg-Gly-Asp- (RGD) containing protein that largely accumulates in the bone matrix (Gaudin-Audrain et al. 2008). Bone markers expressed in the later stage of osteoblast maturation include bone sialoprotein (BSP) – which is also an RGD-containing protein – osteonectin, and osteocalcin (OC) (Boskey & Robey 2013).

2.2 Stem cells

The main characteristics of stem cells are their ability to differentiate into several cell types and proliferate by keeping their differentiation capacity (Sarkar et al. 2013). Stem cells can be classified into four main types: 1) Embryonic stem cells (ESCs) and 2) adult stem cells are naturally occurring stem cell types, whereas 3) induced pluripotent CSs (IPSCs) are engineered, and 4) cancer cells are pathologically occurring stem cell-like cells (Alvarez et al. 2012).

ESCs can be derived from the inner cell mass of the blastocyst before the implantation stage (Alvarez et al. 2012). They are received for research from fertilisation treatments of couples with their informed consent (Trounson 2007). ESCs are pluripotent, meaning that they can differentiate into any cells types of an embryo but they lack the capacity to generate complete living organisms (Wobus, Boheler 2005). The major drawback in using ESCs in tissue engineering is their potential tumorigenicity, especially the tendency to form teratomas and teratocarcinomas, and the fact that only an allogeneic cell source can be used (Ben-David, Kopper & Benvenisty 2012).

IPSCs were first reported in 2006 when Takahashi and Yamanaka showed that the enforced expression of a limited number of genes critical to the maintenance of pluripotency enables the reprogramming of somatic cells into pluripotent stem cells. Since then, research groups all over the world have been producing IPSCs by delivering several different gene cocktails into the cell nucleus using various different delivery systems (Rezanejad & Matin 2012). Even though IPSCs have shown several advantages over ESCs in tissue engineering, since they possess fewer ethical and immunogenic issues, there are still major challenges regarding their use in clinical treatments. These challenges include risk of tumorigenesis, incomplete reprogramming, retroviral gene-transfer-induced mutagenesis, redifferentiation, and an insufficient number of cells for patient treatment (Csete 2010).

Adult stem cells are present in the vast majority of adult tissues and are responsible for maintenance and repair of the host tissue (Hodgkinson, Yuan & Bayat 2009). Even though some adult stem cells are restricted to the lineages they are found within, not all are tissue-specific, so some are therefore capable of differentiating across mesodermal, endodermal and ectodermal lineages (Hodgkinson, Yuan & Bayat 2009). For instance, haematopoietic stem cells have been reported to yield cells in the epithelium of lung, liver, gastrointestinal track, and skin in addition to their capacity to differentiate into all blood cell lineages (Daley 2013).

The MSCs that are found in several tissues also demonstrate the plasticity of adult stem cells; they are most abundant and accessible in adipose tissue and bone marrow (Gazit et al. 2013). They are multipotent, giving rise to osteogenic, chondrogenic, adipogenic, myogenic and other mesenchymal cell lineages (Wen et al. 2013). Adult stem cells do not have a unique marker for multipotency because the expression of the markers may change during their culture *in vitro*, even though they retain their multipotentiality (Jones & McGonagle 2008). Therefore, multipotency is commonly examined by studying the expression of several surface antigens and their differentiation ability (Gazit et al. 2013). The Society for Cellular Therapy has proposed minimal criteria for defining human MSCs: (1) they must be plastic-adherent in standard culture conditions and develop colony-forming unit fibroblasts, (2) they

must express CD105, CD73, and CD90 and lack expression of CD45, CD34, CD14 or CD11b, CD79alpha or CD19, and HLA-DR surface molecules, and (3) they must differentiate into osteoblasts, adipocytes and chondroblasts *in vitro* (Dominici et al. 2006). Interestingly, several studies have shown that MSCs can escape immune recognition and inhibit immune responses, which makes them attractive cells for clinical use as an allogeneic cell source (Gazit et al. 2013). Immunosuppressive properties of bone marrow MSCs (BMSCs) have been reported *in vitro* and *in vivo*, but those in ASCs have been less studied (Lindroos, Suuronen & Miettinen 2011, Leto Barone et al. 2013). So far, they have been shown to be immunoprivileged for their lack of the HLA-DR expression that belongs to major histocompatibility complex class II (Lindroos, Suuronen & Miettinen 2011, Gonzalez-Rey et al. 2009, Gonzalez-Rey et al. 2010). Immunosuppression of MSCs is widely studied in organ transplantation, where MSCs are administered by intravenous injection to transplant recipients (Alagesan, Griffin 2014). In addition, several clinical trials have been conducted to examine immunomodulatory properties for other immunologic disorders, such as Crohn's disease (Lindroos, Suuronen & Miettinen 2011).

2.3 Adipose stem cells

ASCs are an MSC source abundantly found in adipose tissue. They are easy to isolate and, in comparison to BMSCs, the MSC yield is substantially higher (Lindroos, Suuronen & Miettinen 2011). The number of ASCs in 300 ml of lipoaspirate is normally around 10 million, with greater than 95% purity (Boquest et al. 2006). ASCs have similar characteristics to BMSCs, but some slightly different differentiation propensities occur (Vishnubalaji et al. 2012).

ASCs are commonly isolated from adipose tissue by collagen digestion followed by centrifugal separation. This separates floating adipocytes from the pelleted stromal vascular fraction, which contains fibroblasts, circulating blood cells, pericytes, and endothelial cells in addition to adipocyte progenitors and ASCs. ASCs can be separated from the stromal vascular fraction by their plastic-adherent property. (Gimble, Katz & Bunnell 2007, Zuk et al. 2001)

ASCs have been reported to differentiate towards various cell types, with the emphases being on adipose tissue and skeletal tissues. Differentiation towards adipocytes, osteoblasts, chondroblasts, and myocytes have been long confirmed, but differentiation towards neurogenic lineages (Cardozo, Gómez & Argibay 2012), cardiomyocytes (Lee et al. 2009), tenocytes (Cheng et al. 2014, Yang et al. 2013), endothelial cells (Zhang et al. 2011), and nucleus pulposus (Zhang et al. 2014) has also been reported.

The number of clinical trials with ASCs has increased rapidly over recent years. They have been (or are being) studied for several different purposes, such as osteoarthisis, osteoporotic fractures, graft versus host disease, treatment of tendon injuries, type 1 diabetes, Crohn's disease, and incontinence (18 Mar 2014: clinicaltrials.gov). With regard to bone regeneration, clinical case studies have been conducted for treating severe bone defects, especially in cranio-maxillofacial treatments (Farre-Guasch et al. 2013, Sandor et al. 2014, Mesimäki et al. 2009, Thesleff et al. 2011). A review of thirteen clinical case studies exploiting resorbable scaffold materials seeded with ASCs reported successful integration of the construct to the surrounding skeleton in ten cases (Sandor et al. 2014). However, the actual role of ASCs in regeneration is yet to be determined.

2.3.1 Osteogenic differentiation of adipose stem cells

Two families of growth factors have been shown to stimulate osteogenic differentiation of ASCs and other MSCs in native tissues: a portmanteau of the Wingless and integration1 (Wnt) family, and bone morphogenic proteins (BMPs) (Fakhry et al. 2013). Wnt family members play an essential role during tissue development and homeostasis (Pinzone et al. 2009). Wnt3 and Wnt10b activate the canonical signalling pathway that is essential for bone development (Fakhry et al. 2013, Day et al. 2005). Non-canonical Wnt members may also be involved in ossification (Guo, Jin & Cooper 2008). BMPs belong to the transforming growth factor-β (TGF-β) superfamily and trigger cellular responses mainly through a portmanteau of the Sma in Drosophila and Mad in C. elegans (Smad) pathway (Massague 1998), but they can also activate the mitogen-activated protein kinase pathway (Guicheux et al. 2003). BMPs are important in skeleton formation and have an effect on runt-related 2 (runx2) and osterix expression, which are transcription factors involved in the osteogenic differentiation of MSCs (Li & Cao 2006, Zaidi 2007). Some of the most common osteogenic markers for ASC characterisation along maturation stages are presented in Figure 2.

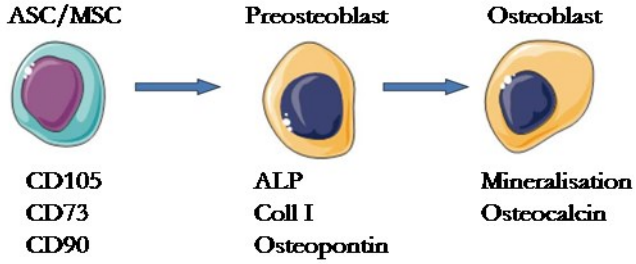

Figure 2. The expression of osteogenic markers during the osteogenic differentiation stages of ASCs. Modified from Fakhry et al. (2013). ASC: Adipose stem cell; MSC: mesenchymal stem cell; CD: cluster of differentiation; ALP: alkaline phosphatase; Coll I: collagen type I.

2.3.2 Chemical factors

Chemical factors that have been used to induce osteogenic differentiation of ASCs *in vitro* include glucocorticoids, ascorbic acid and growth factors, especially from BMPs. The most standard contents in osteogenic medium (OM) are ascorbic acid, dexamethasone, β-glycerophosphate and/or 1,25 vitamin D3 (Lindroos, Suuronen & Miettinen 2011, Kyllonen et al. 2013a). Ascorbic acid is used in OM mainly because of its inducing effect on proliferation and coll I production (Choi et al. 2008, Potdar & D'Souza 2010). ASCs have also been reported to maintain their phenotype and differentiation potential when subjected to 250 μM of ascorbic acid in culture medium (Potdar & D'Souza 2010). Dexamethasone treatment *in vitro* has been reported by Song, Caplan & Dennis (2009) to induce osteogenic differentiation of MSC *in vivo*. The effect in osteogenic markers *in vitro* was seen after 3 and 4 wks of induction rather than at earlier time points. It has also been reported to facilitate the culture expansion of MSCs (Park et al. 2011) and maintain stemness during expansion (Xiao et al. 2010). In addition, 100 nM of dexamethasone has been shown to reduce inter- and intraindividual variations of BMSCs in osteoblastic differentiation (Alm et al. 2012). However, dexamethasone in high concentrations has been shown to inhibit osteogenic differentiation (Wang et al. 2012). β-glycerophosphate alone has been shown to promote calcium phosphate deposition and it is closely linked to high ALP activity of bone cell cultures (Coelho & Fernandes 2000).

The choice of serum also plays an important role in differentiation because serum protein contents vary widely (Kyllonen et al. 2013a, Kocaoemer et al. 2007). For instance, foetal bovine serum (FBS) has been reported to induce weaker osteogenic

differentiation in comparison to human serum (Kyllonen et al. 2013a). Lots can also vary noticeably within one serum type, which makes the use of serum challenging for cell culturing (Wappler et al. 2013). To overcome the variability and risks of disease transmission, xeno-free and serum-free medium replacements have been studied (Kyllonen et al. 2013a, Kocaoemer et al. 2007, Lindroos et al. 2009, Rajala et al. 2010, Patrikoski et al. 2013, Khanna-Jain et al. 2012, Sensebe 2008, Spees et al. 2004).

BMPs, namely BMP-2, -4, -6 and -7, are the most commonly used growth factors *in vitro* for inducing osteogenic differentiation of ASCs (Kyllonen et al. 2013b, Kang et al. 2004, Luu et al. 2007). However, contrasting effects have been recently reported for their efficiency *in vitro* (Kyllonen et al. 2013b). At present, only BMP-2 and BMP-7 have been approved by the US Food and Drug Administration (FDA) for clinical use, in spinal fusion applications and tibial fractures respectively (Elbackly, Mastrogiacomo & Cancedda 2014). Other commonly used growth factors in bone tissue engineering include TGF-β, fibroblast growth factor-2 (FGF-2), platelet-derived growth factor (PDGF), vascular endothelial growth factor (VEGF), and insulin-like growth factor (Elbackly, Mastrogiacomo & Cancedda 2014, Bai et al. 2013). The use of growth factors is not without disadvantages, as they may pose a risk of cancer (Leroith, Scheinman & Bitton-Worms 2011, Tu et al. 2014) and other adverse effects (Carragee, Hurwitz & Weiner 2011). They are also ineffective as well as costly (Tu et al. 2014, Garrison et al. 2007).

2.4 Electrical stimulation in tissue engineering applications

2.4.1 Physical stimulation in bone tissue

In purely mechanical stimulation, bone responds to changes in mechanical loads by increasing or decreasing its strength via a tissue-level negative feedback system called the mechanostat (Frost 2004). This can be exploited and mimicked *in vitro* to reinforce or replace chemical induction of MSCs. Mechanical stimulation is extensively studied in bone tissue engineering with MSCs and several different stimulation strategies have been tested, such as vibration loading (Tirkkonen et al. 2011), stretch loading (Du et al. 2012), fluid flow (Knippenberg et al. 2005), and ultrasound (Uddin & Qin 2013).

Bone tissue is stimulated not only by mechanical stresses during bodily movements, but also by electrical currents and fields induced by mechanical loading. These currents and fields cause a flow of electrolytes and the generation of electric charges due to the piezoelectric properties of bone tissue (Ciombor & Aaron 1993).

These inherent electrical currents and fields play an essential role in bone growth and remodelling. Fukada and Yasuda (1964) were the first to report bone formation under tension dominated by a positive charge, and they observed the reverse in the case of a negative charge and compression.

2.4.2 Electrical stimulation: From physiological phenomena to medical applications

ES has gained interest in tissue engineering in recent years, especially in nerve, cardiac, and skeletal tissue applications. The fact that endogenous electric fields play an important role not only as action potentials in nerves and muscles but also in controlling cellular functions in non-excitable cells makes ES an attractive means in controlling stem cell adhesion, proliferation, migration and differentiation without extensive use of chemical factors (Titushkin & Cho 2009, Balint, Cassidy & Cartmell 2013, Titushkin et al. 2011). Electric fields have long been known to take part in embryonic development and regeneration, regulating the cell behaviour and spatial patterns, such as left–right organ asymmetry (Sundelacruz, Levin & Kaplan 2008, Sundelacruz, Levin & Kaplan 2008, McCaig et al. 2005, Erickson & Nuccitelli 1984, Serena et al. 2009, Reid, Song & Zhao 2009). For instance, inherent electric fields play an essential role in wound healing, giving "a kick start" to the cellular processes immediately after the epithelium is breached; chemical gradients, on the other hand, can take from minutes to hours to establish (McCaig, Song & Rajnicek 2009, Goldman & Pollack 1996). Inherent electric fields are monitored in evaluating the state of wound healing by commercially available devices, such as the Dermacorder® (Nuccitelli et al. 2011). Furthermore, ES applications are extensively studied for excitable cells, such as neuronal and cardiac cells, to direct growth and differentiation (Thompson et al. 2010, Ghasemi-Mobarakeh et al. 2011, Kim et al. 2011a, Wang et al. 2013a, Llucià-Valldeperas et al. 2013, Tandon et al. 2011). In addition, Ciombor and Aaron's (1993) remarks regarding the piezoelectric properties of bone and reports on the favourable effects of ES on bone regeneration have led to the development of ES devices for treating severe bone defects (Griffin & Bayat 2011, Kooistra, Jain & Hanson 2009).

2.4.3 Delivery of external electrical stimulation

ES delivery systems can be divided into direct and indirect stimulation. In direct stimulation, electrodes are in contact with the cell culture or implanted into the patient

(Balint, Cassidy & Cartmell 2013, Merrill, Bikson & Jefferys 2005). The method is simple and therefore commonly used in *in vitro* experimental set-ups. However, there are several disadvantages, such as the possible corrosion of the electrodes, changes in pH, reduced levels of molecular oxygen, and the generation of harmful faradic products, such as reactive oxygen species, in the culture medium. (Balint, Cassidy & Cartmell 2013, Merrill, Bikson & Jefferys 2005, Ercan & Webster 2010, Hess et al. 2012a) Stimulation may also be biased due to the formation of a capacitive layer on the electrodes (Balint, Cassidy & Cartmell 2013, Merrill, Bikson & Jefferys 2005). The risks of corrosion, faradic products and pH change can be reduced by using biphasic pulses (Ercan & Webster 2010, Kim et al. 2009).

Indirect stimulation, which can be classified into capacitive stimulation, inductive stimulation, or both, is non-invasive and used in many therapeutic devices and *in vitro* experimental set-ups (Balint, Cassidy & Cartmell 2013). In capacitive stimulation systems, parallel metal layers, acting as electrodes, are placed outside the culture medium with a small gap between them, and then a homogenous electric field is created between the electrodes (Balint, Cassidy & Cartmell 2013). The field created has uniform electromagnetic properties across the stimulation area; however, the method requires high voltages (e.g. 100 V) and therefore poses some limitations (Hess et al. 2012a). Inductive stimulation utilises coils placed around the cell culture area in order to create an electromagnetic field (EMF) and to subsequently induce small magnitude electrical currents and potentials near the targeted cells (Balint, Cassidy & Cartmell 2013, Merrill, Bikson & Jefferys 2005). When two coils are situated so that the distance between them is equal to their radius, they create nearly a homogenous magnetic field in between them (Bodamyali et al. 1998). Combined stimulation includes a static and an AC magnetic field. The disadvantages of using an inductive stimulation system include the heat in the coils created by the generation of an EMF and that the system requires very accurate placement of the coils due to inseparable interplay of the EMF and electric fields; the wrong placement can lead to different biological effects. (Hess et al. 2012a) Using the above-mentioned delivery systems, ES can be applied in various ways, from the simplest direct current (DC), generated by batteries, to alternating currents (ACs) with different frequencies and waveforms (square, saw tooth, sinusoidal) using different voltages and current densities (Balint, Cassidy & Cartmell 2013). Stimulation systems are presented in Figure 3.

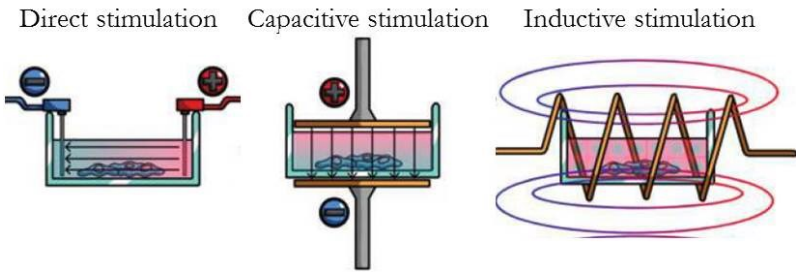

Figure 3. Electrical stimulation systems for *in vitro* applications. Modified from Balint, Cassidy & Cartmell (2013).

2.4.4 Coupling mechanisms of electrical signals with the cell membrane

In vivo electricity mainly arises from cells constantly pumping ions across their cell membrane, resulting in membrane potential (Balint, Cassidy & Cartmell 2013). Sundelacruz, Levin & Kaplan (2008) examined the changes in membrane potential of hASCs under adipogenic and osteogenic differentiation. The resting membrane potential was reported to be -37 mV under osteogenic differentiation and -47 mV under adipogenic differentiation. The cells were shown to hyperpolarise during both differentiation pathways, with the adipogenic differentiation being more substantial. Interestingly, the membrane potential could be manipulated to facilitate the differentiation pattern of ASCs. When hyperpolarisation was induced by pharmacological means, osteogenic markers were upregulated. Other studies have also reported that more immature proliferative cells exhibit a strongly depolarised membrane potential and terminally differentiated cells exhibit a strongly hyperpolarised membrane potential (Sundelacruz, Levin & Kaplan 2013, Levin 2007). On the other hand, induced depolarisation of MSC-derived osteoblasts and adipocytes has reported to lead to suppression of the osteoblast or adipocyte phenotype even under differentiation-inducing soluble factors (Sundelacruz, Levin & Kaplan 2013). The underlying mechanisms of polarisation affecting the cell behaviour have been tracked to interactions with actin and tubulin cytoskeleton organisations (Nin, Hernández & Chifflet 2009, Chifflet, Hernandez & Grasso 2005).

The cell membrane potential, which is within a range of 10^6–10^7 V/m, halts weaker external DC electric fields from entering the cell. Therefore, the effects of external electric fields of the physiological range are at least partly mediated by the internal signalling pathways via the same cell surface sensors that are involved in mechanotransduction and chemotaxis (Balint, Cassidy & Cartmell 2013, Erickson & Nuccitelli 1984, Hammerick et al. 2010, Zhao 2009, Lin et al. 2008, Funk, Monsees &

Özkucur 2009). The intracellular calcium level is a key component in responding to electrical signals (Balint, Cassidy & Cartmell 2013, Titushkin et al. 2011). Cytosolic free calcium in mouse ASCs has been reported to increase 30 s after electric field initiation (Hammerick et al. 2010). Increase in intracellular calcium levels is at least partially due to the calcium/calmodulin pathway, which is affected differently depending on the method of stimulation (Balint, Cassidy & Cartmell 2013). As direct and capacitive coupled stimuli cannot penetrate the cell membrane, they are suggested to couple with cell membrane receptors that activate phospholipase C (PLC) (Titushkin & Cho 2009), and/or voltage-gated calcium channels, raising the intracellular Ca^{2+} and prostaglandin E2 levels (Titushkin & Cho 2009, Titushkin et al. 2011). Instead, EMF can induce potentials and currents in the cytoplasm, releasing intracellular calcium from reservoirs, such as the endoplasmic reticulum (Balint, Cassidy & Cartmell 2013, Li et al. 2006).

Integrins and other extracellular glycoproteins are also suggested to respond to ES at low frequencies (0.1–10 Hz) of sinusoidal electric fields (~1 V/cm) and may therefore share a common transduction mechanism with mechanical forces exerted on glycoproteins (Hart 2006, Hart 2008). Integrins transmit the mechanical torque, triggered either by ES or fluid shear, directly to the actin cytoskeleton (Titushkin et al. 2011). In addition, redistribution and clustering of integrins and activation of some focal adhesion proteins during ES is mediated by PLC or focal adhesion-mediated pathways to alter the Ca^{2+} dynamics, which in turn controls integrin-mediated cell adhesion and migration (Titushkin et al. 2011, Sjaastad & Nelson 1997). Therefore, it is highly likely that ES-regulated Ca^{2+} dynamics also control focal adhesions (Titushkin et al. 2011). Cytoskeletal elasticity of the cell membrane in MSCs is reported to decrease during ES, which is likely to be through actin cytoskeleton reorganisation (Titushkin et al. 2011, Hammerick et al. 2010, Titushkin & Cho 2009). MSC elasticity has been reported to decrease to values similar to those found in mature osteoblasts when MSCs are put under chemical osteoinduction (Titushkin & Cho 2007, Pablo Rodríguez et al. 2004). Changes in MSC mechanics can in turn activate other mechanosensors other than extracellular glycoproteins, such as stretch-activated cation channels in the cell membrane (Cho et al. 1999). Titushkin and Cho (2009) found that ES causes ATP depletion in MSCs and osteoblasts, which induces the inhibition of linker proteins between the cell membrane and the cytoskeleton; in addition, it modulates Ca^{2+} dynamics. Inhibition of linker proteins triggered membrane disruption from the cytoskeleton and was more pronounced in mature osteoblasts, since they possess stronger membrane-cytoskeleteon interaction. The consequences of the separation of cellular functions are still unclear. The diverse mechanism through which ES affects MSC functions is summarised in **Figure 4**.

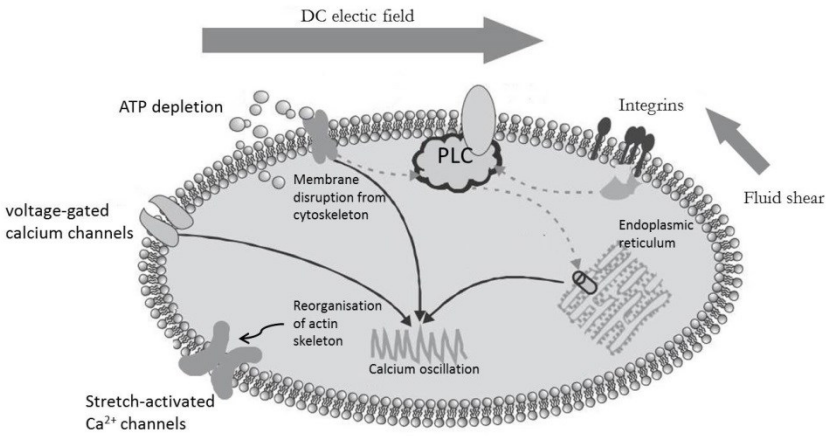

Figure 4. The coupling mechanisms of ES in MSCs. Modified from Titushkin et al. (2011). ATP: adenosine triphosphate; PLC: phospholipase C.

2.4.4.1 Potential mechanisms in osteogenic differentiation of mesenchymal stem cells under electrical stimulation

Undoubtedly, the above-mentioned ES coupling mechanisms play a major part in the initiation of the osteogenic differentiation cascade of MSCs. However, the specific signals that determine the osteogenic differentiation pathway in MSCs is unclear. As ES can couple in various different ways with MSC-signalling molecules depending on the nature of the ES (e.g. the strength of the electric field, frequency), the emphasis on the signalling pathways to result in osteogenic differentiation can be very different as well. BEC stimulation was reported to increase extracellular-signal-regulated kinase (Erk) p38 activation of the mitogen-activated protein kinase (MAPK) pathway (Kim et al. 2009), which is known to be involved in VEGF production and cell proliferation (Matsuda et al. 1998). In addition, messenger ribonucleic acid (mRNA) expression of the hypoxia-inducible factor, which is known to upstream VEGF transcription, was noticed to increase 30 min after ES. BEC was also reported to mediate signals through a voltage-gated calcium channel and another L-type calcium channel. Calcium signalling was found to have a greater effect on proliferation than the MAPK pathway under BEC. (Kim et al. 2009) Sun et al. (2007) found that intracellular calcium oscillation spikes of hBMSCs (in MM) were changed under ES to resemble the oscillation spikes measured from fully differentiated osteoblasts. The same effect on oscillation was achieved with chemical osteoinduction.

2.4.5 External electrical stimulation in osteogenic differentiation of mesenchymal stem cells

Even though ES has long been used for treatments in bone defects, the use of ES in bone tissue engineering has only been studied more intensively over the last five years (Kooistra, Jain & Hanson 2009). To date, various ES patterns have been applied to induce osteogenic differentiation of MSCs (Kim et al. 2009, Hammerick et al. 2010, Titushkin & Cho 2009, Sun et al. 2007, McCullen et al. 2010, Creecy et al. 2013, Hess et al. 2012b, Balint et al. 2013, Hronik-Tupaj et al. 2011) or maturation of osteoblasts (Zhuang et al. 1997, Zhang et al. 2013, Supronowicz et al. 2002, Meng, Zhang & Rouabhia 2011, Meng, Rouabhia & Zhang 2013) in 2 dimensional (2D) or 3-dimensional (3D) cell cultures. The applied ES patterns for MSCs *in vitro* are reviewed in **Table 2**. The studies involving DC electric fields have mainly concentrated on the effect on orientation and migration (Tandon et al. 2009b, Sun, Titushkin & Cho 2006, Zhao et al. 2011). MSCs have been reported to align perpendicularly to the direction of the electric field (Hammerick et al. 2010, Tandon et al. 2009b). In addition, the coupling of electric fields in the cell membrane (Sun, Titushkin & Cho 2006) and the cytoskeleton tension of MSCs (Titushkin & Cho 2009) have been studied with a DC electric field.

AC ES studies in bone tissue engineering have focused on examining proliferation and differentiation of MSCs (Kim et al. 2009, Hammerick et al. 2010, Sun et al. 2007, McCullen et al. 2010, Creecy et al. 2013, Hess et al. 2012b, Balint et al. 2013, Hronik-Tupaj et al. 2011, Hwang et al. 2012). The ES conditions vary widely between the studies, which makes the comparison of the ES parameters challenging. However, AC electric fields ranging from 20 mV/cm up to 10 V/cm have shown to be suitable ranges for MSC stimulation at certain frequencies (McCullen et al. 2010, Hronik-Tupaj et al. 2011). In addition, current densities of 1.5−40 μA/cm² have been applied to MSCs to study osteogenic differentiation. OM conditions used in combination with ES have given a stronger MSC response to ES in terms of osteogenic differentiation when compared to similar ES conditions in a maintenance medium (MM). This suggests synergistic effects between chemical osteogenic induction and ES (Kim et al. 2009, Hess et al. 2012b). Synergistic phenomenon has also been observed when mechanically stimulating hASCs in OM (Tirkkonen et al. 2011).

Several ES parameters have been reported to enhance ALP activity (Kim et al. 2009, Hess et al. 2012b), ECM mineralisation in OM (Kim et al. 2009, Sun et al. 2007, McCullen et al. 2010) and upregulate OC (Creecy et al. 2013, Hess et al. 2012b, McCullen et al. 2010), OPN (Hammerick et al. 2010, Hess et al. 2012b), Coll I, runx2 (Hammerick et al. 2010), VEGF (Kim et al. 2009, Tandon et al. 2009b, Hwang et al. 2012), insulin-like growth factor 1 (IGF-1), BMP-2, bFGF (FGF-2), TGF-β1,

interleukin-8 (IL8) and (C-X-C motif) ligand 2 (CXCL-2) (Hwang et al. 2012). However, some ES parameters used have not upregulated runx2 (Hess et al. 2012a, Creecy et al. 2013), osterix (Creecy et al. 2013), OPN (Kim et al. 2009, Creecy et al. 2013), OC, BSP or Coll I (Kim et al. 2009), even though other osteogenic markers were upregulated in the studies. Proliferation has been reported with frequencies of 1 Hz with sinusoidal waves (Sun et al. 2007, McCullen et al. 2010) and 100 Hz with pulsed BEC (Kim et al. 2009, Hwang et al. 2012), whereas set-ups using 10 Hz (Hess et al. 2012b) or 50 Hz (Hammerick et al. 2010) have not shown enhancement in proliferation. The difference between a 2D and 3D environment under ES has been studied by Hwang et al. (2012); they reported that the 3D environment gave a stronger expression of chemokine receptors (C-X-C motif) receptor 4 (CXCR4) and IL8, which are related to the homing capabilities of MSCs in 3D.

In addition to traditional markers, the effect of ES on heat shock proteins has been studied, as these proteins are upregulated during stress, including oxidative stress, but are also reported to affect osteogenic differentiation of MSCs (Norgaard, Kassem & Rattan 2006). Upregulation of heat shock protein 27 has been observed in a high frequency (60 kHz) AC electric field (Hronik-Tupaj et al. 2011). Oxidative stress may also compromise bone regeneration by formation of reactive oxygen species (ROS), such as hydrogen peroxide and xanthine/xanthine oxidase (Mody et al. 2001). Only one of the above-mentioned ES studies with MSCs has examined the production of ROS during ES; it did not detect any accumulation of ROS when stimulating mouse ASCs with pulsed ES (Hammerick et al. 2010). Other ES studies with embryonic stem cells (Serena et al. 2009) and neural cells (Riquelme et al. 2011) have reported generation of ROS during ES at the level that promoted favourable cell behaviour. Serena et al. (2009) used electric field pulses of 1 V/mm for 1 or 90 s, and Riquelme et al. (2011) used an electric field of 20–25 V/cm with 1 ms pulses at a frequency of 50 or 10 Hz.

The choice of electrical parameters has a significant impact on cellular response. However, to date, comparison of different electrical parameters has been addressed in only a few studies (Hu et al. 2014, McCullen et al. 2010, Creecy et al. 2013, Hwang et al. 2012). McCullen et al. (2010) tested the effect of several different electrical potentials under 1 Hz of sinusoidal ES on hASCs. Of the potentials 1, 3 and 5 V/cm, 5 V/cm was found to induce the highest proliferation in hASCs, whereas 1 V/cm was the best potential in terms of mineralisation. Hu et al. (2014) tested the effect of different DC voltages on rat BMSCs seeded on PPy films and found decreased viability when using the highest voltage, 3.5 V. In addition, the longest stimulation time, 12 h, already showed decreased viability with lower voltages. From the tested ES durations, 2, 4 and 12 h, calcium deposition was the highest when 4 h of ES was applied. Kim et al. (2009) found pulsed BEC to induce a significantly higher

proliferation in the 2D culture system. Proliferation was the highest with a longer pulse and a lower current density when compared to a shorter pulse and a higher current density. However, when Hwang et al. (2012) applied the same parameters in 3D in the other study, no significant enhancement in proliferation was observed. Instead, the 3D environment required a stronger current – a 40 $\mu A/cm^2$ current density – to promote proliferation. Both studies with pulsed BEC promoted significantly higher VEGF and BMP-2 synthesis, and gene expression. Hwang et al. also compared 2D and 3D environments in VEGF expression, finding a significantly stronger effect of ES in 3D in comparison to 2D.

Table 2. A review of the applied ES patterns for MSCs in osteogenic differentiation *in vitro*.

Culture system	Cell source	ES parameters	Culture period	Cell substrate	Main results with effective ES parameters				
					Proliferation	ALP activity	Gene expression	Mineralisation	Authors
2D, OM	hASCs	1, 3 or 5 V/cm, sinusoidal 1 Hz 4h/d	14 d	Interdigitated electrodes on glass (Cr, Au, 25 "fingers")	++ (5 V/cm, 7d)	N/A	N/A	+ (1 V/cm, 7 d), ++ (14 d)	McCullen et al. 2010
3D, MM	hBMSCs	Sinusoidal 10 Hz AC either 10 or 40 μA, 6h/d	14 d	Coll I gel and BMP-2- and BMP-6-incorporated	N/A	N/A	OC: ++ (10 and 40 μA, 14 d) OPN: 0 Runx2: 0 Osterix: 0	N/A	Creecy et al. 2013
3D, MM and OM	hBMSCs	Rectangular pulses: 7 ms, 3.6 mV/cm, 10 Hz ES for 4 h followed by a 4 h break	28 d	PCL scaffolds coated with Coll I and Coll I/high-sulphated HA derivative	0 (neither MM or OM)	++ (7, 21, 28 d, OM)	OPN: ++(14 and 28 d) OC:++ (28 d) Runx2: 0 ALP: 0	N/A	Hess et al. 2012
2D, MM and OM	hBMSCs	Pulsed BEC, 100 Hz, 1) 250 μs pulse with 1.5 μA/cm2 or 2) 25 μs with 15 μA/cm2 continuous ES during 7 d	21 d	Au-deposited silicon plate	+++ (group1; 3 and 5 d), ++ (group 2; 5 d), in MM only	++ (group 2 tested only, 10 d)	Tested in OM only. VEGF: + (1, 2, 3, 7 d) IGF: ++ (2, 3 d) TGF-β1: ++ (3, 7 d) BMP-2: ++ (3 d)	++ (21 d)	Kim et al. 2009
3D vs. Monolayer, general, MM	hBMSCs	Biphasic, 100 Hz, 1) 10, 20, or 40 μA/cm², pulse 125 μs, 2) 1.5 μA/cm², pulse 250 μs	4 d	Collagen sponge	++ (3D, 40 μA/cm², 2 d)	N/A	Monolayer: IGF, VEGF: ++ (4 d) BMP-2: + (4 d) IL-8: + CXCL2: 0 Fibronectin: 0 stromal cell-derived factor-1: - 3D: IGF ++ (2 d) BMP-2, FBF-2, TGF-β, IL-8, CXCL2, VEGF: +++ (4 d)	N/A	Hwang et al. 2012
2D, calcium oscillation, MM and OM	hBMSCs	0.1 and 1 v/cm DC or 1 Hz sinusoidal AC, 30 min/d	10 d	Not specified	+ (OM, 0.1 V/cm tested only, day 10	++ (OM, 0.1 V/cm tested only, 10 d)	N/A	+ (10 d, OM)	Sun *et al.* 2007

Culture system	Cell source	ES parameters	Culture period	Cell substrate	Main results with effective ES parameters				Authors
					Proliferation	ALP activity	Gene expression	Mineralisation	
2D, OM	hMSCs	20 mV/cm, 60 kHz, 40 min/d	28 d	Glass dish	N/A	N/A	ALP: ++ (20 d) Coll I: ++ (5, 15, 20 d) Heat shock protein 27: ++ (15 d), – (5 d) Heat chock protein 70: – (10, 15 d), ++(20 d)	0 (28 d)	Hronik-Tupaj et al. 2011
2D, MM and OM	mouse ASCs	Pulsed ES, 6 V/cm, 50 Hz, 6h/d	21 d	Tissue culture dish	0 (MM tested only)	++ (7 d)	ALP: ++ (7 d) OPN: ++ (7 d) Coll I: ++ (7 d) Runx2: ++ (7 d) OC: 0 (21 d)	0 (21 d)	Hammerick et al. 2010
2D, OM	rat BMSCs	0.035, 0.35 or 3.5 V/cm	12 h	PPy films with different pyrrole concentrations	N/CA	N/A	N/A	++ (0.035, 0.35 V/cm for 4 h); 0 (3.5 V/cm)	Hu et al. 2014
2D, MM	hASCs	6 V/cm DC	4 h	Glass slide	N/A	N/A	Connexin-43: ++(2 h) VEGF: ++ (2, 4 h) FGF-2: ++ (2 h) OPN: 0	N/A	Tandon et al. 2009
2D, MM	hBMSCs	10–600 mV/mm	10 h	Chamber slides	N/A	N/A	N/A	0 (qualitative, wk 4)	Zhao et al. 2011

++/+++: Significant increase/upregulation; +: upregulated; N/A: not applicable; 0: no effect; –: decrease/downregulation, but not significant. AC: alternating current; ALP: alkaline phosphatase; BMP: bone morphogenic protein; Coll I: collagen type I; CXCL2: Chemokine (C-X-C motif) ligand 2; DC: direct current; FGF: fibroblast growth factor; HA: hyaluronic acid; hASC: human adipose stem cell; hBMSC: human bone marrow stromal cell; IGF-1: insulin-like growth factor 1; IL-8: interleukin 8; MM: maintenance medium; OC: osteocalcin; OM: osteogenic medium; OPN: osteopontin; PCL: polycaprolactone; PPy: polypyrrole; runx2: runt-related 2; TGF- β: transforming growth factor- β; VEGF: vascular endothelial growth factor

2.5 Biomaterials in bone applications

Biomaterials are intended to interface with biological systems to evaluate, treat, augment or replace any tissue, organ or function in the body (Nair & Laurencin 2007). Nair and Laurencin (2007) list some of the most essential requirements of the biomaterial:

- Biomaterial should not evoke an inflammatory or toxic response in body;
- The degradation of the material should match with the regeneration process and healing of the body;
- The mechanical properties of the material should closely match the mechanical properties of the target tissue and the material should sustain suitable mechanical properties alongside degradation;
- The degradation product should not be toxic and the body should be able to process and clear it;
- Biomaterial should have an acceptable shelf life.

Biomaterials can be classified into polymeric (synthetic and natural), metallic, ceramic and composite materials. In bone applications, materials from every biomaterial group have been exploited. Non-degradable materials – such as titanium alloys, stainless steel, and certain ceramics – are excluded from this review.

Biodegradable polymers can degrade through a hydrolytic or an enzymatic route. Most of the natural polymers go through enzymatic degradation, whereas synthetic polymers degrade mainly hydrolytically. The advantages of using natural polymers are in their inherent bioactivity, the ability to present receptor-binding ligands to cells, and in their susceptibility to cell-triggered proteolytic degradation. However they may trigger a strong immunogenic response because they are complex to purify, and they may pose a risk of disease transmission. Therefore, many synthetic polymers are still commonly used in clinical applications due to their more predictable properties and batch-to-batch uniformity. In addition, their properties can easily be tailored for specific applications. (Nair & Laurencin 2007)

Hydrolytically degrading polymers are commonly used as implants because the enzymatically degrading polymers have varying degradation properties depending on the target tissue's and patients' enzymatic activity (Katti et al. 2002). Several synthetic polymers are approved for use in bone graft substitute by the FDA, including poly(α-hydroxy esters), PLA, polyglycolide (PGA), poly(lactide-co-glycolide) (PLGA) and poly(caprolactone) (Nair & Laurencin 2007).

Ceramics have long been used as materials in bone applications because they can closely mimic the mineral matrix of the bone tissue. They primarily include calcium phosphates, calcium sulphates or bioactive glass. Calcium phosphate bone substitutes are usually made of tricalcium phosphate (TCP) or hydroxyapatite that, among other calcium phosphate-based biomaterials, are considered osteoconductive – meaning that they allow bone growth within the material and provide attractive surfaces for osteoblasts to attach to (Brown, Kumbar & Laurencin 2013). Hydroxyapatite-based bone grafts are slow to degrade in comparison to other calcium phosphates, which limits their use in bone tissue engineering (Brown, Kumbar & Laurencin 2013, Navarro et al. 2008). TCP is less brittle and more osteoinductive than hydroxyapatite. It is mainly used for filling small bone defects (Calori et al. 2011). TCPs can be classified into α-TCP and β-TCP according to their crystal structures, yet they both possess similar chemistry, with a Ca/P ratio of 1:5 (Barrere, van Blitterswijk & de Groot 2006). α-TCP is more soluble than β-TCP and is a major reagent in the composition of bone cements (Barrere, van Blitterswijk & de Groot 2006). From those, β-TCP is more stable up to 1125 °C and is more extensively used for bone regeneration (Barrere, van Blitterswijk & de Groot 2006). Bioactive glasses are amorphous materials usually containing SiO_2 as a network former and Na_2O, CaO and P_2O_5 as modifying oxides (Brown, Kumbar & Laurencin 2013, Rahaman et al. 2011). This composition can be found in Bioglass (45S5) that was developed by Cao and Hench (1996) in the 1970s. Some Bioglass formulations are reported to induce three times faster bone growth in comparison to hydroxyapatite (Fujishiro, Oonishi & Hench 1997). Bioactive glass has the ability to form a hydroxyapatite-like layer on its surface through certain chemical reactions when implanted into the body, which contributes to the formation of a firm bond with hard and soft tissues (Kokubo, Takadama 2006).

Composite materials combine two or more of the elements described above to exploit the beneficial properties of the materials. Commonly used approaches in orthopaedic materials involve combining synthetic polymers to bring flexibility of ductile polymers and ceramics to gain higher compression strength and introduce bioactivity to the implant (Rezwan et al. 2006). From these, poly(lactide-co-glycolide) (PLGA)-TCP composites will be more closely detailed below.

2.5.1 Lactide-based polymers: PLLA, PLGA

Lactide (LA) -based polymers are classified as poly (α-esters), and more specifically, poly(α-hydroxy acids) that mainly degrade by bulk erosion. They are thermoplastic

polymers that degrade through the hydrolytically labile ester linkages in their backbone. (Nair & Laurencin 2007)

Lactide is a chiral molecule with two optically active isoforms: L-lactide and D-lactide. Usually the polymerisation of these monomers leads to semi-crystalline polymers, but the combination of racemic D-L-lactide and mesolactide also results in amorphous polymers (Nair & Laurencin 2007). L-lactide is a naturally occurring isomer and its polymer poly(L-lactide) (PLLA) possesses ~37% crystallinity in its structure, the degree depending on molecular weight and processing parameters (Nair & Laurencin 2007). The glass transition temperature of PLLA is 60–65 °C and the melting temperature is approximately 175 °C (Nair & Laurencin 2007, Middleton & Tipton 2000). PLLA is a slow degrading polymer with good tensile strength, low extension and high modulus (~4.8 GPa) which makes it a suitable polymer for load-bearing applications (Nair & Laurencin 2007). The final hydrolysis product, lactic acid, is a human metabolic by-product that is processed in the citric acid cycle into water and carbon dioxide (Maurus, Kaeding 2004).

PLGA is one of the most investigated LA-based polymers with different lactide chimeras (L- and DL-lactides) and different LA-GA compositions. In the composition range of 25–75%, poly(L-lactide-co-glycolide) (PLLGA) forms amorphous polymers. The bulk erosion of PLGA is faster than PLLA's due to its higher hydrophilicity but the degradation rate depends on the LA/GA ratio, molecular weight, and the shape and structure of the matrix. (Nair & Laurencin 2007)

The major advantage of the PLGA is its easy processability, controllable degradation rates, and that their FDA approval for use in humans (Nair & Laurencin 2007). PLGA provides a good adhesion surface and supports proliferation of cells, and is therefore widely studied for tissue engineering applications (Katti et al. 2004, Borden et al. 2002, Lu & Chen 2004). In addition, guided tissue regeneration and drug delivery devices have been developed.

2.5.2 Lactide-based medical devices

Several orthopaedic products are currently made of PLLA, including suture anchors, soft tissue fixation screws and meniscal stringers (Nair & Laurencin 2007). High molecular weight PLLA has been reported to totally resorb within 2 to 5.6 years *in vivo* (Middleton & Tipton 2000, Bergsma et al. 1995). Due to the bulk erosion, PLLA can lose its mechanical properties already 6 months after hydrolysation, even though significant changes in mass will not occur for a long time (Nair & Laurencin 2007).

PLGA has also been developed and investigated for a wide range of biomedical applications, one of the most famous on the market being multifilament sutures,

namely Vicryl® and PANACRYL® from Ethicon, Inc. Other commonly used applications are different meshes, suture reinforcements, skin replacement materials, and duramater substitutes (Nair & Laurencin 2007). In orthopaedics, PLGA is used in the form of screws, pins and nails (Bioretec Ltd. 2014). The shape-memory effect has been applied for PLLA and PLGA to facilitate, for instance, functions in stents (Xue, Dai & Li 2010) or orthopaedic devices (Bioretec Ltd. 2014). ActivaScrew™, which is intended for bone repair, has a shape memory effect with lengthwise compression and expansion in the diameter, preventing the screw from loosening.

Due to the bulk degradation of PLLA and PLGA, zero-order kinetics is challenging to achieve. Another disadvantage – especially in PLGA – is its acidic degradation product, which can increase the risk of inflammation *in vivo* (Nair & Laurencin 2007, Athanasiou, Niederauer & Agrawal 1996). To overcome the acidic degradation products and lack of bioactivity of PLLA and PLGA, they have been combined with several materials, such as β-TCP (Debusscher et al. 2009), hydroxyapatite (Wang et al. 2013b), and titania nanoparticles (Liu, Slamovich & Webster 2006).

2.5.3 PLGA-β-TCP composites for orthopaedics

One of the composites used to improve compatibility with bone tissue is β-TCP, whose incorporation into the structure improves dissolution properties, enhances formation of bone, provides structural strength more closely mimicking that of native bone tissue, and buffers the acidic degradation products of PLGA (Ehrenfried, Patel & Cameron 2008, Kang et al. 2011, Kang et al. 2013). β-TCP is commercially used as a bone filler, root canal filler and artificial tooth root (Kokovic, Todorovic 2011). However, β-TCP faces some disadvantages when used alone in bone applications because its degradation rate does not quite match with bone absorption – it is slightly too quick to degrade (Kwon et al. 2002). It is also brittle, making it susceptible to scaffold collapse (Liu, Lun 2012).

PLGA-β-TCP composite screws are commercially used in anterior cruciate ligament (ACL) fixation. MILARGO® interference screws use a homogenous mixture of 30% β-TCP and 70% PLGA by weight. When tested in a canine model, implant sites were filled with bone after 36 months of implantation and no residual screw material was observed (Barber, Dockery & Hrnack 2011). PLGA-β-TCP composites have also been investigated as drug releasing devices for bone regeneration (Luginbuehl et al. 2010). For instance, incorporation of tetracycline has been tested for prevention of bone infections (Luginbuehl et al. 2010), whereas icaritin, a metabolic compound of certain flavonoids reported to stimulate osteogenic differentiation of

MSCs (Sheng et al. 2013), and BMP-2 have been tested for enhancement of bone regeneration (Chen et al. 2013, Yu et al. 2008).

2.6 Electrically conductive polypyrrole in tissue engineering

CPs are gaining interest in the field of tissue engineering as they allow direct delivery of electrical, electrochemical and mechanical stimulus to cells (Balint, Cassidy & Cartmell 2014). Their chemical, electrical and physical properties can be tailored for specific applications by incorporating different biological moieties, such as enzymes and antibodies (Higgins et al. 2012). To date, several different CPs, such as PPy, poly(3,4-ethyl-enedioxythiophene) (PEDOT) and polyaniline (PANI) have been tested for tissue engineering (Balint, Cassidy & Cartmell 2014). Of those, PPy is the most studied CP; it can be easily modified with different bioactive molecules and polymerised at ambient temperatures (Balint, Cassidy & Cartmell 2014). It is used in numerous biomedical applications, such as drug delivery systems (Richardson et al. 2009, Thompson et al. 2011), biosensors (Ates 2013), as a biomaterial in scaffolds (Aznar-Cervantes et al. 2012, Sajesh et al. 2013), nerve guidance channels (Abidian et al. 2012), neural probes (Gomez et al. 2007) blood conduits (Alikacem et al. 1999) and actuators (Liu et al. 2009).

The conductivity of PPy arises from a combination of several factors. PPy consists of single and double bonds that allow electrons to delocalise and move freely between atoms, but it also requires dopants acting as a charge carrier between the polymer chains (Balint, Cassidy & Cartmell 2014). PPy is in its oxidised form when conductive, and it requires presence of negative dopants to stabilise the backbone and neutralise the net charge (Bredas, Street 1985). When electrical potential is applied in PPy, the dopants start to move in or out of the polymer chain, depending on the polarity, simultaneously removing or adding electrons (Ravichandran et al. 2012). This disrupts the stable backbone and allows the charge to be passed along the polymer in the form of polarons or bipolarons that can travel along the polymer chain (Balint, Cassidy & Cartmell 2014). Large dopants give PPy greater electrical stability because they are integrated in the polymer; they do not leach out and get replaced by ions from the electrolyte (Balint, Cassidy & Cartmell 2014, Liu et al. 2009, Wallace & Spinks 2007, Shi et al. 2004). In PPy, the conductivity is present especially because of bipolarons. The conductivity of PPy can be up to 7.5×10^3 S/cm (Dai 2004). However, the conductivity strongly depends on the concentration and the nature of the dopants (Kaynak, Rintoul & George 2000).

2.6.1 Biocompatibility of polypyrrole

PPy has been reported to be compatible with several cell types, such as MSCs (Serra Moreno et al. 2012, Hu et al. 2014), skeletal muscle cells (Gilmore et al. 2009), neurons (Thompson et al. 2011), cardiomyocytes (Kai et al. 2011), endothelial cells (Garner et al. 1999), and osteoblasts (Meng, Zhang & Rouabhia 2011). In addition, PPy is reported to be biocompatible *in vivo* in several tissues, such as in subcutaneous tissue in rats (Jiang et al. 2002), the intraperitoneum in mice (Ramanaviciene et al. 2007), neural tissue in rats (Wang et al. 2004a, Williams, Doherty 1994), brain tissue in rats (George et al. 2005) and the myocardium in rats (Mihardja, Sievers & Lee 2008). In addition, PPy has been reported to cause no haemolysis or changes in blood coagulation (Zhang et al. 2001) and has implanting PPy caused no changes in spleen, kidney and liver indexes in mice (Ramanaviciene et al. 2007). Subacute toxicity, acute toxicity, pyrogens, haemolysis, allergens and micronuclei have also been studied with PPy, showing no abnormalities (Wang et al. 2004a). One major disadvantage is that PPy is not inherently biodegradable. However, the erosion products of PPy have shown to be less cytotoxic than those of silver or TiO_2 particles, which are common wear products of orthopaedic implants (Kim et al. 2011b, Palomäki et al. 2010).

However, some contrasting results exist for PPy *in vivo*. Human MSCs were shown to grow better on silk fibroin mats when compared to those coated with PPy (Aznar-Cervantes et al. 2012). Moreover, the thickness of PPy layer was reported to correlate directly with tissue response, with endothelial cells adhering less on thicker surfaces (Alikacem et al. 1999). A similar study revealed that endothelial cells did not synthesise deoxyribonucleic acid (DNA) on a neutral PPy surface, whereas cells on oxidised surfaces did not seem to have an effect on cell shape and function (Wong, Langer & Ingber 1994). Jakubiec et al. (1998) reported that a highly conductive PPy-coated polyester weakened endothelial cell growth, migration and viability. The optimal level of conductivity was found to be 10^3–10^4 Ω/square. In one study, a fibronectin coating was required for bovine aortic endothelial cells to properly adhere to PPy (Ateh, Navsaria & Vadgama 2006). In addition, PPy nanoparticles have shown to reduce human lung fibroblasts and mouse alveolar macrophage viability (Kim et al. 2011b). The variation in biocompatibility of PPy is suggested to arise from different fabrication protocols used in the experiments. For instance, rinsing, extraction and aging is shown to have an effect on biocompatibility (Ferraz et al. 2012).

When comparing current knowledge of PPy properties to the general biocompatibility requirements of biomaterials mentioned in Chapter 6.1, the main challenges arise in the non-biodegradability and poor mechanical properties of PPy, while inflammatory and toxic response can be minimised by adequate fabrication methods. The mechanical properties of PPy can be modified when used in

composites, which will be further described in Chapter 2.6.3. The self-life of PPy has been addressed by one study, where aging of nanocellulose-PPy during four weeks of storage was reported to have a negative effect on its biocompatibility (Ferraz et al. 2012).

2.6.2 Fabrication of conducting and bioactive polypyrrole

PPy can be polymerised via two main routes, either chemically or electrochemically. Chemical polymerisation involves an oxidation agent, such as ferric chloride or ammonium persulphate, and it is often used in commercial applications as it allows bulk manufacturing and provides many different possible routes of polymerisation (Guimard, Gomez & Schmidt 2007). However, chemically produced films yield lower conductivity in comparison to electrochemically produced films. It is also highly sensitive to the choice and purity of the reagents, reaction times and temperature (Balint, Cassidy & Cartmell 2014).

The polymerisation proceeds through oxidation of pyrrole to give a radical cation that reacts with a neutral monomer. The monomer oxidises and deprotonates, forming a dimer that is also oxidised into a dimeric radical cation. This further reacts with the new monomer, giving a trimer, and the reaction continues, monomer by monomer. (Tan & Ghandi 2013)

In electrochemical polymerisation, presented in **Figure 5**, voltage is applied through electrodes that are placed in a solution with pyrrole monomers and negatively charged molecules as dopants. Monomer deposits and oxidises on the positively charged working electrode during the applied current, forming insoluble polymer chains. (Balint, Cassidy & Cartmell 2014, Guimard, Gomez & Schmidt 2007)

Three main methods can be used in PPy electrochemical deposition: the galvanostatic, potentiostatic, and potentiodynamic. In potentiostatic deposition, the voltage is controlled and the current varies. To control the amount of polymer deposited, the method requires a coulometer. In galvanostatic polymerisation, the current is controlled, meaning that the rate of deposition is steady and controllable. (Wallace, Smyth & Zhao 1999)

In potentiodynamic deposition, the polymerising potential sweeps between a low and high potential limit in cycles, resulting in each polymer layer becoming electrically active before the next layer is deposited (Mondal, Prasad & Munichandraiah 2005, Girija, Sangaranarayanan 2006).

The electrochemical method allows high control over the thickness and morphology of the films and allows formation of very thin films (Balint, Cassidy & Cartmell 2014). However, the amount of dopant that can be incorporated into the

structure is limited (Meng et al. 2008, Castano et al. 2004) and the substrate that the polymer is deposited on must be conductive and it is restricted by geometry and surface area (Shi et al. 2004, Zhang et al. 2001). In addition, electrochemically synthesising PPy in composites is very difficult, whereas chemical synthesis easily allows the combination of PPy with different polymers (Shi et al. 2004, Meng et al. 2008).

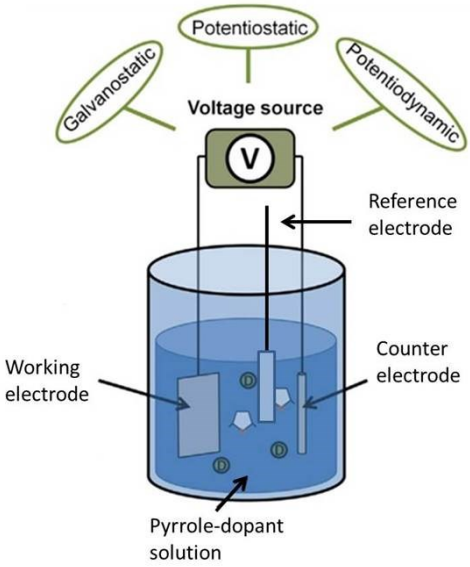

Figure 5. An electrochemical polymerisation set-up. Modified from Balint, Cassidy and Cartmell (2014).

2.6.3 Modification of PPy

PPy is a non-thermoplastic, rigid and brittle polymer and is insoluble after synthesis, which makes PPy difficult to process after synthesis (Meng et al. 2008). However, several modifications of PPy have been made to modify its material properties, such as its bioactivity, biodegradability, porosity and conductivity. Modifications can be divided into four main types: absorbing molecules after PPy polymerisation (Ahuja et al. 2007), entrapping molecules inside the polymer (Cosnier 1999), covalently bonding the molecule to the monomer (De Giglio, Sabbatini & Zambonin 1999), and simply exploiting the doping process (Gelmi, Higgins & Wallace 2010). Scaffolds with

conductive PPy cues are usually made by chemical polymerisation as electrochemical means require distinct conditions to succeed in 3D (Peramo et al. 2008).

Different negatively charged biomolecules, such as certain proteins and GAGs, are commonly exploited as dopants in electrochemical polymerisation (Serra Moreno et al. 2012, Serra Moreno et al. 2009, Meng, Zhang & Rouabhia 2011, Thompson et al. 2011, Gilmore et al. 2009, Gelmi, Higgins & Wallace 2010, Collier et al. 2000, Serra Moreno et al. 2008, Richardson et al. 2007). The choice of the dopant can significantly alter the surface and bulk properties of PPy (Higgins et al. 2012) such as surface roughness, film thickness, Young's modulus, mechanical actuation (Gelmi, Higgins & Wallace 2010), and conductivity (Gilmore et al. 2009). Application of AC ES to the doped PPy films causes films to undergo expansion and contraction as the electrolyte ions move in and out of the polymer to compensate the charge imbalance on the polymer backbone (Gelmi, Higgins & Wallace 2010). Depending on the dopant's properties, such as size and morphology, the dopant can be released from the matrix upon ES, which is called dedoping, and replaced by the electrolyte's anions, such as Cl^- (Serra Moreno et al. 2012, Higgins et al. 2012). This is exploited in drug release (Thompson et al. 2011, Richardson et al. 2007) and in mechanical actuation applications (Gelmi, Higgins & Wallace 2010, Martinez, Otero & Jager 2014), where the ion exchange profile can be controlled by AC ES.

Biodegradation of PPy has been tested with several methods, either by synthesising it in a composite (Zhang et al. 2013, Sajesh et al. 2013, Shi et al. 2004, Meng et al. 2008) or modifying the PPy backbone (Zelikin et al. 2002). PPy can be easily synthesised as a composite with a biodegradable polymer, such as PLLA (Shi et al. 2004, Meng et al. 2008). However, this most likely compromises conductivity and it does not render the actual PPy backbone degradable (Balint, Cassidy & Cartmell 2014). An attempt to try to overcome this has involved modifying the backbone itself by adding hydrolysable side groups (Zelikin et al. 2002). However, the conductivity of the resulting polymer could not be measured and the method did not solve the problem of inherent biodegradation, as it still leaves smaller PPy backbone chains after erosion. Nevertheless, gradual erosion of short (< 50 kDa) PPy chains allows them to be moved by renal clearance (Knauf et al. 1988).

2.6.4 Polypyrrole in bone tissue engineering

PPy provides an interesting platform for osteogenic cells even without the application of ES. Heparin (HE) -doped PPy (PPy-HE) and PPy-HA induced osteogenic differentiation in mouse MSCs when early (runx2, osterix and ALP acitivity) and late osteogenic markers (mineralisation) were observed, even in the absence of OM (Serra

Moreno et al. 2012). An earlier study by Serra Moreno et al. (2009) tested osteoblast viability, adhesion and osteogenic markers on similar PPy-He and PPy-HA films; they reported good cell viability, organised actin filaments, and well-maintained focal contacts in the cells. Normal osteoblast metabolism was also maintained according to the ALP activity. Thin, erodible PPy films have been reported to enhance proliferation of hMSCs, when compared to tissue-culture-treated plastic, and to support osteogenic differentiation assessed by mRNA expression of Coll I, BSP and OPN (Zelikin et al. 2002). In addition, thin PPy films made by admicellar polymerisation supported the osteogenic differentiation of rat MSCs while being comparable to standard cell culture polystyrene (PS) dishes (Castano et al. 2004).

The combination of PPy and ES for osteogenic differentiation of MSCs is still little studied. So far, only one study has addressed the issue by applying DC via chemically polymerised PPy films seeded with rat MSCs (Hu et al. 2014). PPy films, with different concentrations of pyrrole and oxidant, all induced significantly enhanced ECM mineralisation when compared to tissue culture PS. The mineral content increased with increasing pyrrole concentration, and ALP activity occurred earlier on PPy films than tissue culture PS. In addition, mRNA expression of Runx2 and OCN, regulated by Runx2, were upregulated on the PPy films with similar trends as in calcium deposition. When a DC electric field was applied, an increasing concentration of pyrrole, with increased conductivities, showed an increased calcium deposition. Osteogenic differentiation was significantly enhanced with the combination of ES and PPy in comparison to unstimulated PPy.

Osteoblast behaviour in combination with ES and PPy films has been more frequently studied. Meng, Rouabhia and Zhang (2013) tested osteoblast adhesion, proliferation and differentiation on PPy-He-PLLA membranes where PPy and HE were polymerised in a water-in-oil emulsion using an oxidant, and then blended with PLLA. DC electric fields of 100−400 mV/mm were applied through the films. The favourable intensity was 200 mV/mm; this induced a significant proliferation with 6 h of ES, a significant increase in ALP protein concentration (6 and 8 h of ES) and a significant upregulation of mRNA expression and the protein content of OC (6 and 8 h of ES). However, ALP mRNA expression was downregulated at 2 and 4 h of ES. An earlier study by Meng, Zhang and Rouabhia (2011) showed an increase in osteogenic gene markers of osteoblasts under ES of 200 mV/mm using similar films.

Zhang et al. (2013) tested DC stimulation (50, 100, 150, 200, and 250 μA for 4 h per day) with osteoblasts on chitosan films containing PPy nanoparticles, and they also further modified the film surface by covalently immobilising BMP-2. The conductivity increased with the increasing PPy content of the films and did not decrease significantly during 28 days of incubation. Higher metabolic activity was observed when increasing the PPy content from 4%. The cause for this was suggested to be due

to a higher surface roughness. ES seemed to induce stronger metabolic activity in osteoblasts than the immobilised BMP-2 alone. Moreover, the combination of BMP-2 and ES resulted in the highest metabolic activity, osteogenic marker expression and calcium deposition.

2.6.5 Patent landscape and clinical interests of polypyrrole in bone applications

To date, no commercial applications of PPy exist in the field of orthopaedics or bone regeneration. However, a few studies have addressed clinically relevant issues, mainly concentrating on functionalisation of titanium implants with PPy to overcome issues in osseointegration and corrosion (De Giglio, Sabbatini & Zambonin 1999, De Giglio et al. 2001, De Giglio et al. 2000). In addition, a few patents are closely related to the coating of bone implants with PPy and its composites. A PPy-hydrogel composite coating on titanium surfaces has been patented for enhancing bone cell and bone growth (Xu et al. 2008). In another patent, a calcium phosphate/magnesium oxide bioceramic coating has been patented for developing bone fixation materials, such as magnesium-based bone plates, bone screws, and the like (Qu et al. 2012).

With regard to bone tissue engineering, several different variations of PPy exist in the patent field. Panero et al. (2004) have patented a conductive composite consisting of HA and its derivatives, including PPy. The patented constructs can have several shapes formed by a HA matrix that encompasses electrically conductive PPy and HA films. Their intended use is to accelerate tissue regeneration processes in nerve and bone regeneration. Interestingly, biodegradable CP patents that include PPy are more abundant than scientific publications regarding this topic. Shastri et al. (2002) patented a biodegradable CP that includes pyrrole moieties to control cell function, proliferation and differentiation. Another patent includes a biodegradable conducting material in which oligomers of pyrrole and other conductive moieties are grafted with a biodegradable polymer matrix, such as chitosan (Shipu et al. 2009). In addition, a biodegradable conducting polymer has been patented that combines heteroaromatic conductive segments of pyrrole and thiophene with flexible aliphatic chains via degradable ester linkages (Schmidt & Rivers 2002). It is intended for several areas of tissue engineering, such as peripheral nerve generation and bone repair.

A cell culture system involving ES applied via a conducting polymer has also been patented. In this system, the conducting polymer acts as a substrate for anchorage-dependent cells. Changes in the polymer's oxidation state during ES are used to alter proliferation, differentiation, or other functions of cells. (Wong, Ingber & Langer 1998) An electrical stimulator, including a conductive substrate, has been

patented to stimulate and record physiological signals of animal-derived cells (Xing et al. 2003). Another patent exploits EMF stimulation via electroactive material to induce bone cell regeneration of BMSCs (Shastri et al. 1998).

A patent search was made using Espacenet Worldwide database (http://www.epo.org/) and United States Patent and Trademark Office (http://www.uspto.gov/). The number of relevant hits concerning PPy in bone tissue engineering is presented in Table 3. As shown by the results, only a few applications are found with each search type. However, more general patents, such as polymeric coatings on implants, may also cover PPy in their description, but they are not included in the search.

Table 3. Patents related to PPy in bone applications. Irrelevant patents, such as neural or heart valve applications, were excluded from this search. The survey was last checked 15 Jun 2014.

Search source	Key words	Relevant hits
United States Patent and Trademark Office	"polypyrrole" (abstract) and "bone"	1
	"conductive polymer" (abstract) and "tissue engineering"	3
Espacenet World Wide Database	"polypyrrole" and "bone" in the title or abstract	2
	"polypyrrole" and "orthopaedic" in the title or abstract	1
	"polypyrrole" and "implant" in the title or abstract	1
	"Polypyrrole" and "tissue engineering"	1
	"conductive polymer" and "tissue engineering" in the title or abstract	3
Total		**12**

3 Aims of this dissertation

The main aim of this dissertation was to examine conductive PPy coatings *in vitro* and *in vivo* for bone regeneration. The aim in examining *in vitro* was to evaluate PPy as a substrate for hASCs in 2D and 3D environments. *In vivo*, the aim was to evaluate PPy as a coating for biodegradable orthopaedic implants. The specific aims of each study are listed below:

I. To compare the effects of two electrochemically synthesised PPy films, one doped with CS and the other with HA, on attachment, viability, proliferation, and osteogenic differentiation of hASCs under ES;
II. To evaluate the effect of chemically PPy-coated non-woven PLA fibres on hASC attachment, viability, proliferation, and early osteogenic differentiation. In addition, to examine how certain ES patterns affect hASCs when applied through the PPy-coated and uncoated PLA scaffolds;
III. To examine the *in vivo* effects of a chemically polymerised PPy coating in terms of biocompatibility (acute, systematic and chronic effects) and bone regeneration, aiming at better implant-tissue contact in load-bearing orthopaedic fixation applications.

4 Materials and methods

4.1 Biomaterial fabrication

The pyrrole for all the studies was purchased from Sigma Aldrich (St. Louis, MO., USA). HA extracted from Streptococcus equi (Sigma-Aldrich) was used in Study **I**, and CS (chondroitin-4-sulphate, C4S) extracted from bovine trachea (Sigma Aldrich) was used in studies **I** and **II**. Pyrrole was distilled for purity in a vacuum before use. Distilled water and ethanol (Altia Oyj, Rajamäki, Finland) were used in all the polymerisations. Before the cell culture, the films (**I**) and scaffolds (**II**) produced were sterilised by gamma irradiation (BBF Sterilisationsservice GmbH, Kernen, Germany), with an irradiation dose of >25 kGy. This dose range has not been reported to significantly alter the conductivity of the films (Ercan, Günal & Güven 1995, Wolszczak, Kroh & Abdel-Hamid 1995).

4.1.1 Polypyrrole films

PPy-CS and PPy-HA films in Study **I** were electrochemically grown on a sputter-coated polyethylene-naphthalate film (PEN)/Au films (125 μm Dupont Teonex®) in a solution of 0.07 ml of pyrrole and 1 mg of HA or CS per 1 ml of distilled water. An Au-coating (VTT Technical Research Center of Finland) with a thickness of 50 nm acted as a working electrode, a platinum mesh as a counter electrode, and an Ag/AgCl as a reference electrode. A constant potential of 1.0 V was applied to the films until a polymerisation charge of 300 mC/cm^2 had passed through the working electrode.

4.1.2 Polypyrrole-coated scaffolds

In Study **II**, 16-ply multifilament fibres were made by extrusion (Gimac Microextruder TR 12/24 B.V.O., Gimac, Gastronno, Italy) and hot drawing, resulting in a single filament diameter of 10–20 μm. The fibres were cut and carded using a manually operated drum carder (Elite Drum Carder; Louët BV, CW Lochem, The Netherlands) to produce non-woven scaffolds. Several cards were then combined by needle punching using a James Hunter Needle Punching Machine (James Hunter Machine Co., North Adams, MA. USA) and cut 10 x 10 x 2 mm-sized scaffolds.

During the optimisation of PPy coatings, the pyrrole concentration was varied between 0.03–0.3 M, the CS concentration between 0.5–2 mg/ml, the ammonium peroxydisulfate (APS) concentration (Sigma Aldrich) between 0.01–0.1 M, and the polymerisation time was varied from 30 s to 15 min at ambient temperature. The optimisation resulted in the following concentrations used for the scaffolds: [pyrrole]=0.036 M, [APS]=0.1 M and [CS]=1 mg/ml, polymerisation time 150 s.

CS and APS were dissolved separately in distilled water prior to the polymerisation. Subsequently, CS and APS solutions were combined, and pyrrole was added immediately with vigorous stirring. Next, the samples were placed in a polymerisation bath. Before the polymerisation, the non-woven scaffolds were pre-treated in ethanol, and after the polymerisation, rinsed thoroughly with water and air-dried.

4.2 Material characterisation

4.2.1 Atomic force microscopy

The films in Study **I** and individual fibres in Study **II** were characterised by atomic force microscopy (AFM; Park Systems XE-100, Korea) to evaluate the surface morphology and the roughness of the sample surfaces. Roughness (Ra) values of the PPy films (**I**) were imaged in a dry (air) and wet (PBS) state after soaking the films in OM (for detailed contents, see 4.2.6) for 4 days. The dried samples were imaged in air using non-contact AFM with a silicon probe (ACTA-905M, Applied NanoStructures, Inc., Santa Clara, USA). Before imaging, sample surfaces were carefully rinsed with deionised water and dried in ambient air. A nominal resonance frequency of 300 kHz, a cantilever spring constant of 40 N/m and a tip radius of < 10 nm were used as parameters for imaging at a scan rate of 0.5 Hz to acquire 5x5 μm^2 images. The wet samples, pre-incubated in OM, were imaged using a contact mode AFM with Silicon nitride probes (HYDRA-6R100N, Applied Nanostructures, Inc.). A nominal force constant of 0.28 N/m and a tip radius with a curvature of < 8 nm were applied to image 20x20 μm^2 areas, with scanning parameters of 7 nN and 20 nN force set points. Eventually, images of 12x12 μm^2 were taken with a scan rate of 1 Hz. Raw 512x512 pixel data were used for the Ra value analysis.

In Study **II**, PPy-coated fibres were imaged in air by non-contact AFM using silicon probes. A pyramid-shaped tip and an aluminium reflective coating (radius < 10 nm) with a nominal resonance frequency of 300 kHz and a cantilever spring constant of 4 N/m were used for imaging. A scan rate of 0.5 Hz and scans of 5x5 μm^2 were applied.

The surface roughness was analysed with Park Systems XEI 1.7.5 image analysis software (Suwon, Korea). In the case of the PPy films (**I**), 10 randomly chosen 4x4 μm^2 areas were calculated. The data were 4^{th} order plane-fitted to expose the nanoscale details of the PPy surfaces. With regard to the roughness data acquired from the coated fibres (**II**), the analysed area size was varied in order to guarantee the reliability of the result. The raw data was 0^{th} order flattened along the fibre axes, which were parallel to the slow axis of the AFM, to present the surface topography of the curved surfaces.

4.2.2 Scanning electron microscopy

Scanning electron microscopy (SEM; JSM – 6360 LV SEM, JEOL, Japan) was used in Study **II** to image coated and uncoated scaffolds. A low acceleration voltage (3 kV) was used to prevent sample damage and to induce contrast between electrically conductive and insulating areas. For the uncoated scaffold, the imaging was first done without a metallic surface coating and then sputter-coated to result in a thin, 20 nm gold layer coat (SCD 050, Balzers AG, Liechtenstein).

4.2.3 Hydrolysis measurements

Gamma irradiated scaffolds in Study **II** were incubated in sealed plastic specimen chambers containing either PBS or maintenance medium (MM; for detailed contents, see 4.2.6) at +37 °C for up to 42 days. The ISO-15814:1999(E) standard was followed to set the test conditions. The pH of the buffer solution was measured and changed every 3 to 4 days in order to prevent the acidic autocatalytic hydrolysis of PLA.

4.2.4 Measuring electrical properties of the electrodes, cell culture medium, and PPy coatings

Electrochemical impedance spectroscopy (EIS) measurements were conducted for the PPy films (**I**) and the coated and uncoated scaffolds (**II**). EIS in Study **I** was conducted in PBS. Doped PPy films on gold-coated Mylar with an area of 1 cm^2 were used as a working electrode. Platinum mesh acted as a counter electrode and Ag/AgCl with 3.0 M NaCl as a reference electrode. Impedance spectra were obtained using a 100 mHz to 100 kHz range, applying an AC amplitude of ±200 mV (CH 660D Electrochemical Analyzer/Workstation, CH Instruments, Austin, USA). All EIS

measurements were performed at the resting potential of the films, ranging from +70 to +195 mV, versus the reference electrode to prevent destruction of the films. The average impedance and standard deviation (SD) at 10 Hz and 100 Hz were calculated from the impedance values of the three samples per film type.

Impedance spectra in Study **II** was measured from circular parallel 1 cm^2 PEN/Au-film electrodes and parallel rigid TiN-coated steel electrodes (electrode material TiN) in Dulbecco's Modified Eagle Medium (DMEM) using a HP 4192A impedance analyser (Agilent Technologies, Santa Clara, USA). In this measurement, a 100 **Ω** series resistor and an excitation sinusoidal peak-to-peak voltage of 50 mV was used. Subsequently, the impedance of the insulating uncoated scaffold and the electrically conductive coated scaffold as well as the plain DMEM was measured between the rigid TiN electrodes (Oerlikon Balzers Sandvik Coating, Finland), which provided an electrochemically stable, smooth, and mechanically rigid construction for the measurement cell. Constant phase element analysis (CPE) was conducted using a curve fitting tool provided in OriginPro 8.5.1 software (Originlab Corporation, Northampton, MA, USA) applying the protocols described by Tandon et al. (2009a). Ohm's law and the impedances measured at 1 Hz and 10 kHz were used to calculate the current densities in the 24-well stimulation set-up.

Cyclic voltammetry (CV) of the films in Study **I** was recorded in PBS with the same instrument and similar electrode set-up as in the impedance recordings of the films. Measurements were performed at a scan rate of 50 mV/s and a potential from -0.6 to 0.5 V.

After the cell culture experiments in Study **I**, the through-plane electrical conductivity of PPy films was monitored in air using a simple two-wire test set-up (Fluke 170 multimeter, Washington, USA). The applied top and bottom electrodes were round Au contact electrodes (contact area of 16 mm^2) and the PEN/Au films, respectively.

In Study **II**, the DC conductivity of air-dry scaffolds was measured directly after the synthesis and during the hydrolysis test using custom made copper flat alligator clips (contact area 6 mm^2) and a Fluke 189 multimeter (Fluke Corporation, Everett, USA).

4.2.5 Electrospray ionisation mass spectroscopy

In Study **II**, gamma sterilised, coated and uncoated samples of 10 mg were hydrolysed for 30 days at +60 °C in 1.0 ml distilled water. Subsequently, the samples were analysed with a single quadrupole Perkin Elmer SQ 300-electrospray mass spectrometry (MS) system (PerkinElmer, Massachusetts, USA) with a positive ion

mode. The drying gas (nitrogen) temperature was set at +175 °C and the flow rate at 8 l/min. To screen the onset of the PLA oligomers cracking, the capillary exit voltage was varied between 60 V and 200 V. The MS was operated in a scan mode (mass range 200–1000) using a dwell time of 0.1 ms. The hydrolysis solution was passed through a 0.45 μm polytetrafluoroethylene filter, 0.5 ml methanol was added to the mixture (water/MeOH 2:1 v/v), and the sample was injected through a syringe pump into the mass spectrometer at a flow rate of 5 μl/min.

4.2.6 Adipose stem cell isolation and cell culture

The adipose tissue for each study was obtained via tissue harvests from three female patients, with an average age of 54 ± 22 years in Study **I** and 54 ±12 years in Study **II**. Surgical procedures were conducted at the Department of Plastic Surgery, Tampere University Hospital. The tissue harvest and the use of hASCs were conducted in accordance with the Ethics Committee of the Pirkanmaa Hospital District (R03058). Samples from the adipose tissue were manually cut into small pieces and digested with collagenase type I (1.5 mg/ml; Invitrogen, California, USA) at $+37^0$C for 45–60 min with intermittent agitation. After centrifugation, the uppermost layer of fat and connective tissue was discarded and the pelleted stromal vascular fraction was passed through a filter of 100 μm (Falcon®, Becton Dickinson Labware, New Jersey, USA) to remove cellular debris. After two more centrifugation and washing steps, the remaining pellet was expanded in T-75 PS flasks (Nunc, Roskilde, Denmark) in MM consisting of a DMEM/Ham's Nutrient mixture F-12 (1:1; Invitogen), 10% FBS (Invitrogen) (**I)** or HS (**II)** (PAA Laboratories GmbH, Pasching, Austria), 1% L-glutamine (GlutaMAX I; Invitrogen) and 1% antibiotics/antimycotic (100 U/ml penicillin, 0.1 mg/ml streptomycin; Invitrogen). Cells were passaged when reaching a confluence level of 80%, and passages 4 and 5 were used for the experiments. The OM was changed for the hASCS at the beginning of ES in Study **I,** consisting of 250 μM ascorbic acid 2-phosphate (Sigma-Aldrich), 5 nM dexamethasone (Sigma-Aldrich), and 10 mM b-glycerofosfate (Sigma-Aldrich) supplemented to the MM.

4.2.7 Electrical stimulation of adipose stem cells

A similar electrical stimulator set-up was used in both *in vitro* studies (**Figure 6**). PEN/Au films, which were either electrochemically coated with PPy (**I**) or used without a PPy coating (**II**), were attached to custom-made, bottomless 24-well plates (Greiner Bio-One GmbH, Frickenhausen, Germany). These working electrodes were

attached to the well plate with biomedical grade Silastic® Q7-4720 liquid silicone rubber. The top electrodes were bent strips of PEN/Au-films partially extending into the cell culture medium. The individual wells were electronically connected in parallel by the connection of four parallel strips. The electrode surface area was 1 cm^2 for the top electrode and 1.5 cm^2 for the bottom electrode in each well. The distance between the top and the bottom electrodes was 2 mm, which matched the thickness of the scaffold in Study **II**.

ES was performed in a cell-culturing incubator at +37 °C and 5% CO_2 during the 14-day culture period. Samples were stimulated for 4 h a day with a BEC of ±0.2 V amplitude. The waveforms for the 1 Hz (**II**) and 100 Hz (**I** and **II**) BEC were 250 ms (+200 mV) / 250 ms (-200 mV) / 500 ms (0 mV) and 2.5 ms (+200 mV) / 2.5 ms (-200 mV) / 5 ms (0 mV) respectively. Corresponding non-stimulated samples acted as controls. The measured DC current after the 2.5 ms and the 250 ms pulses was in the range of 40–50 $\mu A/cm^2$, corresponding to a cell impedance of 5 k**Ω**.

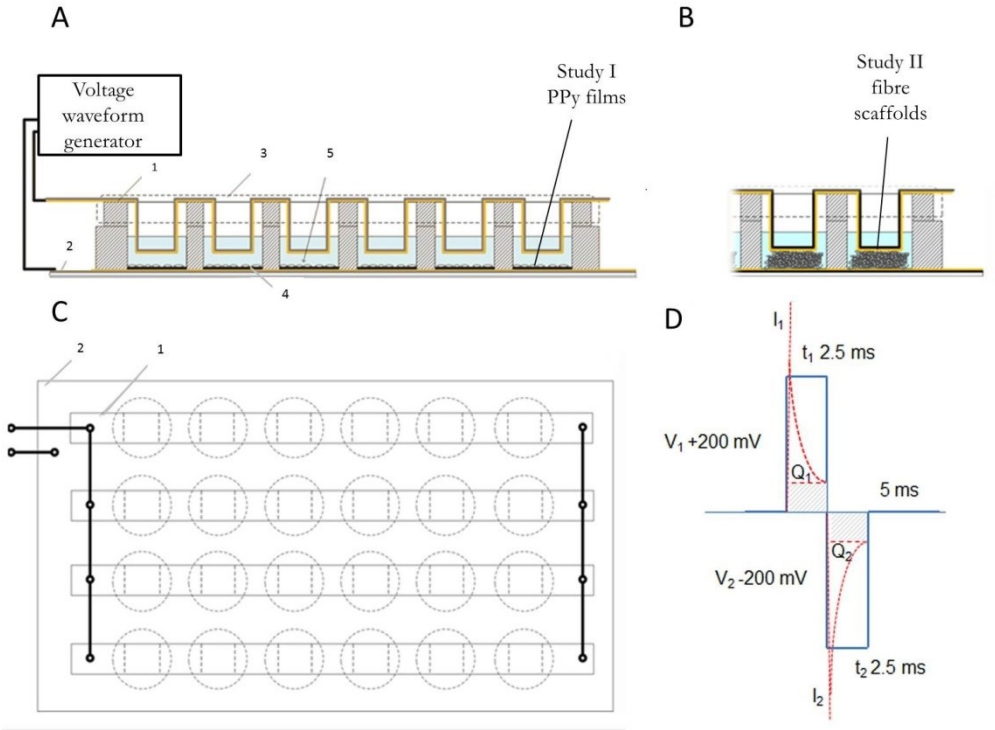

Figure 6. A schematic illustration of the stimulation device geometry. A) Side projection from Study **I**. Numbers 1 and 2 represent the corresponding areas in Figures A and C. The strips of the counter electrode (3) are embedded in the medium. A PEN/Au-film coated with PPy-HA or PPy-CS (4) acts as a working electrode. Human ASCs (5) are seeded on PPy films. B) A side projection from two wells in Study **II** where hASC-seeded fibre scaffolds are squeezed between working and counter electrodes. Study **II** used a similar ES configuration as Study **I** but without the PPy coating on the PEN/Au films. C) A schematic illustration of the stimulation device geometry as a plan (projection). D) A voltage waveform at 100 Hz was applied to the samples in both *in vitro* studies. Biphasic pulses are shown as a blue coloured line. Transient net current is presented with a dashed line. The electrical double layer charging of the Au electrodes is presented as Q_1 and Q_2.

4.3 Adipose stem cell characterisation

4.3.1 Adipose stem cell surface marker expression

In both *in vitro* studies, cells were characterised with a fluorescence-activated cell sorter (FACSAria; BD Biosciences, Erembodegem, Belgium) at passage 1 before the experiments. Monoclonal antibodies against the following surface markers were used: CD14, CD19, CD49d-PE, CD90-APC, CD106-PECy5 (BD Biosciences); CD45-FITC (Miltenyi Biotech, Bergisch Gladbach, Germany); CD34-APC, HLAABC-PE, HLA-DR-PE (Immunotools GmbH, Friesoythe, Germany); and CD105-PE (R&D Systems Inc, MN, USA). Analysis was performed on 10,000 cells per sample, and unstained cell samples were used to compensate the background autofluorescence of the cells.

4.3.2 The attachment, morphology, viability and cell number of the adipose stem cells

Cell morphology and viability in studies **I** and **II** were evaluated qualitatively using live/dead staining (Molecular Probes, Eugene, USA). The samples were incubated with 0.5 μM of CellTracker™ Green (5-chloromethylfuorescein diacetate, CMFDA; Molecular Probes) and Ethidium homodimer-1 (EthD-1; Molecular Probes) in PBS at room temperature for 45 min. Viable cells with green fluorescence and dead cells with red fluorescence were imaged with a fluorescence microscope (Olympus IX51, Olympus Finland PLC, Vantaa, Finland). In Study **I**, standard PS culturing plates (without ES; Nunc, Roskilde, Denmark) served as a control for the cell viability and morphology evaluation.

In both *in vitro* studies, cell proliferation was studied with a CyQuant® Cell Proliferation Assay Kit (Molecular Probes), which is based on the absorbance of DNA-binding fluorescent dye. On the day of the analysis, the samples were carefully washed with PBS and cells were permeabilised with 0.1% Triton-X 100 buffer (Sigma-Aldrich) in PBS and stored at -70 °C until the analysis. After thawing, 20 μl of the cell lysate was pipetted on a microplate (Nunc, Roskilde, Denmark) and mixed with CyQuant® GR dye and the kit's own lysis buffer according to the manufacturer's protocol. The fluorescence of the GR dye bound to cellular nucleic acids was measured with a microplate reader (Victor 1420 Multilabel Counter, Wallac, Turku, Finland) at 480/520 nm.

4.3.3 Alkaline phosphatase activity

In both *in vitro* studies, ALP activity was determined from the same Triton-X 100 lysates as in the cell proliferation assay using an ALP Kit (Sigma-Aldrich) according to the manufacturer's protocol. In brief, the samples were incubated with 50% alkaline buffer solution (2-amino-2-methyl-1-propanol, 1.5 mol/l, pH 10.3; Sigma-Aldrich) and 50% of p-nitrophenyl phosphate (Sigma-Aldrich) at +37 °C for exactly 15 min. The reaction was stopped by adding 1.0 mol/l sodium hydroxide. The colour intensity was measured at 405 nm using a microplate reader (Victor 1420).

4.3.4 Mineralisation

The mineralisation of the ECM was studied with Alizarin Red staining in Study **I**. Samples were fixed in ice cold 70% ethanol for 60 min at room temperature and then rinsed with distilled water before the addition of 2% Alizarin Red solution (pH 4.2; Sigma-Aldrich) for 5 min. After rinsing the samples twice with distilled water and once with 70% ethanol, they were incubated in cetylpyridium chloride (Sigma-Aldrich) for 3 h. Supernatant was pipetted on a microplate (Nunc) and the absorbance was measured at 544 nm (Victor 1420).

4.4 *In vivo* experiment

4.4.1 Polypyrrole-coated bioabsorbable bone fixation screws

PPy was chemically polymerised in the presence of CS on PLGA-β-TCP-composite screws (ActivaScrew™ TCP, Bioretec, Tampere, Finland). The screws were 2 mm in diameter and 10 mm in length, and had X-ray visible β-TCP in the tip. The screws were soaked in pyrrole in ethanol solution (1.3 mol/l) for 67 min and then transferred into a freshly prepared aqueous solution of $FeCl_3$ (0.5 mol/l) and 1 mg/ml CS for 15 min. The coated screws were carefully rinsed with deionised water in an ultrasonic bath and air-dried. The coated and uncoated screws were sterilised by gamma irradiation of 17.5–26 kGy (by a commercial supplier). The stainless steel screws (Synthes 211.010, diameter 2.0 mm, length 10 mm) acting as references for foreign body reaction were sterilised by autoclaving them at +121 ^{0}C.

4.4.2 Implantation of bioactive screws

The animal experiments, authorised by the Animal Ethics Committee of the Zhongshan Hospital, Fudan University, China [SYXK(2008)-039], were carried out on 23 female New Zealand white rabbits with a mean weight of 3.1 ± 0.1 kg. According to the standard ISO 10993-6 for biocompatibility studies, the rabbit is the smallest possible animal model for the testing of bone implants.

The animals were randomly separated into four groups presented in Table 4: the rabbits receiving coated screws were called the coated group and those receiving uncoated bioabsorbable screws were called the control group. In the coated group, rabbits were implanted with three PPy-coated screws in the left leg (n=9). The right leg was left intact in the 12-week subgroup of the coated group, whereas for the 26-week subgroup, steel screws were implanted in the right leg in similar manner when compared to the left leg. In the control group, steel screws were implanted in the right leg (n=9), similar to coated group, and uncoated screws were implanted in the left (n=9). For the torsion tests at the 12-week time point, five rabbits were operated on, receiving three coated screws (n=15) in the left leg and three uncoated screws (n=15) in the right leg.

Table 4. The experimental groups in Study **III**.

	12-week implantation period	**26-week implantation period**
Rabbits with uncoated screws	Uncoated group, 12-week subgroup	Uncoated group, 26-week subgroup
Rabbits with coated screws	Coated group, 12-week subgroup	Coated group, 26-week subgroup

The surgery was performed under sedation and general anaesthesia with an intramuscular (i.m.) injection of diazepam (2 mg/kg; SunRise Pharma, Shanghai, China) and ketamine (40 mg/kg; GuTian Pharma, Fujian, China), which was also used for maintaining the anaesthesia (40 mg/kg). To prevent drying of the eyes, NaCl (0.9%; HuaLu Pharma, Shandong, China) was applied.

The medial side of the distal femur and the upper tibia were exposed with two mini-incisions. A 1.5 mm drill bit was used to drill a 10 mm deep implant hole, which was slightly countersunk to fit the head of the screw flush with the bone surface. After tapping the hole (2 mm), screws were inserted. Two screws were implanted into the proximal tibia and one screw into the distal femur. After saline irrigation, the wound

was closed by suturing in two layers with nonabsorbable surgical sutures (Ping'an medical equipment CO. LTD, Huai'an, China). To prevent infection, penicillin (130,000 U/kg; HuaBei Pharma, Hebei, China) was used as an antibiotic by i.m. intraoperatively and on the first postoperative day. Animals were dosed with a subcutaneous (s.c.) injection of buprenorphine hydrochloride (0.03 mg/kg; Drug Research Pharma, Tianjin, China) for analgesia once a day for 3 days after the operation. Radiographs of both hind legs were taken in the medio-lateral projections (49 kV, 5.0 mA, 33 ms, digital X-ray machine, Siemens, Germany) 8 wks postoperation to monitor the correct placement of the implants. Twelve and 26 wks after the implantation, the animals were euthanised with an overdose of ketamine hydrochloride (GuTian Pharma, Fujian, China). Tetracycline (30 mg/kg; Sigma, USA) was injected i.m. 8 days and 1 day before euthanasia to detect new bone formation.

4.4.3 In vivo characterisation methods

4.4.3.1 Clinical signs

The appearance, behaviour, and the food and water consumption of the rabbits was observed twice daily on weekdays and once daily on weekends. After the procedure, the implantation sites were examined for the first 5 days and weekly throughout the study. Body temperature and weight were measured prior to the implantation and 48 h, 2, 4, 12 and 26 wks after implantation.

4.4.4 Haematology and clinical chemistry

Haematology and clinical chemistry were performed prior to the implantation and 48 h, 2, 4, 12 and 26 wks postoperation to evaluate the subchronic toxicity of the coated screws. Blood samples were drawn from the readily accessible central auricular artery under anaesthesia without overnight deprivation of food. The haematological analyses were conducted with an automatic haemocyte analyser (XS-1000i and CA1500, Sysme, Japan) and chemical analyses with a biochemical automatic analyser (P800/P2400, Roche, Switzerland) at Labway Clinical Laboratory Limited (Shanghai, China).

4.4.5 Organ examination

To avoid drying and subsequently false low values, organs were weighed immediately after dissection. For bilateral organs (adrenals, kidneys, ovaries and oviducts), the left and right organs were weighed together. Subchronic toxicity was examined from organ weights, macroscopic examinations and histology of internal organs. All the organ samples were fixed in 10% neutral buffered formalin (XingYinHe Chemical Ltd, Hubei, China), dehydrated, and embedded in paraffin (FangZheng Chemical Ltd, Sichuan, China). Paraffin blocks were cut into thin sections of 5 μm and stained with Haematoxylin and Eosin (Vaijayanthimala et al. 2012). The samples were examined under an optical microscope (Axio Imager M1, Zeiss, Jena, Germany) using AxioVision SE64 software (Zeiss, Jena, Germany).

4.4.6 Soft tissue examination

Soft tissue around the head of the screws (uncoated, coated and steel screws) was selected for routine histology. The processing of the tissue samples was done by the same method as the organ samples. The coated and uncoated samples were evaluated semi-quantitatively. The quantitative comparison was made from inflammatory polymorphonuclear cells, lymphocytes, plasma cells, macrophages and giant cells. Qualitative comparison was made from the extent of necrosis, neovascularisation, fibrosis and fatty infiltrate.

4.4.7 Torsion test

Torsion tests (Iijima et al. 2008) were performed on the day of euthanasia 12 wks postoperation to characterise the attachment strength of the bone to the screws. Newly formed bone and adherent soft tissue were carefully dissected around the screw head. A hexagonal screwdriver linked with the sensor of a digital torque meter (HDP-5, Tuojing Measuring Instrument Limited Co., Shanghai, China) was used to rotate the screws in order to capture the peak value of twist force (F_{max}, Nm) during the course of loosening the screws.

4.4.8 Micro-CT examination

The bone specimens including the implanted screws were harvested and osseous tissue surrounding the coated and uncoated screws in the rabbit femur and tibiae were scanned non-destructively by micro-computed tomography (μCT-80; Scanco Medical AG, Zurich, Switzerland for the 12-week samples and Siemens Inveon Micro-CT/PET, Munich, Germany for the 26-week samples). The μCT images, with a pixel size of 20 μm, were recorded on a 1024×1024 charge-coupled device detector. The images were segmented after scanning using a nominal threshold value of 220. Measurement of the total volume and mineral density of the sample areas was performed automatically with FEA software (Scanco Medical AG, Zurich, Switzerland). In order to cover the surrounding tissue in the scan, a circular area with a diameter of 2.2 mm was selected to scan the sample area around the screw axis. To calculate the relative amount of the mineralised tissue, the scan was repeated with a 2.0 mm diameter and deducted from the first area.

4.4.9 Tetracycline labelling

The bone specimens, including the implants, were harvested and dehydrated in acetone for 1 month and embedded in methyl metacrylate (MMA) (Suicheng Chemical Ltd, Guangzhou, China) without decalcification. The MMA blocks were then sliced to a 200 μm thickness (E300CP, Norderstedt, Germany) and polished to 20 μm slices. The distances between the two tetracycline fluorescence lines were measured from several spots under a light microscope (Axioimager, Axiovision).

4.4.10 Hard tissue examination

The tetracycline-labelled samples were also used for hard tissue examination by adding toluidine blue（ZiYi Chemical Ltd, Shanghai, China） to the slices for 15 min (Deng et al. 2008). Subsequently, coverslips were mounted at room temperature for two days. The slices were analysed and the number of osteoblasts and chondroblasts were counted from the bone-implant interface under an optical microscope (Axio Imager) (Di Iorio et al. 2006).

4.5 Statistical analysis

The statistical analyses for Ra values, DNA content, ALP activity and mineralisation (**I** and **II**) as well as for blood samples, torsion test, micro-CT, tetracycline-labelling, samples, hard tissue histology, weight and temperature (**III**) were performed with SPSS, version 17 (**II** and **III**) and 19 (**I**). A one-way analysis of variance (ANOVA) with Bonferroni post hoc correction was used in Study **I** for comparison of PPy-HA and PPy-CS, including the control and ES groups, and in Study **II** for comparison of the time points (1 d vs. 7 d vs. 14 d) and the stimulation groups (control vs. 1 Hz vs. 100 Hz). Fisher's Least Significant Difference (LSD) was used for one-way ANOVA to analyse blood samples in Study **III**. Student's t-test was used for comparison of the time points (7 d vs. 14 d) in Study **I** and for comparison of the scaffolds (coated vs. uncoated) in Study **II.** In Study **III**, Student's t-test was used for comparison of the coated and uncoated group within the time points for the torsion test, micro-CT, tetracycline-labelling, hard tissue histology, weight, and temperature. Ra values of the films (**I**) were also analysed with Student's t-test and the equal variance assumption was checked by Levene's Test. The data from the three repeated experiments in studies **I** and **II** were combined and presented as mean ± SD. In Study **III**, all quantitative data were presented as mean ± standard error of mean (SEM). The results were considered statistically significant when $p<0.05$.

5 Results

5.1 *In vitro* experiments

5.1.1 Material characterisation

5.1.1.1 Atomic force microscopy

In Study **I**, PPy-HA films had significantly lower Ra values on dry films and significantly higher values on wet films (in PBS) when compared to PPy-CS (**Table 5**). The nanoscopic details of the dry films (**Figure 7**) showed the PPy-CS surface texture consisting mainly of nodules of 40–50 nm in diameter and 5–10 nm in height. The nodules were organised into a porous web. PPy-HA had larger nodules of 150–160 nm in diameter and 30–35 nm in height. The sparsely distributed protrusions on both films were similar in size, 500 nm in diameter and 100 nm in height.

Nanoscopic textures of the films could not be observed in PBS in Study **I**. Instead, imaging in PBS revealed a strong undulating morphology on both films, consisting of uniformly spread small 800–1000 nm nodules (**Figure 7**) and sparsely spread 4–10 μm circular protrusions covered with nodules (not visible in the flattened image data in **Figure 7**). The typical height range of the nodules was 100–150 nm for PPy-HA (**Figure 7**D) and 200–300 nm for PPy-CS (**Figure 7**C). The hills caused by the undulating morphology and the protrusions were significantly higher than the nodules, which were 400–500 nm for PPy-CS and 600–800 nm for PPy-HA. The protrusions on PPy-HA had a more oval shape, while those on PPy-CS were more circular. Therefore, the Ra values represented the height of the protrusions as well as height and shape of the nodules.

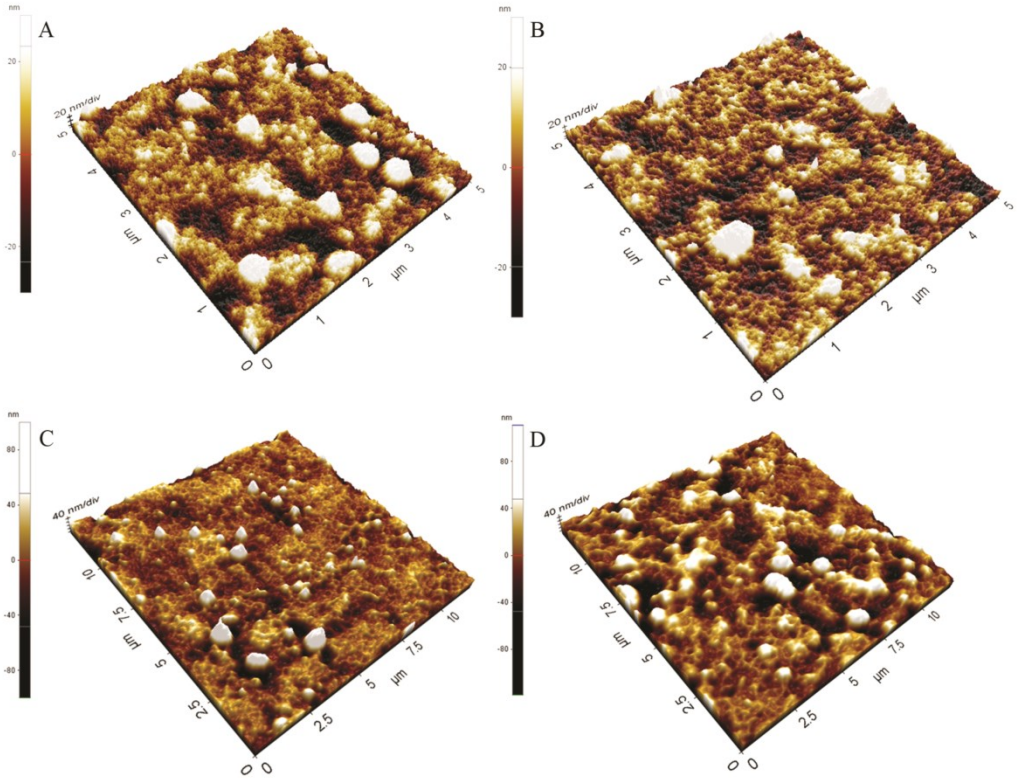

Figure 7. AFM images of dry PPy-CS (A) and PPy-HA (B) films in a scanned area of 5x5 µm in Study **I**. Sparsely distributed white areas represent protrusions. Z-scale in the images is 20 nm/division. AFM images of wet PPy-CS (C) and PPy-HA (D) in PBS have 800–1000 nm nodules seen as white areas. The scanned area is 12x12 µm. The Z-scale of the images is 40 nm/division.

In Study **II**, the coated fibres were still fully covered with PPy after 20 days of hydrolysis (**Figure 8**). The surface morphology of the PPy coating smoothened over the time and the Ra values decreased significantly from 160 nm to less than 80 nm. Day 0 showed the typical morphology of a chemically coated PPy surface in PBS where the fibres were extensively covered by fine nodules of 200 nm in diameter. The nodular morphology was still detected on day 10, but showed smoother areas and coarser nodules (>400 nm). The fraction of the smoother areas had further increased on day 20. The roughness analysis was consistent and independent of the chosen surface area in the images, which were 5 x 5 μm^2 in size with 2 x 2 μm^2 subareas.

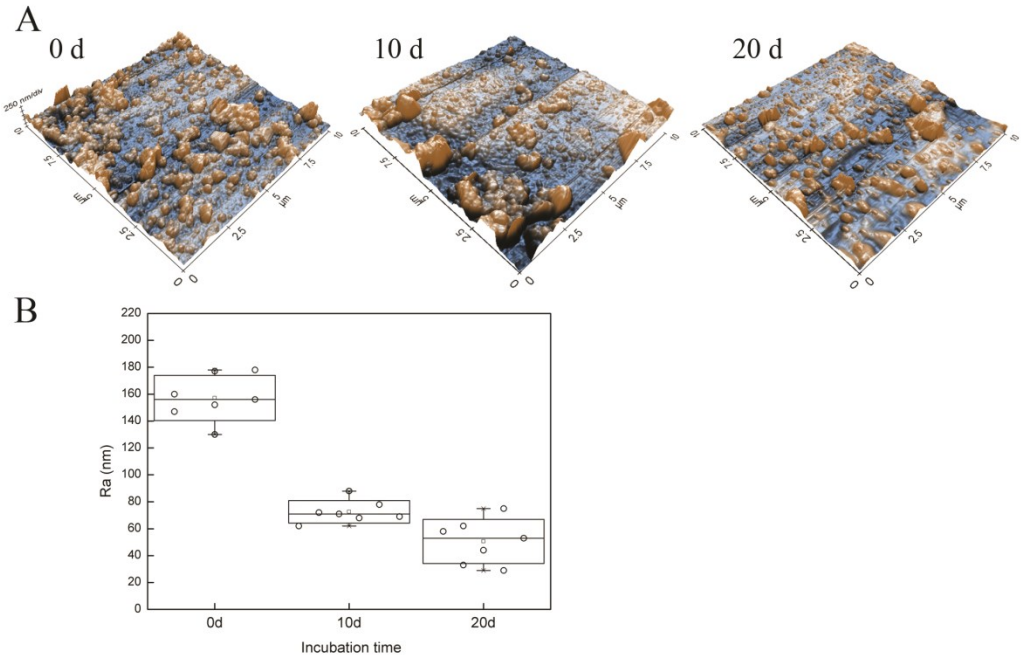

Figure 8. AFM images (A) of a coated scaffold at day 0, 10 and 20 in a scanning area of 10 x 4 μm in Study **II**. The surface of the coated scaffold (B) gradually loses its fine granular morphology and smoothens during incubation. The Z-scale of the images is 600 nm. Ra: surface roughness.

5.1.1.2 Scanning electron microscopy

The coated PLA fibres in Study **II** were covered with a conductive layer because they did not build up any electrostatic charge in SEM imaging (**Figure 9**). Metallised PLA fibres appeared substantially smoother when compared to coated fibres.

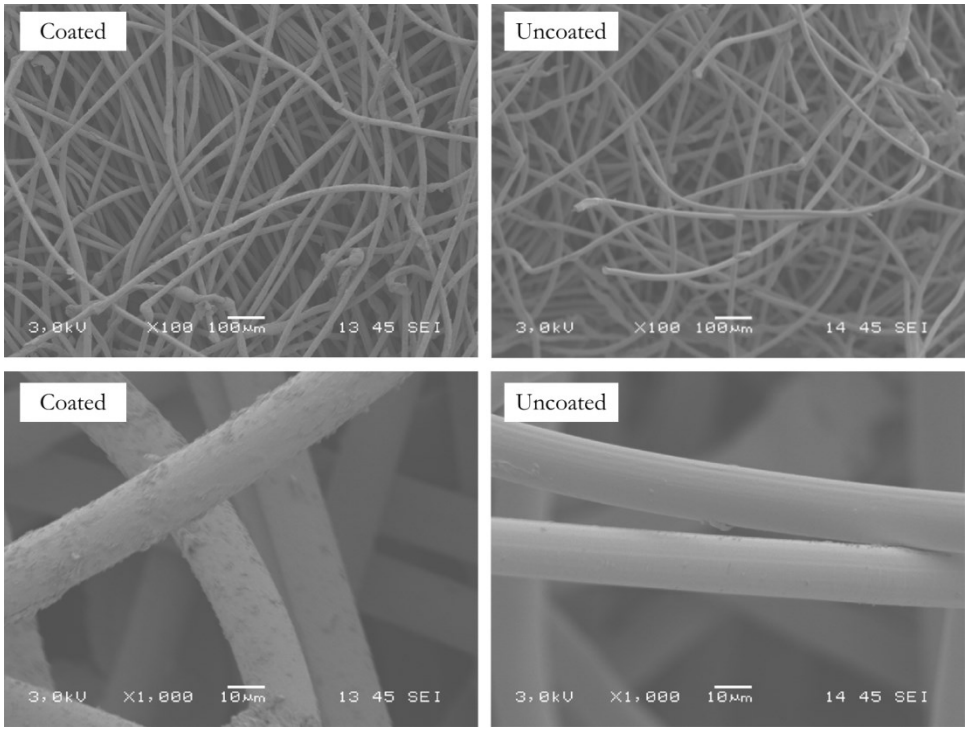

Figure 9. SEM images of the coated (left) and the uncoated (right) scaffold in Study **II**. The PLA scaffold is sputtered with a gold layer 20 nm thick. The images were taken with a 3 kV acceleration voltage.

5.1.1.3 Measuring electrical properties of the electrodes, cell culture medium, and PPy coatings

In Study **I**, the impedance values of PPy-HA and PPy-CS films did not vary significantly (Table 5), yet PPy-CS showed slightly higher impedance values at 10 and 100 Hz. Both films showed a similar trend in the impedance spectra (**Figure 10**).

Table 5. Surface roughness and impedance values of PPy films in Study **II**.

Sample	Ra in air (nm)	Ra in PBS (nm)	Impedance at 10 Hz in PBS (Ohm)	Impedance at 100 Hz in PBS (Ohm)
PPy-CS	14 ± 0.8	320 ±28	54 ±13	45 ±6
PPy-HA	8.6 ± 0.2	420 ± 40	51 ±6	45 ±2

PBS: phosphate buffered saline; PPy-HA: hyaluronic acid-doped PPy; PPy-CS: chondroitin sulphate-doped PPy; Ra: surface roughness.

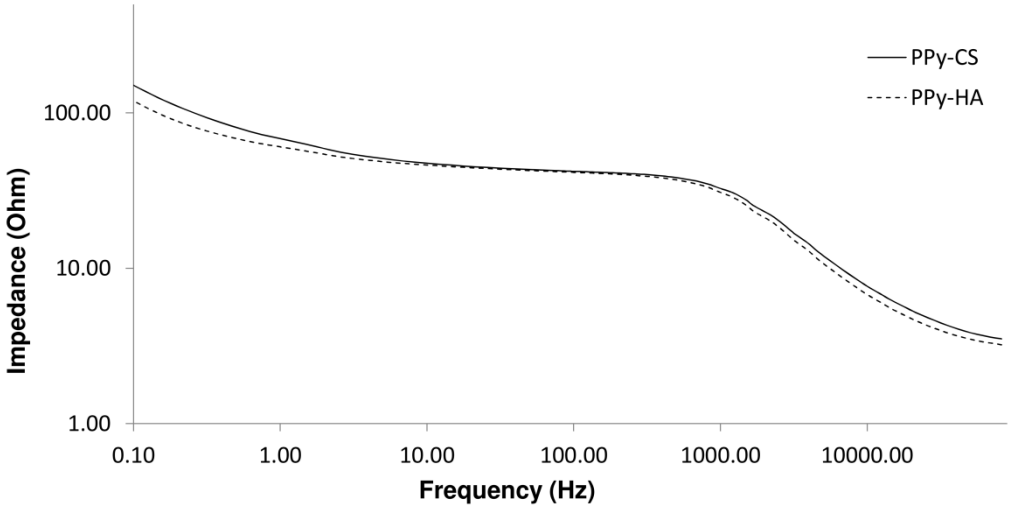

Figure 10. The impedance spectra of PPy-CS and PPy-HA films in PBS in Study **I**. PPy-CS: chondroitin sulphate-doped PPy; PPy-HA: hyaluronic acid-doped PPy.

The results of the impedance measurement for Study **II** are summarised in Table 6.|Z|cell is the magnitude of cell impedance, CPE represents the capacitance of the cell and η is a fit parameter describing the "ideality" of capacitance in the CPE model (Tandon et al. 2009a). The resistance of the coated scaffolds significantly increased during the first day. The resistance of the air-dried samples immediately after the synthesis was 50 ± 20 k**Ω**; this increased to 90 ± 40 k**Ω** after rinsing with deionised water at day 0, as illustrated in **Figure 11**. According to the measured data, the coated and uncoated scaffolds both had a significant effect on cell impedance in DMEM. The low frequency impedances in particular were significantly lower for the cell containing the scaffolds in DMEM (either coated or uncoated) than for the cell containing only

the medium. As expected, the coated scaffold induced the most significant decrease in cell impedance at lower frequencies. The ideality coefficient η of the coated scaffold was low (0.83), which suggests that the capacitive CPE model did not describe the cell impedance spectrum in this case. Contrary to expectations, the uncoated scaffold also decreased the cell impedance. Impedance at a low frequency was 3-fold higher and the capacitance was 10-fold lower for the Au electrodes than for the TiN electrodes.

Table 6. Summary of the impedance data from Study **II**.

Sample	$\|Z\|_{cell}$ at 1 Hz (Ω)	$\|Z\|_{cell}$ at 10 kHz (Ω)	CPE capacitance (μF)	Ideality coeff. η
PEN/Au/film	240,000	15	2	0.97
TiN	83,000	17	20	0.94
TiN/uncoated scaffold	13,000	26	20	0.90
TiN/coated scaffold	1700	12	14	0.83

PEN: polyethylene-naphthalate; |Z|cell: the magnitude of cell impedance.

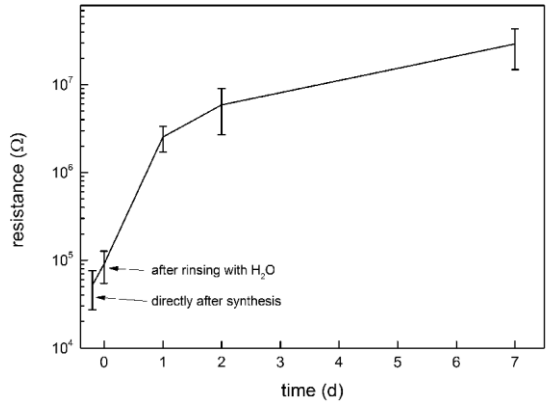

Figure 11. The resistance of the coated scaffold in air in Study **II**.

Impedances derived from sinusoidal test signals were used for estimating the magnitude of the stimulation current during the biphasic pulses. The calculated theoretical current densities were $I_{1,2,\ DC}$ ±13.3 μA/cm² for the DC current and $I_{1,2,max}$ ±16.7 mA/cm² for the transient current. The real transient current density, which could not be directly measured with the system used, was limited by the current amplifier to roughly ±0.4 mA/cm².

In Study **I**, both films showed well-defined voltammetric profiles, but PPy-CS had slightly higher electrochemical activity and doping level when compared to PPy-HA. This was evidenced by the integrated surface areas covered by the respective voltammogram (**Figure 12**). The conductivity of the films was confirmed to be at similar levels (10^{-3} S/cm) as before the experiment when measured in air (data not shown).

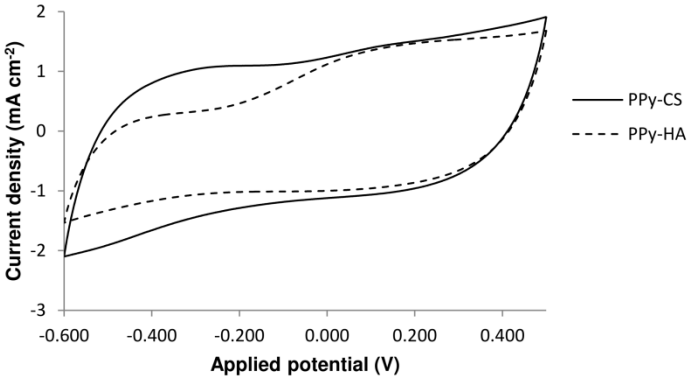

Figure 12. The CV profiles of PPy-CS and PPy-HA films in PBS in Study **I**. PPy-CS: chondroitin sulphate-doped PPy; PPy-HA: hyaluronic acid-doped PPy.

5.1.1.4 Electrospray ionisation mass spectroscopy

In Study **II**, the coated and uncoated scaffolds had very similar ESI-MS spectra (**Figure 13**) which contained peaks of PLA hydrolysis products (Andersson et al. 2010) and the corresponding Na peaks. Peaks related to potential degradation products of PPy or CS, such as oxidised pyrrole oligomers or oligosaccharides, were not found in the studied m/z range of 200–1000.

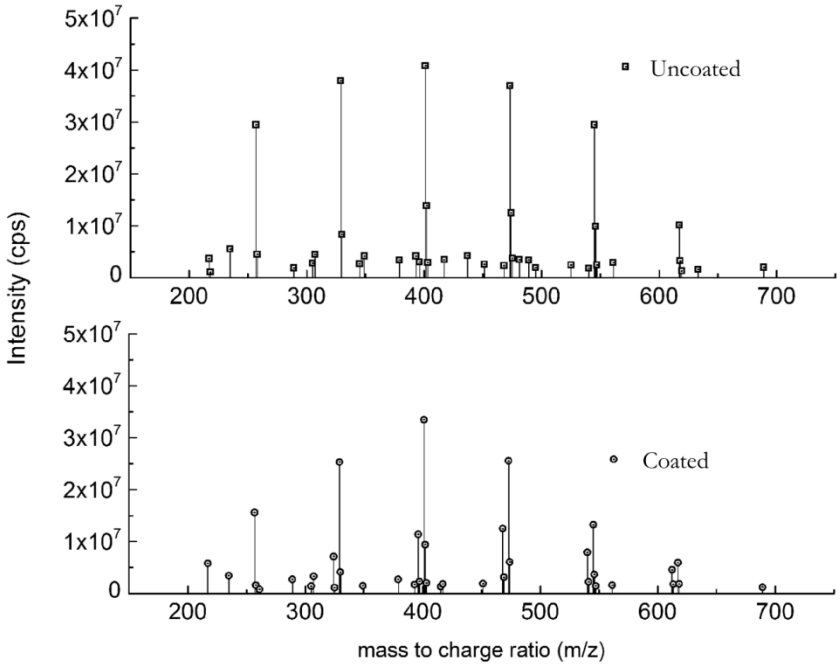

Figure 13. The hydrolysis products of coated and the uncoated scaffolds shown in ESI-MS spectra in Study **II**. All peaks were found in an m/z range of 200–700.

5.1.2 Adipose stem cell surface marker expression

The surface marker analysis was performed on all the cell lines used in the studies. The expression levels are presented in Table 7. According to the guidelines recommended for multipotency of MSCs (Dominici et al. 2006, Lindroos et al. 2010, McIntosh et al. 2006), the expression is considered positive when ≥75%, moderate in the range of 2–50% and there is a lack of expression when ≤2%. The positive expression of CD73, CD90 and CD105, which are the required positive markers in MSC identification, was apparent in both studies. Of those, however, CD105 showed a highly varying expression in Study **II**. Lack of expression was measured in both studies from CD14, CD19, CD45 and CD106. Moderate expression was detected in both studies from CD34, CD49d and HLA-ABC. Of those, the expression of CD34 greatly varied in Study **I**. Moreover, in Study **I**, HLA-DR was expressed moderately, whereas in Study **II** it was not expressed by hASCs.

Table 7. Surface marker expression of undifferentiated hASCs in Studies **I** and **II**. The results are presented as mean percentage ± SD of surface marker expression.

Surface protein	Antigen	Study **I**	Study **II**
CD14	Serum lipopolysaccharide-binding protein	1.7 ± 0.8	1.9 ± 2.3
CD19	B lymphocyte-lineage differentiation antigen	0.9 ± 0.4	0.5 ± 0.2
CD34	Sialomucin-like adhesion molecule	9.3 ± 8.75	26.4 ± 32.3
CD45	Leukocyte common antigen	1.1 ± 0.3	2.3 ± 1.7
CD49d	Integrin a2, VLA-4	11 ± 13	51.5 ± 14.4
CD73	Ecto-50-nucleotidase	91.2 ± 12.7	88.9 ± 2.7
CD90	Thy-1 (T-cell surface glycoprotein)	99 ± 0.3	98.1 ± 0.3
CD105	SH-2, endoglin	85.3 ± 12.1	82.5 ± 21.8
CD106	VCAM-1 (vascular cell adhesion molecule)	0.7 ± 0.3	1.7 ± 2.4
HLA-ABC	Major histocompatibility class I antigens	9.2 ± 7.0	22.7 ± 12.0
HLA-DR	Major histocompatibility class II antigens	7.0 ± 0.4	0.7 ± 0.3

CD: cluster of differentiation.

5.1.3 The attachment, morphology, viability and number of the adipose stem cells

The majority of the hASCs were viable in all of the experimental groups in both studies. However, crucial differences in spreading and attachment of the cells were seen in Study **I**, where hASCs strongly aggregated and detached on the PPy-HA surfaces (**Figure 14** E–H). In contrast, the cells on PPy-CS films (**Figure 14** A–D) showed substantially higher cell density and homogenous spreading even when compared to cells on PS (**Figure 14** I–J). Interestingly, the cells on PS were unevenly spread, forming a net-like pattern on the surface. Cell density increased with time on both PPy-CS and PS, whereas this could not be evaluated from PPy-HA due to the high detachment of the cells.

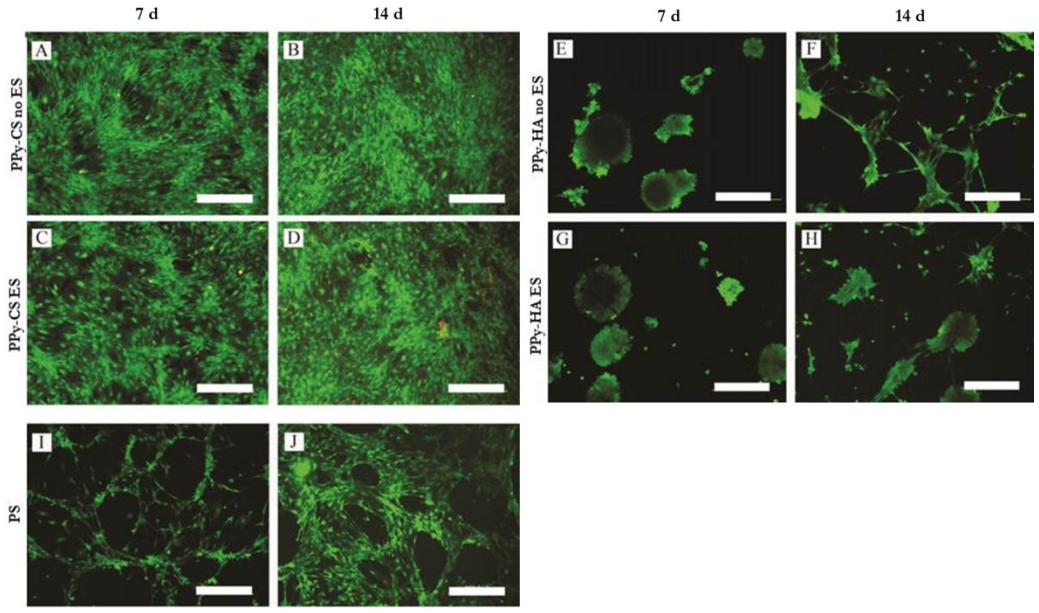

Figure 14. Cell viability, attachment and morphology were evaluated by live/dead imaging in Study **I**. The PPy-CS controls (A–B) and the ES group (C–D) were the most favourable films for hASCs and did not show any differences between the groups. Cells on the PPy-HA controls (E–F) as well as on PPy-HA ES films (G–H) aggregated equally. PS (I–J) acted as a control over cell morphology. The scale bar is 500 μm. ES: electrical stimulation; PPy-CS: chondroitin sulphate-doped PPy; PPy-HA: hyaluronic acid-doped PPy; PS: polystyrene.

In Study **II,** hASCs showed a clearly flatter and more elongated morphology in the coated scaffolds compared to the uncoated scaffolds (**Figure 15**) on day 14. This was also evident on both sides of the scaffolds, as well as on the cross-section of the scaffolds (data not shown). No differences in viability, morphology or attachment between the controls and stimulated groups were observed, nor were substantial differences in viability, morphology or attachment seen between the control and stimulation groups in either of the studies. Therefore, ES did not seem to compromise the viability of the cells.

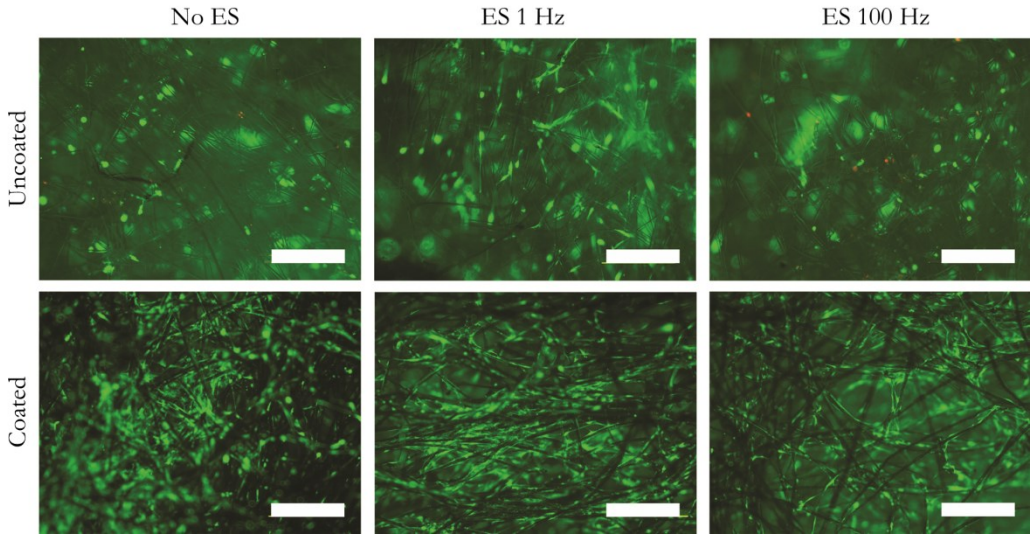

Figure 15. Live/dead images of hASCs on coated and uncoated scaffolds at the 14-day time point in Study **II**. The scale bar is 500 μm. ES: electrical stimulation.

Cell proliferation was evaluated quantitatively in both studies by measuring the total DNA content. In the control group on day 7, hASCs on PPy-CS showed a significantly higher cell number in comparison to those on PPy-HA in Study **I** (Figure 16). No differences were observed in the other groups, but the trend where PPy-CS induced a higher cell number remained similar in the stimulated groups. However, on day 14, the controls in PPy-CS and PPy-HA were at similar levels. The cell number increased significantly with time on both films in the control group, but only the PPy-CS samples showed a significant increase in the cell number under ES.

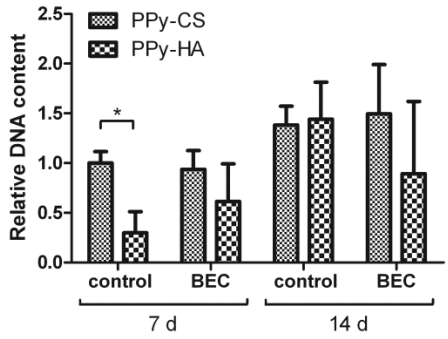

Figure 16. The relative DNA content of the hASCs in Study **I**. The results are expressed as mean ±SD and *=p<0.05. ES: electrical stimulation; PPy-CS: chondroitin sulphate-doped PPy; PPy-HA: hyaluronic acid-doped PPy.

In Study **II**, the cell number was significantly higher in the coated scaffolds when compared to uncoated scaffolds at all the time points, with the exception of the 7 d control and the 7 d 100 Hz (**Figure 17**). A significantly increased cell number was detected in 1 Hz group between day 1 and day 7 and in the control group between day 7 and day 14. No effect of ES on proliferation was observed in either of the stimulation groups.

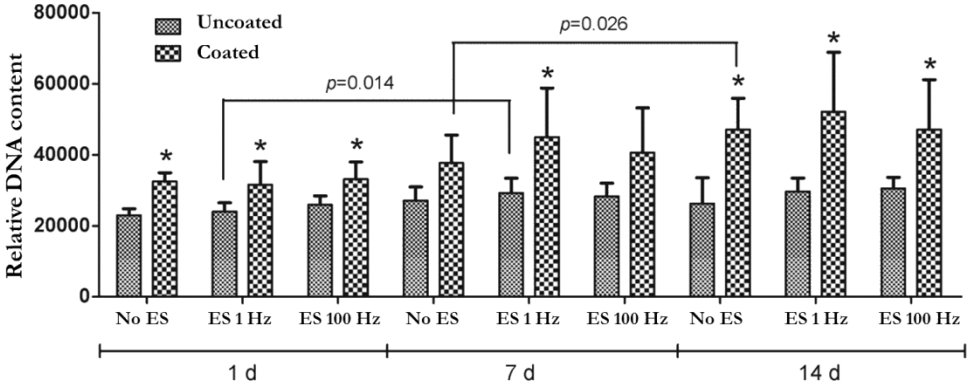

Figure 17. The relative DNA content of the hASCs in Study **II**. The results are expressed as mean ±SD and *= p<0.05. ES: electrical stimulation.

5.1.4 Osteogenic differentiation of adipose stem cells

In Study **I**, both film types supported early osteogenic differentiation according to ALP activity, and no significant differences between the films were found (**Figure 18**). However, a significant increase in ALP activity with time was seen only in hASCs on PPy-CS in both the control and the ES group. In Study **II**, ALP activity was at a higher level in the case of hASCs on coated scaffolds in all groups at 7 and 14 d (**Figure 19**). However, no significant differences were detected. One donor line did not show detectable ALP activity at any of the time points in Study **II**. Therefore, the data from only two donor lines is shown. Moreover, ALP activity varied substantially between the two donor lines.

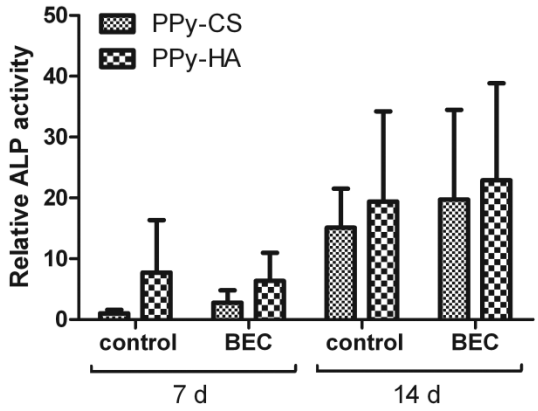

Figure 18. The relative ALP activity of the hASCs in Study **I**. The results are expressed as mean ±SD. ES: electrical stimulation.

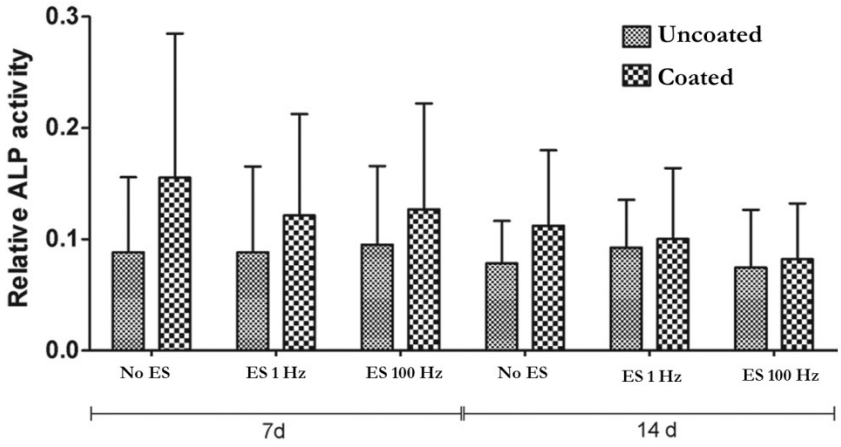

Figure 19. The relative ALP activity of the hASCs in Study **II**. The results are expressed as mean ±SD. ALP: alkaline phosphatase; ES: electrical stimulation.

No significant effect of ES was seen on ALP activity in either of the film or scaffold types in Studies **I** and **II** (**Figure 18** and **Figure 19**). However, in Study **I**, in late osteogenic differentiation at day 14, PPy-CS was superior to PPy-HA, inducing significantly higher mineralisation in the ES group. However, the PPy-CS and PPy-HA controls showed similar mineralisation levels (**Figure 20**). Mineralisation slightly increased with ES in both films types, and thus was not significant. In Study **I**, one donor line was excluded from the mineralisation data as it did not show detectable mineralisation levels. No effect of ES on ALP activity was detected.

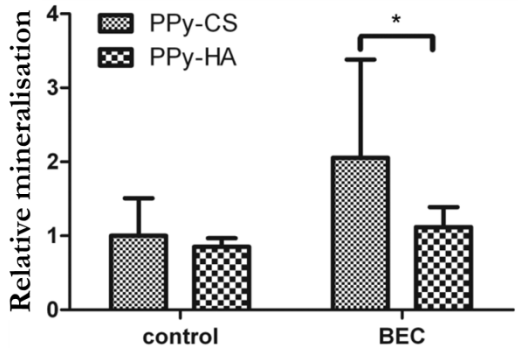

Figure 20. Relative ECM mineralisation in Study **I**. The results are expressed as mean ±SD, and *= $p<0.05$.

5.2 *In vivo* experiment

5.2.1 Post-operative examination

All rabbits recovered well from the operation even though one rabbit had a decubitus ulcer and another had a slight opening of surgical wound 3 wks postoperation. X-ray markers of the biodegradable screws were visible and in the right position (Figure 21) 8 wks postoperation.

The weight of the rabbits steadily increased with time, showing no differences between the experimental groups. Body temperature also remained stable in both groups during the study, and no differences were found.

Figure 21. A radiograph of a rabbit 8 wks postoperation in Study **III**. The β-TCB markers are shown by the red arrows and the steel screws by the yellow arrows.

5.2.2 Haematology and clinical chemistry

Monocyte, platelet counts, and blood urea nitrogen were significantly higher in the uncoated group when compared to the coated group 2 wks postoperation. The uncoated group also had a significantly higher blood cell count and platelet count 12 wks postoperation. No statistically significant differences were found between the groups at any other time point. When choosing the blood samples prior to the surgery as a baseline, no significant differences were found in the uncoated group. In the coated group, creatinine values per weight significantly increased 2 wks and 4 wks postoperation, but were still within the normal range. The creatinine values recovered back to baseline at the 12-week time point.

5.2.3 Organ and soft tissue examination

No significant differences in weight, appearance or histology of the organs were found between the groups. The heads of the coated, uncoated and steel screws were covered by new calluses that were more apparent in the 26-week subgroup.

Macroscopic examination showed no notable differences between the implantation site, and only slight haematoma, oedema or encapsulation was found in the surrounding soft tissue. No substantial differences in semi-quantitative evaluation were found either at the 12-week or 26-week time points. According to the semi-quantitative evaluation, the irritation level was slightly higher for the coated screws when compared to the uncoated screws.

5.2.4 Implant-tissue contact and new bone formation

Significantly higher torsional forces were required for the coated screws when compared to the uncoated screws when retracting them from the bone tissue (**Figure 22**). Five coated screws and two uncoated screws broke during the twist test.

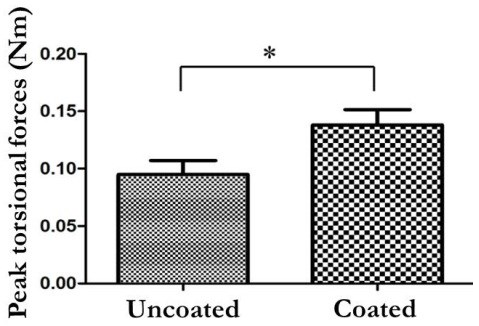

Figure 22. The peak values of the torsion forces of the coated and the uncoated screws in bone tissue in Study **III**. *= $p<0.05$.

Postoperative micro-CT measurements revealed a significantly greater amount of mineralised tissue in the coated samples than in the uncoated samples at both time points. Mineralised areas were found around most of the samples. Results for the 26-week subgroup are presented in **Figure 23**.

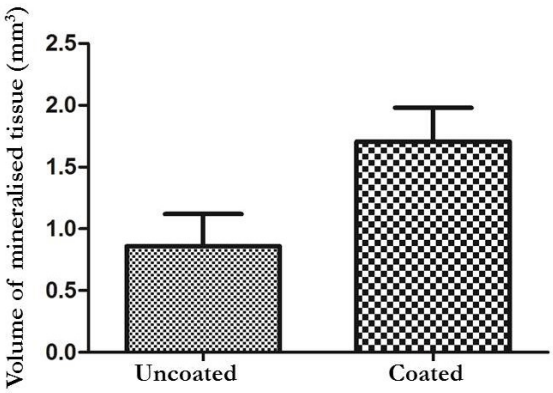

Figure 23. A quantitative evaluation of the mineralised areas around the screws 26 wks postoperation in Study **III** (B). *= $p<0.05$.

Tetracycline injections with 7 d intervals resulted in two tetracycline-labelled lines that illustrated the bone formation front in the hard tissue histology samples (**Figure 24**a). A significantly longer distance between the two tetracycline lines was found in the coated samples compared to the uncoated samples in both subgroups, as shown in **Figure 24**(b) and (c). This is directly proportional to the new bone formation rate, which indicates a significantly higher rate for the coated samples.

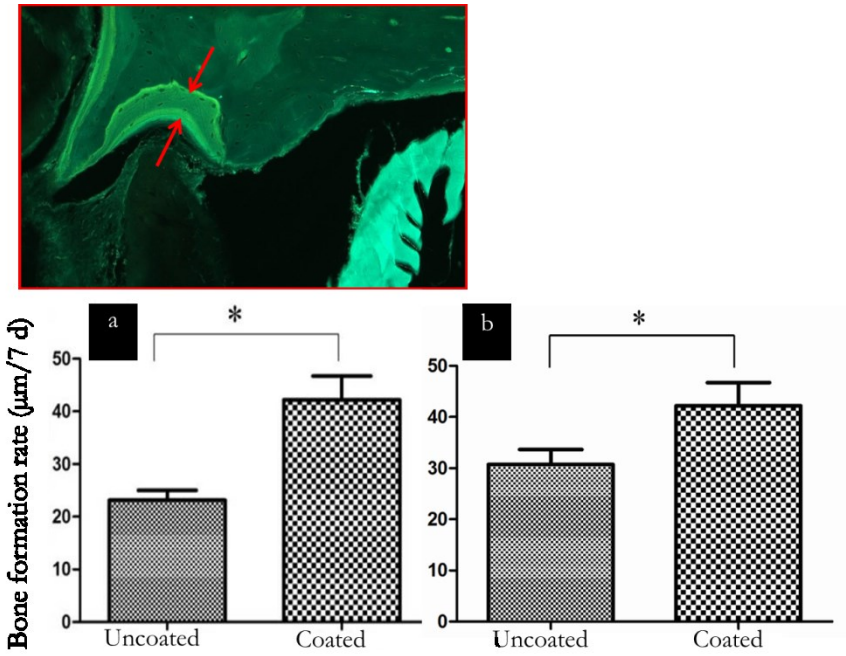

Figure 24. A quantitative evaluation of the bone formation rate measured from the average distance between the two tetracycline lines (a) in Study **III**. The scale bar is 100 µm. The coated screws induced a significantly higher bone formation rate compared to the uncoated screws 12 wks (b) and 26 wks (c) postoperation. *=$p<0.05$.

With regard to the hard tissue histology 12 wks postoperation, a darker blue band, indicating new bone, was found in the coated samples when compared to the uncoated samples (**Figure 25**). After a postoperation period of 26 wks, the dark blue band was similar between the uncoated and coated samples (**Figure 26**). The implant-bone interface was larger in the uncoated group compared to the coated group at the 12-week time point, as illustrated by a white band at the interface of the uncoated samples. No inflammation was detected from any of the samples. The PPy coating, stained with Toluidine blue, was apparent in the 12-week subgroup and some traces were found in a few coated samples in the 26-week subgroup. However, the presence of PPy had decreased substantially with time. Toluidine blue also stained PLGA, which showed as colourful stripes dominated by blue, green and yellow, in the 12-week subgroup. In addition, the total number of osteoblasts and chondroblasts at the bone-implant contact was significantly higher in the coated groups at both time points (data not shown).

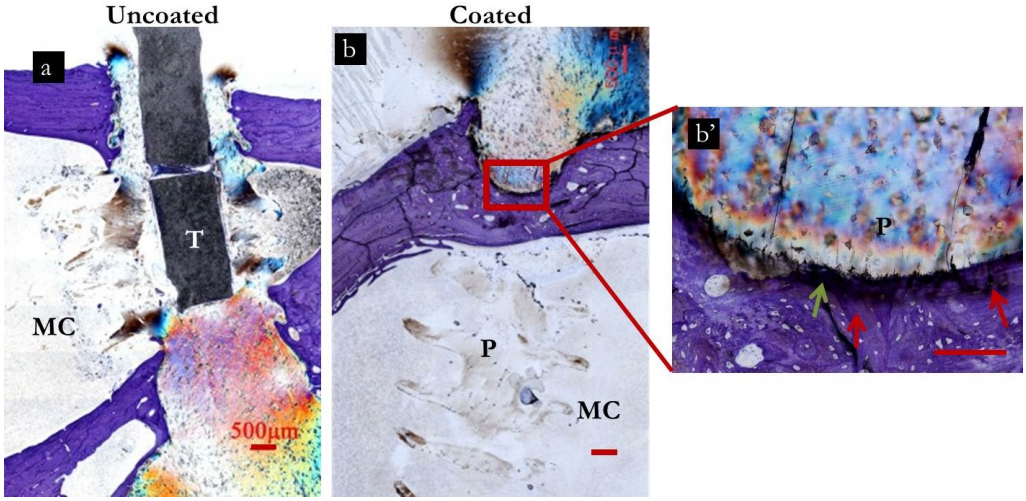

Figure 25. The hard tissue histology of the uncoated (a) and the coated (b and b') screw 12 wks postoperation in Study **III**. The samples were stained with Toluidine blue. The scale bar is 500 µm for figures a and b and 100 µm for figure b'. New bone is marked with red arrows. The PPy coating is marked with a green arrow. MC: marrow cavity; P: PLGA-β-TCP; T: β-TCP.

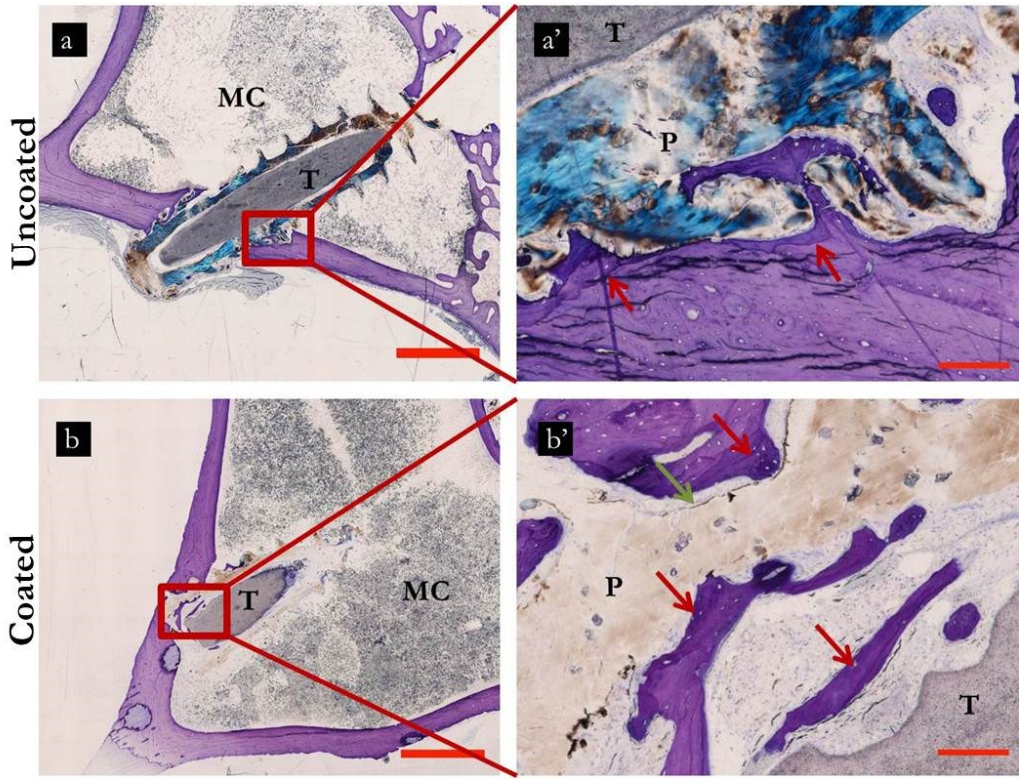

Figure 26. The hard tissue histology of the uncoated (a and a') and the coated (b and b') screw 26 wks postoperation in Study **III**. Samples were stained with Toluidine blue. The scale bar is 500 μm for a and b, and 100 μm for a' and b', which are magnifications from a and b respectively. New bone is marked with red arrows. Some traces of PPy coating were still found and are marked with the green arrow. MC: marrow cavity; P: PLGA-β-TCP; T: β-TCP.

6 Discussion

6.1 Effect of polypyrrole dopant *in vitro*

Surface chemistry is evidently a major factor in cell adhesion (Rivera-Chacon et al. 2013). Surface topography also plays an important role in controlling cell fate, as demonstrated in several topographical studies on titanium surfaces (Mendonca et al. 2011, Osathanon et al. 2011, Gittens et al. 2011, Kaivosoja et al. 2013, Myllymaa et al. 2010). Nano- and microroughness together have been reported to play an important role in the adhesion, proliferation and osteogenic differentiation of MSCs (Gittens et al. 2011). In Study **I**, CS- and HA-doped electrochemically polymerised PPy films were compared, revealing great differences in cell attachment. PPy-CS promoted cell attachment and homogenous spreading of the cells across the films, whereas PPy-HA triggered heavy aggregation and cell detachment. With regard to the AFM data of the films in PBS, PPy-HA revealed significantly higher Ra values and oval-shaped protrusions when compared to the lower Ra values of PPy-CS and its round-shaped protrusions. Moreno et al. (2009) reported poor attachment of mouse osteoblasts on rougher and more irregular PPy-HA surfaces in comparison to smooth PPy-HA films that were electrochemically polymerised with low (0.1 mA/cm^2) current densities. Moreover, similar results to Study **I** were found by Gelmi, Higgins & Wallace (2010), who reported larger nodules for electrochemically synthesised PPy-HA when compared to that of PPy-CS; they also reported that the PPy-HA nodules were more irregularly sized.

Surface morphology is not only affected by dopant content but also by the duration of the polymerisation or applied charge passing through the electrochemical cell during PPy synthesis (Gilmore et al. 2009). Increased polymerisation times increase the film thickness and subsequently result in a higher surface roughness of the films (Gilmore et al. 2009), whereas higher current densities are reported to yield rougher surfaces even though the total charge passing the electrical cell is kept constant (Serra Moreno et al. 2009, Serra Moreno & Panero 2012). In Study **I**, potentiostatic electrochemical synthesis was used, implying that the current density varied during the polymerisation. Therefore, a controlled surface morphology on the films was more challenging to achieve. However, the charge passing through the electrical cell was observed to increase steadily during the polymerisation in a similar fashion for both films.

Earlier reports indicate that the higher surface roughness and distinct topographical features of PPy-HA films were the most probable factors for hASC aggregation on

PPy-HA films (Serra Moreno et al. 2009, Gelmi, Higgins & Wallace 2010). According to the strong green fluorescence and the absence of red fluorescence in the viability assay in Study **I**, the aggregation of the cells on PPy-HA did not seem to compromise viability. This kind of surface could be exploited for anti-adhesion purposes, such as in chondrogenic differentiation, where cell aggregation is one of the earliest signs of chondrogenesis (Wu et al. 2010).

Other film properties that may have had an impact on hASC response are mechanical factors, such as the mechanical properties of the film and film actuation during ES. For example, Gelmi et al. (2010) reported that Young's modulus was higher for PPy-HA than for PPy-CS films. Moreover, PPy-CS showed a higher level of strain in electrochemical actuation, which was deduced to result from the lower Young's modulus of PPy-CS. Dopand chemistry and size may therefore have a substantial impact on the mechanical cues experienced by cells. These factors should be elucidated in future studies.

HA and CS were chosen for dopants because they are both frequently exploited in bone tissue engineering (Serra Moreno et al. 2012, Serra Moreno et al. 2009, Jha et al. 2011, Wollenweber et al. 2006, Rentsch et al. 2009). In a study where rat BMSCs were cultured on several different immobilised GAG surfaces, HA and CS were the only GAGs found to promote proliferation even without the addition of fibronectin or vitronectin (Uygun, Stojsih & Matthew 2009). Interestingly, in a similar study Mathews et al. (2014) reported the CS to have the weakest effect on osteoblast differentiation of BMSCs over the other GAGs tested, namely HA, HE, and dermatan sulphate. Moreover, HA provided the most favourable condition for osteogenic differentiation and ECM formation.

The significant increase in Ra values from dry to wet PPy films suggests that the films absorbed significant amounts of water. This was substantially stronger in PPy-HA films. Study **I** did not address the degree of water uptake, but earlier studies have reported a 19% swelling of similar PPy-CS films after soaking in PBS for 4 d (Serra Moreno et al. 2008) and 18.9% of water uptake by PPy-HA after 7 d of soaking in PBS (Serra Moreno et al. 2012). The aging of the films in PBS was reported to change the film morphologies to become rougher and more porous (Serra Moreno & Panero 2012). Another reason for changes in morphology in both films in Study **I** could be the ion exchange between PPy and the electrolyte. This does not necessarily require external potential changes; this was demonstrated by Serra Moreno and Panero (2012), who reported 97.55% HE content in PPy-HE films after 30 d soaking in PBS.

In order to reach further conclusions on the effect of PPy film properties on hASCs, more thorough characterisation should be done in future. For example, zeta potential characteristisation would bring valuable understanding about the electrical surface properties of PPy films in the function of pH (Mehmet et al. 2014). In

addition, the chemical composition could be characterised by energy-dispersive X-ray spectroscopy.

In Study **I**, proliferation was significantly lower with PPy-HA on day 7 but increased to a similar level as PPy-CS on day 14 in the non-stimulated group. Hence, despite the aggregation of the hASCs, PPy-HA films supported the increase in the cell number with time. Both films equally promoted ALP activity, which was at the highest level on day 14 in both groups and films types. Interestingly, mineralisation was found to be significantly higher in PPy-CS samples in the ES group, even though PPy-HA and PPy-CS showed similar levels of mineralisation in the control group. This suggests synergistic effects between PPy-CS and ES on the late osteogenic differentiation of hASCs in comparison to PPy-HA under ES. Earlier studies have not addressed PPy-CS impact on the mineralisation of osteoblastic cells. Only PPy-HA has been reported to increase ECM mineralisation of mice BMSCs (Serra Moreno et al. 2012).

6.2 Polypyrrole-coated polylactide fibre scaffolds for bone tissue engineering

Different strategies to fabricate PPy composite scaffolds have been tested by mixing PPy with ECM components, such as collagen (Yow et al. 2011) and ECM-like natural polymers, namely chitosan (Wan et al. 2005), alginate, (Sajesh et al. 2013) and gelatin (Vishnoi, Kumar 2013). One study has also addressed the use of PPy-coated PLA fibres for neurite outgrowth by synthesising poly(glutamic acid)–sodium dodecyl sulphate-codoped-PPy nanoparticles on a PLA fibre surface (Zeng et al. 2013). Other PPy composites tested for tissue engineering applications are fabricated as membranes and films (Hu et al. 2014, Zhang et al. 2013, Meng, Rouabhia & Zhang 2013, Shi et al. 2004, Castano et al. 2004, Lee, Lee & Schmidt 2009, Huang et al. 2010, Beattie et al. 2006). When compared to the earlier studies, Study **II** took a simpler approach to fabricating conductive 3D structures by minimising the use of chemicals needed for the process. The supporting PLA non-woven fibre structure was chosen for its biocompatibility and its favourable and well-characterised degradation and mechanical properties.

The PPy coating was chemically synthesised on PLA non-woven fibre scaffolds by immersing it into the mixture of pyrrole, oxidant and CS, which was found to be a suitable dopant in Study **I**. Coated scaffolds showed superior performance in comparison to uncoated scaffolds due to the better viability and morphology of hASCs on the coated scaffolds during the 14 days of the experiment. The morphology of the hASCs was elongated and flattened against the PPy coating, suggesting that the

coating provided plenty of suitable adhesion sites for the cells. By contrast, hASCs on plain PLA fibres were rounder and smaller. Moreover, the cell number was found to be significantly higher in PPy-coated scaffolds in most of the experimental groups. PPy-coated scaffolds also supported early osteogenic differentiation of hASCs; however, no significant differences were detected. ALP activity was at the highest level on day 7 and showed a slight decrease in all the groups at day 14. This could either indicate that osteogenic differentiation of hASCs had proceeded to a late differentiation stage at the 14-day time point, or that the cells experienced dedifferentiation during the decrease in ALP activity.

According to the results of Study **II**, PPy-coated fibres provided favourable *in vitro* conditions for hASCs over the plain PLA fibres. Before the actual experiments, PPy polymerisation conditions were optimised by varying the pyrrole and oxidant concentrations from 0.03–0.3 M and 0.01–0.1 M respectively, and polymerisation duration from 30 s to 15 min. The best coating ([pyrrole]=0.036 M, [APS]=0.1 M and [CS]=1 mg/ml, polymerisation time 150 s) was chosen for its highest conductivity and its uniformity (data not shown). Hu et al. (2014) tested the different oxidant and pyrrole concentrations in more detail with PPy membranes, using the same oxidant as used in Study **II**. They reported a thicker PPy layer and higher conductivity with increasing concentrations of pyrrole. The highest concentration, [pyrrole] = 0.5 M, [APS] = 0.1 M, was closest to Study **II**. The sheet conductivity for the films was measured at 0.25 mS (Hu et al. 2014). The roughness of the chemically synthesised PPy films has been reported to increase with increasing film thickness when fabricated with admicellar polymerisation (Castano et al. 2004). It is likely that the same phenomenon occurs in the chemical polymerisation without the use of a surfactant. The challenge lies in determining whether the optimal combination of conductivity and roughness in PPy coatings can be achieved.

The coated fibre surface was covered by fine nodules in Study **II**. Although direct comparison of the surface morphologies between studies **I** and **II** is challenging, given that they were done in different dimensions, some rough comparisons of the roughness and morphology of the PPy coatings can be made. Nodule sizes on the coated fibres, in comparison to the nodules found on the electrodeposited PPy films in Study **I**, were smaller, which was reflected in substantially lower Ra values for coated fibres. Ra values for PPy-CS films for Study **I** were ~320 nm whereas they were ~80 nm in Study **II** after soaking the fibres for 10 days in PBS. Hence, the relatively smoother surface of the chemically polymerised PPy coating on the fibres could have provided a more favourable surface roughness for the cells when compared to the PPy-CS film.

With regard to the degradation of the PPy coating in Study **II**, no traces of PPy or CS were found in the hydrolysed samples after 30 d under hydrolysis; only PLA

degradation products were detected. However, morphological changes in the PPy coating were evident during the course of 20 d of hydrolysis in PBS because the Ra values decreased substantially. The fibres were still fully covered by PPy after a 20-day incubation in PBS. Whether the morphological changes were due to PLA or PPy degradation, water uptake, ion exchange, or some other factor is unclear.

It is also unclear what role CS played in PPy coating properties. Viscosity measurements revealed CS rapidly splitting into fragments during the chemical oxidation of PPy (data not shown). However, the presence of CS rendered PPy surface permanently hydrophilic, but no traces of CS hydrolysis products were detected. This confirms that other polymerisation methods, such as emulsion polymerisation, should be used, if a strong presence of CS or other GAGs is required (Meng, Rouabhia & Zhang 2013, Meng et al. 2008).

According to measurements in Study **II**, the PPy coating clearly promoted lower impedance values when compared to the plain medium. Surprisingly, uncoated scaffolds resulted in lower impedance values in comparison to the medium, although this was to a lesser extent when compared to PPy-coated scaffolds. The relative permittivity of the medium (~80) is much higher than that of the dry PLA polymer (~3.5; Buchner, Hefter 2009, Pluta, Jeszka & Boiteux 2007). Even though PLA is an insulator, the surface ionic conductivity may have increased on the fibre surface. It is unclear how long the PPy coating stayed conductive during the cell culture in Study **II**. The DC and AC conductivity of the coated fibres was confirmed to be substantially higher than DMEM after 2 d of soaking in DMEM. However, an enhanced current flow along the PPy coating may have been exceeded since it is difficult to discriminate between ionic and electronic conductivity, and therefore current may have partly gone through DMEM.

6.3 Polypyrrole promotes bone regeneration *in vivo*

To date, very little is known about the impact of PPy on bone tissue even though several studies *in vitro* suggest its high potential in bone regeneration applications (Serra Moreno et al. 2012, Hu et al. 2014, Castano et al. 2004, Zelikin et al. 2002). As Study **II** revealed the excellent viability of hASCs with the chemically produced PPy coating, Study **III** took a step further to exploit the coating on bioabsorbable PLGA-β-TCP composite screws and to test it *in vivo* in a rabbit model. To minimise the number of rabbits, following the principles of the 3Rs (Gauthier, Griffin 2005), but still to receive quantitative and reliable data, three parallel screws were implanted in each hind leg of the rabbits. Moreover, suitable target tissues were found in the femur and tibia in order to test the screws in load-bearing conditions.

Coated screws did not induce acute, subchronic or chronic toxicity, as evaluated by the clinical signs, organ examination, soft tissue examination of the implant area, and haematology and clinical chemistry. Moreover, coated screws showed high compatibility with bone tissue throughout the 26-week-long implantation period, as neither inflammatory cells nor allergic reactions were found in the implant area according to the hard tissue histology. Coated screws were stored in appropriate sterile packages for ten months at ambient temperature before implantation and can therefore be considered to possess a reasonable self life, yet this will need to be further elucidaded with appropriate characterisation methods.

Interestingly, the PPy coating was found to significantly promote new bone formation in the implant site according to the micro-CT and the cell count from hard tissue histology samples in both the 12- and the 26-week subgroups. Hard tissue histology also showed bone tissue in a closer proximity to the coated implant surface than in the uncoated screws in the 12-week subgroup. This could explain why significantly higher torsional forces were required to retract coated screws from the bone tissue compared with the forces required for uncoated screws. During the torsion test, five coated screws broke, whereas this happened only twice for uncoated screws. This could either be due to stronger tissue-implant attachment or a higher degradation rate of the coated screws. In addition, the faster bone turnover of the coated screws compared with the uncoated was evidenced by the tetracycline labelling in the hard tissue samples showing greater distance between the two tetracycline-labelled lines at both time points. Tetracycline binds to newly mineralised bone tissue and can therefore be exploited to expose the present bone formation front at the time of administration (Pautke et al. 2010, Frost 1963).

The PPy coating was evident in the hard tissue histology samples in the 12-week subgroup, where the PLGA-β-TCP matrix was clearly present, but it started to show signs of degradation, as indicated by the deformations in the screw shape. Some traces of PPy were found in the 26-week subgroup. However, the PLGA-β-TCP matrix had heavily degraded by the 26-week time point, also causing PPy coating to crack and erode. The significantly increased creatinine levels in the coated group 2 wks and 4 wks after surgery suggest that PPy coating started to erode 2 wks after implantation; however, the erosion evidenced between twelve and 26-week time points did not affect renal functioning. Moreover, all the increased levels were still within normal range. The time course of the degradation and bone formation is similar to an earlier study conducted with PLA rods in rabbit bone tissue (Saikku-Bäckström et al. 2000). In this study, new bone formation was reported to commence between 6 and 12 wks after the implantation, and the molecular weight of the rods had decreased to less than 30% in 24 wks.

6.4 Electrical stimulation as a potential differentiation method in bone tissue engineering

ES has shown to affect MSC functioning in several ways *in vitro* depending on the electrical parameters used and the surrounding environment. Even though hASCS have shown great potential in bone tissue engineering due to their numerous advantages over BMSCs, the effect of ES on hASCs has so far only been addressed by a few studies in 2D (McCullen et al. 2010, Tandon et al. 2009b) and no studies exist in the 3D environment.

In studies **I** and **II,** pulsed BEC with a zero net charge was chosen because it prevents accumulation of charged proteins and keeps the pH at steady levels at low frequency (< 500 Hz) ranges (Kim et al. 2009, Bodamyali et al. 1999, Huang, Carter & Shepherd 2001). Large pH changes have a major effect on enzyme activity, such as ALP activity (Monfoulet et al. 2014), and changes in ionic conductivity of neural membrane have also been reported (Chesler 1990).

Earlier studies have discovered that resting periods between mechanical stimulation of bone restore the mechanosensitivity of desensitised bone cells (Robling, Burr & Turner 2001, Srinivasan et al. 2002, LaMothe & Zernicke 2004). LaMothe and Zernicke (2004) found the longest resting period, 8 h, to be the best recovery time. Tandon et al. (2009b) tested the short-term effects of DC (6 V/cm) in MM, reporting upregulation of several bone formation-related genes after 2 or 4 h of ES. Acute (~5 min) and chronic (4 h) effects of 1 Hz sinusoidal ES on hASCS were tested by McCullen et al. (2010), mapping the cell response under different potentials. The ES experiments were conducted in OM, resulting in an upregulated proliferation and mineralisation on certain potentials. Based on these earlier studies, 4 h stimulation and a 20 h rest period was chosen for studies **I** and **II**. The applied voltage, ±1 V/cm, was within safe physiological ranges that were previously screened by McCullen et al. (2010).

ES was first tested in a hASC monolayer under chemical osteoinduction in Study **I** by exploiting the electrochemically polymerised PPy-CS and PPy-HA films. The only noticeable effect of ES was seen in ECM mineralisation, which was higher on both films when compared to the control groups without ES, but this difference was not statistically significant. Interestingly, ES triggered significantly higher ECM mineralisation in hASCs on PPy-CS in comparison to those on PPy-HA. CV measurements in Study **I** revealed a slightly higher electrical activity of PPy-CS when compared to PPy-HA, which could partly explain the synergy between PPy-CS and ES. Higher electrical activity of similar PPy-CS films has also been demonstrated in an earlier study where PPy-CS had a higher total impedance in comparison to PPy-HA (Serra Moreno & Panero 2012). In Study **I**, the impedance of both films was at a

similar level, yet the impedance of PPy-CS slightly increased in low (<10 Hz) frequencies in comparison to PPy-HA. Cell response to ES may also be strongly dependent of the electrical properties of PPy. Hu et al. (2014) demonstrated how higher conductivity of PPy can lead to stronger ECM mineralisation of rat MSCs.

In Study **II**, an additional ES group with low frequency (1 Hz) was added and the hASC response was tested in 3D without chemical osteoinduction. ES was applied through coated scaffolds, which were expected to mediate the current along the PPy surface. Similar yet uncoated scaffolds were hypothesised to affect cells mainly via the electric field generated across the scaffold. There were no positive or negative effects observed in any of the groups in terms of viability, proliferation or early osteogenic differentiation. The results in Study **II** are supported by studies that report osteogenic differentiation of MSCs only responds to ES under chemical osteogenic induction (Titushkin et al. 2011, Kim et al. 2009, Hess et al. 2012b). However, the presence of OM during ES in Study **I** did not trigger a significant effect on osteogenic differentiation, apart from the earlier-mentioned effect on mineralisation. Proliferation of hBMSCs has been reported in MM in response to pulsed BEC (Kim et al. 2009), but Study **II** was the first to test the effect of ES on proliferation of hASCs in MM. The phenomena that hASCs may require chemical induction in order to respond to physical stimulus by osteogenic differentiation is already documented in a mechanical stimulation study by Tirkkonen et al. (2011); hASCs responded to vibration loading only in OM, and no significant effect was seen in MM. As ES and mechanical stimulation at least partly share the same internal signalling pathways, the analogue from mechanical stimulation to ES may be applicable (Balint, Cassidy & Cartmell 2013, Erickson & Nuccitelli 1984, Hammerick et al. 2010, Zhao 2009, Lin et al. 2008, Funk, Monsees & Özkucur 2009).

6.5 Donor variation of adipose stem cells

MSCs are a heterogeneous mixture of cells, and it was recently reported that a single MSC may use a distinct molecular mechanism to reach the common cell fate (Jääger et al. 2014). The differentiation potential and marker expression of MSCs varies greatly between donors, as evidenced by several studies (Alm et al. 2012, Bieback et al. 2012, Siddappa et al. 2007, Capra et al. 2012). For instance in Study **I**, HLA-DR was moderately expressed, but it ought to be negative according to the recommendations (Dominici et al. 2006). However, it has been reported to be more highly expressed in early passages and to decrease upon subsequent passage (McIntosh et al. 2006). Moderate expression was also detected from HLA-ABC in both *in vitro* studies.

HLA-ABC has earlier shown a varying expression – from moderate to positive – in hASCs (Lindroos et al. 2010, McIntosh et al. 2006).

High donor variability was observed in the osteogenic differentiation capability of hASCs in studies **I** and **II**. One donor line in Study **I** showed no detectable mineralisation in any of the groups. Similarly, one donor line in Study **II** showed no detectable ALP activity. Dexamethasone-induced variation in ALP activity in hBMSCs has been reported in the past (Alm et al. 2012, Siddappa et al. 2007). However, the age, gender, and source of isolation were reported not to affect the variability (Siddappa et al. 2007). Study **I** was conducted in OM, suggesting that dexamethasone could partly induce variability via ALP activity (Yadav et al. 2011, Whyte 2010). Study **II** was conducted in MM, but it also showed great variability in ALP activity. Donor variation is problematic in clinical treatments and therefore an allogenous MSC source from patients with the most optimal ASC characteristics has been considered. However, several issues, such as the immunosuppressive characteristics of ASCs, must be studied more closely (Lindroos, Suuronen & Miettinen 2011).

6.6 Future perspectives

Regenerative bone applications have advanced from simple biodegradable implants and scaffolds providing mechanical support to electrospun composite structures with drug releasing properties (Kolambkar et al. 2011, Fisher & Mauck 2013). Moreover, ECM-derived approaches, such as well-studied decellularised implants, have been further developed to construct complex tissues (Fisher & Mauck 2013), such as lung tissue (Petersen et al. 2010). Nevertheless, "conventional" lactide-based bioabsorbable polymers still prevail in load-bearing bone applications because, in addition to having good biocompatibility, they are easy to fabricate with controllable chemical and mechanical properties (Nair & Laurencin 2007, Makarov et al. 2013). However, the lack of bioactivity and the evident foreign body reaction that causes the formation of a fibrous capsule around the implant hinders the regeneration of the bone tissue (Kangas et al. 2006, Närhi et al. 2003). Studies **II** and **III** show that a simplistic approach of coating bioabsorbable lactide-based biomaterials with electroactive PPy can significantly improve proliferation of hASCs *in vitro*, and enhance new bone formation and attachment of the bone tissue to the implant surface *in vivo*. Importanly according to Study **III**, PPy coating seems to fulfil the requirements of not evoking an inflammatory or toxic response in body. The electroactive PPy coating could therefore introduce new opportunities for enhancing bone regeneration, not only by enabling immobilisation or incorporation of biomolecules onto its surface (Hu et al. 2014, Higgins et al. 2012), but also by mediating ES and thereby controlling cell fate as well

as the release profiles of possible bioactive molecules in the structure (Thompson et al. 2010, Thompson et al. 2011, Liu et al. 2009, Richardson et al. 2007, Esrafilzadeh et al. 2013). Even though the results in Study **III** showed that the erosion products of PPy as a coating did not seem to disturb bone regeneration, more studies investigating its erosion process *in vivo* should be conducted. This is particularly important when it comes to applying PPy in the bulk material. Furthermore, development of biodegradable and mechanically feasible, but still conductive PPy derivatives should be the focus of the future research as these areas do not meet the requirements of biomaterials described in Chapter 2.5.

Clinical case studies have provided evidence of the high potential of hASCs in bone tissue engineering (Sandor et al. 2014, Mesimäki et al. 2009, Thesleff et al. 2011, Kulakov et al. 2008, Lendeckel et al. 2004, Pak 2011, Taylor 2010). In order to gain recognition as an efficient treatment method, the *in vitro* cell culture time must be shortened by increasing the efficacy of the cell expansion and differentiation, and safety issues must be minimised. For instance, the role of MSCs in cancer is still under examination (Barkholt et al. 2013). ES could be used to accelerate the *in vitro* cell culture time or to provide an alternative to growth factors in regulating cell growth and differentiation. Moreover, ES has been reported to have antibacterial effects (Kloth 2005, Daeschlein et al. 2007), which could significantly facilitate the success and safety of *in vitro* products. As shown by the promising results with pre-osteoblasts, ES and PPy could also be combined with mechanical stimulation in future applications (Liu et al. 2013). However, before advancing into more complex systems, a more systematic approach must be taken to evaluate the impact of ES patterns on MSCs. As shown by earlier studies, certain types of ES can actually be mechanically sensed by the receptors (Hart 2006, Hart 2008). More information is therefore needed on the effect of ES at the single cell-level to determine the mechanism behind ES coupling with cell receptors to better evaluate the safety of ES at cellular level. Apart from comparing different parameters of ES, it must also be noted that the sensitivity of MSCs may change during osteogenic differentiation. For instance, stiff actin stress fibres of MSCs are more sensitive to ES than softer and more stable actin fibres in osteoblasts (Titushkin et al. 2011).

At present, the guidelines for minimal manipulation of cells, defined by the FDA, do not accept the combining of cells with a drug or device (U.S. Food and Drug Administration 2009). Given that electric fields play an important role in the function and regeneration of tissues (Sundelacruz, Levin & Kaplan 2008, Sundelacruz, Levin & Kaplan 2008, McCaig et al. 2005, Erickson & Nuccitelli 1984, Serena et al. 2009, Reid, Song & Zhao 2009), the controlled use of ES could provide more natural means of stimulating cells in comparison to extensively used drugs. However, the concept of minimal manipulation, as defined by the FDA, is very vague and does not give

detailed guidelines or examples (U.S. Food and Drug Administration 2009). The European Medicines Agency (EMA) considers expansion and differentiation of cells to be substantial manipulation and therefore beyond minimal manipulation (Committee for Advanced Therapies. 2011). It can therefore take a long time before worldwide regulations meet the products that science has to offer.

7 Conclusions

In this study, electroactive PPy coating was examined as a substrate for hASCs in bone tissue engineering with and without ES, and then further evaluated *in vivo* for orthopaedic applications. The main conclusions and findings from the studies are:

I. The electrochemically synthesised PPy-CS film supports hASCS attachment and homogenous spreading with and without ES in comparison to PPy-HA. On the PPy-HA film, hASCs formed aggregations owing to poor attachment to the substrate. Furthermore, a significantly higher mineralisation was detected in the case of PPy-CS films in comparison to PPy-HA, suggesting synergistic effects between PPy-CS and ES. No significant differences were found between unstimulated controls and electrically stimulated samples.

II. The chemically polymerised PPy coating on non-woven PLA fibre scaffolds with and without ES promoted significantly higher proliferation of hASCs when compared to the uncoated counterpart. In addition, the PPy coating induced favourable cell morphology and supported the early osteogenic differentiation of hASCs. In comparison to the non-stimulated samples, neither of the two ES patterns significantly affected cell viability or proliferation or ALP activity.

III. The chemically polymerised PPy coating on bioabsorbable PLGA-β-TCP composite screws for bone fixation proved to be biocompatible after the maximum 26 wks of implantation, showing no acute, systematic or chronic toxicity. Moreover, coated screws promoted significantly greater new bone formation according to micro-CT imaging and hard tissue histology compared to the uncoated screws. The rate of new bone formation was also significantly greater on the coated samples, as evidenced by the tetracycline labelling. In addition, superior attachment of coated screws to the bone tissue was evidenced by the torsion test.

PPy coating is recommended as a conductive hASCs substrate for bone tissue engineering and as multifunctional implant coating for bone regeneration purposes.

Acknowledgements

The work for this dissertation was conducted in the Adult Stem Cell Group, BioMediTech, University of Tampere during the years 2010–2014.

First and foremost, I would like to thank my supervisors. I am deeply grateful to my supervisor, Docent Suvi Haimi for her sedulous and highly professional guidance throughout my PhD studies. She did not only find the right way to challenge me to get the best out of me but she also gave highly valuable mentoring in the world of academic networking. I would not be a PhD without her. I also want to thank Docent Susanna Miettinen for being an excellent group leader of our "Mese group". Her leadership allowed an inspirational athmosphere, great team spirit and a strong base of scientific expertise to build on.

I truly appreciate the guidance of the reviewers of this dissertation, Associate Professor Joselito Razal and Professor Reijo Lappalainen. They gave me highly valuable comments and constructive criticism under a strict schedule.

I am also grateful to my follow-up group, Professor Jari Hyttinen and Sari Vannhatupa, PhD who gave me encouragement and valuable comments to finalise my PhD studies. I also want to thank people in "Regea" for creating a great work spirit and providing help and valuable advice.

The research that has resulted in my PhD has been a great team effort in this multidisclipinary field and for that I especially would like to acknowledge Jani Pelto, who provided me a highly useful "engineering aspect", which motivated me to think outside the box. I am also deeply grateful to my former collegue Aliisa Siljander who mentored me in the lab and gave valuable insights in the world of research in the beginning of my researcher career. My gratitude also goes to all other co-authors, Elina Talvitie, Minna Kellomäki, Bettina Mannerström, MingDong Zhao, Cao Lu, Wang Hui-Ren, and Jiang Yun-Qi.

I also want to thank all our group members, who have together created a very pleasant work environment. Special thanks go to Anna-Maija Honkala, Miia Juntunen and Sari Kalliokoski for their highly professional technical assistance and advice in cell culture work. I also owe my gratitude to my collegues and office mates, Laura Kyllönen, Sanni Virjula, and Sanna Huttunen for the delightful scientific and less scientific discussions shared in our office. I especially want to thank my collegue, Mimmi Patrikoski for her friendship and sharing the challenges of the research life – and life in general.

I want to express my gratitude to my dear and inspirational friend, Emily Trestrail, who kindly offered her help in getting my English writing in shape.

A special thanks to my dear lifelong friend Miia Pavela, with whom I shared the pains and joys of growing up. Thank you for just being there no matter how much

distance and time was sometimes between us. I also want to thank Mikko Pelkonen and Petra Knuuttila for sharing their friendship and being such good listeners.

I am truly grateful to my bubbly family "Omenainen". I want to thank my parents, Pirjo and Juha Hämäläinen who supported me throughout my life and gently guided me to the path of life that I am following now. Special thanks to my mother, Pirjo for sharing her expertise in quality assurance of medicinal products and half-secretly leading me to the field of biotechnology. I am also deeply grateful to my sister Enna and brother Samu just for being there and making my life very much less boring.

Finally, I am deeply grateful to my husband Hannes for his love and support at all times and keeping my feet on the ground when I was demanding a little too much from the life.

This work was financially supported by TEKES, the Finnish Funding Agency for Technology and Innovation, the competitive research funding of the Pirkanmaa Hospital District, University of Tampere, the Science Centre of Tampere City, and the Paulo Foundation.

8 References

Abidian, M.R., Daneshvar, E.D., Egeland, B.M., Kipke, D.R., Cederna, P.S. & Urbanchek, M.G. 2012, "Hybrid Conducting Polymer-Hydrogel Conduits for Axonal Growth and Neural Tissue Engineering", *Advanced Healthcare Materials,* vol. 1, no. 6, pp. 762-767.

Ahuja, T., Mir, I.A., Kumar, D. & Rajesh 2007, "Biomolecular immobilization on conducting polymers for biosensing applications", *Biomaterials,* vol. 28, no. 5, pp. 791-805.

Alagesan, S. & Griffin, M.D. 2014, "Autologous and allogeneic mesenchymal stem cells in organ transplantation: what do we know about their safety and efficacy?", *Current opinion in organ transplantation,* vol. 19, no. 1, pp. 65-72.

Alikacem, N., Marois, Y., Zhang, Z., Jakubiec, B., Roy, R., King, M.W. & Guidoin, R. 1999, "Tissue Reactions to Polypyrrole-Coated Polyesters: A Magnetic Resonance Relaxometry Study", *Artificial Organs,* vol. 23, no. 10, pp. 910-919.

Alm, J.J., Heino, T.J., Hentunen, T.A., Vaananen, H.K. & Aro, H.T. 2012, "Transient 100 nM dexamethasone treatment reduces inter- and intraindividual variations in osteoblastic differentiation of bone marrow-derived human mesenchymal stem cells", *Tissue Engineering.Part C, Methods,* vol. 18, no. 9, pp. 658-666.

Alvarez, C.V., Garcia-Lavandeira, M., Garcia-Rendueles, M.E., Diaz-Rodriguez, E., Garcia-Rendueles, A.R., Perez-Romero, S., Vila, T.V., Rodrigues, J.S., Lear, P.V. & Bravo, S.B. 2012, "Defining stem cell types: understanding the therapeutic potential of ESCs, ASCs, and iPS cells", *Journal of Molecular Endocrinology,* vol. 49, no. 2, pp. R89-111.

Andersson, S.R., Hakkarainen, M., Inkinen, S., Sodergard, A. & Albertsson, A.C. 2010, "Polylactide stereocomplexation leads to higher hydrolytic stability but more acidic hydrolysis product pattern", *Biomacromolecules,* vol. 11, no. 4, pp. 1067-1073.

Asselmeier, M.A., Caspari, R.B. & Bottenfield, S. 1993, "A review of allograft processing and sterilization techniques and their role in transmission of the human immunodeficiency virus", *The American Journal of Sports Medicine,* vol. 21, no. 2, pp. 170-175.

Ateh, D.D., Navsaria, H.A. & Vadgama, P. 2006, "Polypyrrole-based conducting polymers and interactions with biological tissues", *Journal of the Royal Society, Interface / the Royal Society,* vol. 3, no. 11, pp. 741-752.

Ates, M. 2013, "A review study of (bio)sensor systems based on conducting polymers", *Materials Science and Engineering: C,* vol. 33, no. 4, pp. 1853-1859.

Athanasiou, K.A., Niederauer, G.G. & Agrawal, C.M. 1996, "Sterilization, toxicity, biocompatibility and clinical applications of polylactic acid/ polyglycolic acid copolymers", *Biomaterials,* vol. 17, no. 2, pp. 93-102.

Awad, H.A., O'Keefe, R.J., Lee, C.H. & Mao, J.J. 2014, "Chapter 83 - Bone Tissue Engineering: Clinical Challenges and Emergent Advances in Orthopedic and

Craniofacial Surgery" in *Principles of Tissue Engineering (Fourth Edition)*, eds. R. Lanza, R. Langer & J. Vacanti, Academic Press, Boston, pp. 1733-1743.
Aznar-Cervantes, S., Roca, M.I., Martinez, J.G., Meseguer-Olmo, L., Cenis, J.L., Moraleda, J.M. & Otero, T.F. 2012, "Fabrication of conductive electrospun silk fibroin scaffolds by coating with polypyrrole for biomedical applications", *Bioelectrochemistry,* vol. 85, no. 0, pp. 36-43.
Bai, Y., Yin, G., Huang, Z., Liao, X., Chen, X., Yao, Y. & Pu, X. 2013, "Localized delivery of growth factors for angiogenesis and bone formation in tissue engineering", *International immunopharmacology,* vol. 16, no. 2, pp. 214-223.
Balint, R., Cassidy, N.J. & Cartmell, S.H. 2013, "Electrical stimulation: a novel tool for tissue engineering", *Tissue engineering.Part B, Reviews,* vol. 19, no. 1, pp. 48-57.
Balint, R., Cassidy, N.J., Araida Hidalgo-Bastida, L. & Cartmell, S. 2013, "Electrical Stimulation Enhanced Mesenchymal Stem Cell Gene Expression for Orthopaedic Tissue Repair", *Journal of Biomaterials and Tissue Engineering,* vol. 3, no. 2, pp. 212-221.
Balint, R., Cassidy, N.J. & Cartmell, S.H. 2014, "Conductive polymers: Towards a smart biomaterial for tissue engineering", *Acta Biomaterialia,* no. 14, pp. S1742-7061.
Barber, F.A., Dockery, W.D. & Hrnack, S.A. 2011, "Long-term degradation of a poly-lactide co-glycolide/beta-tricalcium phosphate biocomposite interference screw", *Arthroscopy : The Journal of Arthroscopic & Related Surgery : Official Publication of the Arthroscopy Association of North America and the International Arthroscopy Association,* vol. 27, no. 5, pp. 637-643.
Barkholt, L., Flory, E., Jekerle, V., Lucas-Samuel, S., Ahnert, P., Bisset, L., Büscher, D., Fibbe, W., Foussat, A., Kwa, M., Lantz, O., Mačiulaitis, R., Palomäki, T., Schneider, C.K., Sensebé, L., Tachdjian, G., Tarte, K., Tosca, L. & Salmikangas, P. 2013, "Risk of tumorigenicity in mesenchymal stromal cell–based therapies—Bridging scientific observations and regulatory viewpoints", *Cytotherapy,* vol. 15, no. 7, pp. 753-759.
Barrere, F., van Blitterswijk, C.A. & de Groot, K. 2006, "Bone regeneration: molecular and cellular interactions with calcium phosphate ceramics", *International Journal of Nanomedicine,* vol. 1, no. 3, pp. 317-332.
Beattie, D., Wong, K.H., Williams, C., Poole-Warren, L.A., Davis, T.P., Barner-Kowollik, C. & Stenzel, M.H. 2006, "Honeycomb-structured porous films from polypyrrole-containing block copolymers prepared via RAFT polymerization as a scaffold for cell growth", *Biomacromolecules,* vol. 7, no. 4, pp. 1072-1082.
Ben-David, U., Kopper, O. & Benvenisty, N. 2012, "Expanding the Boundaries of Embryonic Stem Cells", *Cell Stem Cell,* vol. 10, no. 6, pp. 666-677.
Bergsma, J.E., Rozema, F.R., Bos, R.R.M., Boering, G., de Bruijn, W.C. & Pennings, A.J. 1995, "In vivo degradation and biocompatibility study of in vitro pre-degraded as-polymerized polylactide particles", *Biomaterials,* vol. 16, no. 4, pp. 267-274.

Bertrand, J., Cromme, C., Umlauf, D., Frank, S. & Pap, T. 2010, "Molecular mechanisms of cartilage remodelling in osteoarthritis", *The International Journal of Biochemistry & Cell Biology,* vol. 42, no. 10, pp. 1594-1601.

Bieback, K., Hecker, A., Schlechter, T., Hofmann, I., Brousos, N., Redmer, T., Besser, D., Kluter, H., Muller, A.M. & Becker, M. 2012, "Replicative aging and differentiation potential of human adipose tissue-derived mesenchymal stromal cells expanded in pooled human or fetal bovine serum", *Cytotherapy,* vol. 14, no. 5, pp. 570-583.

Bioretec Ltd. 2014, *Bioretec.* Available: http://www.bioretec.com/ [2014, 04/5].

Bodamyali, T., Bhatt, B., Hughes, F.J., Winrow, V.R., Kanczler, J.M., Simon, B., Abbott, J., Blake, D.R. & Stevens, C.R. 1998, "Pulsed Electromagnetic Fields Simultaneously Induce Osteogenesis and Upregulate Transcription of Bone Morphogenetic Proteins 2 and 4 in Rat Osteoblastsin Vitro", *Biochemical and biophysical research communications,* vol. 250, no. 2, pp. 458-461.

Bodamyali, T., Kanczler, J.M., Simon, B., Blake, D.R. & Stevens, C.R. 1999, "Effect of Faradic Products on Direct Current-Stimulated Calvarial Organ Culture Calcium Levels", *Biochemical and biophysical research communications,* vol. 264, no. 3, pp. 657-661.

Boquest, A.C., Shahdadfar, A., Brinchmann, J.E. & Collas, P. 2006, "Isolation of stromal stem cells from human adipose tissue.", *Methods in molecular biology (Clifton, N.J.),* vol. 325, pp. 35-46.

Borden, M., Attawia, M., Khan, Y. & Laurencin, C.T. 2002, "Tissue engineered microsphere-based matrices for bone repair: design and evaluation", *Biomaterials,* vol. 23, no. 2, pp. 551-559.

Boskey, A.L. & Robey, P.G. 2013, "Chapter 11 - The Regulatory Role of Matrix Proteins in Mineralization of Bone" in *Osteoporosis (Fourth Edition)*, eds. R. Marcus, D. Feldman, D.W. Dempster, M. Luckey & J.A. Cauley, Academic Press, San Diego, pp. 235-255.

Boyce, B.F., Yao, Z. & Xing, L. 2009, "Osteoclasts have multiple roles in bone in addition to bone resorption", *Critical reviews in eukaryotic gene expression,* vol. 19, no. 3, pp. 171-180.

Bredas, J.L. & Street, B.G. 1985, "Polarons, bipolarons, and solitons in conducting polymers", *Accounts of Chemical Research,* vol. 18, no. 10, pp. 309-315.

Brown, J.L., Kumbar, S.G. & Laurencin, C.T. 2013, "Chapter II.6.7 - Bone Tissue Engineering" in *Biomaterials Science (Third Edition)*, eds. B.D. Ratner, A.S. Hoffman, F.J. Schoen & J.E. Lemons, Academic Press, pp. 1194-1214.

Buchner, R. & Hefter, G. 2009, "Interactions and dynamics in electrolyte solutions by dielectric spectroscopy", *Physical Chemistry Chemical Physics,* vol. 11, no. 40, pp. 8984-8999.

Calori, G.M., Mazza, E., Colombo, M. & Ripamonti, C. 2011, "The use of bone-graft substitutes in large bone defects: Any specific needs?", *Injury,* vol. 42, Supplement 2, no. 0, pp. S56-S63.

Cao, W. & Hench, L.L. 1996, "Bioactive materials", *Ceramics International,* vol. 22, no. 6, pp. 493-507.

Capra, E., Beretta, R., Parazzi, V., Vigano, M., Lazzari, L., Baldi, A. & Giordano, R. 2012, "Changes in the proteomic profile of adipose tissue-derived mesenchymal stem cells during passages", *Proteome science,* vol. 10, no. 1, pp. 46-5956-10-46.

Cardozo, A.J., Gómez, D.E. & Argibay, P.F. 2012, "Neurogenic differentiation of human adipose-derived stem cells: Relevance of different signaling molecules, transcription factors, and key marker genes", *Gene,* vol. 511, no. 2, pp. 427-436.

Carragee, E.J., Hurwitz, E.L. & Weiner, B.K. 2011, "A critical review of recombinant human bone morphogenetic protein-2 trials in spinal surgery: emerging safety concerns and lessons learned", *The spine journal : official journal of the North American Spine Society,* vol. 11, no. 6, pp. 471-491.

Castano, H., O'Rear, E.A., McFetridge, P.S. & Sikavitsas, V.I. 2004, "Polypyrrole Thin Films Formed by Admicellar Polymerization Support the Osteogenic Differentiation of Mesenchymal Stem Cells", *Macromolecular Bioscience,* vol. 4, no. 8, pp. 785-794.

Chen, S.-., Lei, M., Xie, X.-., Zheng, L.-., Yao, D., Wang, X.-., Li, W., Zhao, Z., Kong, A., Xiao, D.-., Wang, D.-., Pan, X.-., Wang, Y.-. & Qin, L. 2013, "PLGA/TCP composite scaffold incorporating bioactive phytomolecule icaritin for enhancement of bone defect repair in rabbits", *Acta Biomaterialia,* vol. 9, no. 5, pp. 6711-6722.

Cheng, X., Tsao, C., Sylvia, V.L., Cornet, D., Nicolella, D.P., Bredbenner, T.L. & Christy, R.J. 2014, "Platelet-derived growth-factor-releasing aligned collagen–nanoparticle fibers promote the proliferation and tenogenic differentiation of adipose-derived stem cells", *Acta Biomaterialia,* vol. 10, no. 3, pp. 1360-1369.

Chesler, M. 1990, "The regulation and modulation of pH in the nervous system", *Progress in neurobiology,* vol. 34, no. 5, pp. 401-427.

Chifflet, S., Hernandez, J.A. & Grasso, S. 2005, "A possible role for membrane depolarization in epithelial wound healing", *American journal of physiology.Cell physiology,* vol. 288, no. 6, pp. C1420-30.

Cho, M.R., Thatte, H.S., Silvia, M.T. & Golan, D.E. 1999, "Transmembrane calcium influx induced by ac electric fields", *FASEB journal : official publication of the Federation of American Societies for Experimental Biology,* vol. 13, no. 6, pp. 677-683.

Choi, K., Seo, Y., Yoon, H., Song, K., Kwon, S., Lee, H. & Park, J. 2008, "Effect of ascorbic acid on bone marrow-derived mesenchymal stem cell proliferation and differentiation", *Journal of Bioscience and Bioengineering,* vol. 105, no. 6, pp. 586-594.

Ciombor, D.M. & Aaron, R.K. 1993, "Influence of electromagnetic fields on endochondral bone formation", *Journal of cellular biochemistry,* vol. 52, no. 1, pp. 37-41.

Clarke, B. 2008, "Normal bone anatomy and physiology", *Clinical journal of the American Society of Nephrology : CJASN,* vol. 3 Suppl 3, pp. S131-9.

Coelho, M.J. & Fernandes, M.H. 2000, "Human bone cell cultures in biocompatibility testing. Part II: effect of ascorbic acid, β-glycerophosphate and dexamethasone on osteoblastic differentiation", *Biomaterials,* vol. 21, no. 11, pp. 1095-1102.

Cohen Jr., M.M. 2006, "The new bone biology: Pathologic, molecular, and clinical correlates", *American Journal of Medical Genetics Part A,* vol. 140A, no. 23, pp. 2646-2706.

Collier, J.H., Camp, J.P., Hudson, T.W. & Schmidt, C.E. 2000, "Synthesis and characterization of polypyrrole?hyaluronic acid composite biomaterials for tissue engineering applications", *Journal of Biomedical Materials Research,* vol. 50, no. 4, pp. 574-584.

Committee for Advanced Therapies. 2011, *Reflection paper on stem cell-based medicinal products*, European Medicines Agency.

Cosnier, S. 1999, "Biomolecule immobilization on electrode surfaces by entrapment or attachment to electrochemically polymerized films. A review", *Biosensors and Bioelectronics,* vol. 14, no. 5, pp. 443-456.

Creecy, C.M., O'Neill, C.F., Arulanandam, B.P., Sylvia, V.L., Navara, C.S. & Bizios, R. 2013, "Mesenchymal stem cell osteodifferentiation in response to alternating electric current", *Tissue engineering.Part A,* vol. 19, no. 3-4, pp. 467-474.

Csete, M. 2010, "Translational prospects for human induced pluripotent stem cells", *Regenerative Medicine,* vol. 5, no. 4, pp. 509-19.

Cypher, T.J. & Grossman, J.P. 1996, "Biological principles of bone graft healing", *The Journal of Foot and Ankle Surgery,* vol. 35, no. 5, pp. 413-417.

Daeschlein, G., Assadian, O., Kloth, L.C., Meinl, C., Ney, F. & Kramer, A. 2007, "Antibacterial activity of positive and negative polarity low-voltage pulsed current (LVPC) on six typical Gram-positive and Gram-negative bacterial pathogens of chronic wounds", *Wound Repair and Regeneration,* vol. 15, no. 3, pp. 399-403.

Dai, L. 2004, "Conducting polymers" in *Intelligent macromolecules for smart devices: from materials synthesis to device applications.*, ed. L. Dai, Springer, London, pp. 41-80.

Daley, G.Q. 2013, "Chapter 48 - Hematopoietic Stem Cells" in *Handbook of Stem Cells (Second Edition)*, eds. R. Lanza & A. Atala, Academic Press, San Diego, pp. 553-557.

Day, T.F., Guo, X., Garrett-Beal, L. & Yang, Y. 2005, "Wnt/beta-catenin signaling in mesenchymal progenitors controls osteoblast and chondrocyte differentiation during vertebrate skeletogenesis", *Developmental cell,* vol. 8, no. 5, pp. 739-750.

De Giglio, E., Guascito, M.R., Sabbatini, L. & Zambonin, G. 2001, "Electropolymerization of pyrrole on titanium substrates for the future development of new biocompatible surfaces", *Biomaterials,* vol. 22, no. 19, pp. 2609-2616.

De Giglio, E., Sabbatini, L., Colucci, S. & Zambonin, G. 2000, "Synthesis, analytical characterization, and osteoblast adhesion properties on RGD-grafted polypyrrole coatings on titanium substrates", *Journal of biomaterials science.Polymer edition,* vol. 11, no. 10, pp. 1073-1083.

De Giglio, E., Sabbatini, L. & Zambonin, P.G. 1999, "Development and analytical characterization of cysteine-grafted polypyrrole films electrosynthesized on Pt- and Ti-substrates as precursors of bioactive interfaces", *Journal of biomaterials science.Polymer edition,* vol. 10, no. 8, pp. 845-858.

Debusscher, F., Aunoble, S., Alsawad, Y., Clement, D. & Le Huec, J.C. 2009, "Anterior cervical fusion with a bio-resorbable composite cage (beta TCP-PLLA): clinical and radiological results from a prospective study on 20 patients", *European spine journal : official publication of the European Spine Society, the European Spinal Deformity Society, and the European Section of the Cervical Spine Research Society,* vol. 18, no. 9, pp. 1314-1320.

Deng, F., Ling, J., Ma, J., Liu, C. & Zhang, W. 2008, "Stimulation of intramembranous bone repair in rats by ghrelin", *Experimental physiology,* vol. 93, no. 7, pp. 872-879.

Di Iorio, E., Barbaro, V., Ferrari, S., Ortolani, C., De Luca, M. & Pellegrini, G. 2006, "Q-FIHC: Quantification of fluorescence immunohistochemistry to analyse p63 isoforms and cell cycle phases in human limbal stem cells", *Microscopy research and technique,* vol. 69, no. 12, pp. 983-991.

Dominici, M., Le Blanc, K., Mueller, I., Slaper-Cortenbach, I., Marini, F., Krause, D., Deans, R., Keating, A., Prockop, D. & Horwitz, E. 2006, "Minimal criteria for defining multipotent mesenchymal stromal cells. The International Society for Cellular Therapy position statement", *Cytotherapy,* vol. 8, no. 4, pp. 315-317.

Du, H.M., Zheng, X.H., Wang, L.Y., Tang, W., Liu, L., Jing, W., Lin, Y.F., Tian, W.D. & Long, J. 2012, "The osteogenic response of undifferentiated human adipose-derived stem cells under mechanical stimulation", *Cells, tissues, organs,* vol. 196, no. 4, pp. 313-324.

Ehrenfried, LisaMaria, Patel, MunnawwarH. & Cameron, RuthE. 2008, "The effect of tri-calcium phosphate (TCP) addition on the degradation of polylactide-co-glycolide (PLGA)", *Journal of Materials Science: Materials in Medicine,* vol. 19, no. 1, pp. 459-466.

Elbackly, R.M., Mastrogiacomo, M. & Cancedda, R. 2014, "Chapter 56 - Bone Regeneration and Bioengineering" in *Regenerative Medicine Applications in Organ Transplantation*, eds. G. Orlando, J. Lerut, S. Soker & R.J. Stratta, Academic Press, Boston, pp. 783-797.

Elefteriou, F. 2008, "Regulation of bone remodeling by the central and peripheral nervous system", *Archives of Biochemistry and Biophysics,* vol. 473, no. 2, pp. 231-236.

Ercan, B. & Webster, T.J. 2010, "The effect of biphasic electrical stimulation on osteoblast function at anodized nanotubular titanium surfaces", *Biomaterials,* vol. 31, no. 13, pp. 3684-3693.

Ercan, I., Günal, i. & Güven, O. 1995, "Conductance of polypyrole irradiated with gamma rays to low doses", *Radiation Physics and Chemistry,* vol. 46, no. 4–6, Part 1, pp. 813-817.

Erickson, C.A. & Nuccitelli, R. 1984, "Embryonic fibroblast motility and orientation can be influenced by physiological electric fields", *The Journal of cell biology,* vol. 98, no. 1, pp. 296-307.

Esko, J., Koji, K., Koji & Lindahl, U. 2009, "**Chapter 16 Proteoglycans and Sulfated Glycosaminoglycans**" in ***Essentials of Glycobiology.***, eds. A. Varki, R. Cummings, J. Esko, et al, 2nd edn, Cold Spring Harbor Laboratory Press, Cold Spring Harbor (NY).

Esrafilzadeh, D., Razal, J.M., Moulton, S.E., Stewart, E.M. & Wallace, G.G. 2013, "Multifunctional conducting fibres with electrically controlled release of ciprofloxacin", *Journal of Controlled Release,* vol. 169, no. 3, pp. 313-320.

Fakhry, M., Hamade, E., Badran, B., Buchet, R. & Magne, D. 2013, "Molecular mechanisms of mesenchymal stem cell differentiation towards osteoblasts", *World journal of stem cells,* vol. 5, no. 4, pp. 136-148.

Farre-Guasch, E., Prins, H.J., Overman, J.R., Ten Bruggenkate, C.M., Schulten, E.A., Helder, M.N. & Klein-Nulend, J. 2013, "Human maxillary sinus floor elevation as a model for bone regeneration enabling the application of one-step surgical procedures", *Tissue engineering.Part B, Reviews,* vol. 19, no. 1, pp. 69-82.

Ferraz, N., Strømme, M., Fellström, B., Pradhan, S., Nyholm, L. & Mihranyan, A. 2012, "In vitro and in vivo toxicity of rinsed and aged nanocellulose?polypyrrole composites", *Journal of Biomedical Materials Research Part A,* vol. 100A, no. 8, pp. 2128-2138.

Fisher, M.B. & Mauck, R.L. 2013, "Tissue engineering and regenerative medicine: recent innovations and the transition to translation", *Tissue engineering.Part B, Reviews,* vol. 19, no. 1, pp. 1-13.

Frost, H.M. 2004, "A 2003 update of bone physiology and Wolff's Law for clinicians", *The Angle Orthodontist,* vol. 74, no. 1, pp. 3-15.

Frost, H.M. 1963, "Measurement of human bone formation by means of tetracycline labelling", *Canadian journal of biochemistry and physiology,* vol. 41, pp. 31-42.

Fujishiro, Y., Oonishi, H. & Hench, L.L. 1997, "Quantitative comparison of in vivo bone generation with particulate" in *Bioceramics*, eds. L. Sedel & C. Rwy, Elsevier, New York, NY, pp. 283-286.

Fukada, E. & Yasuda, I. 1964, "Piezoelectric Effects in Collagen", *Japanese Journal of Applied Physics,* vol. 3, no. 2, pp. 117-121.

Funk, R.H.W., Monsees, T. & Özkucur, N. 2009, "Electromagnetic effects – From cell biology to medicine", *Progress in histochemistry and cytochemistry,* vol. 43, no. 4, pp. 177-264.

Garner, B., Georgevich, A., Hodgson, A.J., Liu, L. & Wallace, G.G. 1999, "Polypyrrole-heparin composites as stimulus-responsive substrates for endothelial cell growth", *Journal of Biomedical Materials Research,* vol. 44, no. 2, pp. 121-129.

Garrison, K.R., Donell, S., Ryder, J., Shemilt, I., Mugford, M., Harvey, I. & Song, F. 2007, "Clinical effectiveness and cost-effectiveness of bone morphogenetic

proteins in the non-healing of fractures and spinal fusion: a systematic review", *Health technology assessment (Winchester, England),* vol. 11, no. 30, pp. 1-150, iii-iv.
Gaudin-Audrain, C., Gallois, Y., Pascaretti-Grizon, F., Hubert, L., Massin, P., Basle, M.F. & Chappard, D. 2008, "Osteopontin is histochemically detected by the AgNOR acid-silver staining", *Histology and histopathology,* vol. 23, no. 4, pp. 469-478.
Gauthier, C. & Griffin, G. 2005, "Using animals in research, testing and teaching", *Revue scientifique et technique (International Office of Epizootics),* vol. 24, no. 2, pp. 735-745.
Gazdag, A.R., Lane, J.M., Glaser, D. & Forster, R.A. 1995, "Alternatives to Autogenous Bone Graft: Efficacy and Indications", *The Journal of the American Academy of Orthopaedic Surgeons,* vol. 3, no. 1, pp. 1-8.
Gazit, Z., Pelled, G., Sheyn, D., Kimelman, N. & Gazit, D. 2013, "Chapter 45 - Mesenchymal Stem Cells" in *Handbook of Stem Cells (Second Edition)*, eds. R. Lanza & A. Atala, Academic Press, San Diego, pp. 513-527.
Gelmi, A., Higgins, M.J. & Wallace, G.G. 2010, "Physical surface and electromechanical properties of doped polypyrrole biomaterials", *Biomaterials,* vol. 31, no. 8, pp. 1974-1983.
George, P.M., Lyckman, A.W., LaVan, D.A., Hegde, A., Leung, Y., Avasare, R., Testa, C., Alexander, P.M., Langer, R. & Sur, M. 2005, "Fabrication and biocompatibility of polypyrrole implants suitable for neural prosthetics", *Biomaterials,* vol. 26, no. 17, pp. 3511-3519.
Ghasemi-Mobarakeh, L., Prabhakaran, M.P., Morshed, M., Nasr-Esfahani, M.H., Baharvand, H., Kiani, S., Al-Deyab, S.S. & Ramakrishna, S. 2011, "Application of conductive polymers, scaffolds and electrical stimulation for nerve tissue engineering", *Journal of Tissue Engineering and Regenerative Medicine,* vol. 5, no. 4, pp. e17-e35.
Gilmore, K.J., Kita, M., Han, Y., Gelmi, A., Higgins, M.J., Moulton, S.E., Clark, G.M., Kapsa, R. & Wallace, G.G. 2009, "Skeletal muscle cell proliferation and differentiation on polypyrrole substrates doped with extracellular matrix components", *Biomaterials,* vol. 30, no. 29, pp. 5292-5304.
Gimble, J.M., Katz, A.J. & Bunnell, B.A. 2007, "Adipose-derived stem cells for regenerative medicine", *Circulation research,* vol. 100, no. 9, pp. 1249-1260.
Girija, T.C. & Sangaranarayanan, M.V. 2006, "Investigation of polyaniline-coated stainless steel electrodes for electrochemical supercapacitors", *Synthetic Metals,* vol. 156, no. 2–4, pp. 244-250.
Gittens, R.A., McLachlan, T., Olivares-Navarrete, R., Cai, Y., Berner, S., Tannenbaum, R., Schwartz, Z., Sandhage, K.H. & Boyan, B.D. 2011, "The effects of combined micron-/submicron-scale surface roughness and nanoscale features on cell proliferation and differentiation", *Biomaterials,* vol. 32, no. 13, pp. 3395-3403.
Goldman, R. & Pollack, S. 1996, "Electric fields and proliferation in a chronic wound model", *Bioelectromagnetics,* vol. 17, no. 6, pp. 450-457.

Gomez, N., Lee, J.Y., Nickels, J.D. & Schmidt, C.E. 2007, "Micropatterned Polypyrrole: A Combination of Electrical and Topographical Characteristics for the Stimulation of Cells", *Advanced Functional Materials,* vol. 17, no. 10, pp. 1645-1653.

Gonzalez-Rey, E., Anderson, P., Gonzalez, M.A., Rico, L., Buscher, D. & Delgado, M. 2009, "Human adult stem cells derived from adipose tissue protect against experimental colitis and sepsis", *Gut,* vol. 58, no. 7, pp. 929-939.

Gonzalez-Rey, E., Gonzalez, M.A., Varela, N., O'Valle, F., Hernandez-Cortes, P., Rico, L., Buscher, D. & Delgado, M. 2010, "Human adipose-derived mesenchymal stem cells reduce inflammatory and T cell responses and induce regulatory T cells in vitro in rheumatoid arthritis", *Annals of the Rheumatic Diseases,* vol. 69, no. 1, pp. 241-248.

Griffin, M. & Bayat, A. 2011, "Electrical Stimulation in Bone Healing: Critical Analysis by Evaluating Levels of Evidence", *Eplasty,* vol. 11.

Guicheux, J., Lemonnier, J., Ghayor, C., Suzuki, A., Palmer, G. & Caverzasio, J. 2003, "Activation of p38 Mitogen-Activated Protein Kinase and c-Jun-NH2-Terminal Kinase by BMP-2 and Their Implication in the Stimulation of Osteoblastic Cell Differentiation", *Journal of Bone and Mineral Research,* vol. 18, no. 11, pp. 2060-2068.

Guimard, N.K., Gomez, N. & Schmidt, C.E. 2007, "Conducting polymers in biomedical engineering", *Progress in Polymer Science,* vol. 32, no. 8–9, pp. 876-921.

Gunson, D., Gropp, K.E. & Varela, A. 2013, "Chapter 63 - Bone and Joints" in *Haschek and Rousseaux's Handbook of Toxicologic Pathology (Third Edition)*, eds. W.M. Haschek, C.G. Rousseaux & M.A. Wallig, Academic Press, Boston, pp. 2761-2858.

Guo, J., Jin, J. & Cooper, L.F. 2008, "Dissection of sets of genes that control the character of wnt5a-deficient mouse calvarial cells", *Bone,* vol. 43, no. 5, pp. 961-971.

Hammerick, K.E., James, A.W., Huang, Z., Prinz, F.B. & Longaker, M.T. 2010, "Pulsed direct current electric fields enhance osteogenesis in adipose-derived stromal cells", *Tissue engineering.Part A,* vol. 16, no. 3, pp. 917-931.

Hart, F.X. 2008, "The mechanical transduction of physiological strength electric fields", *Bioelectromagnetics,* vol. 29, no. 6, pp. 447-455.

Hart, F.X. 2006, "Integrins may serve as mechanical transducers for low-frequency electric fields", *Bioelectromagnetics,* vol. 27, no. 6, pp. 505-508.

Heinegård, D. 2009, "Proteoglycans and more - from molecules to biology", *International journal of experimental pathology,* vol. 90, no. 6, pp. 575-586.

Hess, R., Neubert, H., Seifert, A., Bierbaum, S., Hart, D.A. & Scharnweber, D. 2012a, "A novel approach for in vitro studies applying electrical fields to cell cultures by transformer-like coupling", *Cell biochemistry and biophysics,* vol. 64, no. 3, pp. 223-232.

Hess, R., Jaeschke, A., Neubert, H., Hintze, V., Moeller, S., Schnabelrauch, M., Wiesmann, H., Hart, D.A. & Scharnweber, D. 2012b, "Synergistic effect of defined artificial extracellular matrices and pulsed electric fields on osteogenic differentiation of human MSCs", *Biomaterials,* vol. 33, no. 35, pp. 8975-8985.

Higgins, M.J., Molino, P.J., Yue, Z. & Wallace, G.G. 2012, "Organic Conducting Polymer–Protein Interactions", *Chemistry of Materials,* vol. 24, no. 5, pp. 828.

Hodgkinson, T., Yuan, X. & Bayat, A. 2009, "Adult stem cells in tissue engineering", *Expert Review of Medical Devices,* vol. 6, no. 6, pp. 621-40.

Hronik-Tupaj, M., Rice, W.L., Cronin-Golomb, M., Kaplan, D.L. & Georgakoudi, I. 2011, "Osteoblastic differentiation and stress response of human mesenchymal stem cells exposed to alternating current electric fields", *Biomedical engineering online,* vol. 10, pp. 9.

Hu, W., Hsu, Y., Cheng, Y., Li, C., Ruaan, R., Chien, C., Chung, C. & Tsao, C. 2014, "Electrical stimulation to promote osteogenesis using conductive polypyrrole films", *Materials Science and Engineering: C,* vol. 37, no. 0, pp. 28-36.

Huang, C., Carter, P. & Shepherd, R. 2001, "Stimulus Induced pH Changes in Cochlear Implants: An In Vitro and In Vivo Study", vol. 29, no. 9, pp. 791-802.

Huang, J., Hu, X., Lu, L., Ye, Z., Zhang, Q. & Luo, Z. 2010, "Electrical regulation of Schwann cells using conductive polypyrrole/chitosan polymers", *Journal of Biomedical Materials Research Part A,* vol. 93A, no. 1, pp. 164-174.

Hwang, S.J., Song, Y.M., Cho, T.H., Kim, R.Y., Lee, T.H., Kim, S.J., Seo, Y.K. & Kim, I.S. 2012, "The implications of the response of human mesenchymal stromal cells in three-dimensional culture to electrical stimulation for tissue regeneration", *Tissue engineering.Part A,* vol. 18, no. 3-4, pp. 432-445.

Iijima, M., Muguruma, T., Brantley, W.A., Okayama, M., Yuasa, T. & Mizoguchi, I. 2008, "Torsional properties and microstructures of miniscrew implants", *American Journal of Orthodontics and Dentofacial Orthopedics : Official Publication of the American Association of Orthodontists, its Constituent Societies, and the American Board of Orthodontics,* vol. 134, no. 3, pp. 333.e1-6; discussion 333-4.

Jääger, K., Fatkina, A., Velts, A., Orav, E. & Neuman, T. 2014, "Variable expression of lineage regulators in differentiated stromal cells indicates distinct mechanisms of differentiation towards common cell fate", *Gene,* vol. 533, no. 1, pp. 173-179.

Jakubiec, B., Marois, Y., Zhang, Z., Roy, R., Sigot-Luizard, M., Dugré, F.J., King, M.W., Dao, L., Laroche, G. & Guidoin, R. 1998, "In vitro cellular response to polypyrrole-coated woven polyester fabrics: Potential benefits of electrical conductivity", *Journal of Biomedical Materials Research,* vol. 41, no. 4, pp. 519-526.

Jha, A.K., Xu, X., Duncan, R.L. & Jia, X. 2011, "Controlling the adhesion and differentiation of mesenchymal stem cells using hyaluronic acid-based, doubly crosslinked networks", *Biomaterials,* vol. 32, no. 10, pp. 2466-2478.

Jiang, X., Marois, Y., Traore, A., Tessier, D., Dao, L.H., Guidoin, R. & Zhang, Z. 2002, "Tissue reaction to polypyrrole-coated polyester fabrics: an in vivo study in rats", *Tissue engineering,* vol. 8, no. 4, pp. 635-647.

Jones, E. & McGonagle, D. 2008, "Human bone marrow mesenchymal stem cells in vivo", *Rheumatology,* vol. 47, no. 2, pp. 126-131.

Kai, D., Prabhakaran, M.P., Jin, G. & Ramakrishna, S. 2011, "Polypyrrole-contained electrospun conductive nanofibrous membranes for cardiac tissue engineering", *Journal of Biomedical Materials Research Part A,* vol. 99A, no. 3, pp. 376-385.

Kaivosoja E, Myllymaa S, Takakubo Y, Korhonen H, Myllymaa K, Konttinen YT, Lappalainen R, Takagi M. 2013, "Osteogenesis of human mesenchymal stem cells on micro-patterned surfaces", *Journal of Biomaterials Applications*, vol. 27, no. 7, pp. 862-71.

Kanczler, J.M. & Oreffo, R.O. 2008, "Osteogenesis and angiogenesis: the potential for engineering bone", *European cells & materials,* vol. 15, pp. 100-114.

Kang, K.S., Hong, J.M., Kang, J.A., Rhie, J.W. & Cho, D.W. 2013, "Osteogenic differentiation of human adipose-derived stem cells can be accelerated by controlling the frequency of continuous ultrasound", *Journal of ultrasound in medicine : official journal of the American Institute of Ultrasound in Medicine,* vol. 32, no. 8, pp. 1461-1470.

Kang, Q., Sun, M.H., Cheng, H., Peng, Y., Montag, A.G., Deyrup, A.T., Jiang, W., Luu, H.H., Luo, J., Szatkowski, J.P., Vanichakarn, P., Park, J.Y., Li, Y., Haydon, R.C. & He, T.C. 2004, "Characterization of the distinct orthotopic bone-forming activity of 14 BMPs using recombinant adenovirus-mediated gene delivery", *Gene therapy,* vol. 11, no. 17, pp. 1312-1320.

Kang, Y., Scully, A., Young, D.A., Kim, S., Tsao, H., Sen, M. & Yang, Y. 2011, "Enhanced mechanical performance and biological evaluation of a PLGA coated beta-TCP composite scaffold for load-bearing applications", *European polymer journal,* vol. 47, no. 8, pp. 1569-1577.

Kangas, J., Pajala, A., Leppilahti, J., Ryhanen, J., Lansman, S., Tormala, P., Waris, T. & Ashammakhi, N. 2006, "Histomorphometric analysis of poly-L/D-lactide 96/4 sutures in the gastrocnemius tendon of rabbits", *The International journal of artificial organs,* vol. 29, no. 9, pp. 893-899.

Katti, D.S., Lakshmi, S., Langer, R. & Laurencin, C.T. 2002, "Toxicity, biodegradation and elimination of polyanhydrides", *Advanced Drug Delivery Reviews,* vol. 54, no. 7, pp. 933-961.

Katti, D.S., Robinson, K.W., Ko, F.K. & Laurencin, C.T. 2004, "Bioresorbable nanofiber-based systems for wound healing and drug delivery: Optimization of fabrication parameters", *Journal of Biomedical Materials Research Part B: Applied Biomaterials,* vol. 70B, no. 2, pp. 286-296.

Kaynak, A., Rintoul, L. & George, G.A. 2000, "Change of mechanical and electrical properties of polypyrrole films with dopant concentration and oxidative aging", *Materials Research Bulletin,* vol. 35, no. 6, pp. 813-824.

Khanna-Jain, R., Mannerstrom, B., Vuorinen, A., Sandor, G.K., Suuronen, R. & Miettinen, S. 2012, "Osteogenic differentiation of human dental pulp stem cells

on beta-tricalcium phosphate/poly (l-lactic acid/caprolactone) three-dimensional scaffolds", *Journal of tissue engineering,* vol. 3, no. 1, pp. 2041731412467998.
Kim, I.S., Song, J.K., Song, Y.M., Cho, T.H., Lee, T.H., Lim, S.S., Kim, S.J. & Hwang, S.J. 2009, "Novel effect of biphasic electric current on in vitro osteogenesis and cytokine production in human mesenchymal stromal cells", *Tissue engineering.Part A,* vol. 15, no. 9, pp. 2411-2422.
Kim, I.S., Song, Y.M., Cho, T.H., Pan, H., Lee, T.H., Kim, S.J. & Hwang, S.J. 2011a, "Biphasic electrical targeting plays a significant role in schwann cell activation", *Tissue engineering.Part A,* vol. 17, no. 9-10, pp. 1327-1340.
Kim, S., Oh, W., Jeong, Y.S., Hong, J., Cho, B., Hahn, J. & Jang, J. 2011b, "Cytotoxicity of, and innate immune response to, size-controlled polypyrrole nanoparticles in mammalian cells", *Biomaterials,* vol. 32, no. 9, pp. 2342-2350.
Kloth, L.C. 2005, "Electrical stimulation for wound healing: a review of evidence from in vitro studies, animal experiments, and clinical trials", *The international journal of lower extremity wounds,* vol. 4, no. 1, pp. 23-44.
Knauf, M.J., Bell, D.P., Hirtzer, P., Luo, Z.P., Young, J.D. & Katre, N.V. 1988, "Relationship of effective molecular size to systemic clearance in rats of recombinant interleukin-2 chemically modified with water-soluble polymers", *The Journal of biological chemistry,* vol. 263, no. 29, pp. 15064-15070.
Knippenberg, M., Helder, M.N., Doulabi, B.Z., Semeins, C.M., Wuisman, P.I. & Klein-Nulend, J. 2005, "Adipose tissue-derived mesenchymal stem cells acquire bone cell-like responsiveness to fluid shear stress on osteogenic stimulation", *Tissue engineering,* vol. 11, no. 11-12, pp. 1780-1788.
Kocaoemer, A., Kern, S., Klüter, H. & Bieback, K. 2007, "Human AB Serum and Thrombin-Activated Platelet-Rich Plasma Are Suitable Alternatives to Fetal Calf Serum for the Expansion of Mesenchymal Stem Cells from Adipose Tissue", *Stem cells,* vol. 25, no. 5, pp. 1270-1278.
Kokovic, V. & Todorovic, L. 2011, "Preimplantation filling of tooth socket with beta-tricalcium phosphate/polylactic-polyglycolic acid (beta-TCP/PLGA) root analogue: clinical and histological analysis in a patient", *Vojnosanitetski pregled.Military-medical and pharmaceutical review,* vol. 68, no. 4, pp. 366-371.
Kokubo, T. & Takadama, H. 2006, "How useful is SBF in predicting in vivo bone bioactivity?", *Biomaterials,* vol. 27, no. 15, pp. 2907-2915.
Kolambkar, Y.M., Dupont, K.M., Boerckel, J.D., Huebsch, N., Mooney, D.J., Hutmacher, D.W. & Guldberg, R.E. 2011, "An alginate-based hybrid system for growth factor delivery in the functional repair of large bone defects", *Biomaterials,* vol. 32, no. 1, pp. 65-74.
Kooistra, B.W., Jain, A. & Hanson, B.P. 2009, "Electrical stimulation: Nonunions", *Indian journal of orthopaedics,* vol. 43, no. 2, pp. 149-155.
Kulakov, A.A., Goldshtein, D.V., Grigoryan, A.S., Rzhaninova, A.A., Alekseeva, I.S., Arutyunyan, I.V. & Volkov, A.V. 2008, "Clinical study of the efficiency of combined cell transplant on the basis of multipotent mesenchymal stromal

adipose tissue cells in patients with pronounced deficit of the maxillary and mandibulary bone tissue", *Bulletin of experimental biology and medicine,* vol. 146, no. 4, pp. 522-525.

Kwon, S., Jun, Y., Hong, S., Lee, I., Kim, H. & Won, Y.Y. 2002, "Calcium Phosphate Bioceramics with Various Porosities and Dissolution Rates", *Journal of the American Ceramic Society,* vol. 85, no. 12, pp. 3129-3131.

Kyllonen, L., Haimi, S., Mannerstrom, B., Huhtala, H., Rajala, K.M., Skottman, H., Sandor, G.K. & Miettinen, S. 2013a, "Effects of different serum conditions on osteogenic differentiation of human adipose stem cells in vitro", *Stem cell research & therapy,* vol. 4, no. 1, pp. 17.

Kyllonen, L., Haimi, S., Sakkinen, J., Kuokkanen, H., Mannerstrom, B., Sandor, G.K. & Miettinen, S. 2013b, "Exogenously added BMP-6, BMP-7 and VEGF may not enhance the osteogenic differentiation of human adipose stem cells", *Growth factors (Chur, Switzerland),* vol. 31, no. 5, pp. 141-153.

LaMothe, J.M. & Zernicke, R.F. 2004, "Rest insertion combined with high-frequency loading enhances osteogenesis", *Journal of applied physiology (Bethesda, Md.: 1985),* vol. 96, no. 5, pp. 1788-1793.

Lecanda, F., Towler, D.A., Ziambaras, K., Cheng, S.L., Koval, M., Steinberg, T.H. & Civitelli, R. 1998, "Gap junctional communication modulates gene expression in osteoblastic cells", *Molecular biology of the cell,* vol. 9, no. 8, pp. 2249-2258.

Lee, J.Y., Lee, J.W. & Schmidt, C.E. 2009, "Neuroactive conducting scaffolds: nerve growth factor conjugation on active ester-functionalized polypyrrole", *Journal of the Royal Society, Interface / the Royal Society,* vol. 6, no. 38, pp. 801-810.

Lee, W.-.C., Sepulveda, J.L., Rubin, J.P. & Marra, K.G. 2009, "Cardiomyogenic differentiation potential of human adipose precursor cells", *International journal of cardiology,* vol. 133, no. 3, pp. 399-401.

Lendeckel, S., Jödicke, A., Christophis, P., Heidinger, K., Wolff, J., Fraser, J.K., Hedrick, M.H., Berthold, L. & Howaldt, H. 2004, "Autologous stem cells (adipose) and fibrin glue used to treat widespread traumatic calvarial defects: case report", *Journal of Cranio-Maxillofacial Surgery,* vol. 32, no. 6, pp. 370-373.

Leroith, D., Scheinman, E.J. & Bitton-Worms, K. 2011, "The Role of Insulin and Insulin-like Growth Factors in the Increased Risk of Cancer in Diabetes", *Rambam Maimonides medical journal,* vol. 2, no. 2, pp. e0043.

Leto Barone, A.A., Khalifian, S., Lee, W.P. & Brandacher, G. 2013, "Immunomodulatory effects of adipose-derived stem cells: fact or fiction?", *BioMed research international,* vol. 2013, pp. 383685.

Levin, M. 2007, "Large-scale biophysics: ion flows and regeneration", *Trends in cell biology,* vol. 17, no. 6, pp. 261-270.

Lewandrowski, K., D. Gresser, J., Wise, D.L. & Trantolo, D.J. 2000, "Bioresorbable bone graft substitutes of different osteoconductivities: a histologic evaluation of osteointegration of poly(propylene glycol-co-fumaric acid)-based cement implants in rats", *Biomaterials,* vol. 21, no. 8, pp. 757-764.

Li, J.K., Lin, J.C., Liu, H.C., Sun, J.S., Ruaan, R.C., Shih, C. & Chang, W.H. 2006, "Comparison of ultrasound and electromagnetic field effects on osteoblast growth", *Ultrasound in medicine & biology,* vol. 32, no. 5, pp. 769-775.

Li, J. & Stocum, D.L. 2014, "Chapter 10 - Fracture Healing" in *Basic and Applied Bone Biology*, eds. D.B. Burr & M.R. Allen, Academic Press, San Diego, pp. 205-223.

LI, X. & Cao, X. 2006, "BMP Signaling and Skeletogenesis", *Annals of the New York Academy of Sciences,* vol. 1068, no. 1, pp. 26-40.

Lin, F., Baldessari, F., Gyenge, C.C., Sato, T., Chambers, R.D., Santiago, J.G. & Butcher, E.C. 2008, "Lymphocyte electrotaxis in vitro and in vivo", *Journal of immunology (Baltimore, Md.: 1950),* vol. 181, no. 4, pp. 2465-2471.

Lindroos, B., Aho, K.L., Kuokkanen, H., Raty, S., Huhtala, H., Lemponen, R., Yli-Harja, O., Suuronen, R. & Miettinen, S. 2010, "Differential gene expression in adipose stem cells cultured in allogeneic human serum versus fetal bovine serum", *Tissue engineering.Part A,* vol. 16, no. 7, pp. 2281-2294.

Lindroos, B., Boucher, S., Chase, L., Kuokkanen, H., Huhtala, H., Haataja, R., Vemuri, M., Suuronen, R. & Miettinen, S. 2009, "Serum-free, xeno-free culture media maintain the proliferation rate and multipotentiality of adipose stem cells in vitro", *Cytotherapy,* vol. 11, no. 7, pp. 958-972.

Lindroos, B., Suuronen, R. & Miettinen, S. 2011, "The Potential of Adipose Stem Cells in Regenerative Medicine", *Stem Cell Reviews,* vol. 7, no. 2, pp. 269-91.

Liu, A., Zhao, L., Bai, H., Zhao, H., Xing, X. & Shi, G. 2009, "Polypyrrole actuator with a bioadhesive surface for accumulating bacteria from physiological media", *ACS applied materials & interfaces,* vol. 1, no. 4, pp. 951-955.

Liu, B. & Lun, D. 2012, "Current Application of β-tricalcium Phosphate Composites in Orthopaedics", *Orthopaedic Surgery,* vol. 4, no. 3, pp. 139-144.

Liu, H., Slamovich, E.B. & Webster, T.J. 2006, "Less harmful acidic degradation of poly(lacticco-glycolic acid) bone tissue engineering scaffolds through titania nanoparticle addition", *International journal of nanomedicine,* vol. 1, no. 4, pp. 541-545.

Liu, L., Li, P., Zhou, G., Wang, M., Jia, X., Liu, M., Niu, X., Song, W., Liu, H. & Fan, Y. 2013, "Increased proliferation and differentiation of pre-osteoblasts MC3T3-E1 cells on nanostructured polypyrrole membrane under combined electrical and mechanical stimulation", *Journal of biomedical nanotechnology,* vol. 9, no. 9, pp. 1532-1539.

Liu, X., Gilmore, K.J., Moulton, S.E. & Wallace, G.G. 2009, "Electrical stimulation promotes nerve cell differentiation on polypyrrole/poly (2-methoxy-5 aniline sulfonic acid) composites", *Journal of neural engineering,* vol. 6, no. 6, pp. 065002-2560/6/6/065002. Epub 2009 Oct 23.

Liu, Y., Wu, G. & de Groot, K. 2010, "Biomimetic coatings for bone tissue engineering of critical-sized defects", *Journal of the Royal Society, Interface / the Royal Society,* vol. 7 Suppl 5, pp. S631-47.

Llucià-Valldeperas, A., Sanchez, B., Soler-Botija, C., Gálvez-Montón, C., Prat-Vidal, C., Roura, S., Rosell-Ferrer, J., Bragos, R. & Bayes-Genis, A. 2013, "Electrical stimulation of cardiac adipose tissue-derived progenitor cells modulates cell phenotype and genetic machinery", *Journal of Tissue Engineering and Regenerative Medicine*.

Lu, Y. & Chen, S.C. 2004, "Micro and nano-fabrication of biodegradable polymers for drug delivery", *Advanced Drug Delivery Reviews,* vol. 56, no. 11, pp. 1621-1633.

Luginbuehl, V., Ruffieux, K., Hess, C., Reichardt, D., von Rechenberg, B. & Nuss, K. 2010, "Controlled release of tetracycline from biodegradable β-tricalcium phosphate composites", *Journal of Biomedical Materials Research Part B: Applied Biomaterials,* vol. 92B, no. 2, pp. 341-352.

Luu, H.H., Song, W., Luo, X., Manning, D., Luo, J., Deng, Z., Sharff, K.A., Montag, A.G., Haydon, R.C. & He, T. 2007, "Distinct roles of bone morphogenetic proteins in osteogenic differentiation of mesenchymal stem cells", *Journal of Orthopaedic Research,* vol. 25, no. 5, pp. 665-677.

Mackie, E.J., Ahmed, Y.A., Tatarczuch, L., Chen, K.-. & Mirams, M. 2008, "Endochondral ossification: How cartilage is converted into bone in the developing skeleton", *The international journal of biochemistry & cell biology,* vol. 40, no. 1, pp. 46-62.

Makarov, C., Berdicevsky, I., Raz-Pasteur, A. & Gotman, I. 2013, "In vitro antimicrobial activity of vancomycin-eluting bioresorbable beta-TCP-polylactic acid nanocomposite material for load-bearing bone repair", *Journal of materials science.Materials in medicine,* vol. 24, no. 3, pp. 679-687.

Martin, T.J., Wah Ng, K. & Sims, N.A. 2013, "Chapter 2 - Basic Principles of Bone Cell Biology" in *Translational Endocrinology of Bone*, ed. G. Karsenty, Academic Press, San Diego, pp. 5-26.

Martinez, J.G., Otero, T.F. & Jager, E.W. 2014, "Effect of the Electrolyte Concentration and Substrate on Conducting Polymer Actuators", *Langmuir : the ACS journal of surfaces and colloids*.

Massague, J. 1998, "TGF-beta signal transduction", *Annual Review of Biochemistry,* vol. 67, pp. 753-791.

Mathews, S., Mathew, S.A., Gupta, P.K., Bhonde, R. & Totey, S. 2014, "Glycosaminoglycans enhance osteoblast differentiation of bone marrow derived human mesenchymal stem cells", *Journal of Tissue Engineering and Regenerative Medicine,* vol. 8, no. 2, pp. 143-152.

Matsuda, N., Morita, N., Matsuda, K. & Watanabe, M. 1998, "Proliferation and Differentiation of Human Osteoblastic Cells Associated with Differential Activation of MAP Kinases in Response to Epidermal Growth Factor, Hypoxia, and Mechanical Stressin Vitro", *Biochemical and biophysical research communications,* vol. 249, no. 2, pp. 350-354.

Maurus, P.B. & Kaeding, C.C. 2004, "Bioabsorbable implant material review", *Operative Techniques in Sports Medicine,* vol. 12, no. 3, pp. 158-160.

McCaig, C.D., Rajnicek, A.M., Song, B. & Zhao, M. 2005, "Controlling cell behavior electrically: current views and future potential", *Physiological Reviews,* vol. 85, no. 3, pp. 943-978.

McCaig, C.D., Song, B. & Rajnicek, A.M. 2009, "Electrical dimensions in cell science", *Journal of cell science,* vol. 122, no. Pt 23, pp. 4267-4276.

McCullen, S.D., McQuilling, J.P., Grossfeld, R.M., Lubischer, J.L., Clarke, L.I. & Loboa, E.G. 2010, "Application of low-frequency alternating current electric fields via interdigitated electrodes: effects on cellular viability, cytoplasmic calcium, and osteogenic differentiation of human adipose-derived stem cells", *Tissue engineering.Part C, Methods,* vol. 16, no. 6, pp. 1377-1386.

McIntosh, K., Zvonic, S., Garrett, S., Mitchell, J.B., Floyd, Z.E., Hammill, L., Kloster, A., Di Halvorsen, Y., Ting, J.P., Storms, R.W., Goh, B., Kilroy, G., Wu, X. & Gimble, J.M. 2006, "The Immunogenicity of Human Adipose-Derived Cells: Temporal Changes In Vitro", *Stem cells,* vol. 24, no. 5, pp. 1246-1253.

Mehmet Cabuk, Yusuf Alan, Mustafa Yavuz, Halil Ibrahim Unal. 2014, "Synthesis, characterization and antimicrobial activity of biodegradable conducting polypyrrole-graft-chitosan copolymer", Applied Surface Science, in press

Mendonca, D.B., Miguez, P.A., Mendonca, G., Yamauchi, M., Aragao, F.J. & Cooper, L.F. 2011, "Titanium surface topography affects collagen biosynthesis of adherent cells", *Bone,* vol. 49, no. 3, pp. 463-472.

Meng, S., Zhang, Z. & Rouabhia, M. 2011, "Accelerated osteoblast mineralization on a conductive substrate by multiple electrical stimulation", *Journal of bone and mineral metabolism,* vol. 29, no. 5, pp. 535-544.

Meng, S., Rouabhia, M., Shi, G. & Zhang, Z. 2008, "Heparin dopant increases the electrical stability, cell adhesion, and growth of conducting polypyrrole/poly(L,L-lactide) composites", *Journal of Biomedical Materials Research Part A,* vol. 87A, no. 2, pp. 332-344.

Meng, S., Rouabhia, M. & Zhang, Z. 2013, "Electrical stimulation modulates osteoblast proliferation and bone protein production through heparin-bioactivated conductive scaffolds", *Bioelectromagnetics,* vol. 34, no. 3, pp. 189-199.

Merrill, D.R., Bikson, M. & Jefferys, J.G.R. 2005, "Electrical stimulation of excitable tissue: design of efficacious and safe protocols", *Journal of neuroscience methods,* vol. 141, no. 2, pp. 171-198.

Mesimäki, K., Lindroos, B., Tornwall, J., Mauno, J., Lindqvist, C., Kontio, R., Miettinen, S. & Suuronen, R. 2009, "Novel maxillary reconstruction with ectopic bone formation by GMP adipose stem cells", *International journal of oral and maxillofacial surgery,* vol. 38, no. 3, pp. 201-209.

Middleton, J.C. & Tipton, A.J. 2000, "Synthetic biodegradable polymers as orthopedic devices", *Biomaterials,* vol. 21, no. 23, pp. 2335-2346.

Mihardja, S.S., Sievers, R.E. & Lee, R.J. 2008, "The effect of polypyrrole on arteriogenesis in an acute rat infarct model", *Biomaterials,* vol. 29, no. 31, pp. 4205-4210.

Mody, N., Parhami, F., Sarafian, T.A. & Demer, L.L. 2001, "Oxidative stress modulates osteoblastic differentiation of vascular and bone cells", *Free Radical Biology and Medicine,* vol. 31, no. 4, pp. 509-519.

Mondal, S.K., Prasad, K.R. & Munichandraiah, N. 2005, "Analysis of electrochemical impedance of polyaniline films prepared by galvanostatic, potentiostatic and potentiodynamic methods", *Synthetic Metals,* vol. 148, no. 3, pp. 275-286.

Monfoulet, L.E., Becquart, P., Marchat, D., Vandamme, K., Bourguignon, M., Pacard, E., Viateau, V., Petite, H. & Logeart-Avramoglou, D. 2014, "The pH in the Microenvironment of Human Mesenchymal Stem Cells Is a Critical Factor for Optimal Osteogenesis in Tissue-Engineered Constructs", *Tissue engineering.Part A.*

Myllymaa S, Kaivosoja E, Myllymaa K, Sillat T, Korhonen H, Lappalainen R, Konttinen YT. 2010, " Adhesion, spreading and osteogenic differentiation of mesenchymal stem cells cultured on micropatterned amorphous diamond, titanium, tantalum and chromium coatings on silicon", Journal of Materials Science: *Materials in Medicine*, vol. 21, no. 1, pp. 329-341

Nair, L.S. & Laurencin, C.T. 2007, "Biodegradable polymers as biomaterials", *Progress in Polymer Science,* vol. 32, no. 8–9, pp. 762-798.

Närhi, T.O., Jansen, J.A., Jaakkola, T., de Ruijter, A., Rich, J., Seppälä, J. & Yli-Urpo, A. 2003, "Bone response to degradable thermoplastic composite in rabbits", *Biomaterials,* vol. 24, no. 10, pp. 1697-1704.

Navarro, M., Michiardi, A., Castano, O. & Planell, J.A. 2008, "Biomaterials in orthopaedics", *Journal of the Royal Society, Interface / the Royal Society,* vol. 5, no. 27, pp. 1137-1158.

Nin, V., Hernández, J.A. & Chifflet, S. 2009, "Hyperpolarization of the plasma membrane potential provokes reorganization of the actin cytoskeleton and increases the stability of adherens junctions in bovine corneal endothelial cells in culture", *Cell motility and the cytoskeleton,* vol. 66, no. 12, pp. 1087-1099.

Norgaard, R., Kassem, M. & Rattan, S. 2006, "Heat Shock-Induced Enhancement of Osteoblastic Differentiation of hTERT-Immortalized Mesenchymal Stem Cells", *Annals of the New York Academy of Sciences,* vol. 1067, no. 1, pp. 443-447.

Nuccitelli, R., Nuccitelli, P., Li, C., Narsing, S., Pariser, D.M. & Lui, K. 2011, "The electric field near human skin wounds declines with age and provides a noninvasive indicator of wound healing", *Wound Repair and Regeneration,* vol. 19, no. 5, pp. 645-655.

Oh, J.K. 2011, "Polylactide (PLA)-based amphiphilic block copolymers: synthesis, self-assembly, and biomedical applications", *Soft Matter,* vol. 7, no. 11, pp. 5096.

Osathanon, T., Bespinyowong, K., Arksornnukit, M., Takahashi, H. & Pavasant, P. 2011, "Human osteoblast-like cell spreading and proliferation on Ti-6Al-7Nb surfaces of varying roughness", *Journal of oral science,* vol. 53, no. 1, pp. 23-30.

Pablo Rodríguez, J., González, M., Ríos, S. & Cambiazo, V. 2004, "Cytoskeletal organization of human mesenchymal stem cells (MSC) changes during their

osteogenic differentiation", *Journal of cellular biochemistry,* vol. 93, no. 4, pp. 721-731.

Pak, J. 2011, "Regeneration of human bones in hip osteonecrosis and human cartilage in knee osteoarthritis with autologous adipose-tissue-derived stem cells: a case series", *Journal of medical case reports,* vol. 5, pp. 296-1947-5-296.

Palomäki J, Karisola P, Pylkkänen L, Savolainen K, Alenius H. 2010, " Engineered nanomaterials cause cytotoxicity and activation on mouse antigen presenting cells", vol 267, no. 1–3, pp.125-31.

Panero, S., Abbati, G., Renier, D. & Crescenzi, V. 2004, *Electrically conductive polymeric biomaterials, the process for their preparation and the use thereof in the biomedical and healthcare field*, A01N 43/04 (20060101); A61K 31/715 (20060101); C07H 1/00 (20060101), Italy.

Park, D.G., Kim, K.G., Lee, T.J., Kim, J.Y., Sung, E.G., Ahn, M.W. & Song, I.H. 2011, "Optimal supplementation of dexamethasone for clinical purposed expansion of mesenchymal stem cells for bone repair", *Journal of orthopaedic science : official journal of the Japanese Orthopaedic Association,* vol. 16, no. 5, pp. 606-612.

Patrikoski, M., Juntunen, M., Boucher, S., Campbell, A., Vemuri, M.C., Mannerstrom, B. & Miettinen, S. 2013, "Development of fully defined xeno-free culture system for the preparation and propagation of cell therapy-compliant human adipose stem cells", *Stem cell research & therapy,* vol. 4, no. 2, pp. 27.

Pautke, C., Vogt, S., Kreutzer, K., Haczek, C., Wexel, G., Kolk, A., Imhoff, A.B., Zitzelsberger, H., Milz, S. & Tischer, T. 2010, "Characterization of eight different tetracyclines: advances in fluorescence bone labeling", *Journal of anatomy,* vol. 217, no. 1, pp. 76-82.

Peramo, A., Urbanchek, M.G., Spanninga, S.A., Povlich, L.K., Cederna, P. & Martin, D.C. 2008, "In situ polymerization of a conductive polymer in acellular muscle tissue constructs", *Tissue engineering.Part A,* vol. 14, no. 3, pp. 423-432.

Petersen, T.H., Calle, E.A., Zhao, L., Lee, E.J., Gui, L., Raredon, M.B., Gavrilov, K., Yi, T., Zhuang, Z.W., Breuer, C., Herzog, E. & Niklason, L.E. 2010, "Tissue-Engineered Lungs for in Vivo Implantation", *Science,* vol. 329, no. 5991, pp. 538-541.

Pinzone, J.J., Hall, B.M., Thudi, N.K., Vonau, M., Qiang, Y.W., Rosol, T.J. & Shaughnessy, J.D.,Jr 2009, "The role of Dickkopf-1 in bone development, homeostasis, and disease", *Blood,* vol. 113, no. 3, pp. 517-525.

Pluta, M., Jeszka, J.K. & Boiteux, G. 2007, "Polylactide/montmorillonite nanocomposites: Structure, dielectric, viscoelastic and thermal properties", *European Polymer Journal,* vol. 43, no. 7, pp. 2819-2835.

Potdar, P.D. & D'Souza, S.B. 2010, "Ascorbic acid induces in vitro proliferation of human subcutaneous adipose tissue derived mesenchymal stem cells with upregulation of embryonic stem cell pluripotency markers Oct4 and SOX 2", *Human cell,* vol. 23, no. 4, pp. 152-155.

Qu, L., Li, M., Ma, C., Wang, J., Zhuang, M. & Wang, J. 2012, *Method for preparing bioceramic coating of polypyrrole calcium phosphate/magnesium oxide.*, Jiamusi University, Peop. Rep. China.

Rahaman, M.N., Day, D.E., Sonny Bal, B., Fu, Q., Jung, S.B., Bonewald, L.F. & Tomsia, A.P. 2011, "Bioactive glass in tissue engineering", *Acta Biomaterialia,* vol. 7, no. 6, pp. 2355-2373.

Rajala, K., Lindroos, B., Hussein, S.M., Lappalainen, R.S., Pekkanen-Mattila, M., Inzunza, J., Rozell, B., Miettinen, S., Narkilahti, S., Kerkela, E., Aalto-Setala, K., Otonkoski, T., Suuronen, R., Hovatta, O. & Skottman, H. 2010, "A defined and xeno-free culture method enabling the establishment of clinical-grade human embryonic, induced pluripotent and adipose stem cells", *PloS one,* vol. 5, no. 4, pp. e10246.

Ramanaviciene, A., Kausaite, A., Tautkus, S. & Ramanavicius, A. 2007, "Biocompatibility of polypyrrole particles: an in-vivo study in mice", *Journal of Pharmacy and Pharmacology,* vol. 59, no. 2, pp. 311-315.

Ravichandran, R., Sundarrajan, S., Venugopal, J.R., Mukherjee, S. & Ramakrishna, S. 2012, "Advances in Polymeric Systems for Tissue Engineering and Biomedical Applications", *Macromolecular Bioscience,* vol. 12, no. 3, pp. 286-311.

Reid, B., Song, B. & Zhao, M. 2009, "Electric currents in Xenopus tadpole tail regeneration", *Developmental biology,* vol. 335, no. 1, pp. 198-207.

Rentsch, B., Hofmann, A., Breier, A., Rentsch, C. & Scharnweber, D. 2009, "Embroidered and surface modified polycaprolactone-co-lactide scaffolds as bone substitute: in vitro characterization", *Annals of Biomedical Engineering,* vol. 37, no. 10, pp. 2118-2128.

Rezanejad, H. & Matin, M.M. 2012, "Induced pluripotent stem cells: progress and future perspectives in the stem cell world", *Cellular reprogramming,* vol. 14, no. 6, pp. 459-470.

Rezwan, K., Chen, Q.Z., Blaker, J.J. & Boccaccini, A.R. 2006, "Biodegradable and bioactive porous polymer/inorganic composite scaffolds for bone tissue engineering", *Biomaterials,* vol. 27, no. 18, pp. 3413-3431.

Richardson, R.T., Thompson, B., Moulton, S., Newbold, C., Lum, M.G., Cameron, A., Wallace, G., Kapsa, R., Clark, G. & O'Leary, S. 2007, "The effect of polypyrrole with incorporated neurotrophin-3 on the promotion of neurite outgrowth from auditory neurons", *Biomaterials,* vol. 28, no. 3, pp. 513-523.

Richardson, R.T., Wise, A.K., Thompson, B.C., Flynn, B.O., Atkinson, P.J., Fretwell, N.J., Fallon, J.B., Wallace, G.G., Shepherd, R.K., Clark, G.M. & O'Leary, S.J. 2009, "Polypyrrole-coated electrodes for the delivery of charge and neurotrophins to cochlear neurons", *Biomaterials,* vol. 30, no. 13, pp. 2614-2624.

Riquelme, D., Alvarez, A., Leal, N., Adasme, T., Espinoza, I., Valdes, J.A., Troncoso, N., Hartel, S., Hidalgo, J., Hidalgo, C. & Carrasco, M.A. 2011, "High-frequency field stimulation of primary neurons enhances ryanodine receptor-mediated

Ca2+ release and generates hydrogen peroxide, which jointly stimulate NF-kappaB activity", *Antioxidants & redox signaling,* vol. 14, no. 7, pp. 1245-1259.
Rivera-Chacon, D.M., Alvarado-Velez, M., Acevedo-Morantes, C.Y., Singh, S.P., Gultepe, E., Nagesha, D., Sridhar, S. & Ramirez-Vick, J.E. 2013, "Fibronectin and vitronectin promote human fetal osteoblast cell attachment and proliferation on nanoporous titanium surfaces", *Journal of biomedical nanotechnology,* vol. 9, no. 6, pp. 1092-1097.
Robling, A.G., Burr, D.B. & Turner, C.H. 2001, "Recovery periods restore mechanosensitivity to dynamically loaded bone", *The Journal of experimental biology,* vol. 204, no. Pt 19, pp. 3389-3399.
Rouwkema, J., Rivron, N.C. & van Blitterswijk, C.A. 2008, "Vascularization in tissue engineering", *Trends in biotechnology,* vol. 26, no. 8, pp. 434-441.
Saikku-Bäckström, A., Tulamo, R.-., Räihä, J.E., Kellomäki, M., Toivonen, T., Törmälä, P. & Rokkanen, P. 2000, "Intramedullary fixation of cortical bone osteotomies with absorbable self-reinforced fibrillated poly-96L/4D-lactide (SR-PLA96) rods in rabbits", *Biomaterials,* vol. 22, no. 1, pp. 33-43.
Sajesh, K.M., Jayakumar, R., Nair, S.V. & Chennazhi, K.P. 2013, "Biocompatible conducting chitosan/polypyrrole–alginate composite scaffold for bone tissue engineering", *International journal of biological macromolecules,* vol. 62, no. 0, pp. 465-471.
Sandor, G.K., Numminen, J., Wolff, J., Thesleff, T., Miettinen, A., Tuovinen, V.J., Mannerstrom, B., Patrikoski, M., Seppanen, R., Miettinen, S., Rautiainen, M. & Ohman, J. 2014, "Adipose stem cells used to reconstruct 13 cases with cranio-maxillofacial hard-tissue defects", *Stem cells translational medicine,* vol. 3, no. 4, pp. 530-540.
Sarkar, D., Zhao, W., Schaefer, S., Ankrum, J.A., Teo, G.S.L., Pereira, M.N., Ferreira, L. & Karp, J.M. 2013, "Chapter II.6.2 - Overview of Tissue Engineering Concepts and Applications" in *Biomaterials Science (Third Edition)*, eds. B.D. Ratner, A.S. Hoffman, F.J. Schoen & J.E. Lemons, Academic Press, pp. 1122-1137.
Schmidt, C.E. & Rivers, T.J. 2002, *Biodegradable, electrically conducting polymer for tissue engineering applications*, 548/524 ; 252/500 edn, A61L 27/00 (20060101); A61L 27/58 (20060101); A61L 27/16 (20060101); C12N 5/00 (20060101); C07D 295/00 (); C07D 207/00 (); H01B 001/12 (), US.
Sensebe, L. 2008, "Clinical grade production of mesenchymal stem cells", *Bio-medical materials and engineering,* vol. 18, no. 1 Suppl, pp. S3-10.
Serena, E., Figallo, E., Tandon, N., Cannizzaro, C., Gerecht, S., Elvassore, N. & Vunjak-Novakovic, G. 2009, "Electrical stimulation of human embryonic stem cells: Cardiac differentiation and the generation of reactive oxygen species", *Experimental cell research,* vol. 315, no. 20, pp. 3611-3619.
Serra Moreno, J., Panero, S., Artico, M. & Filippini, P. 2008, "Synthesis and characterization of new electroactive polypyrrole–chondroitin sulphate A substrates", *Bioelectrochemistry,* vol. 72, no. 1, pp. 3-9.

Serra Moreno, J. & Panero, S. 2012, "Evaluation of the interface aging process of polypyrrole–polysaccharide electrodes in a simulated physiological fluid", *Electrochimica Acta,* vol. 68, no. 0, pp. 1-8.

Serra Moreno, J., Panero, S., Materazzi, S., Martinelli, A., Sabbieti, M.G., Agas, D. & Materazzi, G. 2009, "Polypyrrole-polysaccharide thin films characteristics: Electrosynthesis and biological properties", *Journal of Biomedical Materials Research Part A,* vol. 88A, no. 3, pp. 832-840.

Serra Moreno, J., Sabbieti, M.G., Agas, D., Marchetti, L. & Panero, S. 2012, "Polysaccharides immobilized in polypyrrole matrices are able to induce osteogenic differentiation in mouse mesenchymal stem cells", *Journal of Tissue Engineering and Regenerative Medicine*.

Shastri, V.P., Zelikin, A., Lynn, D., Langer, R.S. & Martin, I. 2002, *Bioerodible conducting materials*, C08G 73/06 (20060101), U.S.

Shastri, V.R., Rahman, N., Martin, I. & Langer, J., Robert S. 1998, *Electroactive materials for stimulation of biological activity of bone marrow stromal cells*, 435/173.8 edn, C12N 5/00 (20060101); C12M 1/42 (20060101); C12N 13/00 (20060101); C12N 013/00 (), Massachusetts/US.

Sheng, H., Rui, X.F., Sheng, C.J., Li, W.J., Cheng, X.Y., Jhummon, N.P., Yu, Y.C., Qu, S., Zhang, G. & Qin, L. 2013, "A novel semisynthetic molecule icaritin stimulates osteogenic differentiation and inhibits adipogenesis of mesenchymal stem cells", *International journal of medical sciences,* vol. 10, no. 6, pp. 782-789.

Shi, G., Rouabhia, M., Wang, Z., Dao, L.H. & Zhang, Z. 2004, "A novel electrically conductive and biodegradable composite made of polypyrrole nanoparticles and polylactide", *Biomaterials,* vol. 25, no. 13, pp. 2477-2488.

Shipu, L., Yuhua, Y., Qingsing, Z., Xiaoming, C., Tao, W., Youfa, W., Xinyu, W. & Tao, F. 2009, *Degradable conductive biological medical polymer material*, C08B37/08; C08F116/06; C08F8/00; C08G63/91; C08G64/42; C08G67/04; C08G79/02; C08G81/00; H01B1/12, China.

Siddappa, R., Licht, R., van Blitterswijk, C. & de Boer, J. 2007, "Donor variation and loss of multipotency during in vitro expansion of human mesenchymal stem cells for bone tissue engineering", *Journal of Orthopaedic Research,* vol. 25, no. 8, pp. 1029-1041.

Sjaastad, M.D. & Nelson, W.J. 1997, "Integrin-mediated calcium signaling and regulation of cell adhesion by intracellular calcium", *BioEssays : news and reviews in molecular, cellular and developmental biology,* vol. 19, no. 1, pp. 47-55.

Sommerfeldt, D.W. & Rubin, C.T. 2001, "Biology of bone and how it orchestrates the form and function of the skeleton", *European spine journal : official publication of the European Spine Society, the European Spinal Deformity Society, and the European Section of the Cervical Spine Research Society,* vol. 10 Suppl 2, pp. S86-95.

Song, I., Caplan, A.I. & Dennis, J.E. 2009, "In vitro dexamethasone pretreatment enhances bone formation of human mesenchymal stem cells in vivo", *Journal of Orthopaedic Research,* vol. 27, no. 7, pp. 916-921.

Spees, J.L., Gregory, C.A., Singh, H., Tucker, H.A., Peister, A., Lynch, P.J., Hsu, S.C., Smith, J. & Prockop, D.J. 2004, "Internalized antigens must be removed to prepare hypoimmunogenic mesenchymal stem cells for cell and gene therapy", *Molecular therapy : the journal of the American Society of Gene Therapy,* vol. 9, no. 5, pp. 747-756.

Srinivasan, S., Weimer, D.A., Agans, S.C., Bain, S.D. & Gross, T.S. 2002, "Low-Magnitude Mechanical Loading Becomes Osteogenic When Rest Is Inserted Between Each Load Cycle", *Journal of Bone and Mineral Research,* vol. 17, no. 9, pp. 1613-1620.

St. Pierre, C.A., Chan, M., Iwakura, Y., Ayers, D.C., Kurt-Jones, E.A. & Finberg, R.W. 2010, "Periprosthetic osteolysis: Characterizing the innate immune response to titanium wear-particles", *Journal of Orthopaedic Research,* vol. 28, no. 11, pp. 1418-1424.

Stevenson, S. & Horowitz, M. 1992, "The response to bone allografts", *The Journal of bone and joint surgery.American volume,* vol. 74, no. 6, pp. 939-950.

Sun, S., Liu, Y., Lipsky, S. & Cho, M. 2007, "Physical manipulation of calcium oscillations facilitates osteodifferentiation of human mesenchymal stem cells", *The FASEB journal : official publication of the Federation of American Societies for Experimental Biology,* vol. 21, no. 7, pp. 1472-1480.

Sun, S., Titushkin, I. & Cho, M. 2006, "Regulation of mesenchymal stem cell adhesion and orientation in 3D collagen scaffold by electrical stimulus", *Bioelectrochemistry,* vol. 69, no. 2, pp. 133-141.

Sundelacruz, S., Levin, M. & Kaplan, D.L. 2013, "Depolarization alters phenotype, maintains plasticity of pre-differentiated mesenchymal stem cells", *Tissue engineering.Part A.*

Sundelacruz, S., Levin, M. & Kaplan, D.L. 2008, "Membrane potential controls adipogenic and osteogenic differentiation of mesenchymal stem cells", *PloS one,* vol. 3, no. 11, pp. e3737.

Supronowicz, P.R., Ajayan, P.M., Ullmann, K.R., Arulanandam, B.P., Metzger, D.W. & Bizios, R. 2002, "Novel current-conducting composite substrates for exposing osteoblasts to alternating current stimulation", *Journal of Biomedical Materials Research,* vol. 59, no. 3, pp. 499-506.

Takahashi, K. & Yamanaka, S. 2006, "Induction of pluripotent stem cells from mouse embryonic and adult fibroblast cultures by defined factors", *Cell,* vol. 126, no. 4, pp. 663-676.

Tan, Y. & Ghandi, K. 2013, "Kinetics and mechanism of pyrrole chemical polymerization", *Synthetic Metals,* vol. 175, no. 0, pp. 183-191.

Tandon, N., Cannizzaro, C., Chao, P.H., Maidhof, R., Marsano, A., Au, H.T., Radisic, M. & Vunjak-Novakovic, G. 2009a, "Electrical stimulation systems for cardiac tissue engineering", *Nature protocols,* vol. 4, no. 2, pp. 155-173.

Tandon, N., Goh, B., Marsano, A., Chao, P.H., Montouri-Sorrentino, C., Gimble, J. & Vunjak-Novakovic, G. 2009b, "Alignment and elongation of human adipose-

derived stem cells in response to direct-current electrical stimulation", *Conference proceedings : Annual International Conference of the IEEE Engineering in Medicine and Biology Society.IEEE Engineering in Medicine and Biology Society.Conference,* vol. 1, pp. 6517-6521.

Tandon, N., Marsano, A., Maidhof, R., Wan, L., Park, H. & Vunjak-Novakovic, G. 2011, "Optimization of electrical stimulation parameters for cardiac tissue engineering", *Journal of Tissue Engineering and Regenerative Medicine,* vol. 5, no. 6, pp. e115-e125.

Taylor, J.A. 2010, "Bilateral orbitozygomatic reconstruction with tissue-engineered bone", *The Journal of craniofacial surgery,* vol. 21, no. 5, pp. 1612-1614.

Thesleff, T., Lehtimaki, K., Niskakangas, T., Mannerstrom, B., Miettinen, S., Suuronen, R. & Ohman, J. 2011, "Cranioplasty with adipose-derived stem cells and biomaterial: a novel method for cranial reconstruction", *Neurosurgery,* vol. 68, no. 6, pp. 1535-1540.

Thompson, B.C., Moulton, S.E., Richardson, R.T. & Wallace, G.G. 2011, "Effect of the dopant anion in polypyrrole on nerve growth and release of a neurotrophic protein", *Biomaterials,* vol. 32, no. 15, pp. 3822-3831.

Thompson, B.C., Richardson, R.T., Moulton, S.E., Evans, A.J., O'Leary, S., Clark, G.M. & Wallace, G.G. 2010, "Conducting polymers, dual neurotrophins and pulsed electrical stimulation — Dramatic effects on neurite outgrowth", *Journal of Controlled Release,* vol. 141, no. 2, pp. 161-167.

Tirkkonen, L., Halonen, H., Hyttinen, J., Kuokkanen, H., Sievanen, H., Koivisto, A.M., Mannerstrom, B., Sandor, G.K., Suuronen, R., Miettinen, S. & Haimi, S. 2011, "The effects of vibration loading on adipose stem cell number, viability and differentiation towards bone-forming cells", *Journal of the Royal Society, Interface / the Royal Society,* vol. 8, no. 65, pp. 1736-1747.

Titushkin, I., Sun, S., Rao, V. & Cho, M. 2011, "Stem Cell Physiological Responses to Noninvasive Electrical Stimulation" in *The Physiology of Bioelectricity in Development, Tissue Regeneration and Cancer*, ed. C.E. Pullar, CRC Press, pp. 91-120.

Titushkin, I. & Cho, M. 2009, "Regulation of cell cytoskeleton and membrane mechanics by electric field: role of linker proteins", *Biophysical journal,* vol. 96, no. 2, pp. 717-728.

Titushkin, I. & Cho, M. 2007, "Modulation of cellular mechanics during osteogenic differentiation of human mesenchymal stem cells", *Biophysical journal,* vol. 93, no. 10, pp. 3693-3702.

Titushkin, I.A. & Cho, M.R. 2009, "Controlling cellular biomechanics of human mesenchymal stem cells", *Conference proceedings : ...Annual International Conference of the IEEE Engineering in Medicine and Biology Society.IEEE Engineering in Medicine and Biology Society.Conference,* vol. 2009, pp. 2090-2093.

Trounson, A. 2007, "Chapter Thirty - Embryonic stem cells" in *Principles of Tissue Engineering (Third Edition)*, eds. R. Lanza, R. Langer & J. Vacanti, Academic Press, Burlington, pp. 421-429.

Tu, H., Ahearn, T.U., Daniel, C.R., Gonzalez-Feliciano, A.G., Seabrook, M.E. & Bostick, R.M. 2014, "Transforming growth factors and receptor as potential modifiable pre-neoplastic biomarkers of risk for colorectal neoplasms", *Molecular carcinogenesis,* pp. n/a-n/a.

U.S. Food and Drug Administration 2009, *Guidance for Industry and FDA Staff: Minimal Manipulation of Structural Tissue Jurisdictional Update*. Available: http://www.fda.gov/BiologicsBloodVaccines/GuidanceComplianceRegulatoryInformation/Guidances/Tissue/ucm073396.htm [2014, 04/21].

Uddin, S.M. & Qin, Y.X. 2013, "Enhancement of osteogenic differentiation and proliferation in human mesenchymal stem cells by a modified low intensity ultrasound stimulation under simulated microgravity", *PloS one,* vol. 8, no. 9, pp. e73914.

Uygun, B.E., Stojsih, S.E. & Matthew, H.W. 2009, "Effects of immobilized glycosaminoglycans on the proliferation and differentiation of mesenchymal stem cells", *Tissue engineering.Part A,* vol. 15, no. 11, pp. 3499-3512.

Vaijayanthimala, V., Cheng, P., Yeh, S., Liu, K., Hsiao, C., Chao, J. & Chang, H. 2012, "The long-term stability and biocompatibility of fluorescent nanodiamond as an in vivo contrast agent", *Biomaterials,* vol. 33, no. 31, pp. 7794-7802.

Van der Stok, J., Van Lieshout, E.M.M., El-Massoudi, Y., Van Kralingen, G.H. & Patka, P. 2011, "Bone substitutes in the Netherlands – A systematic literature review", *Acta Biomaterialia,* vol. 7, no. 2, pp. 739-750.

Vishnoi, T. & Kumar, A. 2013, "Conducting cryogel scaffold as a potential biomaterial for cell stimulation and proliferation", *Journal of materials science.Materials in medicine,* vol. 24, no. 2, pp. 447-459.

Vishnubalaji, R., Al-Nbaheen, M., Kadalmani, B., Aldahmash, A. & Ramesh, T. 2012, "Comparative investigation of the differentiation capability of bone-marrow- and adipose-derived mesenchymal stem cells by qualitative and quantitative analysis", *Cell and tissue research,* vol. 347, no. 2, pp. 419-427.

Wallace, G.G., Smyth, M. & Zhao, H. 1999, "Conducting electroactive polymer-based biosensors", *TrAC Trends in Analytical Chemistry,* vol. 18, no. 4, pp. 245-251.

Wallace, G. & Spinks, G. 2007, "Conducting polymers - bridging the bionic interface", *Soft Matter,* no. 6, pp. 665.

Wan, Y., Yu, A., Wu, H., Wang, Z. & Wen, D. 2005, "Porous-conductive chitosan scaffolds for tissue engineering II. in vitro and in vivo degradation", *Journal of materials science.Materials in medicine,* vol. 16, no. 11, pp. 1017-1028.

Wang, B., Wang, G., To, F., Butler, J.R., Claude, A., McLaughlin, R.M., Williams, L.N., de Jongh Curry, A.L. & Liao, J. 2013a, "Myocardial scaffold-based cardiac tissue engineering: application of coordinated mechanical and electrical stimulations", *Langmuir : the ACS journal of surfaces and colloids,* vol. 29, no. 35, pp. 11109-11117.

Wang, D.X., He, Y., Bi, L., Qu, Z.H., Zou, J.W., Pan, Z., Fan, J.J., Chen, L., Dong, X., Liu, X.N., Pei, G.X. & Ding, J.D. 2013b, "Enhancing the bioactivity of

Poly(lactic-co-glycolic acid) scaffold with a nano-hydroxyapatite coating for the treatment of segmental bone defect in a rabbit model", *International journal of nanomedicine,* vol. 8, pp. 1855-1865.

Wang, H., Pang, B., Li, Y., Zhu, D., Pang, T. & Liu, Y. 2012, "Dexamethasone has variable effects on mesenchymal stromal cells", *Cytotherapy,* vol. 14, no. 4, pp. 423-430.

Wang, X., Gu, X., Yuan, C., Chen, S., Zhang, P., Zhang, T., Yao, J., Chen, F. & Chen, G. 2004a, "Evaluation of biocompatibility of polypyrrole in vitro and in vivo", *Journal of Biomedical Materials Research Part A,* vol. 68A, no. 3, pp. 411-422.

Wang, Z., Roberge, C., Dao, L.H., Wan, Y., Shi, G., Rouabhia, M., Guidoin, R. & Zhang, Z. 2004b, "In vivo evaluation of a novel electrically conductive polypyrrole/poly(D,L-lactide) composite and polypyrrole-coated poly(D,L-lactide-co-glycolide) membranes", *Journal of Biomedical Materials Research Part A,* vol. 70A, no. 1, pp. 28-38.

Wappler, J., Rath, B., Laufer, T., Heidenreich, A. & Montzka, K. 2013, "Eliminating the need of serum testing using low serum culture conditions for human bone marrow-derived mesenchymal stromal cell expansion", *Biomedical engineering online,* vol. 12, pp. 15-925X-12-15.

Wen, Y., Jiang, B., Cui, J., Li, G., Yu, M., Wang, F., Zhang, G., Nan, X., Yue, W., Xu, X. & Pei, X. 2013, "Superior osteogenic capacity of different mesenchymal stem cells for bone tissue engineering", *Oral surgery, oral medicine, oral pathology and oral radiology,* vol. 116, no. 5, pp. e324-32.

Whyte, M.P. 2010, "Physiological role of alkaline phosphatase explored in hypophosphatasia", *Annals of the New York Academy of Sciences,* vol. 1192, no. 1, pp. 190-200.

Williams, R.,L. & Doherty, P.,J. 1994, "A preliminary assessment of poly(pyrrole) in nerve guide studies", *Journal of Materials Science: Materials in Medicine,* no. 6, pp. 429-433.

Wobus, A.M. & Boheler, K.R. 2005, "Embryonic stem cells: prospects for developmental biology and cell therapy", *Physiological Reviews,* vol. 85, no. 2, pp. 635-678.

Wollenweber, M., Domaschke, H., Hanke, T., Boxberger, S., Schmack, G., Gliesche, K., Scharnweber, D. & Worch, H. 2006, "Mimicked bioartificial matrix containing chondroitin sulphate on a textile scaffold of poly(3-hydroxybutyrate) alters the differentiation of adult human mesenchymal stem cells", *Tissue engineering,* vol. 12, no. 2, pp. 345-359.

Wolszczak, M., Kroh, J. & Abdel-Hamid, M.M. 1995, "Some aspects of the radiation processing of conducting polymers", *Radiation Physics and Chemistry,* vol. 45, no. 1, pp. 71-78.

Wong, J.Y., Langer, R. & Ingber, D.E. 1994, "Electrically conducting polymers can noninvasively control the shape and growth of mammalian cells", *Proceedings of the*

National Academy of Sciences of the United States of America, vol. 91, no. 8, pp. 3201-3204.

Wong, J.Y., Ingber, D.E. & Langer, R.S. 1998, *Method and devices for altering the differentiation of anchorage-dependent cells on an electrically-conducting polymer.*, Massachusetts Institute of Technology, USA; Children's Medical Center Corporation.

Wu, S., Chang, J., Wang, C., Wang, G. & Ho, M. 2010, "Enhancement of chondrogenesis of human adipose derived stem cells in a hyaluronan-enriched microenvironment", *Biomaterials,* vol. 31, no. 4, pp. 631-640.

Xiao, Y., Peperzak, V., van Rijn, L., Borst, J. & de Bruijn, J.D. 2010, "Dexamethasone treatment during the expansion phase maintains stemness of bone marrow mesenchymal stem cells", *Journal of Tissue Engineering and Regenerative Medicine,* vol. 4, no. 5, pp. 374-386.

Xing, W., Yu, Z., Xiang, G., Pan, L. & Cheng, J. 2003, *Apparatus for stimulating an animal cell and recording its physiological signal and production and use methods thereof.*, Capital Biochip Company, Ltd., Peop. Rep. China; Tsinghua University.

Xu, Y., Qu, B., Deng, Y., Liu, Y. & Dai, L. 2008, *Polymer-modified and titanium alloy-based artificial joint medium layer and its preparation method.*, Xiamen University, Peop. Rep. China.

Xue, L., Dai, S. & Li, Z. 2010, "Biodegradable shape-memory block co-polymers for fast self-expandable stents", *Biomaterials,* vol. 31, no. 32, pp. 8132-8140.

Yadav, M.C., Simão, A.M.S., Narisawa, S., Huesa, C., McKee, M.D., Farquharson, C. & Millán, J.L. 2011, "Loss of skeletal mineralization by the simultaneous ablation of PHOSPHO1 and alkaline phosphatase function: A unified model of the mechanisms of initiation of skeletal calcification", *Journal of Bone and Mineral Research,* vol. 26, no. 2, pp. 286-297.

Yang, G., Rothrauff, B.B., Lin, H., Gottardi, R., Alexander, P.G. & Tuan, R.S. 2013, "Enhancement of tenogenic differentiation of human adipose stem cells by tendon-derived extracellular matrix", *Biomaterials,* vol. 34, no. 37, pp. 9295-9306.

Yow, S., Lim, T.H., Yim, E.K.F., Lim, C.T. & Leong, K.W. 2011, "A 3D Electroactive Polypyrrole-Collagen Fibrous Scaffold for Tissue Engineering", *Polymers,* vol. 3, no. 1, pp. 527-544.

Yu, D., Li, Q., Mu, X., Chang, T. & Xiong, Z. 2008, "Bone regeneration of critical calvarial defect in goat model by PLGA/TCP/rhBMP-2 scaffolds prepared by low-temperature rapid-prototyping technology", *International journal of oral and maxillofacial surgery,* vol. 37, no. 10, pp. 929-934.

Zaidi, M. 2007, "Skeletal remodeling in health and disease", *Nature medicine,* vol. 13, no. 7, pp. 791-801.

Zelikin, A.N., Lynn, D.M., Farhadi, J., Martin, I., Shastri, V. & Langer, R. 2002, "Erodible Conducting Polymers for Potential Biomedical Applications", *Angewandte Chemie International Edition,* vol. 41, no. 1, pp. 141-144.

Zeng, J., Huang, Z., Yin, G., Qin, J., Chen, X. & Gu, J. 2013, "Fabrication of conductive NGF-conjugated polypyrrole–poly(l-lactic acid) fibers and their effect on neurite outgrowth", *Colloids and Surfaces B: Biointerfaces,* vol. 110, no. 0, pp. 450-457.

Zhang, J., Neoh, K.G., Hu, X., Kang, E. & Wang, W. 2013, "Combined effects of direct current stimulation and immobilized BMP-2 for enhancement of osteogenesis", *Biotechnology and bioengineering,* vol. 110, no. 5, pp. 1466-1475.

Zhang, P., Moudgill, N., Hager, E., Tarola, N., Dimatteo, C., McIlhenny, S., Tulenko, T. & DiMuzio, P.J. 2011, "Endothelial differentiation of adipose-derived stem cells from elderly patients with cardiovascular disease", *Stem cells and development,* vol. 20, no. 6, pp. 977-988.

Zhang, Z., Li, F., Tian, H., Guan, K., Zhao, G., Shan, J. & Ren, D. 2014, "Differentiation of adipose-derived stem cells toward nucleus pulposus-like cells induced by hypoxia and a three-dimensional chitosan-alginate gel scaffold in vitro", *Chinese medical journal,* vol. 127, no. 2, pp. 314-321.

Zhang, Z., Roy, R., Dugré, F.J., Tessier, D. & Dao, L.H. 2001, "In vitro biocompatibility study of electrically conductive polypyrrole-coated polyester fabrics", *Journal of Biomedical Materials Research,* vol. 57, no. 1, pp. 63-71.

Zhao, M. 2009, "Electrical fields in wound healing—An overriding signal that directs cell migration", *Seminars in cell & developmental biology,* vol. 20, no. 6, pp. 674-682.

Zhao, Z., Watt, C., Karystinou, A., Roelofs, A.J., McCaig, C.D., Gibson, I.R. & De Bari, C. 2011, "Directed migration of human bone marrow mesenchymal stem cells in a physiological direct current electric field", *European cells & materials,* vol. 22, pp. 344-358.

Zhuang, H., Wang, W., Seldes, R.M., Tahernia, A.D., Fan, H. & Brighton, C.T. 1997, "Electrical stimulation induces the level of TGF-beta1 mRNA in osteoblastic cells by a mechanism involving calcium/calmodulin pathway", *Biochemical and biophysical research communications,* vol. 237, no. 2, pp. 225-229.

Zuk, P.A., Zhu, M., Ashjian, P., De Ugarte, D.A., Huang, J.I., Mizuno, H., Alfonso, Z.C., Fraser, J.K., Benhaim, P. & Hedrick, M.H. 2002, "Human adipose tissue is a source of multipotent stem cells", *Molecular biology of the cell,* vol. 13, no. 12, pp. 4279-4295.

Zuk, P.A., Zhu, M., Mizuno, H., Huang, J., Futrell, J.W., Katz, A.J., Benhaim, P., Lorenz, H.P. & Hedrick, M.H. 2001, "Multilineage cells from human adipose tissue: implications for cell-based therapies", *Tissue engineering,* vol. 7, no. 2, pp. 211-228.

9 Original publications

CORRIGENDA

There is one error in the original publications

Study I:
The osteogenic medium contains 250 μM ascorbic acid 2-phosphate, not 250 mM.

Annals of Biomedical Engineering (© 2014)
DOI: 10.1007/s10439-014-1023-7

BMES BIOMEDICAL ENGINEERING SOCIETY™ www.bmes.org

Comparison of Chondroitin Sulfate and Hyaluronic Acid Doped Conductive Polypyrrole Films for Adipose Stem Cells

MIINA BJÖRNINEN,[1,2,3] ALIISA SILJANDER,[1,2,3] JANI PELTO,[4] JARI HYTTINEN,[3,5] MINNA KELLOMÄKI,[3,5] SUSANNA MIETTINEN,[1,2,3] RIITTA SEPPÄNEN,[1,3,5,6] and SUVI HAIMI[1,2,3,7]

[1]Adult Stem Cells, Institute of Biomedical Technology, University of Tampere, Biokatu 8, 33014 Tampere, Finland; [2]Science Centre, Pirkanmaa Hospital District, P.O. BOX 2000, 33521 Tampere, Finland; [3]BioMediTech, Biokatu 10, 33520 Tampere, Finland; [4]VTT Technical Research Centre of Finland, Sinitaival 6, P.O. Box 1300, 33101 Tampere, Finland; [5]Department of Biomedical Engineering, Department of Electronics and Communications Engineering, Tampere University of Technology, P.O. 692, 33101 Tampere, Finland; [6]Department of Eye, Ear, and Oral Diseases, Tampere University Hospital, Division 3, P.O. Box 2000, 33521 Tampere, Finland; and [7]Department of Biomaterials Science and Technology, University of Twente, P.O. Box 217, 7500, AEEnschede, The Netherlands

(Received 7 January 2014; accepted 29 April 2014)

Associate Editor Kent Leach oversaw the review of this article.

Abstract—Polypyrrole (PPy) is a conductive polymer that has aroused interest due to its biocompatibility with several cell types and high tailorability as an electroconductive scaffold coating. This study compares the effect of hyaluronic acid (HA) and chondroitin sulfate (CS) doped PPy films on human adipose stem cells (hASCs) under electrical stimulation. The PPy films were synthetized electrochemically. The surface morphology of PPy–HA and PPy–CS was characterized by an atomic force microscope. A pulsed biphasic electric current (BEC) was applied *via* PPy films non-stimulated samples acting as controls. Viability, attachment, proliferation and osteogenic differentiation of hASCs were evaluated by live/dead staining, DNA content, Alkaline phosphatase activity and mineralization assays. Human ASCs grew as a homogenous cell sheet on PPy–CS surfaces, whereas on PPy–HA cells clustered into small spherical structures. PPy–CS supported hASC proliferation significantly better than PPy–HA at the 7 day time point. Both substrates equally triggered early osteogenic differentiation of hASCs, although mineralization was significantly induced on PPy–CS compared to PPy–HA under BEC. These differences may be due to different surface morphologies originating from the CS and HA dopants. Our results suggest that PPy–CS in particular is a potential osteogenic scaffold coating for bone tissue engineering.

Keywords—Mesenchymal stem cells, Osteogenic, Electrical stimulation, Polysaccharide.

Address correspondence to Suvi Haimi, Adult Stem Cells, Institute of Biomedical Technology, University of Tampere, Biokatu 8, 33014 Tampere, Finland. Electronic mail: suvi.haimi@uta.fi

ABBREVIATIONS

BEC	Biphasic electric current
ES	Electrical stimulation
hASC	Human adipose stem cells
PPy–CS	Chondroitin sulfate doped polypyrrole
PPy–HA	Hyaluronic acid doped polypyrrole
PS	Polystyrene cell culture plate

INTRODUCTION

Conducting polymers are an arising interest in the field of tissue engineering as they can deliver electrochemical as well as electromechanical stimulation to cells. From those polypyrrole (PPy) and poly(3,4-ethylenedioxythiophene) (PEDOT) are the most investigated for biomedical applications owing to their good biocompatibility *in vivo* and *in vitro*.[8] PPy is intensively investigated for bone[9,37,38,46] and neural applications[41,50] due to its easy modification with bioactive agents in ambient conditions and highly adjustable properties, such as surface charge and topography[17,18,44,46] whereas PEDOT studies concentrate more on neural electrodes and nerve grafts[1–5,13,20,21,35,42] mostly owing to PEDOT's higher electrical conductivity and stability compared to PPy.[8] In addition to bone and neural tissue engineering, PPy has so far been studied as bioactive coatings to improve osseointegration,[11] in biosensors,[7] drug delivery systems[50] and actuators.[34] Regards to the comprehensive research supporting

Published online: 14 May 2014

PPy's use in bone tissue engineering, we chose PPy and evaluated the effects of the two most potential bioactive dopants, hyaluronic acid (HA) and chondroitin sulfate (CS) in the PPy films.

In electrochemical polymerization of PPy, charged biomolecules, such as negatively charged glycosaminoglycans (GAGs), can be incorporated into the structure by doping when PPy is electrochemically polymerized by oxidation. Dopants play an important role in mediating the electric charges between the PPy chains.[23] In addition, the surface topography and mechanical properties of PPy can also widely be altered by the choice of dopant.[17,18]

CS and HA are GAGs commonly found in the extracellular matrices (ECMs) of most animal tissues. CS is a major proteoglycan component in organic matrix of the bone and is involved in the mineralization of the bone tissue whereas HA takes part in various cellular processes, such as ECM organization and metabolism.[43] Both GAGs are reported to support osteogenic differentiation of mesenchymal stem cells (MSCs) in scaffold structures *in vitro*.[28,53]

As regards integrating HA and CS into PPy surfaces, HA doped PPy (PPy–HA) has been studied with mouse bone marrow derived MSCs resulting in promoted osteogenic differentiation[46] and with MC3T3-E1 osteoblasts confirming cell differentiation on the surface.[45] In addition, we recently were the first to report an excellent attachment, proliferation and early osteogenic differentiation of hASCs on chemically synthetized PPy–CS coating in non-woven polylactide fiber scaffolds.[38] As both biomolecules are potential dopants for PPy coating in osteogenic applications, a systematic comparison is required to understand their benefits and differences with human MSCs.

Inherent electrical currents and fields are essential in terms of the growth and remodeling of bone tissue. This was first demonstrated by Fukada and Yasuda, who reported bone formation under tension when positive charge was dominating, and the opposite in case of a negative charge and compression.[15] This remark led to the development of electrical stimulation (ES) devices for treating severe bone defects.[22]

Even though ES has been acknowledged as a bone treatment method for several decades, the exploitation of ES to MSCs in bone tissue engineering has been studied only recently.[25,26,31,36] These studies have shown that various types of ES can be applied to improve osteogenic differentiation and proliferation of MSCs, yet no specific parameters for the efficient differentiation of MSC towards mature osteoblasts have so far been identified. In addition, most of the above mentioned studies exploited inert conductive substrates; hence a conductive coating with bioactive molecules and topographical cues may yield interesting synergy mimicking the natural environment in the bone tissue more closely. We therefore wanted to evaluate hASC spreading, proliferation and osteogenic differentiation on PPy surfaces under ES with our novel ES device developed in-house. To the best to our knowledge, this is the first paper to systematically compare HA and CS doped PPy coatings for hASCs.

MATERIALS AND METHODS

Polypyrrole Synthesis

Pyrrole (Sigma-Aldrich, St. Louis, USA) of 0.07 mL and 1 mg of HA from Streptococcus equi (Sigma-Aldrich) or CS A from bovine trachea (Sigma-Aldrich) were added per 1 mL of water. PPy–HA and PPy–CS films were grown electrochemically on a sputter-coated polyethylene-naphthalate film (PEN)/Au films (125 μm Dupont Teonex®), with 50 nm Au-coating (VTT Technical Research Center of Finland) as a working electrode, platinum mesh as a counter electrode and Ag/AgCl as a reference electrode. Constant potential of 1.0 V was applied to the films until 300 mC cm^{-2} polymerization charge had passed the cell. The stimulation plates and plate covers were sterilized by gamma irradiation (BBF Sterilisationsservice GmbH, Kernen, Germany) with an irradiation dose of >25 kGy that has not been reported to significantly alter the conductivity of the films.[12,54]

Surface Characterization of Polypyrrole Film

The surface morphology and roughness (R_a) values of the PPy films were characterized by an atomic force microscope (AFM; Park Systems XE-100, Korea) in both dry and wet conditions due to the significant water absorption and hence swelling phenomenon of wet PPy films in physiological conditions.[39,48] PPy–HA and PPy–CS films were incubated for 4 days in osteogenic medium (OM) containing 250 mM ascorbic acid 2-phosphate (Sigma-Aldrich), 5 nM dexamethasone (Sigma-Aldrich) and 10 mM *b*-glycerofosfate (Sigma-Aldrich) supplemented to maintenance medium consisting of Modified Eagle Medium/Ham's Nutrient mixture F-12 (DMEM/F-12 1:1 Invitogen), 10% fetal bovine serum (FBS; Invitrogen), 1% L-glutamine (GlutaMAX I; Invitrogen) and 1% antibiotics/antimycotic (100 U mL^{-1} penicillin, 0.1 mg mL^{-1} streptomycin; Invitrogen).

To distinguish the swelling effect from the typical polysaccharide doped PPy nodular morphology,[17,18,39,45,47] and in order to image the nanoscopic details of the soft films,[17,38] dried samples were analyzed using non-contact AFM (Park Systems XE-100)

in air using silicon probe ACTA-905M (Applied NanoStructures, Inc.) with a nominal resonance frequency of 300 kHz, spring constant 40 N m^{-1} and tip radius <10 nm. Images of 5×5 μm^2 were acquired with a scan rate of 0.5 Hz. Prior to imaging, the sample surfaces were carefully rinsed with deionized water and dried in ambient air.

The films pre-incubated in OM were imaged in Dulbecco's phosphate-buffered saline (PBS; Lonza Biowhittaker, Switzerland) using a contact mode AFM. Silicon nitride probes HYDRA-6R100N (Applied Nanostructures, Inc., Santa Clara, USA), with a nominal force constant 0.28 N m^{-1} and a tip radius of curvature <8 nm were applied. Areas of 20×20 μm^2 were scanned at 7 and 20 nN force set points for PPy–HA and PPy–CS surfaces respectively. Images of 12×12 μm^2 were acquired with the scan speed of 1 Hz.

R_a value analysis of the raw 512×512 pixel data was conducted. R_a values for 10 randomly chosen 4×4 μm^2 subareas were calculated using Park Systems XEI 1.7.5 image analysis software. AFM image data was 4th order plane fitted to show the nanoscale details of the PPy–HA and PPy–CS surfaces.

Characterization of Electrical Properties of the Films

Electrochemical impedance spectroscopy (EIS) and cyclic voltammetry measurements were taken from 1 cm^2 of doped PPy films on gold Mylar that was acting as working electrode. Platinum mesh acted as counter electrode and Ag/AgCl (3.0 M NaCl) as reference electrode. Impedance measurements were recorded by using CH 660D Electrochemical Analyzer/Workstation (CH Instruments, Austin, USA). Impedance spectra were obtained from 100 mHz to 100 kHz using an AC amplitude of ± 200 mV. All EIS measurements were performed at their resting potential ranging from $+70$ to $+195$ mV vs. the reference electrode to prevent destruction in the films. Average impedance and the standard deviation at 10 and 100 Hz were calculated from three samples per film type.

Cyclic voltammetry of the films was recorded in PBS by CH 660D Electrochemical Analyzer/Workstation in similar electrode setup as impedance recordings. Measurements were performed at the scan rate of 50 mV s^{-1} within the range of -0.6 to 0.5 V.

After the cell culture experiments, the through plane electrical conductivity of PPy films was monitored in air using a simple two-wire test setup (Fluke 170 multimeter, Washington, USA). The top and bottom electrodes applied were a round Au contact electrode (contact area of 16 mm^2) and the PEN/Au film, respectively.

Isolation and Culture of Human Adipose Stem Cells

The adipose tissue was obtained from tissue harvests from surgical procedures on three female donors with an average age of 54 ± 12 years in the Department of Plastic Surgery, Tampere University Hospital. The tissue harvesting and the use of hASCs were conducted in accordance with the Ethics Committee of the Pirkanmaa Hospital District (R03058). The hASC isolation method was presented earlier by Haimi *et al.*[24]. Briefly, the samples from adipose tissue were digested with collagenase type I (1.5 mg (ml; Invitrogen, California, USA). After centrifugation and filtration, the isolated hASCs were maintained and expanded in T-75 cm^2 polystyrene flask (Nunc, Roskilde, Denmark). The experiments were repeated three times, each time using different donors.

Before the cell seeding, PPy–CS and PPy–HA films were rinsed with PBS and pre-treated with maintenance medium at 37 °C for 48 h. PPy–CS and PPy–HA coated plates were cell seeded at passage 3 with a density of 16000 cells cm^{-2}. Cells were allowed to attach for 24 h before initiation of ES. On the first day of stimulation the maintenance medium was replaced by OM and medium was changed twice a week.

Flow Cytometric Surface Marker Expression Analysis

Cells were characterized by a fluorescence-activated cell sorter (FACSAria; BD Biosciences, Erembodegem, Belgium) at passage 1 after primary culture in T-75 flasks. This was described earlier by Lindroos *et al.*[33]. Monoclonal antibodies were used against the following surface markers: CD14, CD19, CD49d-PE, CD90-APC, CD106-PECy5 (BD Biosciences); CD45-FITC (Miltenyi Biotech, Bergisch Gladbach, Germany); CD34-APC, HLAABC-PE, HLA-DR-PE (Immunotools GmbH, Friesoythe, Germany) and CD105-PE (R&D Systems Inc., MN, USA). Analysis was performed on 10,000 cells per sample and unstained cell samples were used to compensate the background autofluorescence levels.

Biphasic Electrical Stimulation of Human Adipose Stem Cells

The stimulation plate assembly was earlier described by Pelto *et al.*[39] As an exception to the previous setup, PPy film was polymerized on the bottom electrode. ES was performed in a cell culturing incubator (37 °C, 5% CO_2). Samples were stimulated for 4 h a day for 14 days with a biphasic electric current (BEC) of ± 0.2 V amplitude, 2.5 ms pulse width and 100 Hz pulse repetition frequency. Non-stimulated samples acted as controls in each film type. The shortest vertical distance

between the top (Fig. 1: 1) and the bottom (Fig. 1: 2) electrodes immersed in each well was 2 mm. The measured steady state direct current after the 2.5 ms pulses was in the range of 40–50 μA cm^{-2}, corresponding to a cell impedance of 5 kΩ. The direction of the current was perpendicular to the PPy films.

Cell Attachment and Viability

Cell attachment and viability were evaluated qualitatively using live/dead staining (Molecular Probes, Eugene, USA). Cells were incubated in PBS-based dye solution containing 0.5 μM of CellTracker^{TM} Green (5-chloromethylfluorescein diacetate, CMFDA; Molecular Probes) and Ethidium homodimer-1 (EthD-1; Molecular Probes) at room temperature for 45 min. Samples were examined with a fluorescence microscope (Olympus IX51, Olympus Finland PLC, Vantaa, Finland). Standard polystyrene (PS) culturing plates (Nunc, Roskilde, Denmark) served as a positive control for the cell viability and morphology evaluation.

Cell Proliferation

Cell proliferation was studied with CyQuant® Cell Proliferation Assay Kit (Molecular Probes). The experiment was performed according to the manufacturer's protocol. Briefly, on the day of the analysis, samples were carefully washed with PBS and cells were suspended in 0.1% Triton-X 100 buffer (Sigma-Aldrich) in PBS and stored at −70 °C until analysis. After thawing, 20 μl of three parallel samples was mixed with CyQuant® GR dye and lysis buffer. The fluorescence was measured with a microplate reader (Victor 1420 Multilabel Counter, Wallac, Turku, Finland) at 480/520 nm.

Osteogenic Differentiation

Alkaline phosphatase (ALP) activity was determined using an ALP Kit (Sigma-Aldrich) according to the manufacturer's protocol. The ALP activity was determined from the same Triton-X 100 lysates as in the cell proliferation assay. The samples were incubated with 50% alkaline buffer solution (2-amino-2-methyl-1-propanol, 1.5 mol L^{-1}, pH 10.3; Sigma-Aldrich) and 50% of stock substrate solution (*p*-nitrophenyl phosphate; Sigma-Aldrich) at 37°C for exactly 15 min. To stop the reaction 1.0 mol L^{-1} sodium hydroxide was added. The intensity of the color was measured at 405 nm using a microplate reader (Victor 1420).

The mineralization of the ECM was studied with Alizarin Red staining. Samples were rinsed with PBS and fixed in ice cold 70% ethanol (Altia Corporation, Helsinki, Finland) for 60 min at room temperature. Samples were then rinsed with distilled water before the addition of 2% Alizarin Red solution (pH 4.2; Sigma-Aldrich) for 5 min. After incubation, samples were rinsed three times with distilled water and once with 70% ethanol. Samples were then incubated in cetylpyridium chloride (Sigma-Aldrich) for 3 hours. Supernatant was pipetted in triplicate on a 96-well plate (Nunc, Roskilde, Denmark) and absorbance measured at 544 nm using a microplate reader (Victor 1420).

Statistical Analysis

The statistical analyses of R_a values, DNA content, ALP activity and mineralization were performed with SPSS, version 19. R_a values of the films were analyzed with Student's *t* test and the equal variance assumption was checked by Levene's Test. A one way analysis of variance (ANOVA) with Bonferroni *post hoc* correction was used to determine the effect of the PPy coating and ES on DNA content, ALP activity and mineralization. The effect of culture duration on proliferation and ALP activity was analyzed using Student's *t* test for independent samples. The cell culture experiments were repeated three times with three par-

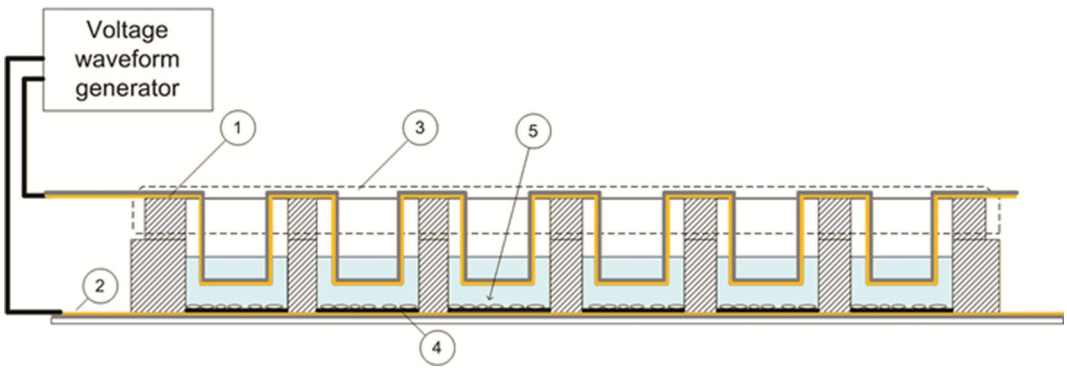

FIGURE 1. (a) Schematic illustration of the stimulation device geometry side projection. Top (1) and bottom (2) electrodes were made of gold coated PEN film. Cells were seeded to the bottom electrode (4) coated with PPy layer.

allel samples, each repetition using a different hASC donor. The data from the three experiments were combined and presented as mean ± standard deviation (SD) and the results were considered statistically significant when $p < 0.05$.

RESULTS

Surface Characterization of Polypyrrole Film

The measured R_a values of the wet and the dry PPy films are presented in Table 1. PPy–HA films had significantly higher R_a values than PPy–CS in PBS, whereas dry PPy–HA film had significantly lower R_a values when measured with non-contact AFM in air.

The non-contact AFM data (Figs. 2a and 2b) show the nanoscopic details of the dry PPy–CS (Fig. 2a) and PPy–HA (Fig. 2b) films. PPy–CS surface texture (Fig. 2a) consisted mainly of nodules, sized 40–50 nm in diameter and 5–10 nm in measurable height, which were organized into a porous web. The surface texture of PPy–HA (Fig. 2b) consisted of larger nodules, 150–160 nm in diameter and 30–35 nm in height. In both films, protrusions were sparsely distributed. The protrusions in the PPy–CS and PPy–HA films were similar in size, 500 nm in diameter and 100 nm in high. The nanoscopic texture was only observed in the dry samples and was not resolvable by AFM in PBS.

Imaging in PBS (contact mode) revealed a strongly undulating morphology of both films consisting of uniformly spread small 800–1000 nm nodules (Figs. 2c and 2d) and sparsely spread 4–10 μm circular protrusions covered with nodules (not visible in the flattened image data in Fig. 2).The nodules were typically of 100–150 and 200–300 nm in height for the PPy–HA (Fig. 2d) and PPy–CS (Fig. 2c) respectively. It is noteworthy that the hills caused by the undulating morphology as well as the protrusions were significantly higher than the nodules, typically 400–500 and 600–800 nm for the PPy–CS and PPy–HA films respectively. The protrusions in the PPy–CS were circular whereas those in PPy–HA were more oval. Hence the R_a values obtained from the AFM in PBS based on raw imaged data were not only representative of the nodules' height and shape but of the height of the protrusions.

Electrical Properties of the Films

The impedance of PPy–HA and PPy–CS films did not vary significantly yet PPy–CS showed slightly higher impedance values at 10 and 100 Hz (Table 1). Both films showed similar trend in the impedance spectra (Fig. 3). Both films showed well-defined voltammetric profiles though PPy–CS had slightly higher electrochemical activity and doping level compared to PPy–HA, as evidenced by the integrated surface areas covered by the respective voltammograms (Fig. 4). The conductivity of the films was confirmed to be in similar 10^{-3} S cm^{-1} levels as before the experiment when measured in air (data not shown).

Flow Cytometric Surface Marker Expression Analysis

Surface marker expression of hASCs was characterized by flow cytometric analysis. The cells used in this study expressed the surface markers CD73, CD90 and CD105 as shown in Table 2. Moderate expression was expressed by CD34, CD49d, HLA-ABC and HLA-DR whereas no expression was detected in CD14, CD19, CD45 and CD106. According to the results, hASCs expressed several of the specific antigens that verify the mesenchymal origin of hASCs.[33]

Cell Attachment and Viability

Cell attachment and viability were determined by live/dead staining which revealed extensive clustering of hASCs on PPy–HA surfaces as shown in Figs. 5e, 5f, 5g and 5h. In contrast, hASCs on PPy–CS were homogenously spread already after 1 week of culture (Figs. 5a, 5b, 5c, and 5d). This homogenous monolayer of hASCs was only evident on PPy–CS, since hASCs cultured on PS (Fig. 5i and 5j) were also sparsely spread on day 7. The increase in cell number over time was most obvious on PS, which had decid-

TABLE 1. R_a values of non-contact AFM data of air-dried PPy films and contact mode AFM of wet films in PBS as well as impedance at 100 Hz frequency.

Sample	R_a in air (nm)	R_a in PBS (nm)	Impedance at 10 Hz in PBS (Ω)	Impedance at 100 Hz in PBS (Ω)
PPy–CS	14 ± 0.8	320 ± 28	54 ± 13	45 ± 6
PPy–HA	8.6 ± 0.2	420 ± 40	51 ± 6	45 ± 2

R_a values were calculated from 10 successive measurements over randomly selected 4 × 4 μm^2 sub-areas. The differences between PPy–CS and PPy–HA were significant in both wet and dry films.

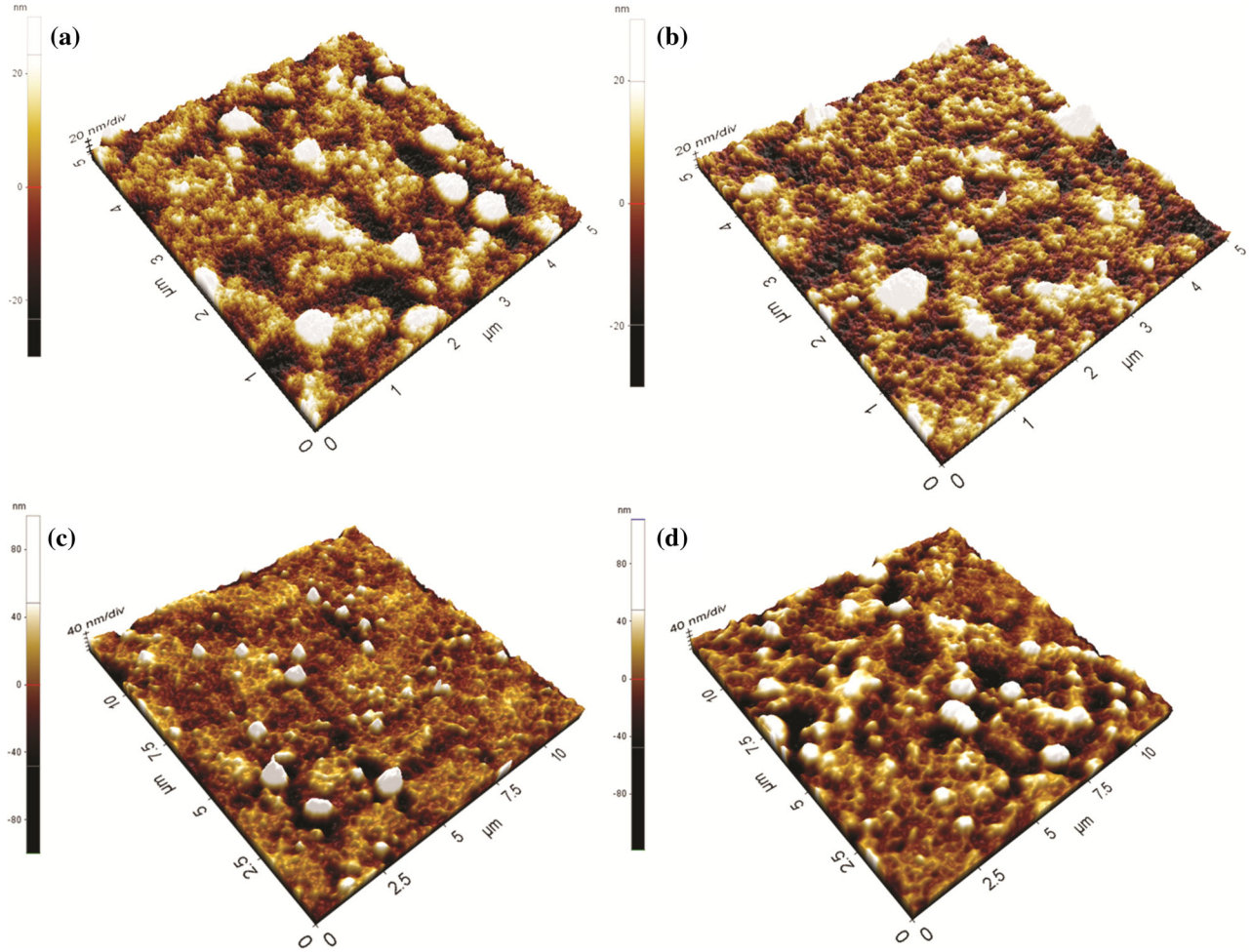

FIGURE 2. Surface topography of dry PPy–CS (a) and PPy–HA (b) films imaged using non-contact AFM in air. The sparsely distributed protrusions are seen as white areas. Scanned area is 5 × 5 μm and Z-scale 20 nm/division. (c) Surface topography images of wet PPy–CS and (d) PPy–HA films imaged with contact AFM in PBS. 800–1000 nm nodules are seen as white areas. Scanned area is 12 × 12 μm and Z-scales of the images are 40 nm/division.

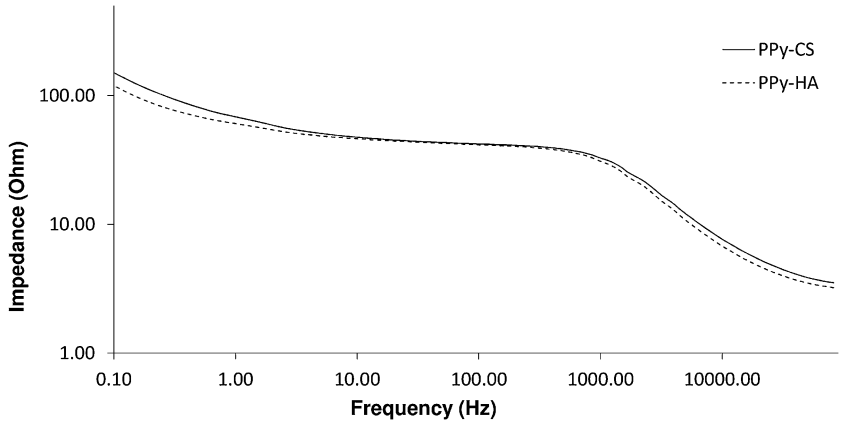

FIGURE 3. Impedance spectra for PPy films recorded in PBS.

edly fewer cells than PPy–CS at both time points. As regards BEC, no notable differences in cell number were seen between the control and stimulated group with neither of the dopants. The majority of the cells were viable on both PPy films at both time points in all experimental groups.

Cell Proliferation

Cell proliferation was evaluated quantitatively by measuring the total DNA content (Fig. 6). In the control group, the cell number on PPy–CS was significantly higher than PPy–HA on day 7. The increase in cell number on PPy–CS followed a similar trend at both time points under BEC compared with PPy–HA. However, no further significant differences were found. Consistently with the live/dead staining, no significant differences in cell number were found between the control and the stimulation group. The cell number increased significantly over time with both PPy–CS and PPy–HA without stimulation. In the stimulated group, only PPy–CS showed a significantly increasing cell number.

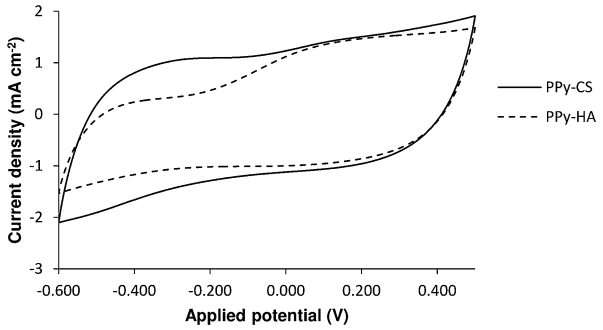

FIGURE 4. Cyclic voltammogram of PPy–CS and PPy–HA in PBS.

Osteogenic Differentiation

Both PPy–HA and PPy–CS supported hASC early osteogenic differentiation (Fig. 7) and no significant differences were detected between these two different material groups. However, ALP activity increased significantly over time only in the PPy–CS with and without stimulation. No significant differences between BEC and control groups were detected.

Under BEC, PPy–CS triggered significantly higher mineralization compared to PPy–HA (Fig. 8), whereas in the control group no significant differences were detected. Consistently with proliferation and ALP activity, no significant differences were found between BEC and the control group. One donor line did not show reliably detectable mineralization at the 14 day time point, therefore only data from two other repetitions are shown.

DISCUSSION

It has recently been reported that nanoscopic roughness in combination with microscale roughness are essential for the adhesion, proliferation and osteogenic differentiation of cells of mesenchymal origin.[19] Moreover, strong cell–ECM interactions enhanced by specific surface characteristics have an important role in osteogenic commitment among MSCs,[14] whereas proliferation is required for effective occupation of the scaffold.

As a main finding, our results demonstrate that CS was a superior dopant to HA by triggering significantly higher proliferation of hASCs after 1 week of culture. Both PPy films supported early osteogenic differentiation of hASCs yet PPy–CS showed significantly higher mineralization than PPy–HA in the stimulation group. Importantly, hASCs cultured on PPy–CS showed typical MSC morphology and already formed a homogenous monolayer on the PPy–CS film by day 7, whereas PPy–HA triggered clustering of the cells

TABLE 2. Surface marker expression of the undifferentiated hASCs after primary culture in maintenance medium.

Surface protein	Antigen	Mean	SD	Expression
CD14	Serum lipopolysaccharide binding protein	1.7	0.8	Negative
CD19	B lymphocyte-lineage differentiation antigen	0.9	0.4	Negative
CD34	Sialomucin-like adhesion molecule	9.3	8.75	Moderate expression
CD45	Leukocyte common antigen	1.1	0.3	Negative
CD49d	Integrin a2, VLA-4	11	13	Moderate expression
CD73	Ecto-50-nucleotidase	91.2	12.7	Positive
CD90	Thy-1 (T cell surface glycoprotein)	99	0.3	Positive
CD105	SH-2, endoglin	85.3	12.1	Positive
CD106	VCAM-1 (vascular cell adhesion molecule)	0.7	0.3	Negative
HLA-ABC	Major histocompatibility class I antigens	9.2	7.0	Moderate expression
HLA-DR	Major histocompatibility class II antigens	7.0	0.4	Moderate expression

Data presented as mean ± SD obtained from the three different hASC donors.

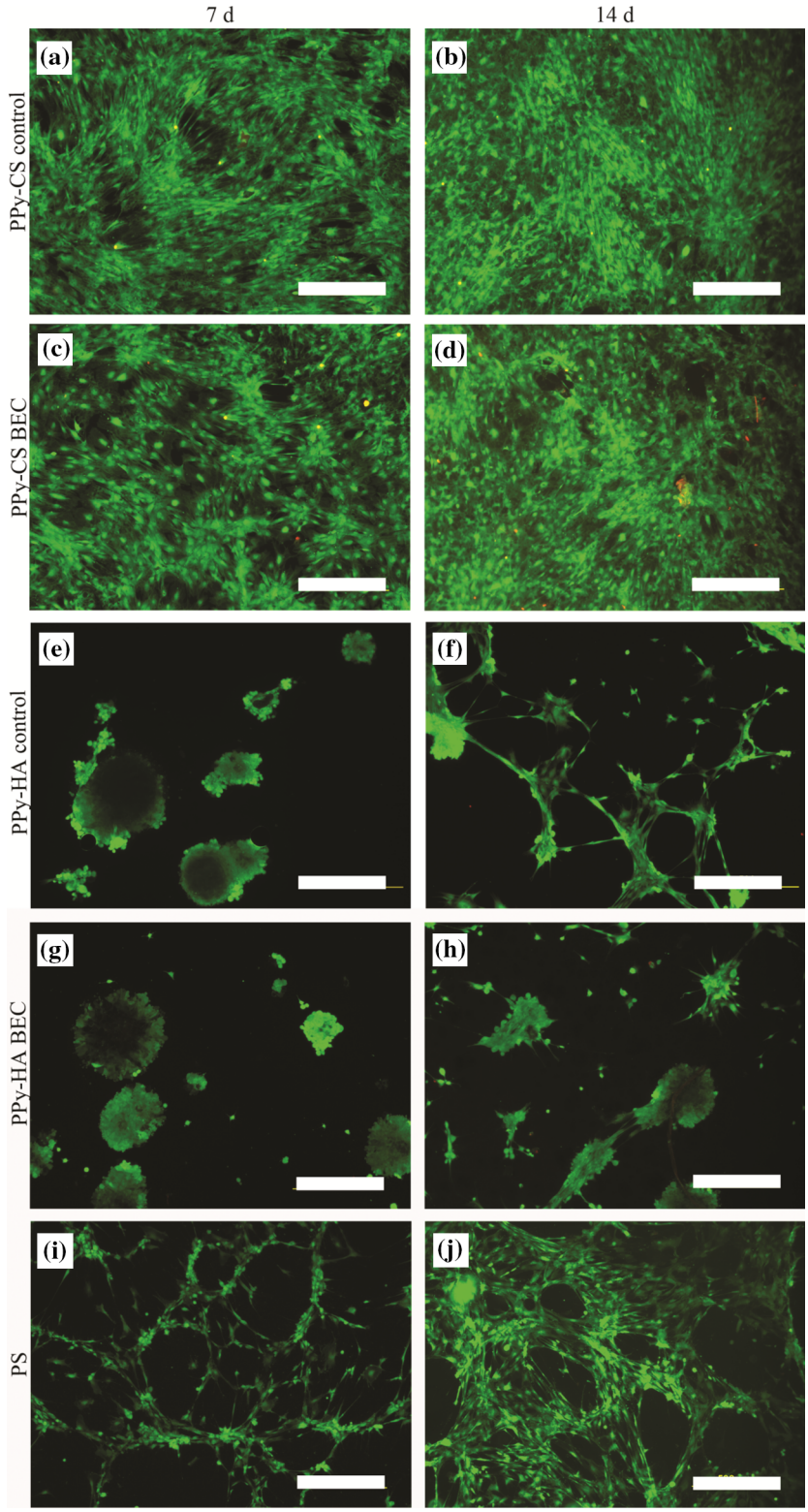

FIGURE 5. Live/dead images of hASCs on PPy–CS controls (a, b) and BEC stimulated group (c, d), PPy–HA controls (e, f) and BEC stimulated group (g, h) and PS (i, j) on days 7 and 14. Scale bar is 500 μm.

leading to detachment from the film. Aggregation of cells is an undesired effect in osteogenic applications and more characteristic of chondrogenic differentiation as it is one of the earliest signs of chondrogenesis. This suggests that PPy–HA could be a potential scaffold coating candidate for chondrogenic applications.[55]

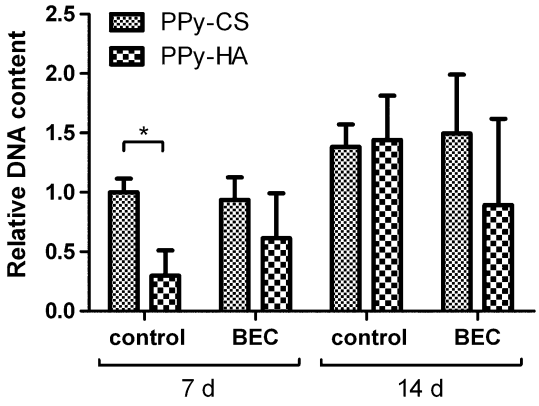

FIGURE 6. Relative DNA content of hASCs cultured for 7 and 14 days on PPy–CS and PPy–HA substrates with and without BEC. PPy–CS had significantly higher DNA content than did PPy–HA in control. The cell number increased significantly over time in the control group, on both PPy–CS and PPy–HA samples. In the stimulated group, only PPy–CS showed significantly increasing cell number. The results are expressed as mean ± SD and *$p < 0.05$.

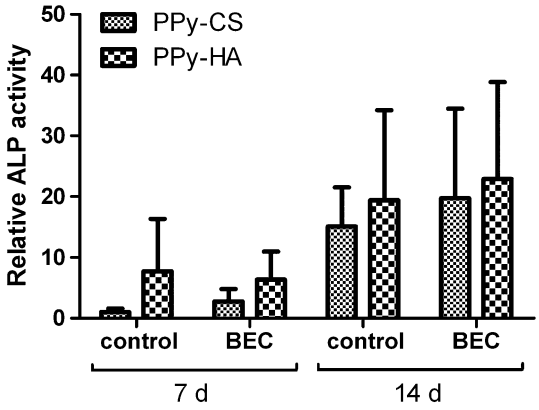

FIGURE 7. Relative ALP activity of hASCs cultured for 7 and 14 days on PPy CS and PPy–HA substrates with and without BEC. ALP activity increased significantly over time on PPy–CS control and BEC group. The results are expressed as mean ± SD.

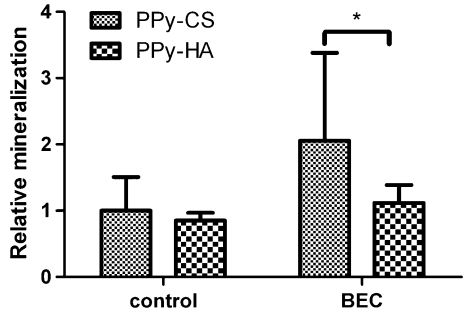

FIGURE 8. Relative ECM mineralization of hASCs cultured for 14 days on PPy CS and PPy–HA substrates with and without BEC. PPy–CS had significantly higher mineralization under BEC compared to PPy–HA. The results are expressed as mean ± SD and *$p < 0.05$.

As both dopants are commonly used macromolecules in bone tissue engineering, the reason why PPy–HA caused clustering of hASC most probably lies in the physical surface properties, such as the morphology, hydrophilicity and elasticity of the PPy–HA surface. Even though the non-uniform microscopic morphology was present in both PPy–CS and PPy–HA wet films, the swollen protrusions were significantly higher in the PPy–HA, consequently reflecting the measured R_a values in contact mode imaging. Similar differences between PPy–HA and PPy–CS morphology have also been reported by Gelmi *et al.*[17] In addition, Gilmore *et al.* compared thin and thick PPy films, formed by different polymerization charges, and examined various dopants. They concluded that PPy–HA did not support myoblast adhesion or differentiation and the elevated R_a values were one of the parameters correlating with the poor performance of PPy–HA. Greater surface thickness of PPy–HA compared to other films, such as PPy–CS, was deduced to lead to the development of greater nodules.[18] Moreover, smooth surface morphology polymerized with low current densities (100–700 μA cm^{-2}) was demonstrated to be the key parameter for MC3T3-E1 osteoblast adhesion on PPy–HA surfaces, whereas those polymerized with higher current densities (~1 mA cm^{-2}) exhibited more irregular surface and did not ensure good cell adhesion.[45] The current density in our study stayed under 700 μA cm^{-2} implying that surface roughness should be within suitable ranges in means of cell adhesion during the ES.

The optimal AFM imaging conditions in PBS for the PPy–CS (force setpoint 20 nN) and PPy–HA (7 nN) films were different from those measured in air, indicating that PPy–HA was softer than PPy–CS in wet state. This was also supported by the occasional adhesion of the AFM tip to the PPy–HA surface. Comparison of AFM images in wet and dry state also showed that both PPy–CS and PPy–HA films absorbed significant amounts of PBS, resulting in swelling, large dimensional changes and softening of the films to hydrogel-like materials. Earlier studies with similar films have estimated the swelling percent to be 11–25%.[39,46,48] In contrast, Gelmi *et al.* did not detect any significant swelling of the PPy–HA and PPy–CS films.[17] Furthermore, the nanoscopic textures of the dry samples were significantly different from those of the wet samples. The characteristic nodular nanomorphology was detected for both PPy films in PBS consistent with earlier reports on PPy–CS and PPy–HA.[17,18,47]

Hills caused by undulating morphology may result from the local detachment of the material from its metallic substrate, which has been previously observed for electropolymerized PPy–HA films on Au microelectrodes upon repeated electrochemical cycling.

However, the characteristic pattern of the microscopic circular protrusions has not been observed on microelectrodes of other substrates.[39]

Regarding electrical properties of the films, the choice of dopant did not pose drastically different impedance either at 10 or at 100 Hz, yet the decrease in impedance was more evident for PPy–CS from 10 to 100 Hz. In contrast to our study, Gilmore *et al.* has earlier compared impedance of electrochemically grown thick PPy–HA and PPy–CS films reporting substantially higher impedance for PPy–HA at 10 Hz.[18] Cyclic voltammetry showed slightly higher electrical activity and doping level of PPy–CS. Higher acidic strength of dopants has been shown to enhance charge carrier (bipolaron) formation in the PPy chains, hence, the stronger acidity of the sulfonic acid groups in CS compared to less acidic carboxylic acid groups in HA could potentially yield higher doping ratio in PPy–CS.[32]

The selected parameters of the ES in our study were based on earlier study with ASCs in osteogenic applications.[25] According to Hammerick *et al.*, ALP activity increased in mouse ASCs in response to pulsed electric field stimulation. We chose a pulsed BEC waveform since it is expected to prevent the accumulation of charged proteins and keep the pH of media at steady levels.[31] In addition to our present work, only one study has examined the effect of a combination of PPy and ES on osteogenic differentiation for conducting a study with SAOS-2 cells.[37] Interestingly, mineralization in our study was significantly higher in PPy–CS compared to PPy–HA in BEC group whereas no differences were detected in control group. Mineralization slightly increased in both groups, being more substantial in PPy–CS, yet not significant. This could suggest synergistic effects of PPy–CS and BEC. The reason why no significant effect of ES on ALP activity could be detected in our study is not clear. One possible reason might be donor variation in means of osteogenic differentiation, which has been reported with MSCs exposed to dexamethasone.[6] In our study, one patient had clearly higher ALP activity than the two others on day 14 (data not shown). In addition, the standard deviation of the stimulated groups was, in general, slightly higher than in the control groups, which may have prevented the detection of some differences between the groups. The reason for greater deviation could be attributable to synergy between BEC and PPy coating, such as overoxidation of PPy during high electrochemical potentials that leads to the loss of conductivity,[10] and de-doping or ion exchange between medium and PPy.[16,27] Moreover, several factors, such as protein deposition from the culture medium and their interactions with redox reactions of the PPy surface[27] or local detachment of PPy film may have affected on the homogenicity of the electrical field. To minimize the bias, three parallel samples were used in all of the assays in every patient lineage. Despite the slight increase in mineralization under BEC, more systematic screening of BEC parameters is needed to find an effective ES pattern for ASCs.

Even though PPy is considered biocompatible by several *in vivo* studies, the longest implantation period has only been six months,[29,40,51,52] PPy is not inherently biodegradable which may pose challenges in its use in tissue engineering. It may be possible that PPy coatings do not fully erode during their use of time and therefore it needs further evaluation of the long term effects in the body. What comes to the inevitable erosion products, PPy nanoparticles have shown to be less cytotoxic compared to silver or TiO_2 nanoparticles that are common wear products of orthopedic implants.[30,49]

CONCLUSION

PPy–CS supported the proliferation and homogenous spreading of hASCs significantly more than PPy–HA. Both PPy–CS and PPy–HA supported early osteogenic differentiation of hASCs over time but mineralization of hASCs was significantly greater with PPy–CS under BEC. PPy–HA is not recommended for osteogenic applications as it promotes the clustering and detachment of hASCs. This is most probably due to different surface properties since PPy–HA had a significantly rougher and softer surface than did PPy–CS in wet conditions. BEC stimulation showed no significant effects on hASC proliferation or osteogenic differentiation. This is the first study to report on the suitability of PPy–CS for bone tissue engineering applications.

ACKNOWLEDGMENTS

The authors would like to thank Ms. Anne Rajala M.Sc, Ms. Ana Luísa Delgado Lima, and Ms. Hanna Juhola for the preparation and of the scaffolds, Ms. Anna-Maija Honkala, Ms. Minna Salomäki M.Sc and Ms Miia Juntunen for their assistance in the cell culture work. This study was financially supported by the Finnish Funding Agency for Technology and Innovation (TEKES), the Academy of Finland and the Competitive Research Funding of Tampere University Hospital (Grant 9K020).

REFERENCES

[1]Abidian, M. R., J. M. Corey, D. R. Kipke, and D. C. Martin. Conducting-polymer nanotubes improve electrical properties, mechanical adhesion, neural attachment, and

neurite outgrowth of neural electrodes. *Small* 6:421–429, 2010.
[2]Abidian, M. R., E. D. Daneshvar, B. M. Egeland, D. R. Kipke, P. S. Cederna, and M. G. Urbanchek. Hybrid conducting polymer–hydrogel conduits for axonal growth and neural tissue engineering. *Adv. Healthc. Mater.* 1:762–767, 2012.
[3]Abidian, M. R., D.-H. Kim, and D. C. Martin. Conducting-polymer nanotubes for controlled drug release. *Adv. Mater.* 18:405–409, 2006.
[4]Abidian, M. R., K. A. Ludwig, T. C. Marzullo, D. C. Martin, and D. R. Kipke. Interfacing conducting polymer nanotubes with the central nervous system: chronic neural recording using poly(3,4-ethylenedioxythiophene) nanotubes. *Adv. Mater.* 21:3764–3770, 2009.
[5]Abidian, M. R., and D. C. Martin. Multifunctional nanobiomaterials for neural interfaces. *Adv. Funct. Mater.* 19:573–585, 2009.
[6]Alm, J. J., T. J. Heino, T. A. Hentunen, H. K. Vaananen, and H. T. Aro. Transient 100 nM dexamethasone treatment reduces inter- and intraindividual variations in osteoblastic differentiation of bone marrow-derived human mesenchymal stem cells. *Tissue Eng. Part C* 18:658–666, 2012.
[7]Ates, M. A review study of (bio)sensor systems based on conducting polymers. *Mater. Sci. Eng. C* 33:1853–1859, 2013.
[8]Balint, R., N. J. Cassidy, and S. H. Cartmell. Conductive polymers: towards a smart biomaterial for tissue engineering. *Acta Biomater.* 10:S1742–7061, 2014.
[9]Castano, H., E. A. O'Rear, P. S. McFetridge, and V. I. Sikavitsas. Polypyrrole thin films formed by admicellar polymerization support the osteogenic differentiation of mesenchymal stem cells. *Macromol. Biosci.* 4:785–794, 2004.
[10]Christensen, P. A., and A. Hamnett. In situ spectroscopic investigations of the growth, electrochemical cycling and overoxidation of polypyrrole in aqueous solution. *Electrochim. Acta* 36:1263–1286, 1991.
[11]De Giglio, E., M. R. Guascito, L. Sabbatini, and G. Zambonin. Electropolymerization of pyrrole on titanium substrates for the future development of new biocompatible surfaces. *Biomaterials* 22:2609–2616, 2001.
[12]Ercan, I., I. Günal, and O. Güven. Conductance of polypyrole irradiated with gamma rays to low doses. *Radiat. Phys. Chem.* 46:813–817, 1995.
[13]Esrafilzadeh, D., J. M. Razal, S. E. Moulton, E. M. Stewart, and G. G. Wallace. Multifunctional conducting fibres with electrically controlled release of ciprofloxacin. *J. Controlled Release* 169:313–320, 2013.
[14]Frith, J. E., R. J. Mills, J. E. Hudson, and J. J. Cooper-White. Tailored integrin-extracellular matrix interactions to direct human mesenchymal stem cell differentiation. *Stem Cells Dev.* 21:2442–2456, 2012.
[15]Fukada, E., and I. Yasuda. Piezoelectric effects in collagen. *Jpn. J. Appl. Phys.* 3:117–121, 1964.
[16]Gandhi, M. R., P. Murray, G. M. Spinks, and G. G. Wallace. Mechanism of electromechanical actuation in polypyrrole. *Synth. Met.* 73:247–256, 1995.
[17]Gelmi, A., M. J. Higgins, and G. G. Wallace. Physical surface and electromechanical properties of doped polypyrrole biomaterials. *Biomaterials* 31:1974–1983, 2010.
[18]Gilmore, K. J., M. Kita, Y. Han, A. Gelmi, M. J. Higgins, S. E. Moulton, G. M. Clark, R. Kapsa, and G. G. Wallace. Skeletal muscle cell proliferation and differentiation on polypyrrole substrates doped with extracellular matrix components. *Biomaterials* 30:5292–5304, 2009.
[19]Gittens, R. A., T. McLachlan, R. Olivares-Navarrete, Y. Cai, S. Berner, R. Tannenbaum, Z. Schwartz, K. H. Sandhage, and B. D. Boyan. The effects of combined micron-/submicron-scale surface roughness and nanoscale features on cell proliferation and differentiation. *Biomaterials* 32:3395–3403, 2011.
[20]Green, R. A., N. H. Lovell, and L. A. Poole-Warren. Cell attachment functionality of bioactive conducting polymers for neural interfaces. *Biomaterials* 30:3637–3644, 2009.
[21]Green, R. A., P. B. Matteucci, R. T. Hassarati, B. Giraud, C. W. Dodds, S. Chen, P. J. Byrnes-Preston, G. J. Suaning, L. A. Poole-Warren, and N. H. Lovell. Performance of conducting polymer electrodes for stimulating neuroprosthetics. *J. Neural Eng.* 10(1):016009, 2013; (Epub 2013 Jan 3).
[22]Griffin, M., and A. Bayat. Electrical stimulation in bone healing: critical analysis by evaluating levels of evidence. *Eplasty* 11:e34, 2011.
[23]Guimard, N. K., N. Gomez, and C. E. Schmidt. Conducting polymers in biomedical engineering. *Prog. Polym. Sci.* 32:876–921, 2007.
[24]Haimi, S., L. Moimas, E. Pirhonen, B. Lindroos, H. Huhtala, S. Räty, H. Kuokkanen, G. K. Sándor, S. Miettinen, and R. Suuronen. Calcium phosphate surface treatment of bioactive glass causes a delay in early osteogenic differentiation of adipose stem cells. *J. Biomed. Mater. Res. Part A* 91A:540–547, 2009.
[25]Hammerick, K. E., A. W. James, Z. Huang, F. B. Prinz, and M. T. Longaker. Pulsed direct current electric fields enhance osteogenesis in adipose-derived stromal cells. *Tissue Eng. Part A* 16:917–931, 2010.
[26]Hess, R., A. Jaeschke, H. Neubert, V. Hintze, S. Moeller, M. Schnabelrauch, H. Wiesmann, D. A. Hart, and D. Scharnweber. Synergistic effect of defined artificial extracellular matrices and pulsed electric fields on osteogenic differentiation of human MSCs. *Biomaterials* 33:8975–8985, 2012.
[27]Higgins, M. J., P. J. Molino, Z. Yue, and G. G. Wallace. Organic conducting polymer–protein interactions. *Chem. Mater.* 24:828, 2012.
[28]Jha, A. K., X. Xu, R. L. Duncan, and X. Jia. Controlling the adhesion and differentiation of mesenchymal stem cells using hyaluronic acid-based, doubly crosslinked networks. *Biomaterials* 32:2466–2478, 2011.
[29]Jiang, X., Y. Marois, A. Traore, D. Tessier, L. H. Dao, R. Guidoin, and Z. Zhang. Tissue reaction to polypyrrole-coated polyester fabrics: an *in vivo* study in rats. *Tissue Eng.* 8:635–647, 2002.
[30]Kim, S., W. Oh, Y. S. Jeong, J. Hong, B. Cho, J. Hahn, and J. Jang. Cytotoxicity of, and innate immune response to, size-controlled polypyrrole nanoparticles in mammalian cells. *Biomaterials* 32:2342–2350, 2011.
[31]Kim, I. S., J. K. Song, Y. M. Song, T. H. Cho, T. H. Lee, S. S. Lim, S. J. Kim, and S. J. Hwang. Novel effect of biphasic electric current on *in vitro* osteogenesis and cytokine production in human mesenchymal stromal cells. *Tissue Eng. Part A* 15:2411–2422, 2009.
[32]Kuwabata, S., J. Nakamura, and H. Yoneyama. The effect of basicity of dopant anions on the conductivity of polypyrrole films. *J. Chem. Soc. Chem. Commun.* 779–780, 1988.
[33]Lindroos, B., S. Boucher, L. Chase, H. Kuokkanen, H. Huhtala, R. Haataja, M. Vemuri, R. Suuronen, and S.

Miettinen. Serum-free, xeno-free culture media maintain the proliferation rate and multipotentiality of adipose stem cells *in vitro*. *Cytotherapy* 11:958–972, 2009.
[34]Liu, A., L. Zhao, H. Bai, H. Zhao, X. Xing, and G. Shi. Polypyrrole actuator with a bioadhesive surface for accumulating bacteria from physiological media. *ACS Appl. Mater. Interfaces* 1:951–955, 2009.
[35]Ludwig, K. A., J. D. Uram, J. Yang, D. C. Martin, and D. R. Kipke. Chronic neural recordings using silicon microelectrode arrays electrochemically deposited with a poly(3,4-ethylenedioxythiophene) (PEDOT) film. *J. Neural Eng.* 3:59–70, 2006.
[36]McCullen, S. D., J. P. McQuilling, R. M. Grossfeld, J. L. Lubischer, L. I. Clarke, and E. G. Loboa. Application of low-frequency alternating current electric fields *via* interdigitated electrodes: effects on cellular viability, cytoplasmic calcium, and osteogenic differentiation of human adipose-derived stem cells. *Tissue Eng. Part C* 16:1377–1386, 2010.
[37]Meng, S., Z. Zhang, and M. Rouabhia. Accelerated osteoblast mineralization on a conductive substrate by multiple electrical stimulation. *J. Bone Miner. Metab.* 29:535–544, 2011.
[38]Pelto, J., M. Bjorninen, A. Palli, E. Talvitie, J. Hyttinen, B. Mannerstrom, R. Suuronen Seppanen, M. Kellomaki, S. Miettinen, and S. Haimi. Novel polypyrrole-coated polylactide scaffolds enhance adipose stem cell proliferation and early osteogenic differentiation. *Tissue Eng. Part A* 19:882–892, 2013.
[39]Pelto, J., S. Haimi, E. Puukilainen, P. G. Whitten, G. M. Spinks, M. Bahrami-Samani, M. Ritala, and T. Vuorinen. Electroactivity and biocompatibility of polypyrrole-hyaluronic acid multi-walled carbon nanotube composite. *J. Biomed. Mater. Res. Part A* 93A:1056–1067, 2010.
[40]Ramanaviciene, A., A. Kausaite, S. Tautkus, and A. Ramanavicius. Biocompatibility of polypyrrole particles: an *invivo* study in mice. *J. Pharm. Pharmacol.* 59:311–315, 2007.
[41]Richardson, R. T., A. K. Wise, B. C. Thompson, B. O. Flynn, P. J. Atkinson, N. J. Fretwell, J. B. Fallon, G. G. Wallace, R. K. Shepherd, G. M. Clark, and S. J. O'Leary. Polypyrrole-coated electrodes for the delivery of charge and neurotrophins to cochlear neurons. *Biomaterials* 30:2614–2624, 2009.
[42]Richardson-Burns, S. M., J. L. Hendricks, B. Foster, L. K. Povlich, D. Kim, and D. C. Martin. Polymerization of the conducting polymer poly(3,4-ethylenedioxythiophene) (PEDOT) around living neural cells. *Biomaterials* 28:1539–1552, 2007.
[43]Salbach, J., T. D. Rachner, M. Rauner, U. Hempel, U. Anderegg, S. Franz, J. C. Simon, and L. C. Hofbauer. Regenerative potential of glycosaminoglycans for skin and bone. *J. Mol. Med. (Berl)* 90:625–635, 2012.
[44]Serra Moreno, J., S. Panero, M. Artico, and P. Filippini. Synthesis and characterization of new electroactive polypyrrole–chondroitin sulphate A substrates. *Bioelectrochemistry* 72:3–9, 2008.
[45]Serra Moreno, J., S. Panero, S. Materazzi, A. Martinelli, M. G. Sabbieti, D. Agas, and G. Materazzi. Polypyrrole-polysaccharide thin films characteristics: electrosynthesis and biological properties. *J. Biomed. Mater. Res. Part A* 88A:832–840, 2009.
[46]Serra Moreno, J., M. G. Sabbieti, D. Agas, L. Marchetti, and S. Panero. Polysaccharides immobilized in polypyrrole matrices are able to induce osteogenic differentiation in mouse mesenchymal stem cells. Med: J. Tissue Eng. Regen., 2012.
[47]Silk, T., Q. Hong, J. Tamm, and R. G. Compton. AFM studies of polypyrrole film surface morphology II. Roughness characterization by the fractal dimension analysis. *Synth. Met.* 93:65–71, 1998.
[48]Smela, E., and N. Gadegaard. Volume change in polypyrrole studied by atomic force microscopy. *J. Phys. Chem. B* 105:9395–9405, 2001.
[49]St. Pierre, C. A., M. Chan, Y. Iwakura, D. C. Ayers, E. A. Kurt-Jones, and R. W. Finberg. Periprosthetic osteolysis: characterizing the innate immune response to titanium wear-particles. *J. Orthop. Res.* 28:1418–1424, 2010.
[50]Thompson, B. C., S. E. Moulton, R. T. Richardson, and G. G. Wallace. Effect of the dopant anion in polypyrrole on nerve growth and release of a neurotrophic protein. *Biomaterials* 32:3822–3831, 2011.
[51]Wang, X., X. Gu, C. Yuan, S. Chen, P. Zhang, T. Zhang, J. Yao, F. Chen, and G. Chen. Evaluation of biocompatibility of polypyrrole *in vitro* and *in vivo*. *J. Biomed. Mater. Res. Part A* 68A:411–422, 2004.
[52]Wang, Z., C. Roberge, L. H. Dao, Y. Wan, G. Shi, M. Rouabhia, R. Guidoin, and Z. Zhang. *In vivo* evaluation of a novel electrically conductive polypyrrole/poly(D,L-lactide) composite and polypyrrole-coated poly(D,L-lactide-*co*-glycolide) membranes. *J. Biomed. Mater. Res. Part A* 70A:28–38, 2004.
[53]Wollenweber, M., H. Domaschke, T. Hanke, S. Boxberger, G. Schmack, K. Gliesche, D. Scharnweber, and H. Worch. Mimicked bioartificial matrix containing chondroitin sulphate on a textile scaffold of poly(3-hydroxybutyrate) alters the differentiation of adult human mesenchymal stem cells. *Tissue Eng.* 12:345–359, 2006.
[54]Wolszczak, M., J. Kroh, and M. M. Abdel-Hamid. Some aspects of the radiation processing of conducting polymers. *Radiat. Phys. Chem.* 45:71–78, 1995.
[55]Wu, S., J. Chang, C. Wang, G. Wang, and M. Ho. Enhancement of chondrogenesis of human adipose derived stem cells in a hyaluronan-enriched microenvironment. *Biomaterials* 31:631–640, 2010.

TISSUE ENGINEERING: Part A
Volume 19, Numbers 7 and 8, 2013

DOI: 10.1089/ten.tea.2012.0111

Novel Polypyrrole-Coated Polylactide Scaffolds Enhance Adipose Stem Cell Proliferation and Early Osteogenic Differentiation

Jani Pelto, MSc,[1] Miina Björninen, MSc,[2–4] Aliisa Pälli, MSc,[2–4] Elina Talvitie, MSc,[4,5] Jari Hyttinen, PhD,[4,5] Bettina Mannerström, PhD,[2–4] Riitta Suuronen Seppanen, MD, DDS,[2,4–6] Minna Kellomäki, PhD,[4,5] Susanna Miettinen, PhD,[2–4] and Suvi Haimi, PhD[2–4,7]

An electrically conductive polypyrrole (PPy) doped with a bioactive agent is an emerging functional biomaterial for tissue engineering. We therefore used chondroitin sulfate (CS)-doped PPy coating to modify initially electrically insulating polylactide resulting in novel osteogenic scaffolds. *In situ* chemical oxidative polymerization was used to obtain electrically conductive PPy coating on poly-96L/4D-lactide (PLA) nonwoven scaffolds. The coated scaffolds were characterized and their electrical conductivity was evaluated in hydrolysis. The ability of the coated and conductive scaffolds to enhance proliferation and osteogenic differentiation of human adipose stem cells (hASCs) under electrical stimulation (ES) in three-dimensional (3D) geometry was compared to the noncoated PLA scaffolds. Electrical conductivity of PPy-coated PLA scaffolds (PLA-PPy) was evident at the beginning of hydrolysis, but decreased during the first week of incubation due to de-doping. PLA-PPy scaffolds enhanced hASC proliferation significantly compared to the plain PLA scaffolds at 7 and 14 days. Furthermore, the alkaline phosphatase (ALP) activity of the hASCs was generally higher in PLA-PPy seeded scaffolds, but due to patient variation, no statistical significance could be determined. ES did not have a significant effect on hASCs. This study highlights the potential of novel PPy-coated PLA scaffolds in bone tissue engineering.

Introduction

Polylactide-based polymers have been extensively used in various applications for over two decades. However, lack of bioactivity has limited their use especially in tissue engineering applications.[1,2] To overcome this problem, several approaches have been developed, such as integrating growth factors, or other bioactive agents into the polymer structure.[3,4] Another potential strategy to functionalize polylactide scaffolds could be the application of conductive polymers as a functional surface coating. Among these conductive polymers, polypyrrole (PPy) has emerged as a promising polymer group for tissue engineering due to its high biocompatibility and its good electroconductive properties.[5]

The surface roughness, hydrophilicity, and elasticity of PPys can be tailored by the choice of the dopants or surfactants used in their synthesis.[6,7] One of the most studied biopolymer dopants is chondroitin sulfate (CS), a naturally occurring ubiquitous glycosaminoglycan.[8,9] CS is found not only in the ECM, but was also discovered on the cell surfaces of most mammalian cells and reported to be involved in osteogenic processes, including development, maturation, remodeling, and repair.[10,11] CS has previously been shown to enhance bone remodeling when applied together with hydroxyapatite/collagen bone cement.[9] Due to the osteogenic potential of CS, we hypothesized that by using CS-doped PPy coating, we could stimulate the osteogenic differentiation of human adipose stem cells (hASCs), a potential mesenchymal stem cell (MSC) group in the field of skeletal tissue engineering.

In an earlier study, we already verified the good biocompatibility of PPy using hASCs.[7] The effect of PPy surfaces with or without electrical stimulation (ES) has been studied with various cell types, such as skeletal muscle cells, neurites, endothelial cells, fibroblasts, osteoblasts, and

[1]VTT Technical Research Centre of Finland, Tampere, Finland.
[2]Adult Stem Cells, Institute of Biomedical Technology, University of Tampere, Tampere, Finland.
[3]Science Centre, Pirkanmaa Hospital District, Tampere, Finland.
[4]BioMediTech, Tampere, Finland.
[5]Department of Biomedical Engineering, Tampere University of Technology, Tampere, Finland.
[6]Department of Eye, Ear, and Oral Diseases, Tampere University Hospital, Tampere, Finland.
[7]Department of Biomaterials Science and Technology, University of Twente, Enschede, Netherlands.

MSCs.[12–17] However, so far, the effects of PPy on osteogenic differentiation of human ASCs have not, to the best of our knowledge, been reported either with or without ES.

ES has been applied to a number of cell types to enhance proliferation and to direct cell differentiation, but mainly to electrically active cells, such as neurons or cardiomyoblasts.[18] Interestingly, a few recent publications have focused on the stimulation of electrically inactive MSCs, demonstrating that ES has a significant impact on ASC proliferation and differentiation.[19–21] ES has also been successfully applied via PPy for different cell types resulting in increased cell proliferation and significant changes in other cell functions.[22–24] This article is the first to report the effects of novel conductive poly-96L/4D-lactide/PPy (PLA-PPy) scaffolds and their combined effects with the ES on hASC viability, proliferation, and early osteogenic differentiation studied in a three-dimensional (3D) culture system.

Materials and Methods

Materials

Medical grade PLA with an inherent viscosity of 2.1 dL g-1 (PURAC biochembv) was used in melt spinning and scaffold manufacturing. Pyrrole monomer, ammonium peroxydisulfate oxidant (APS), and chondroitin 6-sulfate sodium salt from bovine trachea were purchased from Sigma-Aldrich. Pyrrole was distilled in a vacuum before use. Other reagents were used without any further purification. Distilled water was used in the polymerizations.

Synthesis of 3D scaffolds

Polylactide fibers and nonwoven scaffolds. PLA was extruded (GimacMicroextruder TR 12/24 B.V.O.; Gimac) and hot-drawn to 16ply multifilament fiber. The diameters of the single filaments were 10–20 μm. To manufacture the nonwoven scaffolds, the fibers were cut and carded using a manually operated drum carder (Elite Drum Carder; Louët BV). Several cards were then combined by needle punching using a James Hunter Needle Punching Machine (James Hunter Machine Co.) to obtain $10 \times 10 \times 2$ mm size scaffolds.

Chemical oxidative polymerization of PPy. The polymerization parameters were optimized to ensure optimal conductivity and uniformity of the coating; the pyrrole concentration varied between 0.03–0.3 M, the CS concentration between 0.5–2 mg/mL, the oxidant concentration between 0.01–0.1M, and the polymerization time from 30 s to 15 min in an ambient temperature. The following optimized concentrations were used for all the *in vitro* samples: [pyrrole] = 0.036 M, [APS] = 0.1 M, and [CS] = 1 mg/mL, polymerization time 150 s.

Before polymerization, CS and APS were dissolved separately in distilled water. CS and APS solutions were combined and pyrrole added immediately with vigorous stirring. The sample was placed in the polymerization bath. The nonwoven scaffolds were pretreated in ethanol before polymerization. After polymerization, the samples were rinsed thoroughly with water and dried in air. Samples were sterilized by gamma irradiation (BBF Sterilizations service GmbH) with an irradiation dose of >25 kGy.

Characterization

Hydrolysis and conductivity measurements. Gamma irradiated scaffolds were incubated in sealed plastic specimen chambers containing either a phosphate buffer solution PBS (Sörensen, pH 7.4 ± 0.2; Na_2HPO_4 0.0546 mol l-1, KH_2PO_4 0.121 mol l-1) or a maintenance medium consisting of the Dulbecco's modified Eagle's medium/Ham's Nutrient Mixture F-12 (DMEM/F-12 1:1 1 ×; Invitrogen), 10% human serum type AB (HS; PAA Laboratories GmbH), 1% L-glutamine (GlutaMAX I; Invitrogen), and 1% pen-strep (100 U/mL penicillin, 0.1 mg/mL streptomycin; Lonza) at +37°C for up to 42 days. Test conditions were set as specified in ISO-15814:1999(E) standard. The pH of the buffer solution was measured and changed every 3 days twice a week to exclude the acidic autocatalytic hydrolysis of PLA.

Directly after the synthesis and during the hydrolysis test, the direct current (DC) conductivity of air-dry scaffolds was measured using custom-made copper flat alligator clips (contact area 6 mm^2) and Fluke 189 multimeter. Non-sterilized samples were used for conductivity measurement since the electrical properties of PPy have been reported to be stable[25] with the irradiation dose used.

Electrospray ionization mass spectroscopy. Gamma-sterilized, noncoated PLA and PPy-coated samples of 10 mg were hydrolyzed for 30 days at +60°C in 1.0 mL pure water. The hydrolyzed samples were analyzed with a single quadruple Perkin Elmer SQ 300 electrospray mass spectrometry (MS) system (PerkinElmer) in the positive ion mode. The drying gas (nitrogen) temperature was set at +175°C and the drying gas flow rate at 8 L/min. The capillary exit voltage was varied between 60 and 200 V to screen the onset of cracking of the PLA oligomers. The MS was operated in a scan mode (mass range 200–1000) and dwell time was set at 0.1 ms. Briefly, the (hydrolysis) solution was filtered through 0.45-μm PTFE filter, 0.5 mL methanol was added to the mixture (water/MeOH 2:1 v/v) and the sample injected by a syringe pump into the mass spectrometer at a flow rate of 5 μL/min.

Scanning electron microscopy. Noncoated PLA and PPy-coated PLA scaffolds were imaged by JSM–6360 LV SEM (JEOL). Low 3 kV acceleration voltage was applied to prevent sample damage and to induce contrast between electrically conductive and insulating areas. For the non-coated scaffold, the imaging was first done without metallic surface coating and, subsequently, a thin 20-nm sputter-coated gold layer (SCD 050; Balzers AG).

Atomic force microscopy. The morphology of individual PLA-PPy fibers in air was imaged by noncontact mode atomic force microscopy (Park XE-100 AFM; Park Systems). Silicon probes (ACTA-905M, Applied NanoStructures, Inc.) with a nominal resonance frequency of 300 kHz and spring constant of 4 N/m were applied with a pyramidal shaped tip (radius < 10 nm) and an aluminum reflective coating. 5×5 μm^2 scans were taken with a scan rate of 0.5 Hz. The surface roughness of the hydrolyzed sample was determined from the data by Park Systems XEI image processing software (Park Systems). For the roughness data, the analyzed area size was varied to test the consistency of

the result. Roughness analysis was done on the raw data. For the presentation of the surface topography of the curved surfaces, the raw data was 0th order flattened along the fiber axes, which were parallel to the slow axis of the AFM.

Electrical stimulation

Stimulation setup. The scaffolds were placed in custom-made bottomless 24-well plates (Greiner Bio-One GmbH). The two electrodes were in galvanic contact with the cell culture medium in each well (Fig. 1A). The top and the bottom electrodes were sputter-coated polyethylene-naphthalate (PEN)/Au films (125 μm DupontTeonex®, with 50 nm Au-coating applied by VTT). The bottom electrode (PEN/Au film) was attached to the well plate with biomedical grade Silastic® Q7-4720 liquid silicone rubber. The top electrodes were bent strips of PEN/Au-film, partly extending to the cell culture medium (Fig. 1A). The four strips were connected in parallel (Fig. 1B). Hence, the individual wells were also electronically connected in parallel. The electrode surface area was approximately 1 cm^2 for the top electrode and approximately 1.5 cm^2 for the bottom electrode in each well. The distance between the top and the bottom electrodes was approximately 2 mm, matching the thickness of the scaffolds under mild (< 10 kPa) compression. Hence, the fibers of the scaffolds were in physical contact with both the top and bottom electrodes.

Human ASCs were exposed to symmetric biphasic pulsed DC voltage repeated at a frequency of 1 or 100 Hz, ES for 4 h/day. Stimulation waveforms were generated by AFG 3010B (Tektronix Inc.) and the stimulation signal supplied by a laboratory voltage amplifier (VTT). The waveforms for the 1 and 100 Hz stimulation were pulsed DC voltages 250 ms (+200 mV)/250 ms (−200 mV)/500 ms (0 mV) and 2.5 ms (+200 mV)/2.5 ms (−200 mV)/5 ms (0 mV), respectively. A schematic illustration of the voltage is presented in Figure 1C. According to cyclic voltammetry (CV), the PEN/Au-electrodes were electrochemically stable in the ±200 mV potential window (CV data not shown). The transient current generated by the pulsed DC signal was monitored for the 24-well plate assembly with Tektronix TDS 3054B oscilloscope and 100 Ω series resistor. The measured peak current into the 24-well plate assembly in series with the 100 Ω was 2 mA. The measured steady state (DC) current after the 2.5 ms and the 250 ms pulses was in the range of 40–50 μA/cm^2, corresponding to cell impedance of 5 kΩ. Such a low current level could be only roughly measured with the 100 Ω resistor and the oscilloscope. Therefore, the range of the current densities was also based on the impedance spectroscopic data recorded earlier in the DMEM.

The electrical charge of one pulse containing both the transient electrical double layer charging of the Au-electrodes (Q1, Q2 in Fig.1C) and the contribution of the ionic DC current (dashed line in Fig.1C) of the 1 and 100 Hz waveforms were estimated 28.0 and 8.2 μC, respectively. The charging conditions for the top and the bottom electrodes were not balanced electronically and the open circuit voltage of the system was not measured. A nonstimulated group was used as a control.

Impedance of the electrode, cell culture medium, and the nonwoven scaffolds. Impedance spectra of circular parallel 1 cm^2 PEN/Au-film electrodes and parallel rigid TiN-coated steel electrodes (electrode material TiN) in the DMEM were measured using an HP 4192A impedance analyzer. In the measurement a 100 Ω series resistor and excitation voltage of sinusoidal 50 mV_{p-p} was used.

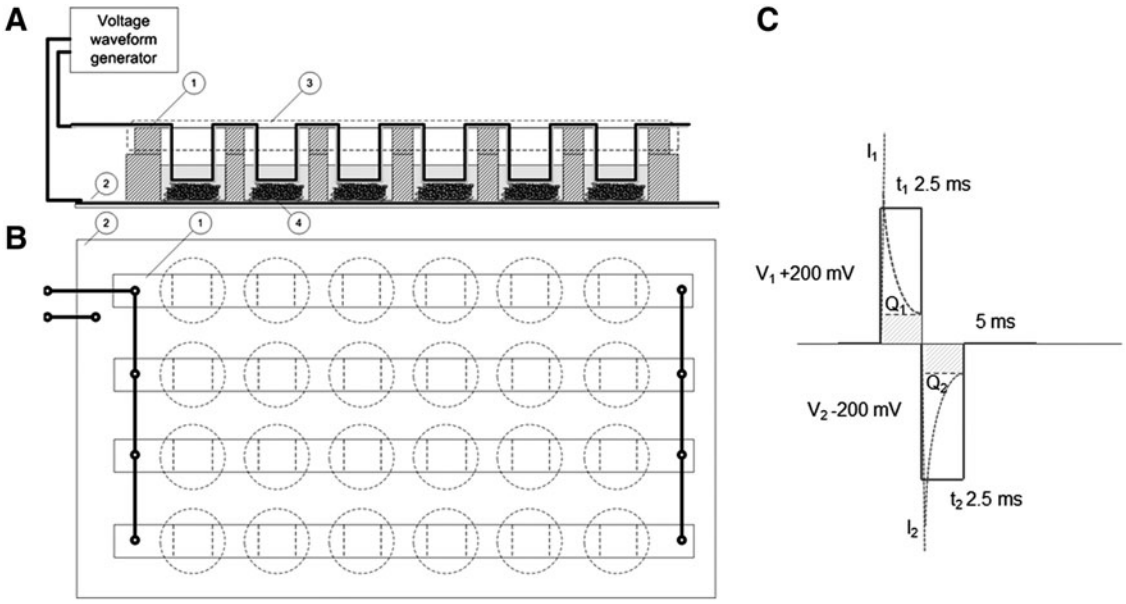

FIG. 1. **(A)** Schematic illustration of the stimulation device geometry as the side projection. Top and bottom electrodes were made of gold-coated polyethylene-naphthalate film. **(B)** The voltage waveform applied to the samples. Biphasic pulses are shown in blue color. The dashed line presents an estimation of the transient net current. Q_1 and Q_2 present both the transient electrical double layer charging of the Au-electrodes. **(C)** Schematic illustration of the stimulation device geometry as the above projection.

Subsequently, the impedance of the insulating PLA scaffold and the electrically conductive PLA-PPy scaffold was measured between the rigid TiN electrodes (OerlikonBalzersSandvik Coating). TiN electrodes were utilized as they provided an electrochemically stable, smooth, and mechanically rigid construction for the measurement cell. Constant phase element analysis (CPE) was done using the curve fitting tool provided in OriginPro 8.5.1 software (Originlab Corporation) using protocols described by Tandon et al.[26]

hASC culture

The experiments were repeated three times, each with a different human hASC line. The cells were isolated from the adipose tissue collected in surgical procedures from three females (aged 39, 43, and 79) at the Department of Plastic Surgery, Tampere University Hospital. Human ASC isolation from the tissue samples was conducted in accordance with the Ethics Committee of Pirkanmaa Hospital District, Tampere, Finland. The minced tissue samples were digested with collagenase type I (1.5 mg/mL; Invitrogen) and cell isolation was performed as previously described.[27] After primary culture in T-75 flasks, hASCs of passage 1 were harvested and analyzed by flow cytometry (FACSAria; BD Biosciences). Monoclonal antibodies against CD14-PE-Cy7, CD19-PE-Cy7, CD45RO-APC, CD49D-PE, CD73-PE, CD90-APC, CD106-PE-Cy5 (BD Biosciences Pharmingen); CD34-APC, HLA-ABC-PE, HLA-DR-PE (Immunotools GmbH Friesoythe); and CD105-PE (R&D Systems, Inc.) were used. Analysis was performed on 10,000 cells per sample, and the positive expression was defined as a level of fluorescence 99% greater than the corresponding unstained cell sample.

Cell expansion and experiments were carried out in the maintenance medium. When the ASCs reached 80% confluence, the cells were passaged. Cells of passages 4 to 5 were used for all experiments. Each scaffold was pretreated with the maintenance medium for 48 h at 37°C in custom-made 24-well plates. The scaffolds were seeded with 87,500 cells in a volume of 30 μL of the maintenance medium and the cells were allowed to attach for 3 h.

Viability. Cell attachment and viability were evaluated qualitatively using live/dead viability assay (Molecular Probes) at 7- and 14-day time points. CellTracker™ Green [5-chloromethylfluorescein diacetate (CMFDA; Molecular Probes) and ethidium homodimer-1 (EthD-1; Molecular Probes) were utilized to dye viable cells (green fluorescence) and dead cells (red fluorescence), respectively, as previously described.[7]

Proliferation and differentiation. The DNA content in the hASC-seeded scaffold constructs was measured after 1, 7, and 14 days' culture using the CyQUANT® Cell proliferation assay kit (Molecular Probes–Invitrogen) according to the manufacturer's protocol and as earlier described.[27] To uniformly extract the DNA, cells were lysed in the scaffold using 0.1% Triton X-100 followed by a freeze–thaw cycle, and then the scaffold was disrupted and the cell lysate carefully collected from the scaffolds for the analysis. The fluorescence was measured with Victor 1420 Multilabel Counter; Wallac). The quantitative alkaline phosphatase (ALP) measurement was performed at time points of 7 and 14 days according to the Sigma ALP procedure (Sigma Aldrich)[27] with minor modifications. Quantitative ALP activity results were normalized to the total amount of DNA measured from the same samples.

Statistical analysis. The statistical analyses were performed with SPSS, version 17. All assays were performed in triplicate and the data were presented as mean ± standard deviation (SD) for both quantitative analyses. The equal variance assumption was checked by the Levene's Test. All statistical analyses were performed at a significance level $p < 0.05$ using one-way analysis of variance (ANOVA) or the T-test. Bonferroni *post hoc* correction for multiple corrections was used. The effects of different culturing periods (1 day vs. 7 days vs. 14 days), scaffold materials (PLA vs. PLA-PPy), and stimulation setup (ES 1 Hz vs. ES 100 Hz vs. control) were evaluated from the combined data of the three experiments.

Results

Effect of hydrolysis on DC electrical conductivity

Incubation of the PPy-coated PLA fiber scaffolds in PBS (pH 7.4) resulted in a significant decrease in DC conductivity during the first day (Fig. 2). Directly after the synthesis the in-plane resistance of the air-dried samples was 50 ± 20 kΩ. Rinsing with deionized water increased the resistance to 90 ± 40 kΩ on day 0. At day 1, the measured resistance was 2.5 ± 0.8 MΩ and steadily increased to 29 ± 14 MΩ on day 7. According to optical microscopy, the surface of the fiber was still fully covered with the PPy coating on day 20. The DC conductivity of the hydrolyzed scaffolds could be partly restored by rinsing with a diluted hydrochloric acid (pH 2) solution and subsequent air drying. Roughly, 5%–10% of the conductivity of the hydrolyzed scaffold was restored by the acid rinse irrespective of the hydrolysis time.

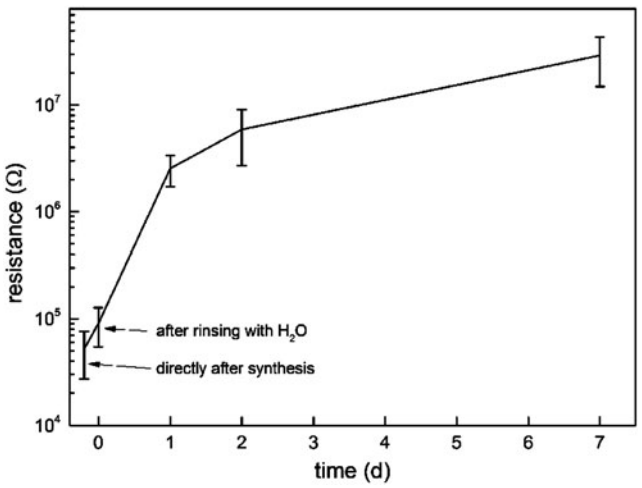

FIG. 2. Resistance of the poly-96L/4D-lactide-polypyrrole (PLA-PPy) scaffold in air ($n = 4$). The samples were rinsed with deionized and air-dried before each measurement. The conductivity of the sample remains at a level relevant for electrical stimulation for at least 2 days.

Table 1. Summary of Impedance Spectroscopic Data Measured in Dulbecco's Modified Eagle's Medium and the Corresponding Constant Phase Element Analyses

Sample	$\|Z\|_{cell}$ *at 1 Hz (Ω)*	$\|Z\|_{cell}$ *at 10 kHz (Ω)*	*CPE capacitance (μF)*	*idealitycoeff. η*
PEN/Au/film	240000	15	2	0.97
TiN	83000	17	20	0.94
TiN/PLA scaffold	13000	26	20	0.90
TiN/PLA-PPy scaffold	1700	12	14	0.83

HP 4192A impedance analyzer, excitation voltage is sinusoidal 50 mVp-p
CPE, constant phase element; PEN, polyethylene-naphthalate; PLA-PPy, poly-96L/4D-lactide-polypyrrole.

Impedance of the electrode, cell culture medium, and the nonwoven scaffolds

The results of the impedance measurement are summarized in the following Table 1.$|Z|_{cell}$ is the magnitude of cell impedance, CPE represents the capacitance of the cell, and η is a fit parameter describing the ideality of capacitance in the CPE model.[26]

According to the measured data, the PLA and the PLA-PPy scaffolds both had a significant effect on cell impedance in the DMEM. The low-frequency impedances specially were significantly lower for the cell containing the scaffolds in the DMEM (either PLA or PLA-PPy) than for the empty cell containing only the medium. As anticipated, the PLA-PPy scaffold induced the most significant decrease in cell impedance at lower frequencies. The ideality coefficient η was low (0.83) for the PLA-PPy scaffold, suggesting that the capacitive CPE model did not describe the cell impedance spectrum in this case. Contrary to expectations, the PLA scaffold also decreased the cell impedance. This was surprising since the relative permittivity of the medium (around 80) is much higher compared with the dry PLA polymer (around 3.5). The result can be explained by a marked enhancement of (low-frequency) ionic conductivity along the PLA fibers. The low-frequency impedance was three-fold higher, and the capacitance was 10-fold lower for the Au-electrodes than for the TiN electrodes.

We used impedances derived from sinusoidal test signals (2.4.2) for estimating the order of magnitude for the stimulation current during the biphasic pulses. The Ohm's law and the impedances measured at 1 Hz and 10 kHz were used for estimating the current densities in the Au-electroded stimulation 24-well setup. Theoretical current densities $I_{1,2,DC} \pm 13.3\,\mu A/cm^2$ $I_{1,2,max} \pm 16.7\,mA/cm^2$ for the DC current and the transient current were calculated, respectively. The real transient current density, which is not directly measurable using our system, was limited by the current amplifier to roughly $\pm 0.4\,mA/cm^2$. The discrepancy between the observed and the calculated values was likely due to the discrepancies between the impedance measurement and the ES setup. However, both the measured and the estimated DC and transient currents were within a physiologically relevant range, but could be considered minimally invasive for the hASCs.[28]

Electrospray ionization mass spectroscopy

The electrospray ionization-MS (ESI-MS) spectra for the PLA-PPy and PLA scaffolds were very similar (Fig. 3). The spectra contained peaks of PLA hydrolysis products[29] and the corresponding Na peaks. No significant peaks associated with potential PPy or CS degradation products, such as oxidized pyrrole oligomers or oligosaccharides, were found in the studied m/z range of 200–1000.

Scanning electron microscopy

According to scanning electron microscopy (SEM) images, the surfaces of the PPy-coated PLA fibers were covered with a conductive layer. This was clearly detected (Fig. 4, left), since the fiber scaffold did not build up any electrostatic charge under the electron beam at 3-kV acceleration voltage. The surface of the metallized (20 nm Au) PLA fibers appeared smooth in comparison to the PPy-coated fibers (Fig. 4, right).

Atomic force microscopy

Figure 5 shows representative topography and the measured surface roughness of individual PPy-PLA fibers after hydrolysis in PBS. The long axis of the fiber in each AFM was set parallel to the slow scan axis (45 degrees in the images in Fig. 5A). On day 0, the fiber surface appears extensively covered by fine nodular material individual nodules being 200 nm in diameter. This presented the typical morphology for PPys prepared by chemical polymerization. On day 10, the nodular surface morphology of the fibers was detected as on day 1. However, smoother areas and coarser (>400 nm) nodules with fine structure had appeared on day 10. On day

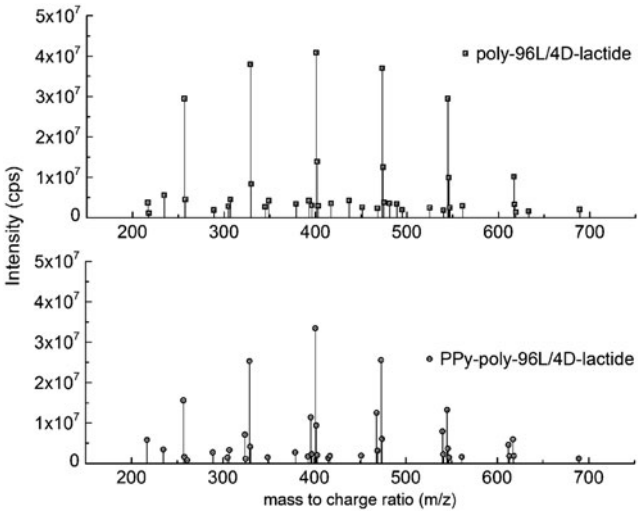

FIG. 3. Electrospray ionization-mass spectrometry spectra of the hydrolysis products from PLA-PPy and PLA scaffolds. All detectable peaks are found in the m/z range of 200–700.

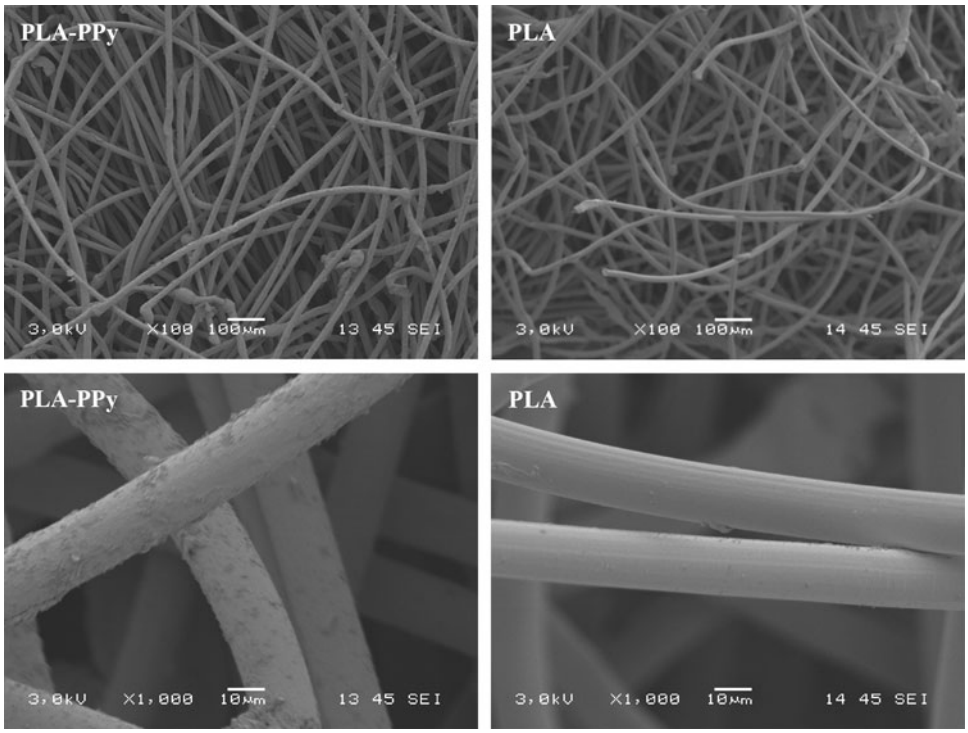

FIG. 4. Scanning electron microscopy image of PLA-PPy scaffold (left) without sputtered gold layer and PLA scaffold (right) with 20 nm gold coating. At 3-kV acceleration voltage, the PPy-coated PLA scaffold could be readily imaged, but the electrically insulating PLA scaffold could not be imaged without a thin coating layer (typically gold or carbon) due to heavy electrostatic charging.

20, the fraction of smoother areas had further increased from day 10. According to optical microscopy, the fibers were still fully covered with PPy after the 20 days in PBS. Hence, the observed changes were probably due to the changes of the PPy coating morphology and/or the hydrolysis of the PLA surface under the PPy coating.

The changes in the AFM images were reflected in the surface roughness values (Ra) derived from the images (Fig. 5B). Within 10 days, the Ra values decreased significantly from about 160 nm to less than 80 nm. The roughness analysis showed a consistency independent of how the analyzed surface area was chosen from the images ($5\times5\,\mu m^2$, $2\times2\,\mu m^2$ subareas).

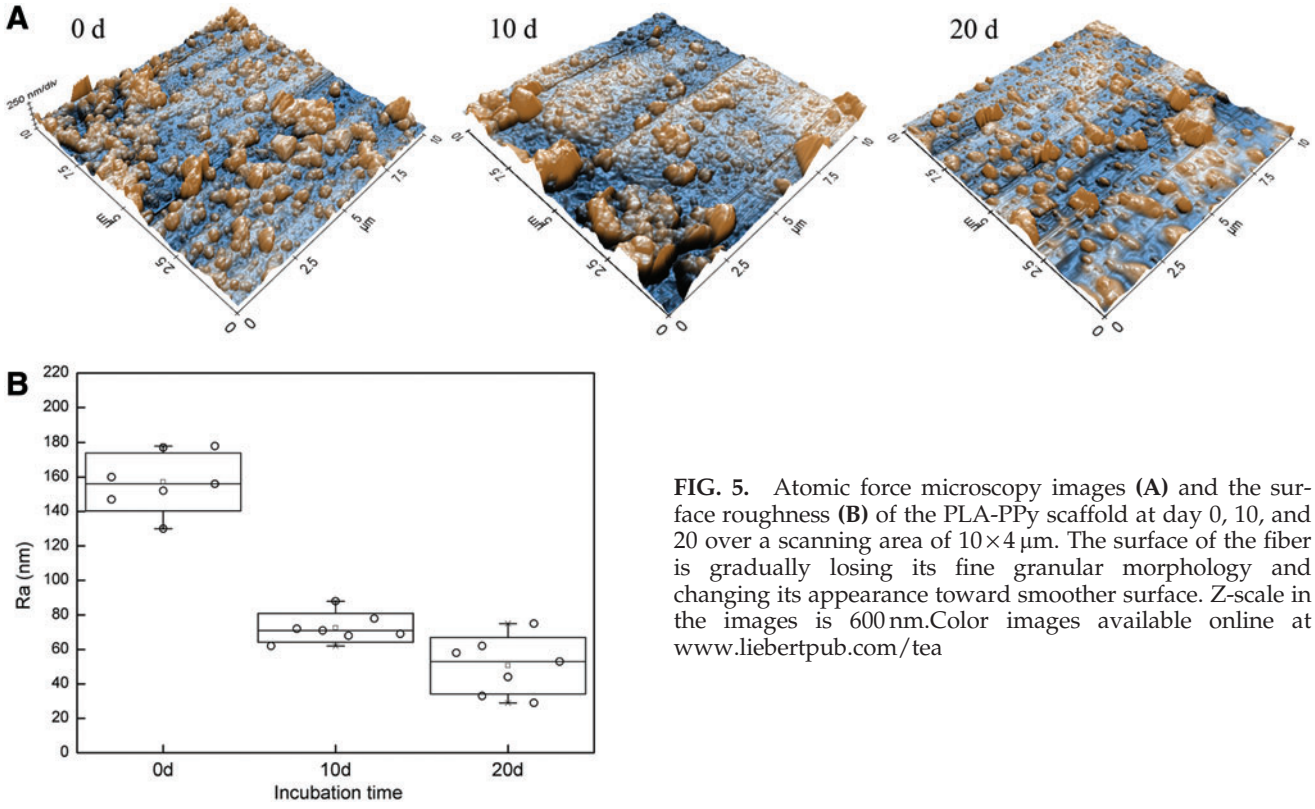

FIG. 5. Atomic force microscopy images **(A)** and the surface roughness **(B)** of the PLA-PPy scaffold at day 0, 10, and 20 over a scanning area of $10\times4\,\mu m$. The surface of the fiber is gradually losing its fine granular morphology and changing its appearance toward smoother surface. Z-scale in the images is 600 nm.Color images available online at www.liebertpub.com/tea

Cell culture

Flow cytometry. The flow cytometric analysis demonstrated that hASCs show high expression of CD105 (endoglin), CD73 (ecto 5′ nucleotidase), and CD90 (Thy-1), moderate expression (<50% >2%) of CD34 (hematopoietic progenitor and endothelial cell marker), and CD49d (integrin α4), while lacking expression (≤2%) of CD14 (monocyte and macrophage marker), CD19 (B cell marker), CD45RO (pan-leukocyte marker), CD106 (vascular cell adhesion molecule 1), and HLA-DR (HLA class II). Surface marker expression characteristics of undifferentiated ASCs from one donor cell line is presented in Figure 6. The results showed that hASCs expressed several of the specific antigens proposed by the Mesenchymal and Tissue Stem Cell Committee of the ISCT[30] defining human stem cells of mesenchymal origin. According to ISCT, CD34 should not be expressed in stem cells of mesenchymal origin; however, it showed moderate expression with high donor variation. However, varying results have been reported for CD34 on hASCs cultured in a medium supplemented with human serum[31–33] and fetal bovine serum.[31,34,35]

Viability. Live/dead staining showed that the majority of hASCs were viable and spread homogenously in both scaffold types with and without ES on day 14 (Fig. 7). By qualitative estimation, the number of hASCs was higher in PLA-PPy scaffolds than in the plain PLA scaffolds at all time points. This difference was evident on the cell seeding surface (Fig. 7) and the bottom surface of the scaffolds as well as inside the scaffolds (Supplementary Figs. S1 and S2; Supplementary Data are available online at www.liebertpub.com/tea). The ES did not seem to have any effect on cell viability or the cell number.

Proliferation and early osteogenic differentiation. The number of hASCs was assessed quantitatively using the CyQUANT proliferation method (Fig. 8), which is based on the relative absorbance values according to the amount of DNA. As demonstrated with live/dead staining, the number of hASCs was higher in PLA-PPy scaffolds at each time point compared to PLA scaffolds. This difference was statistically significant, excluding 7-day time point, in the nonstimulated and in the stimulated (100 Hz) group. In addition, the cell number in PLA scaffolds did not increase over time, whereas the cell proliferation during the 14-day culture period was detected in PLA-PPy scaffolds. Neither did the stimulation of 1 Hz nor 100 Hz show any effect on cell proliferation.

ALP analysis was performed on the same samples as used for DNA amount analysis (Fig. 9). ALP activity of hASCs was higher in PLA-PPy scaffolds in each stimulation group than in the PLA scaffolds at 7 and 14 days. One donor line did not show reliably detectable ALP activity at any of the measured time points. Therefore, data from two other repeats only are shown. The ALP activity values varied notably between the two donor lines; hence, no significant differences were detected between different scaffold types or stimulation groups.

Discussion

As our main finding, the PPy coating enhanced hASC proliferation. A similar trend was also seen in ALP activity, but no significant differences were detected. ALP activity peaked at the 7-day time point, which is typical behavior for ASCs in 3D scaffolds in the maintenance medium.[36] To the best of our knowledge, this is the first study to investigate the effect of ES on hASCs in a 3D culture system on PLA-PPy scaffolds by exploiting the conductivity properties of PPy. For the ES in the 3D culture system, we designed a custom-made stimulation setup, where multiple scaffolds could simultaneously be stimulated. Symmetric biphasic pulsed DC voltage with ±100 mV/mm pulse amplitude (2.5 ms/250 ms pulse duration and

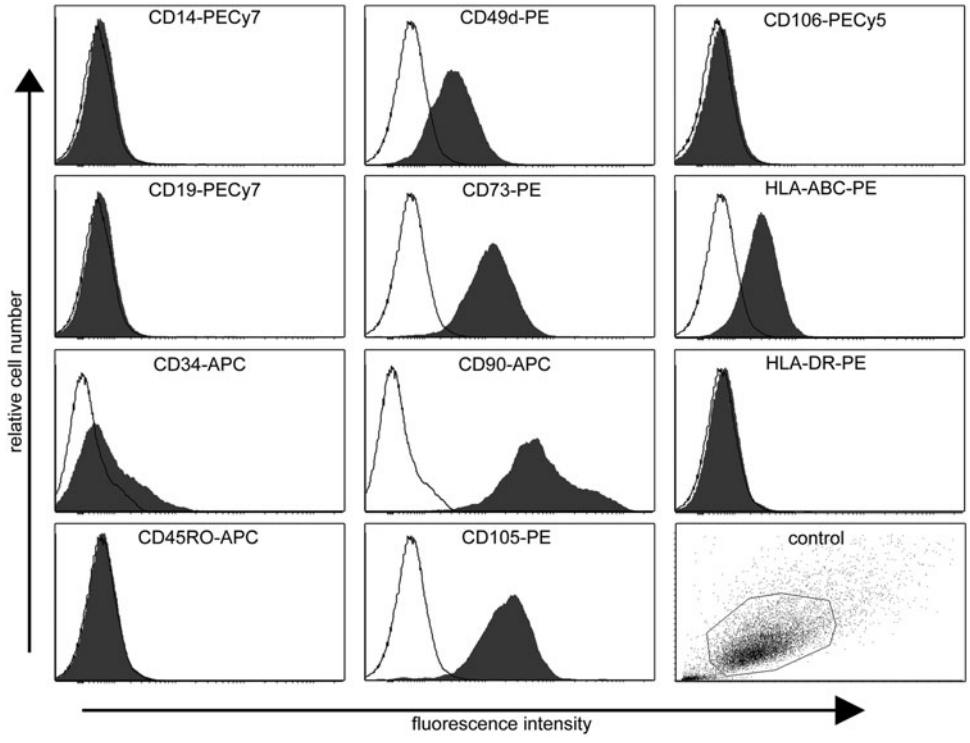

FIG. 6. Surface marker expression characteristics of undifferentiated adipose stem cells (ASCs) from one donor cell line as analyzed by flow cytometry. Relative cell number (*y*-axis) and fluorescence intensity (*x*-axis). Unstained control cells (empty histograms) and cells stained with antibody (filled histograms). Unstained control sample dot plot showing particle size and granularity (side scatter vs. forward scatter).

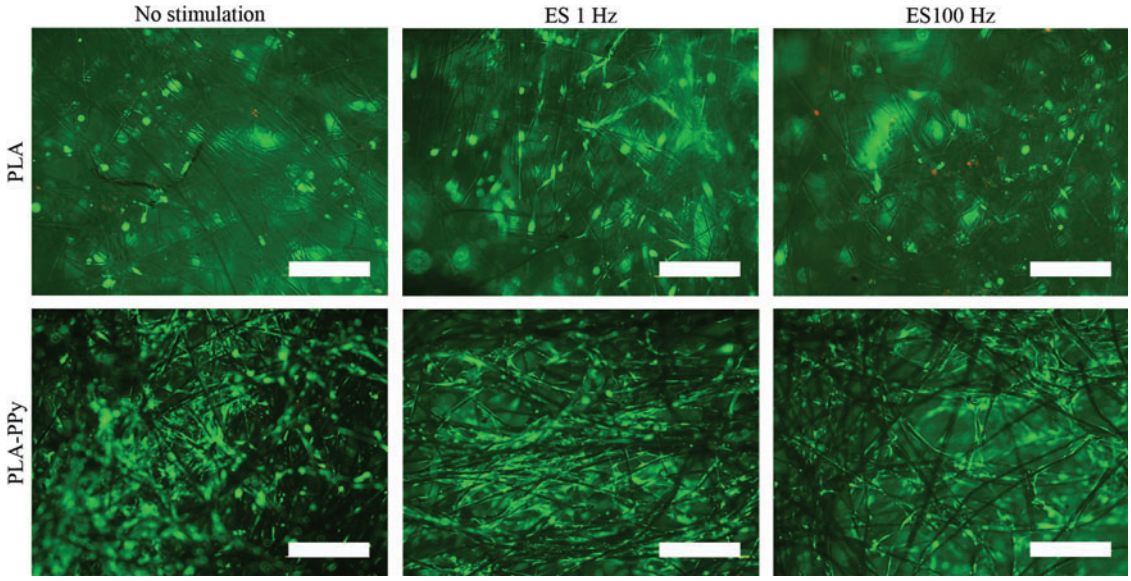

FIG. 7. Representative images of viable (green fluorescence) and dead (red fluorescence) human adipose stem cells at 14-day time point attached to PLA and PLA-PPy scaffolds visualized at top/cell seeding side of the scaffolds. Scale bar is 500 μm. Color images available online at www.liebertpub.com/tea

100 Hz/1 Hz pulse frequencies, respectively), was chosen on the basis of earlier studies demonstrating their physiological relevance, safety, and applicability to stimulating hASCs.[19,21]

ES can be considered a potential way to stimulate hASCs as it offers a means to exert similar influence on cells as, for example, growth factors, but in a safer, more inexpensive and repeatable way.[19] Nevertheless, no significant differences in early osteogenic differentiation or proliferation were detected between electrically stimulated and nonstimulated hASCs in our setup. This result was in contrast to many recent studies reporting favorable effects of ES on hASC osteogenic differentiation. McCullen et al. demonstrated hASC mineralization and differentiation toward bone tissue under ES in a 2D culture system[19] when the osteogenic medium was used (the maintenance medium supplemented with 50 mM ascorbic acid, 0.1 mM dexamethasone, and 10 mM β-glycerofosfate, while Tandon *et al.*[21] demonstrated that hASCs align and elongate in the presence of ES. Similar to our study, no differentiation medium or growth factors were used to increase the differentiation processes. As a result, they did not detect osteogenic differentiation, but rather fibroblastic or vasculogenic differentiation. As our study set out to investigate early osteogenic differentiation, it remains to be determined if differentiation into other lineages occurred.

Hammerick *et al.* used mouse ASCs and stimulated them using very similar parameters to ours. Their results on proliferation were consistent with ours since they did not detect any effect of ES on proliferation during a 10-day culture period. On the other hand, osteogenic differentiation was observed only in combination with ES and the osteogenic medium (the maintenance medium supplemented with 100 mg/mL of ascorbic acid and 10 mM β-glycerophosphate).

It should also be noted that most of the studies of using ES for stem cells have not been done in combination with electrically conductive biomaterial. PPy and ES may have synergistic effects, such as redox activity upon potential changes and bioactive molecules as dopants, which can affect also to the cell response in addition to the applied ES.[6]

The electrical impedance of the Au-electrodes in the DMEM changed significantly in the frequency range of sinusoidal (50 mV) 1–1000-Hz test signals, as confirmed by impedance spectroscopy. Indeed, the nonlinearity of the

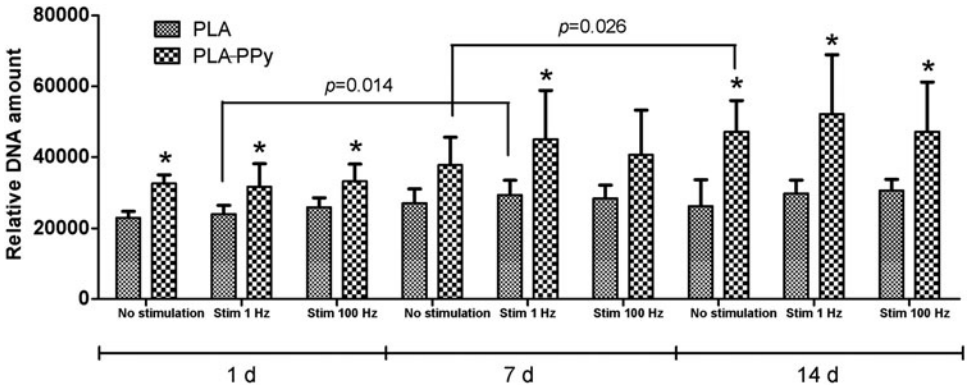

FIG. 8. Relative DNA content of human adipose stem cells cultured for 1, 7, and 14 days in PLA and PLA-PPy scaffolds. The results are expressed as mean ± SD, $n = 3$. The total number of technical samples was 9. *$p < 0.05$ with respect to the corresponding PLA scaffold.

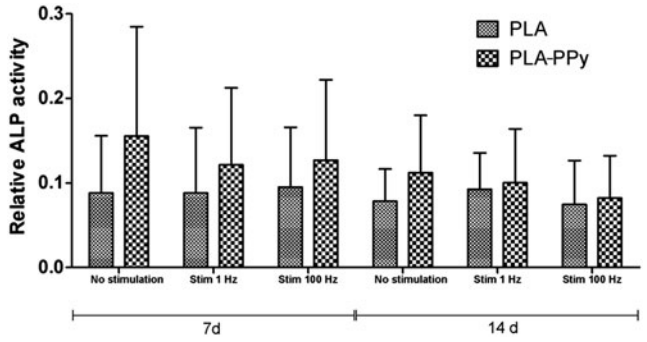

FIG. 9. Relative ALP activity of human adipose stem cells cultured for 7 and 14 days in PLA and PLA-PPy scaffolds. The results are expressed as mean ± SD, $n = 2$. The total number of technical samples was 6.

stimulation cell impedance was found to be an important factor in designing electronic stimulation setups and waveforms for stem cells. As anticipated, the electrically conductive PPy-PLA scaffold placed between the circular 1 cm^2 TiN electrodes decreased the impedance of the TiN/DMEM/TiN cell significantly, in particular, in the lower frequency range. A less significant, but a surprising decrease in cell impedance was also observed for the PLA scaffold, which is an excellent electrical insulator in air. In both cases, a possible explanation would be a marked enhancement of the conductivity of the fibers, extending to the interior of the scaffold. In the case of PLA fibers, the enhancement was likely due to increased surface ionic conductivity. For the PLA-PPy fiber, the enhancement was more easily understood since PPy is an electronic conductor both in air and in a medium. Our results suggest that an electronically conductive PPy can better deliver the stimulation currents to the cells located in the interior of the scaffold, which may have an additional effect on cell response. It is noteworthy that a significant enhancement of the electronic conductivity resulted from only 2–3 wt-% of the conductive PPy in the composite PLA-PPy fibers.

The in-plane DC resistance of air-dried PLA-PPy scaffolds was 50 kΩ on day 0. The DC conductivity of the PPy coating was roughly 10–30 S/m, based on an order of magnitude estimation of the DC conductivity of the PPy-layer and a careful extrapolation of the impedance spectroscopic data to very low frequencies. The estimated conductivity was within the range of the electronic volume conductivity reported for bulk PPy-sulfate powders prepared by APS oxidation in water.[37] Hence, the incorporation of the CS dopant did not adversely affect the electronic conductivity of PPy. The loss of DC conductivity of PPy coating was partly restored by acid doping in pH 2. Therefore, the loss of electronic conductivity was partly due to reversible de-doping of PPy chains in high pH 7.4.[6] Other mechanisms, such as PLA degradation, were also affecting the PPy coating and/or detachment, and cracking of the PPy layer. According to the impedance spectroscopy (1–10 kHz) and the DC measurements, the AC conductivity (electronic and ionic) of the PPy layer remained considerably (>2 decades) higher than the ionic conductivity of the DMEM at least on days 0–2. Although the impedance measurement cannot discriminate between the electronic conductivity and the ionic conductivity of the scaffold material, we find this a clear indication that the scaffold will enhance the stimulation current flow for periods far exceeding 2 days.

Irreversible changes were also apparent in the morphology of the fibers according to AFM topography images, which showed that the appearance of the fibers changed significantly during incubation. According to optical microscopy, the fibers were still fully covered with PPy after the 20 days in PBS. The data suggested extensive morphological changes in the thin PPy layer due to dopant ion exchange, hydration, osmotic pressure, and/or hydrolysis of the PLA surface under the PPy coating. Both factors may have affected the morphology of PPy, the local adhesion of the PPy coating, and consequently, the electronic conductivity of the coating.

Between the electrochemical potentials of the ES signals (±200 mV) used, the PPy remained in oxidized state. Thus, it is unlikely that redox chemistry had any significant effects on PPy morphology. Hydration and hydrolytic degradation of the outermost surface of the PLA may have been affected by the PPy coating and the ES, mainly due to the high ionicity of PPy. However, we found no direct evidence of such effect using SEM, AFM, and ESI-MS. This should be further studied in future.

Under the oxidative polymerization conditions, the CS was rapidly split into fragments (C4–C6) as evidenced by the viscosity measurements (data not shown). Although it was evident that the CS induced permanent hydrophilicity of the PPy coating, the role of the CS dopant in the cell response of PPy coating remained unclear. After hydrolysis in deionized water at +60°C, we did not detect pyrrole oligomers or CS fragments in the hydrolysis products of the PLA-PPy fibers by ESI-MS. It is therefore debatable if molecular fragments of the CS remained in PPy. This needs elucidation since CS fragments have well reported biological activity both *in vitro* and *in vivo*.[38,39] Nevertheless, our results showed that the effect of PPy coating on hASC response was as strong with and without ES, suggesting that the surface chemistry of PPy plays a more important role in triggering cell response than in the electrical conductivity of PPy.

According to the ESI-MS spectra, the influence of PPy coating on the hydrolysis of the PLA scaffold was negligible. According to our interpretation, the thin PPy coating was not hydrolytically degraded in water and had little effect on the hydrolytic degradation of the PLA scaffolds *in vitro*.

In conclusion, the novel PPy-coated scaffolds significantly enhanced hASC proliferation. In addition, early osteogenic differentiation was consistently more enhanced by PPy coating than by plain PLA scaffolds. This study highlights the future potential of PPy-coated PLA scaffolds seeded with hASCs in clinical bone tissue engineering applications. The ES of the relatively noninvasive biphasic pulsed voltage waveforms in 3D geometry did not have a significant effect on hASC proliferation or differentiation on days 1, 7, and 14.

Acknowledgments

The authors would like to thank Ms. Anne Rajala M.Sc, Ms. Ana Luísa Delgado Lima, and Ms. Hanna Juhola for the preparation and hydrolytic testing of the scaffolds, Ms. Anna-Maija Honkala and Ms. Minna Salomäki M.Sc for their assistance in the cell culture work. This study was financially supported by the Finnish Funding Agency for Technology

and Innovation (TEKES), the Academy of Finland and the Competitive Research Funding of Tampere University Hospital (grant 9K020).

Disclosure Statement

No competing financial interests exist.

References

1. Gloria, A., De Santis, R., and Ambrosio, L. Polymer-based composite scaffolds for tissue engineering. J Appl Biomater Biomech **8,** 57, 2010.
2. Niemelä, T., Niiranen, H., Kellomäki, M., and Törmälä, P. Self-reinforced composites of bioabsorbable polymer and bioactive glass with different bioactive glass contents. Part I: initial mechanical properties and bioactivity. Acta Biomater **1,** 235, 2005.
3. Cronin, E.M., Thurmond, F.A., Bassel-Duby, R., Williams, R.S., Wright, W.E., Nelson, K.D., and Garner, H.R. Protein-coated poly(L-lactic acid) fibers provide a substrate for differentiation of human skeletal muscle cells. J Biomed Mater Res Part A **69A,** 373, 2004.
4. Jiang, T., Khan, Y., Nair, L.S., Abdel-Fattah, W.I., and Laurencin, C.T. Functionalization of chitosan/poly(lactic acid-glycolic acid) sintered microsphere scaffolds via surface heparinization for bone tissue engineering. J Biomed Mater Res Part A **93A,** 1193, 2010.
5. Jakubiec, B., Marois, Y., Zhang, Z., Roy, R., Sigot-Luizard, M., Dugré, F.J., King, M.W., Dao, L., Laroche, G., and Guidoin, R. *In vitro* cellular response to polypyrrole-coated woven polyester fabrics: Potential benefits of electrical conductivity. J Biomed Mater Res **41,** 519, 1998.
6. Ateh, D.D., Navsaria, H.A., and Vadgama, P. Polypyrrole-based conducting polymers and interactions with biological tissues. J R Soc Interface **3,** 741, 2006.
7. Pelto, J., Haimi, S., Puukilainen, E., Whitten, P.G., Spinks, G.M., Bahrami-Samani, M., Ritala, M., and Vuorinen, T. Electroactivity and biocompatibility of polypyrrole-hyaluronic acid multi-walled carbon nanotube composite. J Biomed Mater Res Part A **93A,** 1056, 2010.
8. Du Souich, P., García, A.G., Vergés, J., and Montell, E. Immunomodulatory and anti-inflammatory effects of chondroitin sulphate. J Cell Mol Med **13,** 1451, 2009.
9. Schneiders, W., Reinstorf, A., Ruhnow, M., Rehberg, S., Heineck, J., Hinterseher, I., Biewener, A., Zwipp, H., and Rammelt, S. Effect of chondroitin sulphate on material properties and bone remodelling around hydroxyapatite/collagen composites. J Biomed Mater Res Part A **85A,** 638, 2008.
10. Manton, K.J., Haupt, L.M., Vengadasalam, K., Nurcombe, V., and Cool, S.M. Glycosaminoglycan and growth factor mediated murine calvarial cell proliferation. J Mol Histol **38,** 415, 2007.
11. Manton, K.J., Leong, D.F.M., Cool, S.M., and Nurcombe, V. Disruption of heparan and chondroitin sulfate signaling enhances mesenchymal stem cell-derived osteogenic differentiation via bone morphogenetic protein signaling pathways. Stem cells **25,** 2845, 2007.
12. Garner, B., Georgevich, A., Hodgson, A.J., Liu, L., and Wallace, G.G. Polypyrrole-heparin composites as stimulus-responsive substrates for endothelial cell growth. J Biomed Mater Res **44,** 121, 1999.
13. Gilmore, K.J., Kita, M., Han, Y., Gelmi, A., Higgins, M.J., Moulton, S.E., Clark, G.M., Kapsa, R., and Wallace, G.G. Skeletal muscle cell proliferation and differentiation on polypyrrole substrates doped with extracellular matrix components. Biomaterials **30,** 5292, 2009.
14. Richardson, R.T., Thompson, B., Moulton, S., Newbold, C., Lum, M.G., Cameron, A., Wallace, G., Kapsa, R., Clark, G., and O'Leary, S. The effect of polypyrrole with incorporated neurotrophin-3 on the promotion of neurite outgrowth from auditory neurons. Biomaterials **28,** 513, 2007.
15. Shi, G., Rouabhia, M., Meng, S., and Zhang, Z. Electrical stimulation enhances viability of human cutaneous fibroblasts on conductive biodegradable substrates. J Biomed Mater Res Part A **84A,** 1026, 2008.
16. Shi, G., Zhang, Z., and Rouabhia, M. The regulation of cell functions electrically using biodegradable polypyrrole–polylactide conductors. Biomaterials **29,** 3792, 2008.
17. Meng, S., Zhang, Z., and Rouabhia, M. Accelerated osteoblast mineralization on a conductive substrate by multiple electrical stimulation. J Bone Miner Metabol **29,** 535, 2011.
18. McCaig, C.D., Rajnicek, A.M., Song, B., and Zhao, M. Controlling cell behavior electrically: current views and future potential. Physiol Rev **85,** 943, 2005.
19. McCullen, S.D., McQuilling, J.P., Grossfeld, R.M., Lubischer, J.L., Clarke, L.I., and Loboa, E.G. Application of low-frequency alternating current electric fields via interdigitated electrodes: effects on cellular viability, cytoplasmic calcium, and osteogenic differentiation of human adipose-derived stem cells. Tissue Eng Part C Methods **16,** 1377, 2010.
20. Hammerick, K.E., James, A.W., Huang, Z., Prinz, F.B., and Longaker, M.T. Pulsed direct current electric fields enhance osteogenesis in adipose-derived stromal cells. Tissue Eng Part A **16,** 917, 2010.
21. Tandon, N., Goh, B., Marsano, A., Chao, P.H., Montouri-Sorrentino, C., Gimble, J., and Vunjak-Novakovic, G. Alignment and elongation of human adipose-derived stem cells in response to direct-current electrical stimulation. Annual International Conference of the IEEE Engineering in Medicine and Biology Society. Minneapolis, MN: IEEE Engineering in Medicine and Biology Society. 1, 6517, 2009.
22. Schmidt, C.E., Shastri, V.R., Vacanti, J.P., and Langer, R. Stimulation of neurite outgrowth using an electrically conducting polymer. Proc Natl Acad Sci U S A **94,** 8948, 1997.
23. Wong, J.Y., Langer, R., and Ingber, D.E. Electrically conducting polymers can noninvasively control the shape and growth of mammalian cells. Proc Natl Acad Sci U S A **91,** 3201, 1994.
24. Rowlands, A.S., and Cooper-White, J.J. Directing phenotype of vascular smooth muscle cells using electrically stimulated conducting polymer. Biomaterials **29,** 4510, 2008.
25. Wolszczak, M., Kroh, J., and Abdel-Hamid, M. Effects of the radiation processing of conductive polymers. Radiat Phys Chem **1,** 78, 1995.
26. Tandon, N., Cannizzaro, C., Chao, P.H., Maidhof, R., Marsano, A., Au, H.T., Radisic, M., and Vunjak-Novakovic, G. Electrical stimulation systems for cardiac tissue engineering. Nat Protoc **4,** 155, 2009.
27. Haimi, S., Moimas, L., Pirhonen, E., Lindroos, B., Huhtala, H., Räty, S., Kuokkanen, H., Sándor, G.K., Miettinen, S., and Suuronen, R. Calcium phosphate surface treatment of bioactive glass causes a delay in early osteogenic differentiation of adipose stem cells. J Biomed Mater Res Part A **91A,** 540, 2009.
28. Sun, S., Liu, Y., Lipsky, S., and Cho, M. Physical manipulation of calcium oscillations facilitates osteodiffer-

entiation of human mesenchymal stem cells. FASEB J **21,** 1472, 2007.
29. Andersson, S.R., Hakkarainen, M., Inkinen, S., Sodergard, A., and Albertsson, A.C. Polylactide stereocomplexation leads to higher hydrolytic stability but more acidic hydrolysis product pattern. Biomacromolecules **11,** 1067, 2010.
30. Dominici, M., Le Blanc, K., Mueller, I., Slaper-Cortenbach, I., Marini, F., Krause, D., Deans, R., Keating, A., Prockop, D., and Horwitz, E. Minimal criteria for defining multipotent mesenchymal stromal cells. The International Society for Cellular Therapy position statement. Cytotherapy **8,** 315, 2006.
31. Kocaoemer, A., Kern, S., Klüter, H., and Bieback, K. Human AB serum and thrombin-activated platelet-rich plasma are suitable alternatives to fetal calf serum for the expansion of mesenchymal stem cells from adipose tissue. Stem Cells **25,** 1270, 2007.
32. Lindroos, B., Boucher, S., Chase, L., Kuokkanen, H., Huhtala, H., Haataja, R., Vemuri, M., Suuronen, R., and Miettinen, S. Serum-free, xeno-free culture media maintain the proliferation rate and multipotentiality of adipose stem cells *in vitro*. Cytotherapy **11,** 958, 2009.
33. Parker, A.M., Shang, H., Khurgel, M., and Katz, A.J. Low serum and serum-free culture of multipotential human adipose stem cells. Cytotherapy **9,** 637, 2007.
34. Gronthos, S., Franklin, D.M., Leddy, H.A., Robey, P.G., Storms, R.W., and Gimble, J.M. Surface protein characterization of human adipose tissue-derived stromal cells. J Cell Physiol **189,** 54, 2001.
35. Mitchell, J.B., McIntosh, K., Zvonic, S., Garrett, S., Floyd, Z.E., Kloster, A., Di Halvorsen, Y., Storms, R.W., Goh, B., Kilroy, G., Wu, X., and Gimble, J.M. Immunophenotype of human adipose-derived cells: temporal changes in stromal-associated and stem cell-associated markers. Stem cells **24,** 376, 2006.
36. Marino, G., Rosso, F., Cafiero, G., Tortora, C., Moraci, M., Barbarisi, M., and Barbarisi, A. Beta-tricalcium phosphate 3D scaffold promote alone osteogenic differentiation of human adipose stem cells: *in vitro* study. J Mater Sci **21,** 353, 2010.
37. Blinova, N.V., Stejskal, J., Trchová, M., Prokeš, J., and Omastová, M. Polyaniline and polypyrrole: A comparative study of the preparation. Eur Poly J **43,** 2331, 2007.
38. Kang, S.K., Putnam, L., Dufour, J., Ylostalo, J., Jung, J.S., and Bunnell, B.A. Expression of telomerase extends the lifespan and enhances osteogenic differentiation of adipose tissue-derived stromal cells. Stem Cells **22,** 1356, 2004.
39. Grzesik, W.J., Frazier, C.R., Shapiro, J.R., Sponseller, P.D., Robey, P.G., and Fedarko, N.S. Age-related changes in human bone proteoglycan structure. Impact of osteogenesis imperfecta. J Biol Chem **277,** 43638, 2002.

Address correspondence to:
Suvi Haimi, PhD
Department of Biomaterials Science and Technology
University of Twente
P.O. Box 217
Enschede 7500 AE
The Netherlands

E-mail: suvi.haimi@uta.fi

Received: February 22, 2012
Accepted: October 17, 2012
Online Publication Date: January 4, 2013

Polypyrrole coating on poly-(lactide/glycolide)-β-tricalcium phosphate screws enhances new bone formation in rabbits

Ming-Dong Zhao[a,b,*], Miina Björninen[c,d,e,*], Lu Cao[a,*], Hui-Ren Wang[a], Jani Pelto[f], Jari Hyttinen[d,g], Yun-Qi Jiang[a], Minna Kellomäki[d,g], Susanna Miettinen[c,d,e], Suvi Haimic,[d,e,h*], Jian Dong[a,*]

[a] *Department of Orthopaedic Surgery, Zhongshan Hospital, Fudan University, Shanghai 200032, China;*
[b] *Department of Orthopaedic Surgery, Jinshan Hospital, Fudan University, Shanghai 201508, China*
[c] *Adult Stem Cell Group, Institute of Biomedical Technology, University of Tampere, FI-33014, Finland*
[d] *BioMediTech, Biokatu, Tampere, Finland,*
[e] *Science Centre, P.O. BOX 2000, FI-33521 Tampere, Finland*
[f] *VTT Technical Research Centre of Finland, Sinitaival 6, P.O. Box 1300, 33101 Tampere, Finland,*
[g] *Department of Electronics and Communications Engineering, Tampere University of Technology, P.O. 692, 33101 Tampere, Finland (previously Department of Biomedical Engineering)*
[h] *Department of Biomaterials Science and Technology, University of Twente, Enschede, P.O. Box 217 7500 AE Enschede, The Netherlands*

Corresponding authors: Jian Dong, email: dong.jian@zs-hospital.sh.cn and Suvi Haimi, email: suvi.haimi@uta.fi
**Equal contribution*

Abstract

Polypyrrole (PPy) has gained interest as an implant material due to its multifunctional properties and its high compatibility with several cell and tissue types. For the first time, the biocompatibility and osteogenic induction of PPy coating, incorporated with chondroitin sulfate (CS), were studied in vivo by implanting PPy-coated bioabsorbable polymer composite bone fixation screws into New Zealand white rabbits. Uncoated bioabsorbable polymer composite screws and commercially available stainless steel cortical screws were used as reference implants. The rabbits were euthanized 12 and 26 weeks after the implantation. The systemic effects were evaluated from food and water consumption, body weight, body temperature, clinical signs, blood samples, internal organs weights, and histological examination. Local effects were studied from bone tissue and surrounding soft tissue histology. New bone formation was evaluated by micro-computed tomography, tetracycline labelling and, torsion tests.
The coated screws induced bone formation significantly more than the uncoated screws. In addition, none of the implants induced any systemic or local toxicity. The results suggest that PPy is biocompatible with bone tissue and is a potential coating for enhancing osteointegration in orthopedic implants.

Introduction

Poly-(lactide/glycolide) copolymers (PLGA) are widely used as bioabsorbable polymers in bone fracture fixations due to biocompatibility, non-toxicity and good processability [1]. However, common disadvantages of polylactide and its copolymers as a bone implant material are their non-polar and hydrophobic surface properties, which limit cell attachment on the implant surface [2, 3]. Several surface modification methods have been tested for overcoming this problem, including incorporation of growth factors and mixing polymers with osteoconductive calcium phosphates [4-6]. These methods may contribute to distinct properties, such as enhancement of osteointegration in the case of calcium phosphates [6], but they face limitations when highly controllable multifunctionality is desired.

Polypyrrole (PPy) is a promising polymer coating for medical implant materials due to its multifunctional properties, such as controlled drug delivery, biocompatibility and relatively high electrical conductivity [7]. It is the most frequently investigated conductive polymer due to its easy synthesis, good tunability of the surface properties and long-term ambient stability [8]. Furthermore, PPy incorporated with a variety of

biomolecules has been investigated in several osteogenic applications in vitro [9-14]. Among these studies, Pelto et al. studied a chemically polymerized PPy coating on fibrous non-woven polylactide scaffolds seeded with human adipose stem cells (hASCs); they reported enhanced early osteogenic differentiation on the PPy-coated scaffolds [10]. In addition to hASCs, PPy has also proven to be compatible with many other cell types such as endothelial cells, PC-12 cells and osteoblasts [10, 15-17].

The in vitro and in vivo biocompatibility of PPy, in both chemically and electrochemically synthetized forms, has been investigated in depth by Wang et al [18]. When a PPy coated silicone tube was applied to bridge across the gap of the transected sciatic nerve of rat, they observed only a light inflammatory reaction 6 months postoperatively. The PPy extraction solution was found to possess neither acute nor subacute toxicity, which further suggested the high biocompatibility of PPy with nerve tissue. Furthermore, PPy has been demonstrated to have a high in vivo compatibility with several other tissue types, such as the hypodermis of rats, guinea pig brain, and mice peritoneum [18-21]. PPy-coated polyester fabrics have been reported to show a similar or milder inflammation in comparison to non-coated fabrics when implanted into the backs of rats [19]. Moreover, no significant inflammation was detected in another study where PPy/hyaluronic acid and PPy/polystyrene sulfonate composite was implanted into subcutaneous pouches in rats for 6 weeks [22]. PPy has also shown its potential as a blood-contacting material without adverse effects on hemolysis or coagulation [23].

Despite the several in vivo compatibility studies and the proven osteogenic potential of PPy in vitro, the influence and compatibility of PPy in bone tissue in vivo had not been shown before. We therefore investigated the in vivo biocompatibility and new bone formation of the PPy coating on bioabsorbable bone fixation composite screws of polylactide/glycolide copolymer (PLGA) and β-tricalcium phosphate (TCP).

Materials and methods

Polypyrrole coating

Pyrrole monomer, ferric chloride hexahydrate ($FeCl_3$) and chondroitin 6-sulfate A sodium salt (CS) from bovine tracheae were purchased from Sigma-Aldrich (St. Louis, USA). Pyrrole was distilled for purity in a vacuum before use. Other reagents were used without any further purification. Distilled water and ethanol (Altia Oyj, Rajamäki, Finland) were used in the polymerizations. PPy was oxidatively polymerized on

PLGA-β-TCP-composite screws (ActivaScrew™ TCP, Bioretec, Tampere, Finland) consisting of 85:15 PLGA mixed with 10 wt% of β-TCP. The screws were 2 mm in diameter and 10 mm in length (Fig. 1). The PLGA-β-TCP-composite screws had an x-ray positive marker made of β-TCP inserted into the tip of the screws. $FeCl_3$ was used as an oxidant and CS as a counter ion. First, the screws were soaked in pyrrole monomer solution in ethanol (1.3 mol/l, 67 min soaking time) and then transferred into a freshly prepared $FeCl_3$ aqueous solution (0.5 mol/l, 15 min polymerization time) containing 1 mg/ml CS. The coated screws were then carefully rinsed with deionized water in an ultrasonic bath and air-dried. Gamma irradiation of 17.5–26 kGy (by a commercial supplier) was used for the sterilization of the coated and uncoated bioabsorbable screws. The stainless steel screws (Synthes 211.010, diameter 2.0 mm, length 10 mm) were sterilized by autoclaving at 121 ^{0}C.

Figure 1. The coated (black), uncoated (white) bioabsorbable screws and a steel screw, which were implanted into the rabbits' femurs and tibiae. The screws are 2 mm in diameter and 10 mm in length.

Implantation

The animal experiments were authorized by the Animal Ethics Committee of the Zhongshan Hospital, Fudan University, China [SYXK(2008)-039]. The studies were conducted on 17 female New Zealand white rabbits with a mean weight of 3.1 ± 0.1kg. The rabbit was the smallest possible animal model for conducting the study according to the standard ISO 10993-6 for biocompatibility studies for bone implants.

The animals were randomly separated into 2 groups. In the coated group, 3 rabbits had 3 PPy coated screws implanted in the left leg (n=18) and the right leg was left intact. In the control group, uncoated screws were implanted in the left leg (n=18) in a similar manner to coated screws and 3 steel screws were implanted in the right leg (n=36) as a reference for foreign body reaction. For torsion tests, 5 rabbits were operated on, implanting 3 PPy coated screws in the left leg (n=15) leg and 3 uncoated screws in the right leg (n=15).

The surgery was performed under sedation and general anesthesia with diazepam (2 mg kg-1, SunRise Pharma, Shanghai, China) and ketamine (40 mg/kg, GuTian Pharma, Fujian, China) by intramuscular injection (i.m.). NaCl (0.9 %) (HuaLu Pharma, Shandong, China) was applied to the eyes to prevent drying. Anesthesia was maintained by administrating 40 mg/kg ketamine by i.m.

Two mini-incisions were made on the medial side of the distal femur, exposing the distal femur and the upper tibia. The implant hole was drilled with a 1.5 mm drill bit to a depth of 10 mm and slightly countersunk (2.0 mm) to fit the head of the screw flush with the bone surface. The holes were tapped (2.0 mm) and the screws were inserted (Fig. 2). One screw was implanted into the distal femur and 2 screws into the proximal tibia. The wound was closed with non-absorbable surgical sutures (Ping'An Medical Equipment CO. Ltd, Huai'an, China) by suturing in 2 layers after saline (HuaLu Pharma, Shandong, China) irrigation. Penicillin (130,000 U/kg, HuaBei Pharma, Hebei, China) was used as an antibiotic by i.m. intraoperatively and on the first postoperative day to prevent infection. For analgesia, animals were dosed with a subcutaneous injection of buprenorphine hydrochloride (0.03 mg/kg, Drug Research Pharma, Tianjin, China) once a day for 3 days after the operation.

To monitor the correct placement of the implants, post-operative radiographs of both hind legs were taken in the medio-lateral projections (49 kV, 5.0 mA, 33 ms, digital X-ray machine, Siemens, Germany) 8 weeks postoperatively. The animals were euthanized 12 and 26 weeks postoperatively with an overdose of ketamine hydrochloride (GuTian Pharma, Fujian, China). For tetracycline fluorescence detection, tetracycline (30 mg/kg, Sigma, USA) was injected intramuscularly 8 and 1 days before euthanasia.

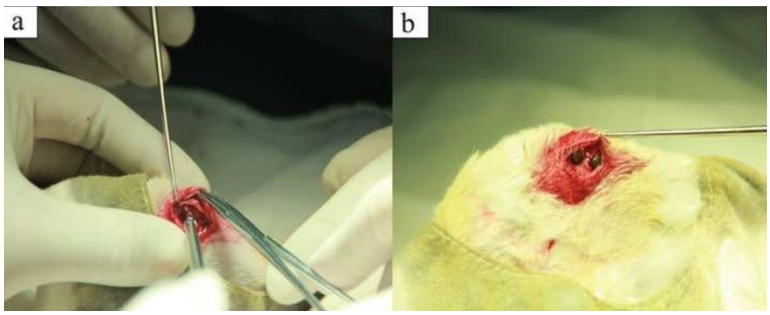

Figure 2. Implantation of two coated screws through one mini-incision in the upper tibia.

Clinical signs

The rabbit's appearance, behavior and food and water consumption were observed twice daily on weekdays and once daily on weekends. Implantation sites were examined for the first 5 days postoperatively and weekly throughout the study. Body temperature and weight were measured prior to the implantation as well as 48 hours and 2, 4, 12 and 26 weeks postoperatively.

Hematology and clinical chemistry

For subchronic toxicity testing of the coated screws, hematology and clinical chemistry were performed prior to the implantation as well as 48 hours, and 2, 4, 12 and 26 weeks postoperatively. The blood samples were drawn from the central auricular artery under anesthesia without overnight deprivation of food. The hematological analyses were performed on an automatic hemocyte analyzer (XS-1000i and CA1500, Sysmex, Japan) and chemical analyses on a biochemical automatic analyzer (P800/ P2400, Roche, Switzerland) at Labway Clinical Laboratory Limited (Shanghai, China).

Organ examination

Organs were weighed immediately after dissection to avoid drying and subsequently false low values. For bilateral organs, the left and right organs were weighed together. Subchronic toxicity was examined from organ weights, macroscopic examinations during necropsy, and histology of the internal organs. All the organ samples were fixed in 10 % neutral buffered formalin (XingYinHe Chemical Ltd, Hubei, China) and the samples were dehydrated and embedded in paraffin (FangZheng Chemical Ltd, Sichuan, China). Paraffin blocks were cut into thin sections of 5 μm in thickness and stained with Hematoxylin and Eosin [24]. Histological evaluation was performed under an optical microscope (Axio Imager M1, Zeiss, Jena, Germany) with AxioVision SE64 software (Zeiss, Jena, Germany).

Soft tissue examination

Soft tissue of 3 mm thickness around the head of the screws (uncoated, coated and steel screws) was selected for routine histology. The soft tissue samples were processed in the same manner as the organ samples. The coated and uncoated screw

samples were evaluated semi-quantitatively, including the quantitative comparison of inflammation polymorphonuclear cells, lymphocytes, plasma cells, macrophages and giant cells, as well as qualitative comparison of the extent of necrosis, neovascularization, fibrosis and fatty infiltrate.

Torsion test

To characterize the attachment strength of the bone to the screws, torsion tests [25] were performed on the day of euthanasia. Adherent soft tissue and newly formed bone tissue were carefully dissected around the screw head. The front tooth structure of metal rod was locked with the screw head. A hexagonal screwdriver linked to the sensor of a digital torque meter (HDP-5, Tuojing Measuring Instrument Limited Co, Shanghai, China) was then used to rotate the screws in order to capture the peak value of the torsion force (Fmax, Nm) during the course of screw's loosening. The longitudinal axis of a hexagonal screwdriver was aligned with the metal rod's fixed direction. According to the manufacturer's guideline, the absorbable screws start to degrade after 16 weeks, hence the torsion test was carried out 12 weeks after implantation.

Micro-CT examination

The bone specimens with the implanted screws were harvested and bony tissue surrounding the coated and uncoated screws in the rabbit's femur and tibia was scanned non-destructively by micro-CT (μCT-80, Scanco Medical AG, Zurich, Switzerland at the 12-week time point; Inveon PET/CT, Siemens AG, Munich, Germany at the 26-week time point). As the diameter of the screw was 2 mm, a circular area with a diameter of 2.2 mm was selected for scanning the screw and its surrounding tissue. A similar scan was repeated with a 2.0 mm diameter and deducted from the first area. The relative amount of mineralized tissue (including new and old bone tissue) was calculated from the residual area. At the 12-week time point, the micro-CT (μCT-80) images were recorded on a 1024×1024 charge-coupled device detector, with the pixel size set to 20 μm. 3D histomorphometric analysis, including the measurements of total volume and mineral density of the implants, was performed automatically with the FEA software (Scanco Medical AG, Zurich, Switzerland). The samples at the 26-week time point were recorded on a 1888×2048 charge-coupled device detector with an effective pixel size of 9.5 μm. The images were analyzed with

Inveon Research Workplace software (Siemens AG, Munich, Germany). The images were segmented using a nominal threshold value of 220 at both time points.

Tetracycline labelling

The bone specimens including implants were harvested to observe the bone formation around the coated and uncoated screws. The bone samples were dehydrated in acetone for 1 month and embedded in methyl metacrylate (MMA) (Suicheng Chemical Ltd, Guangzhou, China) without decalcification. Subsequently, the MMA blocks were cut into 200 μm slices with the EXAKT cutting system (E300CP, Norderstedt, Germany) and polished to a thickness of 20 μm. Distances between the 2 tetracycline fluorescence lines were measured under a microscope (Axio Imager M1, Zeiss, Jena, Germany) with AxioVision SE64 software (Zeiss, Jena, Germany).

Hard tissue examination

Hard tissue histology was conducted from the tetracycline-labelled samples. After examining the tetracycline fluorescence lines of the slices, toluidine blue (ZiYi Chemical Ltd, Shanghai, China) [26] was added on the slices for 15 min. Subsequently, coverslips were mounted for 2 days at room temperature. The slices were analyzed under an optical microscope (Axio Imager M1). The number of osteoblasts and chondroblasts at the bone-implant contact (BIC) was counted under the microscope [27].

Statistical analysis

The statistical analyses were performed with SPSS version 17 (SPSS, Chicago, IL). One-way analysis of variance (ANOVA) with Fisher's Least Significant Difference (LSD) was used for analyzing blood samples. Student's T test was used to compare the mean values of the coated and uncoated group within the time points for the torsion test, micro-CT, tetracycline labelling hard tissue histology, weight and temperature. All quantitative data is presented as mean ± standard error of mean (SEM) and $p < 0.05$ was considered statistically significant.

Results

Postoperative examination

All rabbits recovered well after surgery despite 1 decubitus ulcer and 1 slight opening of the surgical wound 3 weeks postoperatively. Radiography showed that the X-ray markers of the biodegradable screws were visible and in the correct position (Fig. 3.).

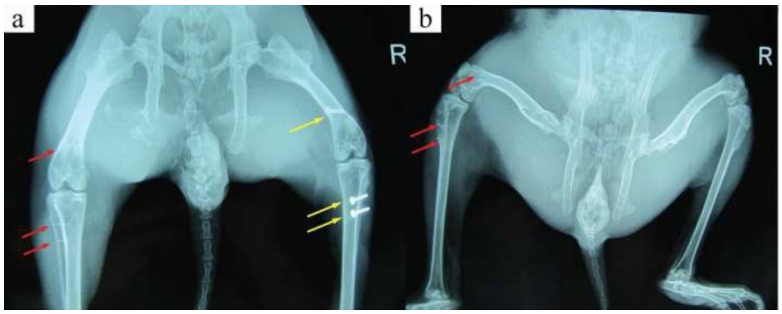

Figure 3. Radiographs of two rabbits (a: uncoated group, b: coated group) eight weeks post-operatively. The red arrows show the β-TCP marker in the bone, the yellow arrows point at the steel screws.

Hematology and clinical chemistry

The monocyte and platelet count and blood urea nitrogen were significantly higher in the uncoated group compared to coated group 2 weeks postoperatively. Furthermore, the white blood cell count and platelet count were significantly higher in the uncoated group than in coated group 12 weeks postoperatively. No significant differences between the coated and uncoated group were found at any other time points. When the blood samples taken prior to surgery were used as a baseline, the values in the uncoated group did not vary significantly. However, in the coated group creatinine values per weight were significantly higher 2 and 4 weeks after the surgery (79.67 ± 3.71 μmol/l and 92.23 ± 5.24 μmol/l respectively), yet still within normal ranges (26.5-115 μmol/l) [28]; the values recovered to baseline level after 12 weeks. At the 26-week time point, there were no statistically significant differences between the coated and uncoated groups.

Organ examination

Macroscopic and microscopic examination of the organs during the necropsy revealed that there were no significant differences in weights and histology between the 2 groups at the 12- and 26-week time points.

Soft tissue examination

All the heads of the coated, uncoated and steel screws were covered by a new callus that was greater in size at the 26-week time point than at the 12-week time point. Only slight hematoma, edema or encapsulation were found in the soft tissue around the 3 implantation sites that did not show obvious differences in macroscopic examination at the 12- and 26-week time points. Semi-quantitative evaluation also showed no differences among the 3 screw types (data not shown) at the 12-week time point. However at the 26-week time point, the irritation level, relative to the corresponding steel screws, was found to be higher in the uncoated screws compared to the coated.

Torsion test

Torsional forces were captured from all of the samples during the course of screws' rotation even though 5 coated screws and 2 uncoated screws broke during the mechanical testing. A significantly higher torsional peak value was measured for the coated screws when compared to the uncoated screws (Fig. 4) at the 12-week time point.

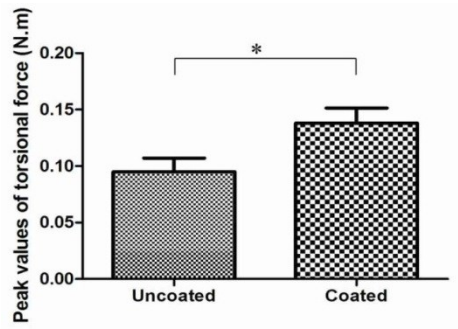

Figure 4. The peak values of the torsion force of the coated screws were significantly higher than those of the uncoated screws at 12 weeks. (*) Significant difference ($p < 0.05$).

Micro-CT evaluation

Micro-CT measurements taken 12 and 26 weeks postoperatively revealed a significantly greater amount of mineralized tissue in the coated samples than in uncoated ones (Fig. 5). Representative images from each group are shown in Fig. 5a. The cylinder shaped β-TCP marker of the bioabsorbable screw shown in the images is surrounded by PLGA-β-TCP composite. Due to the selected micro-CT parameters PLGA-β-TCP composite is not apparent in the figures. Mineralized areas were evident in the surrounding tissue in most of the samples.

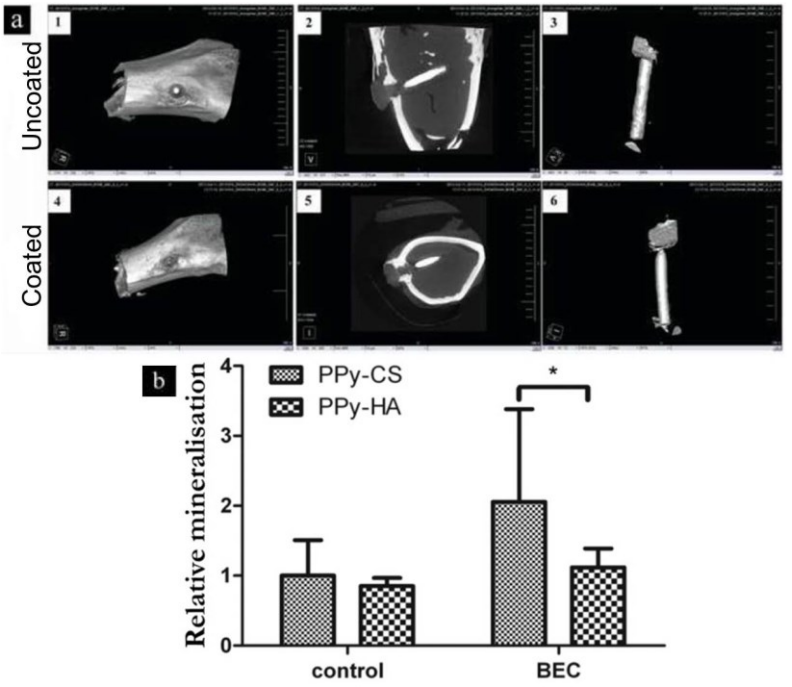

Figure 5. Micro-CT measurements of the implant areas. (a) Representative 3D images of the absorbable implants harvested 26 weeks post-operatively. (a1 and a4) Screw heads facing towards the viewer. (a2 and a5) Side projections of the screws. (a3 and a6) Representative images of the micro-CT measurement area around the screws. (b) Quantitative micro-CT analysis revealed that the bone volume of the coated screws was significantly higher than that of the uncoated screws at the 26-week time point. (*) Significant difference ($p < 0.05$).

Tetracycline fluorescence measurement

Coated samples (Fig. 6b, Fig. 7b) showed a significantly longer distance between the 2 tetracycline lines than the uncoated samples (Fig. 6a, 7a) as presented in Fig. 6c and 7c at the 12- and 26-week time points, respectively. This reflects the significantly greater new bone formation rate of the coated samples.

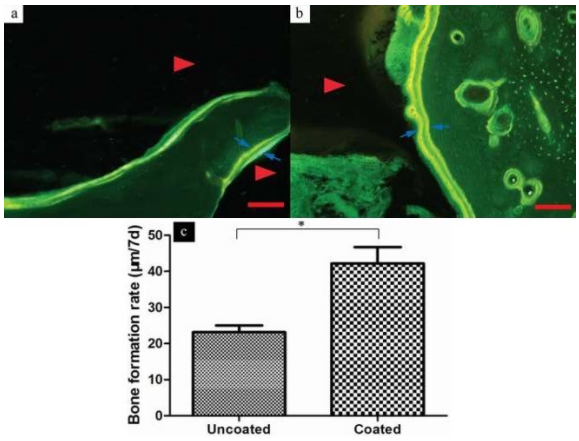

Figure 6. Tetracycline fluorescence measurement between two yellow bands (blue arrows) evaluating the new bone formation rate at 12 weeks. (a) Uncoated group (▶: part of an uncoated screw); (b) Coated group (▶: part of a coated screw). Scale bar 100 μm; (c) Quantitative analysis revealed that the new bone formation rate of the coated screws was significantly higher than that of the uncoated screws at 12 weeks. (*) Significant difference ($p < 0.05$).

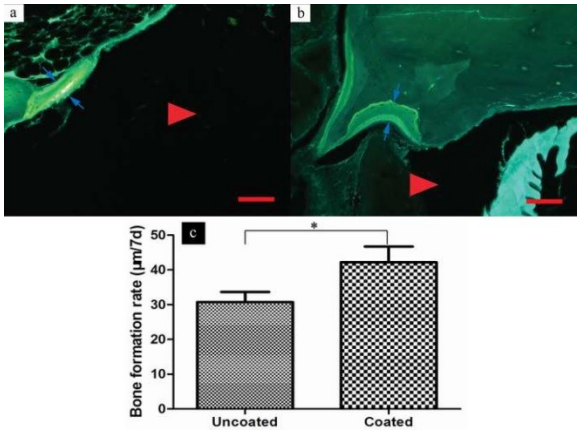

Figure 7. Tetracycline fluorescence measurement between two yellow bands (blue arrows) evaluating the new bone formation rate at 26 weeks. (a) Uncoated group (▶: part of an uncoated screw); (b) Coated group (▶: part of a coated screw). Scale bar 100 μm; (c) Quantitative analysis revealed that the new bone formation rate of the coated screws was significantly higher than that of the uncoated screws at 26 weeks. (*) Significant difference ($p < 0.05$).

Hard tissue histological evaluation

At the 12-week time point, the coated samples (Fig. 8b) showed a darker blue band, indicating a greater amount of new bone compared to the uncoated samples (Fig. 8a). Furthermore, the total number of osteoblasts and chondroblasts at the BIC in the coated group was significantly higher than that in the uncoated group (Fig. 8c.). The parts of the coated and uncoated screws in the marrow cavity were expanded and degraded, while the parts contacting the bone tissues showed good integrity. The expansion had most probably occurred during the sample fixation step with acetone. The solvent was therefore changed to formaldehyde for the 26-weeks samples and no swelling of the screws was observed at that time point. Some fibrotic tissue was apparent under the screw threads, which resulted from the compression irritation of the tissue during the implantation. The BIC showed no inflammation in the coated and uncoated group at either of the time points. However, at the 12-week time point, the BIC of the uncoated group was larger than that of the coated group, as demonstrated by a white band seen in the uncoated samples. In the coated group at the 12-week time point, dark bands were found at the BIC, which resulted from PPy stained by toluidine blue. The colorful stripes shown in both groups were caused by toluidine blue staining in the PLGA-β-TCP matrix.

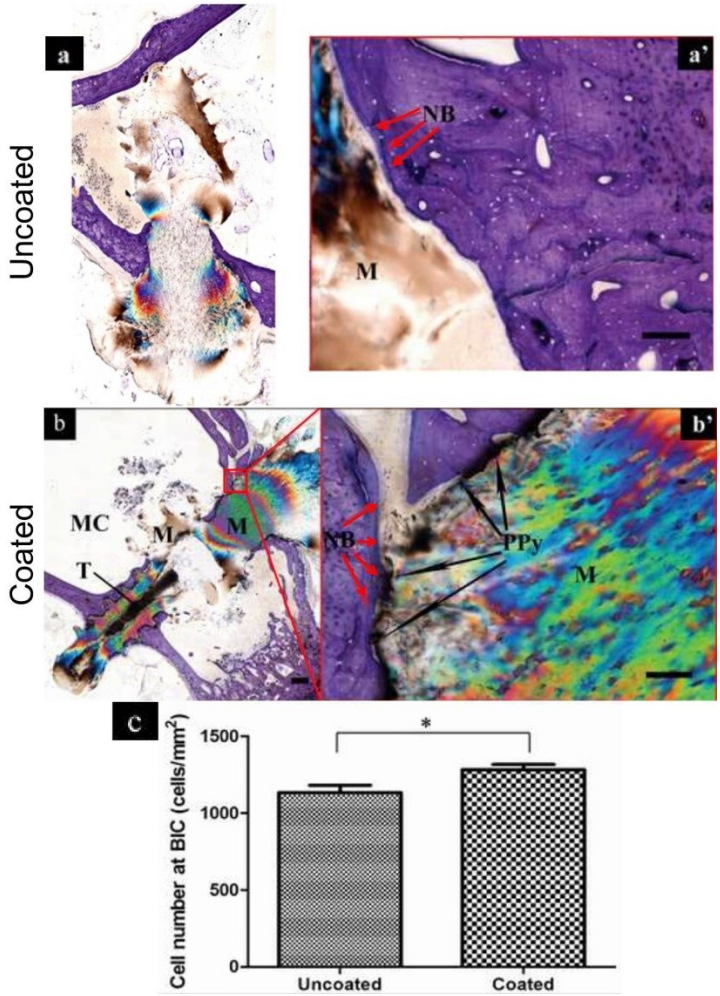

Figure 8. Toluidine blue staining 12 weeks after implantation for hard tissue samples. (a) Uncoated screw (scale bar 500 μm). (a') The magnification of the interface between the uncoated screw and bone revealed a thin detectable new bone (NB) band (scale bar 100 μm). (b) Coated screws (scale bar 500 μm). (b') The magnification of the interface between the coated screw and bone (scale bar 100 μm). NB was clearly detectable as indicated by a thick band on the surface. PPy coating appears as a black band. (MC: marrow cavity, M: PLGA and β-TCP, T: pure β-TCP). (c) The total number of osteoblasts and chondroblasts at the BIC in coated group was significantly higher than that in the uncoated group. (*) Significant difference ($p < 0.05$).

At the 26-week time point, woven bone was found in greater amounts in the coated sample groups than in the uncoated sample groups (Fig. 9), which was demonstrated by a significantly greater number of osteoblasts and chondroblasts (Fig. 9c.). However, the blue band indicating new bone was now similar in the coated and uncoated samples. Small traces of PPy were apparent in the coated samples yet the amount of PPy was notably lower at the 26-week time point than at the 12 week time point. The area of the PLGA-β-TCP composite in both coated and uncoated samples was substantially smaller than those observed at the 12-week time point, and new bone tissue appeared in close proximity to the β-TCP marker.

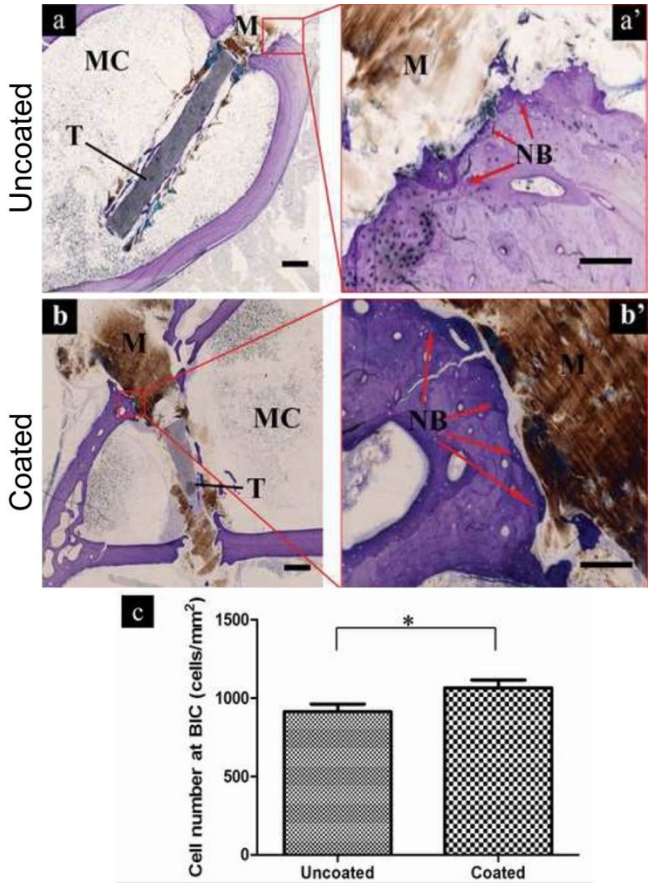

Figure 9. Toluidine blue staining 26 weeks after implantation for hard tissue samples. (a) Uncoated screw (scale bar 500 μm). (a') The magnification of the interface between the uncoated screw and bone revealed a thin detectable new bone (NB) band (scale bar 100 μm). (b) coated screws (scale bar 500 μm). (b') The magnification of the interface between the coated screw and bone (scale bar 100 μm). NB was clearly detectable as indicated by a thick band on the surface. PPy coating appears as a black band. (MC: marrow cavity, M: PLGA and β-TCP, T: pure β-TCP). (c) The total number of osteoblasts and chondroblasts at the BIC in the coated group was significantly higher than that in the uncoated group. (*) Significant difference ($p < 0.05$).

Discussion

In orthopedic surgery, loosening of the implant is the most common cause of failure in internal fixation [29, 30]. Therefore many coating methods have been used to enhance the bonding between bone and the surface of an orthopedic implant to improve its osteointegration [7, 31-36]. Of these coatings, PPy could provide an interesting approach due to its multifunctional properties. For instance, PPy could facilitate exploitation of electrical stimulation in controlled drug delivery [7, 37]. As PPy has previously shown a good biocompatibility with several tissues [10-13] and has excellent cellular attachment properties in vitro [10], we hypothesized that PPy may augment the attachment of the implant in bone tissue, thereby improving new bone formation.

In the present study, systemic toxicity, biocompatibility and osteogenicity of the PPy coating was studied for the first time in vivo. As our main finding, PPy coating significantly promoted new bone formation when compared to the uncoated screws. This was consistently demonstrated by tetracycline labelling and supported by micro-CT and torsion tests. In addition, hard tissue histology showed more new bone tissue and higher number of osteoblasts and chondroblasts around the coated screws compared to the uncoated screws at both time points. At the 12-week time point, the BIC of the coated samples was narrower implying better attachment of the coated screws to the bone tissue compared to the uncoated screws (Fig. 8). At the 26-week time point, the differences between the coated and uncoated samples were less apparent as both screw types had new bone formation at the β-TCP marker surface.

In the torsion tests, the coated screws required significantly greater torsional force to be loosened from the surrounding bone. Five coated screws broke during the torsion tests whereas this occurred only twice with the uncoated screws. This could indicate a stronger attachment of coated screws to bone tissue, their faster degradation rate, or that the coating process had compromised the strength of the screws. The stage of degradation of both screw types at the 12-week time point showed a similar pattern according to the histology. However, this needs to be elucidated in the future with adequate methods.

The rates of the new bone formation with the PLGA-β-TCP screws were in similar ranges as in earlier studies with polylactide-based bioabsorbable bone fixation devices where bone formation was reported to occur between 6 and 12 weeks after implantation in bone tissue [38, 39]. As expected, the bulk degradation of the screws in our study did not occur at the 12-week time point. According to the manufacturer of the PLGA-β-TCP screws, the shear strength of the screws remains at the initial level for 16 weeks and drops to 35% at 26 weeks.

Hard tissue histology at the 12-week time point showed a clear band of PPy stained by toluidine blue around the implants suggesting that it was still consistently distributed around implant and therefore played a key role in tissue attachment. At the 26-week time point, only small traces of PPy were found in the hard tissue histology as the degradation of the inner lying PLGA-β-TCP matrix had caused it to crack and erode. Macrophages did not seem to play a role in PPy elimination at this stage, as none was apparent in the histological samples. PPy is not inherently degradable but its ability to erode may contribute to its final elimination from the body [8, 40]. Small water-soluble PPy chains (1700–3200 Da) have been reported to be excreted by renal clearance [41]. The creatinine values in the coated group were significantly higher 2 and 4 weeks after surgery compared to the coated group indicating slight deterioration in kidney function in the rabbits of the coated group. However, the increased values were still within normal levels. This suggests that the PPy coating started to erode 2 weeks after implantation. The creatinine levels recovered to baseline level 12 weeks postoperatively, showing no further statistical differences and indicating that the major erosion evidenced between 12 and 26 week time points did not affect renal functioning.

PPy did not induce acute, subacute or subchronic toxicity and proved to be compatible with bone tissue. No inflammatory cells or allergic reactions were found around the coated and uncoated screws in the hard tissue histology (Fig. 8 and 9). No abnormal findings in terms of hematoma, edema or encapsulation in any of the samples were found by macroscopic observation. In addition, the histological soft tissue samples around the screw heads showed no abnormal reactions either in the number of polymorphonuclear cells and macrophages or in the amount of necrosis and fatty infiltrate. The PPy coating even seemed to lower the irritation level of the absorbable screw according to the semi-quantitative evaluation. This finding is supported by earlier studies conducted on various tissue types [18, 19, 21, 22]. Moreover, PPy did not show any systemic effect according to hematology and clinical chemistry. Significant differences found between the uncoated and coated group were within normal ranges when compared to the values measured prior to surgery.

Even though several studies have reported the high biocompatibility of PPy, slight adverse reactions have also been reported [14, 42-44]. For instance, different concentrations of PPy monomer used in polymerization can drastically vary cellular events as a higher PPy concentration during admicellar polymerization has been reported to inhibit MSC attachment. It was suggested that the negative effect on cell attachment in the study was due to an unfavorable thickness and hence a changed surface roughness of the PPy layer, and not due to toxic components leaching from the polymer [14]. Thin PPy layers have been reported to result in a better cell attachment in studies conducted in vitro and in vivo [8, 14, 40]. PPy nanoparticles may

also induce slight adverse reactions on cells. This has been reported to be highly dependable on particle size [42, 43]. Moreover, the aging of the PPy has been suggested to have a negative effect on its biocompatibility with nanocellulose-PPy composites, which showed marks of cytotoxicity in several conditions after 4 weeks of storage [44]. The coated screws in our study were stored in appropriate sterile packages for 10 months at ambient temperature before implantation, and the PPy did not show increased cytotoxic signs when compared to uncoated screws. Nevertheless, longer-term effects of the coating require evaluation in the future studies.

The role of CS in this study remains unclear, as the concentration of CS in the PPy coating was not measured. It has, however, been reported to induce permanent hydrophilicity of the PPy coating [10] and its carboxyl groups may facilitate attachment of PPy to bone tissue [32]. The hydrophilic surface characteristics of the coated screws could theoretically facilitate faster water uptake in the implant surface [45].

Conclusion

The PPy coating on PLGA-β-TCP screws significantly enhanced new bone formation during the 26-week implantation period and significantly facilitated the attachment of the screws in bone tissue up to 12 weeks postoperatively. Moreover, the PPy coating and its erosion products did not show any increased adverse reactions locally or systematically. These results highlight the potential of PPy as a multifunctional osteogenic coating material to facilitate better bone tissue-implant interactions.

Acknowledgements

The authors would like to thank Bioretec Ltd. for providing the bioabsorbable polymer composite bone fixation screws for this study; Deng Lianfu (Prof, PhD) and Jorma Pajamäki (MD, PhD) for consultation in bone tissue histology, and Tuija Annala (MSc) for consultation in the experiment configuration. This work was carried out with the financial support of the Shanghai International Science and Technology Partnership Program (11540702700), the Natural Science Foundation of China (81372002), the Finnish Funding Agency for Technology and Innovation (TEKES), the Academy of Finland, the City of Tampere Science Foundation, and the Competitive Research Funding of Tampere University Hospital (grants 9K020 and 9N042).

References

[1] Tian H, Tang Z, Zhuang X, Chen X, Jing X. Biodegradable synthetic polymers: Preparation, functionalization and biomedical application. Prog Polym Sci 2012;37:237-80.

[2] Ajiro H, Takahashi Y, Akashi M, Fujiwara T. Polylactide block copolymers using trimethylene carbonate with methoxyethoxy side groups for dual modification of hydrophilicity and biodegradability. Macromol Biosci 2012;12:1315-20.

[3] Wang S, Cui W, Bei J. Bulk and surface modifications of polylactide. Anal Bioanal Chem 2005;381:547-56.

[4] Son JS, Kim SG, Oh JS, Appleford M, Oh S, Ong JL, et al. Hydroxyapatite/polylactide biphasic combination scaffold loaded with dexamethasone for bone regeneration. J Biomed Mater Res A 2011;99:638-47.

[5] Zhang P, Hong Z, Yu T, Chen X, Jing X. In vivo mineralization and osteogenesis of nanocomposite scaffold of poly(lactide-co-glycolide) and hydroxyapatite surface-grafted with poly(L-lactide). Biomaterials 2009;30:58-70.

[6] Zhou H, Lawrence JG, Bhaduri SB. Fabrication aspects of PLA-CaP/PLGA-CaP composites for orthopedic applications: a review. Acta Biomater 2012;8:1999-2016.

[7] De Giglio E, Guascito MR, Sabbatin L, Zambonin G. Electropolymerization of pyrrole on titanium substrates for the future development of new biocompatible surfaces. Biomaterials 2001;22:2609-16.

[8] Shi G, Rouabhia M, Wang Z, Dao LH, Zhang Z. A novel electrically conductive and biodegradable composite made of polypyrrole nanoparticles and polylactide. Biomaterials 2004;25:2477-88.

[9] Zhang J, Neoh KG, Hu X, Kang ET, Wang W. Combined effects of direct current stimulation and immobilized BMP-2 for enhancement of osteogenesis. Biotechnol Bioeng 2013;110:1466-75.

[10] Pelto J, Bjorninen M, Palli A, Talvitie E, Hyttinen J, Mannerstrom B, et al. Novel polypyrrole-coated polylactide scaffolds enhance adipose stem cell proliferation and early osteogenic differentiation. Tissue Eng Part A 2013;19:882-92.

[11] Serra MJ, Sabbieti MG, Agas D, Marchetti L, Panero S. Polysaccharides immobilized in polypyrrole matrices are able to induce osteogenic differentiation in mouse mesenchymal stem cells. J Tissue Eng Regen Med 2012.

[12] Meng S, Zhang Z, Rouabhia M. Accelerated osteoblast mineralization on a conductive substrate by multiple electrical stimulation. J Bone Miner Metab 2011;29:535-44.

[13] Meng S, Rouabhia M, Zhang Z. Electrical stimulation modulates osteoblast proliferation and bone protein production through heparin-bioactivated conductive scaffolds. Bioelectromagnetics 2013;34:189-99.

[14] Castano H, O'Rear EA, McFetridge PS, Sikavitsas VI. Polypyrrole thin films formed by admicellar polymerization support the osteogenic differentiation of mesenchymal stem cells.

Macromol Biosci 2004;4:785-94.
[15] Garner B, Georgevich A, Hodgson AJ, Liu L, Wallace GG. Polypyrrole-heparin composites as stimulus-responsive substrates for endothelial cell growth. J Biomed Mater Res 1999;44:121-9.
[16] Schmidt CE, Shastri VR, Vacanti JP, Langer R. Stimulation of neurite outgrowth using an electrically conducting polymer. Proc Natl Acad Sci U S A 1997;94:8948-53.
[17] De Giglio E, Sabbatini L, Colucci S, Zambonin G. Synthesis, analytical characterization, and osteoblast adhesion properties on RGD-grafted polypyrrole coatings on titanium substrates. J Biomater Sci Polym Ed 2000;11:1073-83.
[18] Wang X, Gu X, Yuan C, Chen S, Zhang P, Zhang T, et al. Evaluation of biocompatibility of polypyrrole in vitro and in vivo. J Biomed Mater Res A 2004;68:411-22.
[19] Jiang X, Marois Y, Traore A, Tessier D, Dao LH, Guidoin R, et al. Tissue reaction to polypyrrole-coated polyester fabrics: an in vivo study in rats. Tissue Eng 2002;8:635-47.
[20] Cui X, Wiler J, Dzaman M, Altschuler RA, Martin DC. In vivo studies of polypyrrole/peptide coated neural probes. Biomaterials 2003;24:777-87.
[21] Ramanaviciene A, Kausaite A, Tautkus S, Ramanavicius A. Biocompatibility of polypyrrole particles: an in-vivo study in mice. J Pharm Pharmacol 2007;59:311-5.
[22] Collier JH, Camp JP, Hudson TW, Schmidt CE. Synthesis and characterization of polypyrrole-hyaluronic acid composite biomaterials for tissue engineering applications. J Biomed Mater Res 2000;50:574-84.
[23] Zhang Z, Roy R, Dugre FJ, Tessier D, Dao LH. In vitro biocompatibility study of electrically conductive polypyrrole-coated polyester fabrics. J Biomed Mater Res 2001;57:63-71.
[24] Vaijayanthimala V, Cheng PY, Yeh SH, Liu KK, Hsiao CH, Chao JI, et al. The long-term stability and biocompatibility of fluorescent nanodiamond as an in vivo contrast agent. Biomaterials 2012;33:7794-802.
[25] Iijima M, Muguruma T, Brantley WA, Okayama M, Yuasa T, Mizoguchi I. Torsional properties and microstructures of miniscrew implants. Am J Orthod Dentofacial Orthop 2008;134:331-3, 333-4.
[26] Deng F, Ling J, Ma J, Liu C, Zhang W. Stimulation of intramembranous bone repair in rats by ghrelin. Exp Physiol 2008;93:872-9.
[27] Di Iorio E, Barbaro V, Ferrari S, Ortolani C, De Luca M, Pellegrini G. Q-FIHC: quantification of fluorescence immunohistochemistry to analyse p63 isoforms and cell cycle phases in human limbal stem cells. Microsc Res Tech 2006;69:983-91.
[28] Giessler GA, Gades NM, Friedrich PF, Bishop AT. Severe tacrolimus toxicity in rabbits. Exp Clin Transplant 2007;5:590-5.
[29] Scioscia TN, Giffin JR, Allen CR, Harner CD. Potential complication of bioabsorbable screw fixation for osteochondritis dissecans of the knee. Arthroscopy 2001;17:E7.
[30] Cordova LA, Stresing V, Gobin B, Rosset P, Passuti N, Gouin F, et al. Orthopaedic implant failure: aseptic implant loosening--the contribution and future challenges of mouse models in

translational research. Clin Sci (Lond) 2014;127:277-93.
[31] Somayaji SN, Huet YM, Gruber HE, Hudson MC. UV-killed Staphylococcus aureus enhances adhesion and differentiation of osteoblasts on bone-associated biomaterials. J Biomed Mater Res A 2010;95:574-9.
[32] De Giglio E, Cometa S, Calvano CD, Sabbatini L, Zambonin PG, Colucci S, et al. A new titanium biofunctionalized interface based on poly(pyrrole-3-acetic acid) coating: proliferation of osteoblast-like cells and future perspectives. J Mater Sci Mater Med 2007;18:1781-9.
[33] Browne M, Gregson PJ. Effect of mechanical surface pretreatment on metal ion release. Biomaterials 2000;21:385-92.
[34] Bosco R, Edreira ERU, Wolke JGC, Leeuwenburgh SCG, van den Beucken JJJP, Jansen JA. Instructive coatings for biological guidance of bone implants. Surface and Coatings Technology 2013;233:91-8.
[35] Chen Y, Mak AFT, Wang M, Li J, Wong MS. PLLA scaffolds with biomimetic apatite coating and biomimetic apatite/collagen composite coating to enhance osteoblast-like cells attachment and activity. Surface and Coatings Technology 2006;201:575-80.
[36] Edlund U, Danmark S, Albertsson AC. A strategy for the covalent functionalization of resorbable polymers with heparin and osteoinductive growth factor. Biomacromolecules 2008;9:901-5.
[37] Sirivisoot S, Pareta R, Webster TJ. Electrically controlled drug release from nanostructured polypyrrole coated on titanium. Nanotechnology 2011;22:85101.
[38] Saikku-Backstrom A, Tulamo RM, Raiha JE, Kellomaki M, Toivonen T, Tormala P, et al. Intramedullary fixation of cortical bone osteotomies with absorbable self-reinforced fibrillated poly-96L/4D-lactide (SR-PLA96) rods in rabbits. Biomaterials 2001;22:33-43.
[39] Felix LR, Leeuwenburgh SC, Wolke JG, Jansen JA. Bone response to fast-degrading, injectable calcium phosphate cements containing PLGA microparticles. Biomaterials 2011;32:8839-47.
[40] Wang Z, Roberge C, Dao LH, Wan Y, Shi G, Rouabhia M, et al. In vivo evaluation of a novel electrically conductive polypyrrole/poly(D,L-lactide) composite and polypyrrole-coated poly(D,L-lactide-co-glycolide) membranes. J Biomed Mater Res A 2004;70:28-38.
[41] Zelikin AN, Lynn DM, Farhadi J, Martin I, Shastri V, Langer R. Erodible conducting polymers for potential biomedical applications. Angew Chem Int Ed Engl 2002;41:141-4.
[42] Kim S, Oh WK, Jeong YS, Hong JY, Cho BR, Hahn JS, et al. Cytotoxicity of, and innate immune response to, size-controlled polypyrrole nanoparticles in mammalian cells. Biomaterials 2011;32:2342-50.
[43] Vaitkuviene A, Kaseta V, Voronovic J, Ramanauskaite G, Biziuleviciene G, Ramanaviciene A, et al. Evaluation of cytotoxicity of polypyrrole nanoparticles synthesized by oxidative polymerization. J Hazard Mater 2013;250-251:167-74.
[44] Ferraz N, Stromme M, Fellstrom B, Pradhan S, Nyholm L, Mihranyan A. In vitro and in vivo toxicity of rinsed and aged nanocellulose-polypyrrole composites. J Biomed Mater Res A

2012;100:2128-38.
[45] Kallrot M, Edlund U, Albertsson AC. Covalent grafting of poly(L-lactide) to tune the in vitro degradation rate. Biomacromolecules 2007;8:2492-6.